CHAPTER ONE

INTRODUCTION

1.1 Background of the study

Nutrition is a critical and important aspect of quality of human life. Considering the three basic needs of man, food is regarded as the most important of them. Since most food crops are harvested only during a certain time of the year, there is, on the one hand, a temporary surplus during harvest and thereafter a shortage. Postharvest spoilage is still very common, ranging from 20% (Aidoo, 1993), 50% (Okigbo, 2004) to 60% (Dramani, 2013), depending on the type or nature of the product and storage time.

Common food spoilers are fungi and moulds, often present already on the fields and growing on spots that are physically damaged. Also, storage under ambient conditions promotes microbial growth; high humidity causes rapid spoilage of harvested crops (Aidoo, 1993; Okigbo, 2004).

Sequel to these findings, preservation is a useful tool to minimize postharvest losses and increase food security in society. According to WHO (1996), food security can be defined as when all people at all times have access to sufficient, safe, nutritious food to maintain a healthy and active life. Chronic malnutrition, the opposite of food security, is a serious problem in West Africa and it is known to affect a large population of the sub-region. Based on insufficient storage facilities, farmers have to sell their yam tubers quickly during harvest when prices are low. Longer shelf life of the tubers or tuber product would, therefore, increase income and improve the socio-economic situation of these farmers (Dramani 2013).

The discoloration of yam upon peeling is a major limitation. This reduces the consumer's acceptability of the products by developing off-flavours and off-colours. According to Sanful,(2016), for most yam species, the most common cause of discolouration is enzymatic browning which results mainly from the action of polyphenol oxidase and peroxidase. Beside chemical treatment which involves anti-browning agents, there are some methods that are employed traditionally to inhibit enzymatic browning. Thermal treatment such as blanching has been considered as a means of controlling enzymatic browning in a variety of food produce (Kouassi, Nindjin, Tetchi, & Amani. 2010). This type of browning can be prevented by blanching; putting the product in hot water for a short period of time to deactivate the enzyme. Blanching is a common practice before drying of yam (Akissoe, et al.,2005)). In this study, both the aerial yam (Dioscorea bublifera) and water yam (*Dioscorea alata*) undergo this thermal treatment before drying process to improve product quality, increase yield, preserve colour, remove trapped air and also reduce microbial contamination. Blanching can have deleterious effects at high temperature and extended time of treatment resulting in reduced nutritional value from leaching nutrients, thermal degradation or alteration of starch profile and properties.

Drying plays an important role in the preservation of agricultural products. Drying of agricultural products has been of great importance for the preservation of food. Many food products are dried at least once at some point in their preparation (Madamba, et al., 1996).

According to Dincer and Sahin, (2004), Soysal, (2004), drying is an energy intensive process and involves removal of moisture from a crop until the moisture content of the crop is in equilibrium with the surrounding air. It deals with simultaneous heat and mass transfer. Drying is one of the most common techniques used to reduce microbiological activity and to improve the stability of moist material by decreasing their moisture content to a certain constant level. The

main goal of drying agro-products is to reduce the moisture content to a level that halts or controls microbial growth and to reduce deteriorative chemical reaction in order to extend the shelf life of food. Drying is one of the widely used methods in preserving agricultural products. The important aim of drying is to reduce the moisture content and thereby increase the shelf life (Life time) of products by limiting enzymatic and oxidation degradation. In addition, by reducing the amount of water, drying reduces the crop losses, improves the quality of dried products and facilitates its transportation, handling, and storage requirements. Drying is a process comprising simultaneous heat and mass transfer within the materials and between the surface of the material and the surrounding media (Adewale, et al.,2015).

According to Srikiatden and Roberts (2007), drying of foods starts with a constant rate period, which is only determined by the speed of evaporation at the surface. Often, no constant rate period is observed and drying happens at the next stage: the falling rate period, determined by internal diffusion limitation. During drying of foods, it should be noted that the removal of moisture must be at a temperature which will not affect the flavor, texture, colour and the overall quality of the food. Three different drying methods are considered in this study; open sun drying, solar drying system and convective hot air-drying system. Among the three methods of drying, convective hot air-drying system has been to date the most common method employed for dehydrating agricultural and food products. Solar drying has been reported in the literature to affect the concentration of some nutrients (Hassan e al., 2007). Open sun drying is a traditional method of drying and this causes the loss of some nutrients, food losses and contamination by dust, stones and insects (Asumadu & Owusu, 2016).

Aerial yam (*Dioscorea bulbifera*) which is also known as air potatoes is a member of the yam species often considered as a wild species of yam native to Africa and Asia. Aerial yam is a

member of the Dioscoreaceae family which consist of several varieties found in Africa and South Asia (Kayode et al., 2017). Nigeria is a major producer of yam, but Ghana is leading in the production of Aerial yam. Aerial yam is among one of the most underutilized food crops in Nigeria and other parts of the world where it grows and appears in both the wild and edible forms. It has a long vine and it produces tubers (bulbis) which grow at the base of its leaves. This species of yam is not popular among farmers or consumers and does not enjoy the patronage that some of the other edible yam species enjoy. Despite its underutilization, Aerial yam has been shown to possess a myriad of compounds that are said to have several health benefits (Sanful et al., 2015).Water Yam *(Dioscorea alata)* is the most widespread yam species and more important as food in West Africa and the Caribbean than in Asia and in America where it originated and has been competing with the most important species like *Dioscorea rotundata* (Oko & Famurewa, 2015). Water yam is popular and prevalent within Abakiliki agro-ecological zone of Ebonyi state, Nigeria where it is called "Mbala or Nvula" (Native names in Igbo land) (Oselebe & Okporie, 2008). Water yam has low sugar content necessary for diabetic patients. Also, it contains nutrient which has benefits to the body, and it also contains dietary fibre which is important in the diet for the healing and health-promotion. Water yam also contains a lot of minerals like calcium, potassium, iron, phosphorus and copper with high presence of vitamins C and E which have antioxidant properties, and lowers blood pressure levels. Sequel to these findings, it is necessary to preserve this agro-product from spoilage by introducing drying and other processing techniques.

Owing to these overwhelming nutritional, medicinal and economic benefits of these yams, much work has been done to determine its functional properties but not much work has been done on its drying kinetics and its associated engineering properties. Aneke et al, (2018) and Sobukola et

al, (2010) reported some work on the optimization of water yam drying while no report on the optimization of aerial yam drying process was seen by this researcher. This research, therefore, seeks to study the kinetics, drying characteristics, engineering properties of aerial yam and water yam using response surface methodology and numerical finite element analysis. This is with a view to obtaining information which could help in the design and operation of dryers for commercial preservation and production of these vital agro products' flour.

1.2 Statement of the Problem

Basically, food and nutrition are known important modifiers of disease initiation and development. The main causes of illness and death seem to be a chronic degenerative diseases such as cancer, heart disease, arthritis, respiratory diseases, diabetes, and hypertension (Ayoola, et al., 2008). Cognitive impairment and various toxic states could be averted with proper nutrition and diet. Considering the medical importance of aerial yam and water yam as good sources of dietary requirements, efficient preservative techniques should be employed to make these agro-products available in the market. However, there are insufficient preservation facilities and the two agro-materials are seasonal and are not available always throughout the year. Study on the drying of these yams using two drying methods and drying characteristics will provide information for the design and operation of the dryers.

Optimization of the drying process is very important because this will provide sufficient information to industries in the drying of aerial yam and water yam to derive high quality products. Seven drying kinetics models will be investigated to determine the best drying kinetic model for these agro-products. Also, two-dimensional finite element modelling will be employed

to simulate and provide information for the design of dryers, industrial drying and handling of these products.

1.3 Aim and Objectives

The aim of this work is theevaluation of engineering properties and drying characteristics of aerial and water yams. This will lead to the development of a mathematical model to describe the drying.

The objectives of this work include:

1. To determine the engineering properties of aerial and water yam that are relevant to drying.
2. To study the kinetics for the drying process and optimize the drying process using Response Surface Methodology (RSM) via central composite design (CCD).
3. To carry out sensory test (Hedonic test) on the flours produced from the two agro-products.
4. To conduct numerical simulation of the drying process using a two-dimensional finite element model.

1.4 Significance of the Study

Yam is rich in carbohydrates and other essential elements or nutrients. Besides their importance as a food source, yams play a vital and significant role in socio-cultural lives of some producing regions such as the celebrated new yam festivals in Nigeria. West and Central Africa account for about 94% of the world production, Nigeria being the major producer (FAO, 2011; Osunde, 2008). For example, in 2011, the global yam production was about 50 million metric tons with 96% of this coming from Nigeria (FAO, 2011). Since Nigeria is a major producer of yam,

preservative mechanism which drying is an important example should be employed for constant availability of the product for processing.

Researches have shown that experimental drying data should be supported with mathematical modeling in order to improve the efficiency of the dryers and increase the quality of the dried product. The use of mathematical model in finding the drying kinetics of these agro-products is very important. Mathematical modelling and computer simulation will be used in this research to predict the dehydration behaviour of aerial yam and water yam, and thus provides information for designing new dryers and even to control the process (Naghavi & Moheb, 2010).

It is helpful to define what exactly constitutes an engineering property of a certain food. Generally, any attribute affecting the processing or handling of food can be defined as an engineering property. Hence in this research, the engineering property of these agro-products will be studied in detail and reported accordingly to indicate the changes in the chemical and structural orientation of the products.

1.5 Scope of the study

The work covers drying of aerial yam and water yam using two drying methods (solar drying, convective hot-air dryer), drying characteristics and kinetic modelling, comparing the quality of the dried blanched product and unblanched, sensory analysis (hedonic test), numerical analysis of the drying process using a two-dimensional finite element method and optimization of the drying process using response surface methodology.

CHAPTER TWO

LITERATURE REVIEW

2.1 Drying

Drying is a complex process that involves simultaneous coupled transient heat, mass and momentum transport. It is a process whereby the moisture is vaporized and removed from the surface, sometimes in vacuum but normally by means of a carrier fluid passing through or over the moist object. This process has found industrial application ranging from wood drying in the lumber industry to food drying in the food industry. In drying process, the heat may be added to the object from an external source by conduction, convection, or radiation, or the heat can be generated internally within the body by means of electric resistance (Sahin et al., 2002). The effectiveness of a drying process is dependent on different factors which includes method of heat transfer, continuity or discontinuity of the process, direction of the heating fluids with respect to the product (pressure atmospheric, low, deep vacuum). Drying can be accomplished by using different kinds of equipment such as solar dryer, convective hot air dryer, air cabinet, belt drier, tunnel drier, fluidized bed, spray drier, drum dryer, foam drier, freeze-drier, microwave oven (Severini et al., 2005).

Mainly, there are two types of drying which are given below-

i. Natural drying

ii. Mechanical drying

Each of these will be considered in turn.

2.1.1 Natural drying

Natural drying is the method of drying in which natural source of heat such as solar energy is used for drying of food samples. Often known as sun/solar drying, it has found great application in fish, meat, cloth, grain drying and has proved to generate food stuff of high quality and low spoilage. Though solar drying is a cheap, easy and popular method, its application is restricted by the long drying time and need for favorable weather. It is a slow process, very prone to contaminants as well as weather changes. That is why it is not common for commercial scale production. Some of the natural drying methods are listed below.

i. Sun drying

In the tropical regions of the world, the customary method for crop drying is sun drying. Open sun drying usually involves the spreading in thin layers of crops such as maize, rice, coffee, beans, coco yam and fish on concrete floors, large trays, and galvanized sheets or simply on the roadsides until the crop is sufficiently dried (Arinze,1987). This type of drying is normally the only commercially used and feasible method by which agricultural products are dried in developing countries.

It is a simple and inexpensive method of drying agricultural products. Notwithstanding the positive influence of drying on shelf life, Sharma *et al.* (2009) reported several limitations connected with traditional sun drying. During continuous rainfall, crop drying is not possible and the risks of crop losses are high. Sun drying is slow and weather dependent compared to some

other alternative drying systems. Crop quality may be affected considerably due to direct contact with UV-radiation, contamination by dust, dirt, stones and insects, high crop losses from theft and livestock consumption. Also, long exposure to the drying temperatures of open air-drying has an adverse effect on texture, colour, rehydration ratio, nutrient content and other characteristics of the dried product (Hofsetz *et al*., 2008).

Recently, consumer demands have increased for processed products to retain more of their original characteristics, while bacterial and fungal contamination must be prevented. Consequently, this type of drying is not appropriate from food hygiene and food safety point of view. Therefore, any means by which products are dried effectively, quickly and hygienically at a cheaper rate to make them available during the off-season period is highly necessary. Solar dryers may be a good substitute for these problems. A diagram of a sun dying application is shown in Figure. 2.1.

Figure 2. 1: A typical sun drying application

Source: https://www.wonderlandguides.com/backcountry-cooking/dehydrating-food/food-dehydrating-101. Retrieved on 21st February 2019.

ii. Solar Drying

In solar drying, solar-energy is employed either as the sole source of the required heat or as a supplemental source. The airflow into the dryer can be generated by either natural or forced convection. The heating procedure involves the channelling of preheated air by a fan through the product or by directly exposing the product to solar radiation or a combination of both (Ekechukwu & Norton, 1998).

Solar drying has some advantages over other drying methods if the dryer is properly designed. Solar drying is cheap in comparison to other advanced methods of drying since it mainly relies on energy from the sun, requires low or no electric power and the dryers are relatively cheap and easy to construct. This makes it appropriate for use in rural areas with limited electricity and frequent load shedding. They are useful in areas where fuel or electricity is expensive, sunshine is plentiful but air humidity is high. Furthermore, they are useful asa means of heating air for artificial dryers to reduce fuel cost (Fellows, 2000). Solar dryers give faster drying rates by heating the air above ambient, which causes the air to move faster over the product. The sample is completely protected from rain, dust, insects and animals. Faster drying rates decrease the risk of spoilage and improve quality. A diagram of a solar dying application is shown in Figure. 2.2.

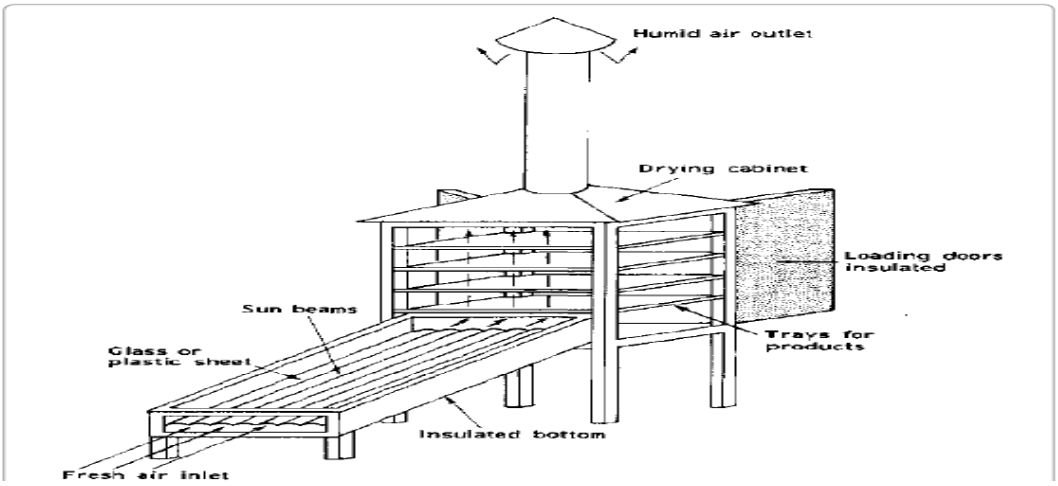

Figure 2. 2: A typical solar dryer application

Source: Tiwari, (2016).

2.1.2 Mechanical drying

Mechanical drying is an advanced method of drying of foods by means of mechanical systems. Hot air is generated by the system which is used for the drying of food material. Numerous mechanical dryers have been developed by researchers in the field of food technology. Several types of mechanical drying systems available in the market are hot air convective drying, freeze drying, microwave drying, vacuum assisted microwave drying, microwave assisted fluidized bed drying etc. Some examples of mechanical dryers are;

i. Microwave drying:

Microwave drying depends on extra energy being supplied that is preferentially absorbed by the sample in the process to enhance evaporation. Microwaves are a form of electromagnetic energy (300 Mhz–300 GHz), produced by magnetrons under the combined force of perpendicular electric and magnetic fields. Microwave heating is a direct heating method. In the rapidly

alternating electric field generated by microwaves, polar materials orient and reorient themselves according to the direction of the magnetic field. The rapid changes in the field (at 2450 MHz), the orientation of the field changes 2450 million times per second and cause rapid molecular reorientation, resulting in friction and heat. Diverse materials have different properties when exposed to microwaves, depending on the degree of energy absorption, which is characterized by the loss factor.

ii. Hot air convective drying

The principle of hot air convective dryer is based on convective heat transfer from heated air to the sample being dried. Hot air is forced through the material with the help of a fan and which aid the moisture diffusion process that results in the drying. This method has been widely used in industries for drying of food products. Different types of dryers have been developed and employed in commercial production (Jayarama & Gupta, 1995). Heated air is blown through the sample by cross flow or by fan generated flow. Hot air convective drying can greatly shorten the drying time from several weeks to several days as compared to solar drying.A diagram of a convective dying application is shown in Figure. 2.3.

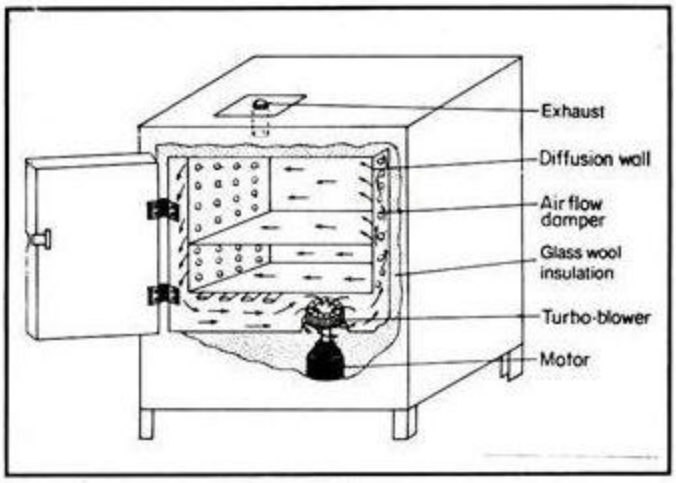

Figure 2. 3: A typical hot air convective dryer

Source: Daniel et al.(2017).

iii. Freeze Drying

Freeze-drying is also known as cryodesiccation. It is a dehydration process normally used to preserve perishable produce or make the products more convenient for transportation. It works by the principle of freezing the material and then decreasing the surrounding pressure to allow the frozen water in the material to sublimate directly from the solid phase to the gas phase.

iv. Oven Drying

An oven dryer is ideal for occasional drying of fruit leathers, banana chips or for preserving excess produce like celery or mushrooms. Since the oven is needed for everyday cooking, it may not be satisfactory for preserving abundant garden produce. By combining the factors of heat, low humidity and air flow, an oven can be used as a dehydrator. Oven drying is slower than dehydrators because it does not have a built-in fan for the air movement, though some

conventional ovens do have a fan. It takes about two times longer to dry food in an oven than if dehydrator is used. Therefore, the oven is not as efficient as a dehydrator and uses more energy.

2.2Drying kinetic model

Thin layer drying models (moisture ratio equations) that define the drying phenomenon of agricultural produce mainly fall into three groups, namely theoretical, semi theoretical and empirical. Nevertheless, for the sake of this research, only semi-theoretical model will be discussed.

2.2.1 Semi –theoretical models

The semi-theoretical model is derived from the simplification of Fick's second law of diffusion or modification of the simplified model, which has been extensively used to describe the drying characteristics. Semi-theoretical models offer a compromise between theory and ease of use; they require less time compared to theoretical thin layer models and do not need assumptions of geometry of typical food, its mass diffusivity and Conductivity (Ozdemir & Devres., 1999). Amongst semi-theoretical thin layer drying models, the Newton (Lewis) model, Page model, the modified Page model, the Henderson and Pabis model, the logarithmic model, the two-term model, the two-term exponential, the diffusion approach model, the modified Henderson and Pabis model, the Verma et al. model and the Midilli–Kucuk model are used extensively.

2.2.2 Lewis model

Lewis in 1921 proposed that the change in moisture content in the falling rate period is proportionate to the instantaneous difference between the moisture content and the expected moisture content when it comes into equilibrium with drying air (Black., 2014). This basically

assumed that the material is thin enough, the velocity high enough and the drying conditions constant enough as shown in eqn. (2.1):

$$\frac{\partial m}{\partial t} = -k(m-m_e) \quad (2.1)$$

Where K is the drying constant for thin layer concepts, m is the moisture content and m_e is the moisture content at equilibrium. This will incorporate the moisture diffusivity, thermal conductivity, interface heat and mass coefficients. If K is independent of the moisture content then we have eqn. (2.2):

$$M_R = \frac{m_t - m_e}{m_i - m_e} = e^{-kt} \quad (2.2)$$

Where K, m_t is the content at time, t and K can be obtained from experimental data. This is known as the Lewis (or Newton) constant, and M_R is the moisture ratio.

2.2.3 Newton model

Newton model posits that the moisture transfer from the foods and agricultural produce can be seen as equivalent to the flow of heat from a body immersed in cool fluid (Ismail & Ibn Idriss., 2013). This model assumes negligible internal resistance, which means no resistance to moisture movement from within the products to the surface of the products. By comparing this phenomenon with Newton's law of cooling, the drying rate is proportional to the variance in moisture content between the material being dried and equilibrium moisture content at the drying air condition as shown in eqn. (2.3):

$$M_R = \exp(-kt) \quad (2.3)$$

Where;

M_R = moisture ratio, dimensionless

k = drying rate constant, h-1

t = drying time, h

This model is used mainly because it is simple. The only disadvantage, however, is that it underestimates the beginning of the drying curve and overestimates the later stages.

Other standard drying kinetic models are presented in Table 2.1, while Table 2.2 presents a review of related works on the drying kinetic models of agricultural products.

Table 2. 1: Standard models reported in the literature used for drying of agricultural products.

S/N	Model	Mathematical function	Reference
1	Wang and Singh	M_R=a$t^2 + bt + c$	Wang and Singh (1978)
2	Verma e*t al*.	M_R=a exp(-kt)+(1-a)exp(-gt)	Motevali *et al*. (2010)
3	Henderson and Pabis	M_R=a exp(-kt)	Motevali *et al*. (2010)
4	Logaritmic	M_R=a exp(-kt)+c	Dandamrongrak *et al*. (2002)

5	Modified page	M_R= exp(-$(kt)^n$	Wang *et al.* (2007)
6	Two term	M_R= a exp($k_o t$) + b exp(−k_1)	Diamente and Munro (1991)
7	Approx. of diffusion	M_R= a exp(-kt)+(1-a)exp(-kbt)	Ertekin and Yaldiz (2004)
8	Page	M_R= exp(-kt^n)	Motevali *et al*. (2010)
9	Modified Henderson and Pabis	M_R= a exp(-kt)+b exp(-gt)+c exp(-ht)	Sharma *et al*. (2009)
11	Midilli *et al.*	M_R= a exp(-kt^n)+bt	Midilli *et al*. (2002)
12	Two term exponential	M_R=a exp(-kt)+(1-a)exp(-kat)	Motevali *et al*. (2010)

Table 2. 2:Thin layer drying models for some farm produce.

S/N	Crop/seed/vegetable	Suitable model	References
1	Okra	Logarithmic	Afolabi, & Agarry, (2014)
2	Bitter leave	Modified Page and Page	Rhoda & Negimote, (2015)
3	Sorghum	Page	Bonner & Kenney, (2012)
4	Carrot	Midi et al	Darvishi et al., (2012)

5	Melon	Midi et al	Azadbakht et al., (2012)
6	Cassava	Exponential	Kajuna et al., (2001)
7	Cocoa	Henderson and Papis	Ndukwu et al., (2010)
8	Corn	Logarithmic	Ajala et al., (2012)
9	Groundnut	Two term and Logarithmic	Kaptso et al., (2013)
10	Yam	Midi et al and Verma et al	Sacilik, (2007)
11	Millet	Modified Page and Page	Ojediran, & Raji, (2010)
12	Breadfruit	Two term	Chinweuba et al., (2016)
13	Soybeans	Midi et al	Rafiee et al., (2009)
14	Cashew kernels	Page	Asiru et al., (2015)
15	Bitter kola	Page	Ehiem, & Eke, (2014)
16	Sugar cane	Midi et al	Goyalde et al., (2009)
17	Scent leave	Page	Rhoda, & Negimote, (2015)
18	Tomato slice	Midi et al	Haney & Hangpin., (2017)
19	Pea Pod	Page	Meenakshi et al, (2014)
20	Turnip	Modified Henderson and Pabis	Gharehbeglou et al, (2014)

2.3 Moisture content

This is a measurement of the total amount of water confined in a food, usually expressed as a percentage of the total weight. It is a suitable measurement for evaluating the dry weight of food and ingredients and it aids the calculation of the total yield. It can also be used to confirm whether the drying of foods has attained a satisfactory level. It is one of the most generally measured properties of food materials. Moisture plays a significant role in postharvest handling

operations such as drying, storage, marketing and roasting of crops such as cocoa, yam, maize and cashew. Moisture measurement during drying is necessary to follow up the drying process and to decide when drying is completed. Marketing worth of a product may be affected by moisture content and may affect the trade negotiations and trust. The roasting temperature and length of roasting may be controlled with the knowledge of product moisture content and this could affect energy requirement during roasting. Moisture level in food materials is essential to food scientists for legal and labeling requirements, economic reasons, microbial stability, food quality and processing among others (Stroshine & Hamann, 1995). Knowledge of the moisture content is often required to predict the behaviour of food sample during processing. It is therefore imperative for food scientists to be able to reliably measure moisture content.

Thiex and van Erem (1999) stated that a number of analytical techniques have been developed for this purpose, which differs in their accuracy, cost, speed, sensitivity, specificity and ease of operation. The choice of an analytical technique for a particular application is dependent on the nature of the food being analyzed and the purpose for which the information is needed.

2.3.1 Methods of measuring moisture content

The methods of determining moisture content in food grains are divided into three broad categories:

Direct measurement: In direct measurement, water content is determined by removing moisture and then measuring weight loss;

Indirect measurement: In this, an intermediate variable is measured and then converted into moisture content. Building up calibration charts before applying indirect measurements is a requirement.

Empirical measurement: This refers to methods such as biting, shaking and crunching, usually used by both producers and small traders. These empirical measurements are both indirect and subjective.

Direct methods are considered to offer true measurements of moisture content and are used to calibrate more practical and faster indirect methods. Direct methods are mostly devoted to research purposes because it requires special equipment (e.g. an oven and analytical balance), and measurements can only be applied in laboratories

Direct measurements

Different methods are used to remove all the water except chemically bound water: heating in an oven, use of microwaves or infrared radiation. For food grains, a reference method has been established and moisture content may be expressed on wet or dry basis. According to Lewis (1987), moisture content MC on wet basis is given by eqn. (2.4).

$$M_{wd} = 100 * \frac{W_e}{W_{d+w_e}} \qquad (2.4)$$

While the moisture content on a dry basis is given as:

$$M_{db} = 100 * \frac{W_e}{W_d} \qquad (2.5)$$

Where; M_{wd} is the moisture content (wet basis), M_{db} is the moisture content (dry basis), W_d is the mass of dry sample and W_e is the mass of wet sample

2.3.2 Effect of moisture content on engineering properties

Biological materials especially food are hygroscopic and absorb moisture under humid conditions until they reach equilibrium with their surroundings. A range of moisture content exists within which optimal performance is attained during processing and storage.

Consequently, the effect of moisture content on the physical, mechanical and thermal properties of the crops is of significance in the designof handling, processing and storage equipment.

Water content is not a thermo-physical property but considerably influences all engineering properties of food and biological materials. If the food is a living commodity, such as fruits and vegetables, its water content will change with maturity, cultivars, stage of growth, and harvest and storage conditions. Values of most thermo-physical properties can be computed directly from the water content (Stroshine & Hamann, 1995). The quantity of moisture in agricultural materials and food product greatly influence the properties such as size and shape, density, force-deformation characteristics, thermal conductivity and heat capacity.

2.3.3 Moisture ratio (M_R)

This is the ratio of the moisture content (kg/kg dry matter) at any given time to the initial moisture content (kg/kg dry matter) (Both relative to the equilibrium moisture content). It can be calculated as in eqn. (2.6) as reported by (Manoj et al., 2012)

$$\mathbf{M_R} = \frac{\mathbf{m_t} - \mathbf{m_e}}{\mathbf{m_o} - \mathbf{m_e}} \qquad (2.6)$$

Where,

M_t – Moisture content of drying sample at any time (%, dry basis)

Me – Equilibrium moisture content (%, db)

Mo – Initial moisture content (%, db)

2.3.4 Drying rate period

Drying curves typically display four defined regions or periods. Not all products will display all four, sometimes only one will appear and although the definition of each period is clear it may be hard to determine in practice. Many agricultural products do not display typical drying curves resulting from lack of constant drying time (Erbay & Icier, 2010). The various drying periods are presented below and displayed in Fig. 2.4,

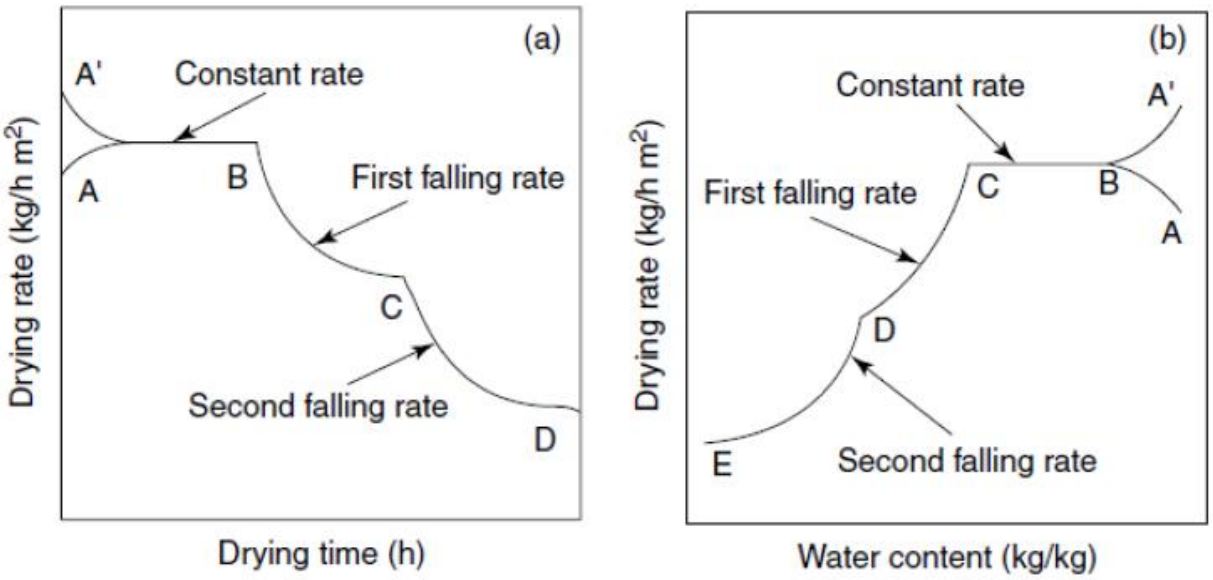

Figure 2.4: A typical drying curve

Source: https://moisturecontrol.weebly.com/drying-curve.html. Retrieved February 21, 2019

2.3.5 Initial drying period

There is often an initial drying rate where the drying rate increases as the surface of the produce is heated to the temperature of the immediate ambient air. A sufficient temperature gradient is required between the air and the product's initial temperature to vaporize the moisture (Singh & Heldman., 2009).

2.3.6 Constant rate period

After the initial period, the curves display a constant drying rate through limited time. During the constant rate period, the surface of the product still contains free moisture, which is vaporized, diffused into the air and taken away by the air (Singh & Heldman., 2009). The rate is controlled by the diffusion process for water removed from the surface and into the air (Menon & Mujumdar., 1987). Critical moisture content (MCcr) is defined as the moisture content at the end in the very last instant of the constant rate period (Menon & Mujumdar., 1987).

2.3.7 First falling drying rate period

Though a general "falling rate" period is normally described, it is due to two different phenomena, which occasionally can be seen evidently by a change in the rate of change of the drying rate. These are called the first and second falling rates. Some products only display one or the other. The falling rate as a whole is described as the time from the critical moisture content until the equilibrium moisture content. Equilibrium moisture content is the point at which the moisture vapour pressure in the solid is equal to the partial pressure of the vapour in the air (Menon & Mujumdar., 1987). During the first falling rate period, moisture must be transferred from within the solid to the surface (modelled as capillary flow) (Menon & Mujumdar., 1987). This is caused by the gradient between the air vapourisation pressure and the vapour vapourisation pressure at the surface (Singh & Heldman., 2009). This continues until the surface film of liquid is entirely evaporated.

2.3.8 Second falling drying rate period

The second falling rate starts when the drying process is controlled by the rate at which moisture can move through the solid. The two possibilities that could be the limiter are the material heat

conduction rate and the material mass diffusion rate. Some other factors come into play in this period – shrinkage may cause internal pressures or case hardening can occur, both of which hinder the drying process. This continues until the product reaches the equilibrium moisture content for the prevailing conditions (Menon & Mujumdar., 1987). Though there are mathematical descriptions available to attempt to describe this period, they often are simplified and depend on geometry (for which only highly simple cases are solved). Cheng, (2009) describes the time for the falling rate for an infinite plate, sphere and cylinder if the diffusion of the moisture is modelled with Crank's basic solution of diffusion, though each situation needs a unique solution based on geometry. But even this contains errors which are presumed to be due to the isothermal assumption.

2.3.9 Moisture diffusivity

The moisture diffusivity of a sample is calculated using eqn. (2.7) (Manoj et al., 2012)

$$\frac{\delta m}{\delta t} = Dm\Delta^2 \qquad (2.7)$$

Where Dm is moisture diffusivity. The solution of the eqn.(2.7) can be used to estimate the diffusivity by converting the solution into a linear relationship between the logarithm of moisture ratio and time. The slope of the plot is represented by constant B in eqn. (2.8) and hence the moisture diffusivity can be determined.

$$LnM_R = A + Bt \qquad (2.8)$$

Where, $A = \frac{8}{\pi^2}$ and $B = [(\pi^2 D_{eff}/L^2)]$ and D_{eff} is the effective diffusivity.

2.3.10 Diffusivity coefficient and activation energy

The diffusion coefficient (Do), is calculated by considering that the Dm changes with drying temperature (T) as an Arrhenius function expressed in eqn. (2.9) (Ndukwu et al., 2010)

$$D_m = D_o \exp\left(-\frac{Ae}{R(T+273.15)}\right) \quad (2.9)$$

Dm is the moisture diffusivity, Ae is the activation energy for moisture diffusion, R is the gas constant, and T is the temperature of drying in degree C. The gradient and the intercept of the Dm plot against T are used to determine the values Ae and Do in Eqn. (2.9).

2.4 Psychrometry of drying

Psychrometry is defined as the study of the thermodynamic properties of moist air and the use of these properties to investigate conditions and processes involving moist air. It is the science of drying. The properties of temperature, humidity, vapor pressure and dew point are measured to estimate air conditions in the structure. While the principles of psychrometry relate to any physical system consisting of gas-vapor mixtures, the most common system of interest is the mixture of water vapor and air, because of its application in heating, ventilating and air conditioning and meteorology.. In human expressions, our thermal comfort is in large part a result of not just the temperature of the surrounding air, but (because we cool ourselves via perspiration) the degree to which that air is saturated with water vapor.

Many substances are hygroscopic, which means that they attract water, usually in proportion to the relative humidity or above a critical relative humidity. Examples of such substances are cotton, paper, cellulose, other wood products, sugar, calcium oxide and many chemicals and fertilizers. Various industries that use these materials are concerned with relative humidity control in production and storage of such materials.

In industrial applications, manufacturers usually try to achieve an optimum between low relative humidity, which increases the drying rate, and energy usage, which decreases as exhaust relative humidity increases. In many industrial applications, it is necessary to avoid condensation that would spoil products or cause corrosion. Molds and fungi can be controlled by keeping relative humidity low.

2.4.1 Psychrometric properties

i. The wet-bulb temperature

This is the temperature reached by a water surface, such as that registered by a thermometer bulb surrounded by a wet cloth, when exposed to air passing over it. The cloth and therefore the thermometer bulb decrease in temperature below the dry-bulb temperature until the rate of heat transfer from the warmer air to the cloth is just equal to the rate of heat transfer required to provide for the evaporation of water from the cloth (wick) into the air stream.

ii. Dry-bulb temperature

The dry-bulb temperature is the temperature indicated by a thermometer exposed to the air in an area protected from direct solar radiation. The term dry-bulb is usually added to temperature to differentiate it from wet-bulb and dew point temperature. In meteorology and psychrometrics the word temperature by itself without a prefix usually means dry-bulb temperature. Technically, it isthe temperature registered by the dry-bulb thermometer of a psychrometer. The name implies that the sensing bulb or element is in fact dry.

iii. Dew point temperature

It is defined as the temperature at which the vapour changes into liquid (condensation). Usually, the level at which water vapor changes into liquid marks the base of the cloud in the atmosphere hence called condensation level. So the temperature value that allows this process (condensation) to take place is called the 'dew point temperature'. A simplified definition is the temperature at which the water vapour turns into dew.

2.4.1 Psychrometric ratio

The psychrometric ratio is the ratio of the heat transfer coefficient to the product of mass transfer coefficient and humid heat at a wetted surface. It may be evaluated with eqn. (2.10).

$$r = \frac{h_c}{h_m c_s} \tag{2.10}$$

where:

r = Psychrometric ratio, dimensionless

h_c = convective heat transfer coefficient, W m^{-2} K^{-1}

h_m = convective mass transfer coefficient, kg m^{-2} s^{-1}

c_s = humid heat, J kg^{-1} K^{-1}

The psychrometric ratio is an important property in the area of psychrometry, as it relates the absolute humidity and saturation humidity to the difference between the dry bulb temperature and the adiabatic saturation temperature.

Mixtures of air and water vapor are the most common systems encountered in psychrometry. The psychrometric ratio of air-water vapor mixtures is approximately one, which means that the difference between the adiabatic saturation temperature and wet bulb temperature of air-water vapor mixtures is small. This property of air-water vapor systems simplifies drying and cooling calculations often performed using psychrometric relationships.

2.4.3 Heat transfer in drying

The rates of drying are generally determined by the rates at which heat can be transferred to the water or to the ice in order to provide the latent heats, nonetheless, under some circumstances, the rate of mass transfer (removal of the water) can be limiting. All three of the mechanisms by which heat is transferred: conduction, radiation and convection may enter into drying. The relative importance of the mechanisms differs from one drying process to another and very often one method of heat transfer predominates to such an extent that it governs the whole process. As an example, in air drying, the rate of heat transfer is given by eqn. (2.11):

$$q = h_s A(T_a - T_s) \tag{2.11}$$

where q is the heat transfer rate in J s^{-1}, h_s is the surface heat-transfer coefficient in J m^{-2} s^{-1} °C^{-1}, A is the area through which heat flow is taking place, m^2, T_a is the air temperature and T_s is the temperature of the surface which is drying, °C.

For example, in a roller dryer where moist material is spread over the surface of a heated drum, heat transfer occurs by conduction from the drum to the foodstuff, so that the equation is given as eqn. (2.12)

$$q = UA\ (T_i - T_s) \tag{2.12}$$

Where U is the overall heat-transfer coefficient, T_i is the drum temperature (usually very close to that of the steam), T_s is the surface temperature of the food (boiling point of water or slightly above) and A is the area of drying surface on the drum. The value of U can be calculated from the conductivity of the drum material and of the layer of foodstuff. Values of U have been quoted as high as 1800 J m^{-2} s^{-1} °C^{-1} under very good conditions and down to about 60 J m^{-2} s^{-1} °C^{-1} under poor conditions.

In a situation where considerable quantities of heat are transferred by radiation, it should be remembered that the surface temperature of the food may be greater than the air temperature. Estimates of surface temperature can be made using the relationships developed for radiant heat transfer though the actual effect of combined radiation and evaporative cooling is complex. Convection coefficients also can be estimated using the standard equations.

In freeze drying, energy must be conveyed to the surface at which sublimation occurs. However, it must be supplied at such a rate as not to increase the temperature at the drying surface above the freezing point. For most freeze drying applications, the heat transfer occurs mainly by conduction. As drying continues, the character of the heat transfer condition changes. Dry material begins to occupy the surface layers and conduction must take place through these dry surface layers which are poor heat conductors so that heat is transferred to the drying region more slowly.

2.4.4 Convective heat and mass transfer coefficient

The most common method of calculating the heat transfer coefficient of most food materials is to combine the heat and the mass transfer coefficients with the Lewis number (Le) as expressed in eqn. (2.13) (Ahromrit &Nemai., 2010)

$$L_e = \frac{h_c}{h_m \rho_a^{\alpha}} \tag{2.13}$$

where: $h_c, h_m, \rho_a^{\alpha}$ and Le are the heat transfer coefficient, mass transfer coefficient, specific heat capacity and Lewis number respectively. The Lewis number (Le) is obtained from eqn. (2.14) (Camargo et al., 2003)

$$L_e = \frac{\Phi}{D_m} \tag{2.14}$$

where Φ is the thermal diffusivity and Dm is moisture diffusivity. The surface mass transfer coefficient is expressed in eqn. (2.15) (Darvishi et al., 2014) as:

$$h_m = \frac{D_m}{d}(2.0 + 0.522\, R_c^{0.5} S_c^{0.33}) \tag{2.15}$$

Where Rc and Sc are Reynold and Schmidt number defined in eqs. (2.16) and (2.17) as:

$$R_e = \frac{v d \rho}{\mu} \tag{2.16}$$

$$S_c = \frac{\mu}{\rho D_m} \tag{2.17}$$

The drying rate is expressed as eqn 2.18 (Manoj et al., 2012);

$$\frac{Dm}{Dt} = \frac{M_i - M_{i+1}}{T_{i+1} - T_i} \tag{2.18}$$

An infinite series solution for Fick's second law of diffusion for un-steady state diffusion which can define the drying rate of a sample slice was used to deduce the moisture diffusivity (Dm).

2.4.5 Analysis of heat and moisture transfer during drying

A complete drying profile comprises of two stages: a constant-rate period and a falling-rate period. It is commonly established that the mechanism of moisture movement within a hygroscopic solid during the falling-rate period could be represented by diffusion phenomenon according to Fick's second law. The governing Fickian equation is exactly in the form of the Fourier equation of heat transfer, in which temperature and thermal diffusivity are substituted with concentration and moisture diffusivity, respectively. Consequently, similar to the case of unsteady heat transfer, one can consider three different situations for the unsteady moisture diffusion, namely, the cases where the Biot number has the following values: Bi $\leq$ 0.1, 0.1< Bi<100, and Bi >100. The first case, corresponding to situations where Bi$\leq$0.1, indicate negligible internal resistance to the moisture diffusivity within the solid object. On the other hand, cases where Bi >100, including negligible surface resistance to the moisture transfer at the solid object, are the most common situation, while cases where 0.1< Bi<100, including the finite internal and surface resistances to the moisture transfer, exist in real applications. The time-dependent heat and moisture transfer equations in Cartesian, cylindrical, and spherical coordinates for an infinite slab, infinite cylinder, and a sphere, respectively, can be written in the following compact form in eqns. (2.19) and (2.20) (Sahin et al., 2002):

$$\left(\frac{1}{y^m}\right)\left(\frac{\partial}{\partial y}\right)\left[y^m\left(\frac{\partial T}{\partial y}\right)\right] = \left(\frac{1}{\alpha}\right)\left(\frac{\partial T}{\partial t}\right) \tag{2.19}$$

For heat transfer and

$$\left(\frac{1}{y^m}\right)\left(\frac{\partial}{\partial y}\right)\left[y^m\left(\frac{m}{\partial y}\right)\right] = \left(\frac{1}{D}\right)\left(\frac{\partial M}{\partial t}\right) \tag{2.20}$$

for moisture transfer, where m=0, 1, and 2 for an infinite slab, infinite cylinder, and a sphere. y=z for an infinite slab, y=r for infinite cylinder and sphere. T represents temperature (°C), M is

moisture content by weight as dry basis (kg/kg), α is thermal diffusivity (m^2/s), D is moisture diffusivity (m^2/s), and t is time (s). The dimensionless temperature (θ) and dimensionless moisture content (φ) can be defined

by eqns. (2.21) and (2.22):

$$\theta = \frac{T - T_1}{T_{a-T_1}} \tag{2.21}$$

$$\varphi = \frac{M - M_e}{M_{i-M_e}} \tag{2.22}$$

where subscripts a, e, and i indicate ambient, equilibrium, and initial conditions, respectively.

2.4.6 Determination of specific energy consumption for drying

The energy consumption for drying in a batch process using the oven and the specific energy consumption are expressed in Eqns.(2.23) and (2.24) (Darvishi et al., 2014).

$$E_c = Av\alpha_a \rho \Delta T D_t \tag{2.23}$$

$$E_s = \frac{E_c}{M_w} \tag{2.24}$$

Where A is the drying tray area (m^2),v is air velocity (m/s), D_t is the total drying time (s), α_a is the specific heat of air (kJ/kg °C) at the D_t, ρ is the density of air (kg/m3), M_w is the mass of water removed from the sample (kg), Ec is the energy consumption (ECD) kWh, and Es is the specific energy consumption SECD (kWh/kg).

2.4.7 Dryer efficiencies

Energy efficiency in drying is of special significance as energy consumption is such a large component of drying costs. Fundamentally, it is a simple ratio of the minimum energy required to the energy actually consumed. But because of the complex relationships of the food, the water, and the drying medium which is often air, a number of efficiency measures can be worked out, each suitable to circumstances and therefore selectable to bring out special features essential in the particular process. Efficiency calculations are beneficial when evaluating the performance of a dryer, looking for improvements, and in making comparisons between the various classes of dryers which may be substitutes for particular drying operation.

Heat has to be supplied to detach the water from the food. The minimum amount of heat that will drive off the required water is that required to supply the latent heat of evaporation, so one measure of efficiency is the ratio of that minimum to the energy actually delivered for the process. Sensible heat can also be added to the minimum as this added heat in the food often cannot be economically recovered.

Another useful measure for air drying is to look at a heat balance over the air, treating the dryer as adiabatic with no exchange of heat with the surroundings. Then the useful heat transferred to the food for its drying corresponds to the drop in temperature in the drying air, and the heat which has to be supplied corresponds to the rise of temperature of the air in the air heater. This adiabatic air-drying efficiency, h, can be defined by eqn. (2.25):

$$\eta_\theta = \frac{T_1 - T_2}{T_{1-T_a}} \qquad (2.25)$$

where T_1 is the inlet (high) air temperature into the dryer, T_2 is the outlet air temperature from the dryer, and T_a is the ambient air temperature. The numerator, the gap between T_1 and T_2, is a major factor in the efficiency.

2.5 Yam

Yam is the collective name for some plant species in the genius *Dioscorea*(family *Dioscoeaceae*) that form edible tubers. It is a perennial herbaceous plant cultivated for the consumption of their starchy tubers in many temperate and tropical world provinces. The tubers themselves are also called "yams", having many cultivar and related species. They are native to Africa, Asia, and the Americas. The palatable tuber has a rough skin hard to peel, but softens after cooking. The skins vary in color from dark brown to light pink. The majority of the vegetable is composed of a much softer material known as the "meat". This material ranges in color from white or yellow to purple or pink in mature yams. Various types of yam are;

2.5.1 Aerial yam

Aerial yam (*Dioscorea bulbifera*) is generally called potato yam or cheeky yam (Ojinnaka, Odimegwu & Ilechukwu., 2016). It is a specie of yam grown all over the world. This bulbils-bearing yam which belongs to the Order *Dioscoreal*, Family *Dioscoreaceae*, and Genus *Dioscorea* is an unpopular specie among the edible yam species. In South-Eastern States in Nigeria it is commonly called “Adu”, Western-Nigeria it is known as “Emina” while in South-South Nigeria it is called “Odu”. It is one of the economically most essential species of yam; it is distinguished from all other species by possessing particular bulbils on the base of leaves petioles (Tewodros, 2008). *They are* members of the Dioscoreaceae family which comprise numerous

varieties found in South Asia and Africa. The tubers are under-utilized and not commercially grown, but are cultivated and consumed among rural inhabitants in parts of Western *Nigeria.*

They are known as air potato, Adun, Odun, Kanduin in some regions of Nigeria though predominantly in the Western and Eastern regions, it is grown for its bulbils and eaten during the famine season (Kayode et. al, 2017). Even though it possesses a characteristic flavour and comparable in nutritional content to the most favorite yam species, it does not possess the same appeal compared to other species of yam. The yam is unpopular; less studied, and received minimal

interest and attention by food processors in Nigeria. The high rate of post-harvest losses of the crop and insufficient method of preservation probably resulted in it's under exploitation as foodstuff and industrial uses. Aerial yam (Fig 2.5) is important to man due to its medical and nutritional benefits.

Figure 2. 5: Aerial Yam

Source: https://www.alamy.com/stock-photo/aerial-tubers.html, retrieved February 25, 2019

i. Medical importance of aerial yam

Aerial yamtuber is a rich source of starch that forms an important dietary supplement (Deb, 2002). Apart from starch, the root tubers of *Dioscorea* species contain protein, fat, fiber and some minerals such as Potassium, Sodium, Phosphorus, Calcium, Magnesium, Copper, Iron, Manganese, Zinc and Sulphur (Deb, 2002). It also has diosgenin, a pharmacologically active component of *Dioscorea* found in root and rhizomes which is one of the most costly and important steroidal drugs used worldwide (Sharma, 2004). Dietary PEs (plant estrogens) of *Dioscorea* can provide a widespread of health benefits including protection against development of cancer, osteoporosis, cardiovascular disease, nephritis, asthma, and diabetes. It is used in the preparation of contraceptives and in the treatment of various genetic disorders (Ayoola et. al., 2008). According to Galani & Patel., (2017), the phytochemical analysis of aerial yam shows that it contains alkaloids, glycosides, protein, fats, steroids, polyphenols, tannins, flavonoid and saponins.

It has been reported that the extraction of constituents from aerial yamusing organicsolvents of little polarity significantly represses the growth of tumor and extends survival of tumor bearing mice and human liver cancer, colon cancer and another tumor cell (Dutta, 2015).

The analgesic and anti-inflammatory properties of aerial yamwere reported by Omodamiro., (2015). According to the report by Omodamiro, (2015), the aqueous and methanol extracts from the dry bulbils of aerial yam L var sativa were evaluated (300 and 600 mg/kg) against pain induced by acetic acid, formalin, pressure and against inflammation induced by carragenaan histamine, serotonin and formalin in experimental animals. The results revealed potent analgesic and anti-inflammatory activities of the extracts which may be due to inhibition of inflammatory mediators such as histamine, serotonin and prostaglandins.

Okigbo et al., (2009) reported the antimicrobial activity of aerial yam. According to the reports, acetone extract, ethyl acetate extract, 95% ethanol extract and methanol extract of aerial yam each indicated a fair antibacterial activity on inhibition of bacterial isolated from animals and poultries using disc method. The acetone extract indicated the most significant anti-bacterial effect when compared to other extract. However, according to the report by Cao et al, (1957), the extract of aerial yam (0.017-0.034mg/ml) was reported to kill DNA virus and inhibit the transcription of RNA virus in direct or indirect inhibitory experiments. From different parts of the ethanol extracts of aerial yam(butanol fraction, ethyl acetate fraction, acetone and ether fraction), the inhibition effect of butanol and ethyl acetate fraction on coxsackie B I-IV virus was better than that of the other two fractions. But their effects on herpes simple virus I were nearly the same. After killing the virus, the cell still could continue to divide and be sub-cultured which was showing that the drug is non-toxic and effective. But the decoction of aerial yam had no inhibitory effect on various types of viruses.

According to Wang et al., (2009), it has been proven that the isolated dihydrodioscorin from aerial yamat 0.1% concentration could inhibit the growth of fungi which could cause disease in several types of plants. However, Vasanthi et al., (2010) reported the cardio-protective activity of aerial yam. In the report, myricetin, epicatechin, isovanilic acid and vanillic acid were shown to be important bioactive components of aerial yam that protects against cardiovascular diseases. Administration of 70% ethanolic extract of aerial yamto rats (150 kg/mg of body weight, 30 days) resulted in significantly improved ventricular performance in terms of aortic flow, left ventricular developed pressure (LVDP) and the first derivative of developed pressure (LV max dp/dt) of aerial yam treated during post ischemic reperfusion. Aerial yam also significantly reduced the size of myocardial infarction by 20 ± 2.64% as compared to the control group.

Cui et al., (2016) investigated the effect of aerial yam on the immune system. In the research, the immune system of mice was studied after oral administration of decoction of aerial yam (1000, 490 and 240 kg/mg body weight) for 15 days. The results showed that the high dose group could considerably suppress the phagocytosis of the mononuclear macrophages. However, the medium dose group markedly enhanced the activities of natural killer cells, the antibody quantity of B cell and the quantity and proliferation of spleen T lymphocytes. This experiment showed that high doses of aerial yamcould suppress the immune function in mice, while medium doses could improve the immune function.

ii. The Nutritional importance of aerial yam

According to Princewill and Ibeji (2015), aerial yam contains not only the vital nutrients like protein, fat, crude fiber they also contain phytochemical (phenol, saponin, oxalate and tannin) which help fight against many human diseases. It is also a good source of minerals such as manganese, iron, potassium and sodium, and contains vitamins A and C which are all necessary for human beings. They have been researched on as, a good source of essential dietary nutrients and a major contribution to the nutrition of West African as a source of carbohydrate, energy, vitamins (especially vitamin C), minerals and protein (Zinash, 2008). Aerial yam has been reported to contain protein in the level of 3.2-13.9% in dry weight (Adejumo, 2013). It also contains other compounds such as peptide, phytochemical, polyphenols etc. which confers healing to the consumer and disease management.

Subhash, et al (2014) reports showed that aerial yam contains crude protein, carbohydrates, crude fiber, and ash content are present with values of 3.4%, 27.51%, 7.50% and 2.94%, respectively

while minerals such as calcium, magnesium, potassium, and phosphorus are also present with values of 0.82, 0.98, 0.53, and 0.38 mg/gm, respectively.

Aerial yam serves as supplement to meals and household income towards poverty mitigation especially at critical moments at the ending and beginning of a year. The nutritional value of aerial yam suggests that it can be fully integrated into the cropping system by farmers in areas where it is found to be adapted (Mbaya, et al., 2013).

iii. Industrial preparation of aerial yam to flour

According to Nwosu (2014), aerial yam can be processed into flour by washing the aerial yam with clean water to remove adhering soil and other undesirable materials. The samples are then sorted, peeled and sliced into sizes of 2 to 3cm in thickness. The resulting sliced sample is soaked in clean water to avoid enzymic browning and also to remove the bitter compound from the sliced samples. The slices are then blanched with hot water at 80^{o}C for 8mins after which the yam slices are transferred into the cabinet oven dryer to dry at 86^{o}C for 4hours. The dried yam slice is milled and screened through a 1mm test sieve to obtain the powdery yam flour.

2.5.2Water yam (*Dioscorea alata)*

Water yam (*Dioscorea alata*), known as purple yam, ube and many other names, is a species of yam, a tuberous root vegetable that originated from South East Asia. It is the species generally spread throughout Asia and the world in general and is second only to white yam in popularity. The shape of the tuber is usually cylindrical but can be extremely variable. It is usually white and "watery" in texture. It seems unnoticed when compared to other varieties of yam and is often considered as food for the poor. It, therefore, plays a very minor role in both local and international yam trade. These misconceptions have contributed to its dwindling popularity in the

country despite its great nutritional and health benefits. Common recipes made from water yam in Nigeria include porridge, yam fritters, pounded yam fufu, yam balls, grated water yams and yam mixed with vegetables. Water yam (Fig 2.6) is important owing to its nutritional and medicinal importance.

Figure 2. 6:Water Yam

Source:https://buzznigeria.com/benefits-water-yam/, retrieved February 25, 2019

i. Nutritional/Medicinal benefits of water yam

Although water yam is different from other yams, it is mucilaginous and so is not that popular for cooking, it is still consumed by many who know not just its nutritional benefits but also its medicinal benefits. It has been established to treat different systemic diseases including hypertension, a condition which may lead to stroke, heart failure, and heart palpitation (Wireko-Manu et al., 2013). Water yam is digested and absorbed slowly by the body and so does not cause blood sugar spike. It is rich in fibre, contains a significant number of antioxidants and vitamin C and helps to suppress blood sugar. Therefore, this makes it suitable for diabetic patients. It also contains a small amount of vitamin E and beta-carotene level (the beta carotene is good for vision, immunity and overall health). The tubers are certainly one of the vegetable-

rich sources that have a lot of minerals, like copper, calcium, potassium, iron and phosphorus. It is a good source of vitamin B6 (Agwu & Avoaja 2012).

According to Wireko-Manu et al., (2013), water yam contains a high level of total dietary fibre (TDF) which makes it appropriate for the management of pile, constipation and diabetes. It is also rich in Vitamin C, beta carotene, vitamin E, calcium, potassium, magnesium, copper and antioxidants. These nutrients are identified to play vital roles in general body upkeep as well as immune functioning, wound healing, suppression of blood sugar, bone growth and anti-ageing. Similarly, according to Agwu and Avoaja (2012), water yam is a good source of vitamin B6 which is needed in the body to breakdown substances called homocysteine which can directly damage blood vessel walls, hence reducing the risk of heart disease. Some other benefits of consuming water yam are (Akissoe et al., 2001):

- It helps to lower blood cholesterol levels.
- It is a good source of female hormone, progesterone, thus it helps to balance female hormones and are good for hormonal imbalance disorder and regulation of menses.
- It decreases blood pressure levels.
- The antioxidants in water yam help to reduce damage by free radicals in the body and slow down the effects of ageing.
- They improve digestive health and help with constipation and irritable bowel syndrome.
- They also have anti-inflammatory properties which help to reduce the risk of chronic diseases.
- It can slow down the ageing process and boost the immune system.
- Vitamin C in water yam helps in wound healing and bone growth.
- It is low in calories so is perfect in weight reduction and management.

- It has been used as worm expeller, laxative and treatment of fever, gonorrhoea, leprosy, and tumors and inflamed haemorrhoid.

ii. Economic importance/ uses of water yam

Tuber is a notable part of the yam plant that has high carbohydrate content (low in fat and protein) and provides a good source of energy. Unpeeled yam has vitamin C. Yam, sweet in flavour, is consumed as boiled yam or fufu or fried in oil and then consumed. Often pounded into a thick paste after boiling and is consumed with soup. Yam can also be processed into flour for use in the making of paste. Its medicinal use as a heart stimulant is attributed to its chemical composition, which consists of alkaloids of saponin and sapogenin. Its use as an industrial starch has also been proven as the quality of some of the species is able to provide as much starch as in cereals (Akissoe et al., 2001).

2.5.3 Yellow yam (*Dioscorea cayenesis*)

Yellow yam *(Dioscorea cayenesis*) derived its common name from its yellow flesh, which is caused by the presence of carotenoids. It is also native to West Africa and is similar to the white yam in appearance. Apart from some morphological, it also has a longer period of vegetation and a shorter dormancy than white yam. This has leaves that are as broad as they are and has cylinder-shaped vines. The prickles where not joined and are long and slender, and cylinder-shaped in cross section, stipules are generally narrow and constricted towards the base. The tuber skin is thick and brittle. This species has a male inflorescence which occurs singly or in pairs, but not in groups(Dumont &Vernier, 2000).

2.5.4 White yam (*Dioscorea rotunda*)

This originated in Africa and is the most generally grown species and is desired by people. It has cylinder-shaped vines with leaves which are long and broad and is typically cultivated in West Indies and the West Africa. The tuber is white and requires about seven months to mature. Tuber is generally thin skinned and the vines twin anti-clockwise. A large number of white yam cultivars occur with differences in their production and post-harvest characteristics(Dumont & Vernier, 2000).

2.5.5 Chinese yam (*Dioscorea esculenta*)

Chinese yam has a vines twin in a clockwise direction and bear alternate, pale green relatively small cordate leaves. The plant produces a bunch of soft sugary tubers at the base of the stem. Tubers are small rounded structures. It matures in about eleven months. The tubers bruise easily and do not store longer before it starts sprouting within a short time (Dumont & Vernier, 2000).

2.5.6 Three-leaf yam (*Dioscorea dumentorum*)

Also called trifoliate yam as a result of its leaves. It originates in Africa where wild cultivars also exist. One noticeable characteristic of this species is the bitter flavour of its tubers. Another undesired characteristic is that the flesh hardens if not cooked soon after harvest. Some wild cultivars are very poisonous. Dumentorum has cylinder-shaped stems with digitate compound leaves of 3, 5, or 7 leaflets. Twining is clockwise. Tubers are bunched and the flesh colour varies from white to creamy white or yellow. Tubers may be bitter and occasionally they are soaked for about three days before being prepared. Tubers reach maturity in about 10 months (Dumont & Vernier, 2000).

2.5.7 Storage of yams

A conservative estimate indicates that about 15 percent of yams produced annually never reach the market, mainly because of post-harvest losses. Losses are due to lack of appropriate storage facilities, a variety of disease, pest and sprouting, even in storage, losses still occur, over one million tons of yam tubers are lost annually in storage in West Africa (Coursey, 1967). Sources of storage losses are rotting, pest respiration and sprouting. Sprouting causes a reduction in the food reserves by translating carbohydrates from the tuber into the sprouts for metabolic processes. There are various methods of yam storage:

i. Scientific methods

Sprouting of *D. rotunda* tuber can be delayed by non-lethal dose of gamma – irradiation (Adesuyi & Mackenzie, 1973). Rotting causes the greatest amount of loss of dry matter in yam storage, it is due mostly to the effects of fungi and bacteria notably Serratia been implicated (Okafor, 1966). To prevent rotting storage, wounding of the tubers during harvesting and handling must be avoided. Curing of yam tubers at 25% and low humidity (55 – 62 percent), for 5 days before storage prevents to a certain degree of storage rot.

Respiration is a serious source of storage loss in yams since harvested tubers are living, they are respiring and the substrate for the respiration is the dry matter which is stored in the tubers. One of the effective ways of reducing respiratory loss is to keep the temperature low, but not below 16^0C.

ii. Traditional methods

Storage of yams by the indigenous peoples of the tropics and subtropics is carried out mostly by traditional methods. These traditional methods which are employed vary from country to country and from region to region. The variations are often related to climate but local natural resources and customs also influence the choice of storage method used. Some traditional methods used by people are:

iii. Burying (clamp) or pit storage

This involves the digging of holes or pit about 1m in diameter in the ground and leaving them with dried leaves and grasses. After selecting good quality yam tubers, they are placed in the pit, alternating each layer of tubers with dried grasses. They are finally covered with a layer of dried grasses and a top layer of soil. This method of yam storage is not very effective due to the lack of sufficient ventilation and the difficulty of inspecting the tubers.

iv. Field storage

Leaving the yams in the field is the simplest method of storage. Tubers are stacked in piles and covered with grasses, sorghum or millet stalks.

v. Barn storage

In the humid areas of West Africa, Yams are often kept in barns. Basically, barns consist of a vertical wooden framework. To this framework, the yam tubers are tied individually by means of tie vines or strings, or they can be laid on simple open work shelving inside the barn.

In some cases, the barns are covered with thatched roofs to protect the tubers from rain and the heat of the sun. Placing yams on the shelves require less time and labour than tying. Shelving

has the advantage that insect infested and rotting yams can be seen easily and removed. The disadvantage with shelving lies in the fact that it is easier for rats to hide amongst the yams. Losses due to delay in some cases can amount to 40 – 50 percent (Olorunda & Adesugi, 1973). Losses can be reduced by protecting the barn from rats by fixing a barrier made of iron sheeting around the barn.

vi. Compound storage

Outside the forest zone, for example in the savanna regions of West Africa, yams can be stored either in the field or in the farm compound. Yams stored in the farm compound are stacked in cribs like those used for maize. The cribs are raised well off the ground with rat guards fitted to the legs.

vii. Cold storage of yam tubers

The application of low temperature storage to yams is limited by the fact that yams are susceptible to low temperature injury at a temperature of 10-12^{0}C or less (Coursey, 1967). The temperature of 16-17^{0}C has been successfully employed to prolong the storage time of yams (Passam, 1977). At 16^{0}C the dormancy and hence the storage life of water yam tubers may be extended by as much as four months, particularly if the tubers are cured prior to storage so as to reduce infection by wound pathogens (Gonzalez & Collazo 1972). The storage of yam tubers at lowered temperature has the advantage of reducing the major sources of storage loss (respiration, sprouting and rotting).

2.5.8 General economic importance of yam

Fresh yam can be eaten fried, boiled, or roasted like potatoes (Wanasundera & Ravindran 1994). Different people prepare yam differently. *Fufu* is prepared from cassava in combination with plantain or cocoyam but in yam producing zones or during the scarcity of plantain and cocoyam, *Fufu* is prepared from boiled yam and cassava. In Benin and Western parts of Nigeria, yam tubers are processed into slightly fermented flour called e*lubo* for a product called *amala*.

Yam tubers can be processed into yam chips and pellets, which are milled to produce yam flour. Mestres *et al*. (2002) reported that there has been an increase in production and marketing of yam chips in Nigeria, Benin, and Togo. In the industry, yam chips can be milled and used for various food products for example biscuit and weaning food. Attempts to manufacture fried yam chips, similar to French fried potatoes have been reported from Puerto Rico and the potential for its production on a commercial level has been highlighted (Abasse, et al., 2003). Yam tubers have also been processed into starch or into poultry and livestock feed just as cassava (Opara, 1999). Yam starch is used in the production of all-purpose adhesives. Producers of cartons, packaging companies, leather and shoes use the adhesives for their products. Recently, several beneficial properties of yams were reported, and the extracts of yam showed antioxidant activity and possessed scavenging properties against free radicals (Farombi, et al., 2000).

2.6 Engineering properties of food crop

General, any attribute that influences the processing or handling of food can be described as an engineering property. The engineering properties of foods are important, if not indispensable, in the process design and manufacture of food products. Most of the engineering properties are

affected by changes in the chemical composition and structural arrangement of foods ranging from the molecular to the macroscopic level. The engineering properties can be classified as:

i. Thermal properties such as specific heat, conductivity, diffusivity, and boiling point rise, freezing point depression.
ii. Mechanical properties such as textural (including strength, compressibility, and deformability) and rheological properties (such as viscosity).
iii. Optical properties, primarily color, gloss and translucency.
iv. Electrical properties, primarily conductivity and permittivity.
v. Structural and geometrical properties such as density, particle size, shape, porosity, surface roughness, and cellularity.
vi. Others, including mass transfer related properties (diffusivity, permeability), surface tension, cloud stability, gelling ability, and radiation absorbance.

2.6.1 Thermal properties of food crop

Most processed and fresh foods receive some type of treatment (heating or cooling) during handling or manufacturing. The design and operation of processes that require heat transfer need special attention due to the heat-sensitivity of the food samples. Thermal properties of foods are associated with the heat transfer control in specified foods and can be categorized as thermodynamic properties (enthalpy and entropy) and heat transport properties (thermal conductivity and thermal diffusivity). The thermo physical properties of foods include the thermodynamic and heat transport properties, physical properties involved in the transfer of heat (freeze and boiling point, mass, density, porosity, and viscosity). These food properties play an

essential role in the design and prediction of heat transfer rates during the handling, processing, canning, storing, and distribution of food products.

The thermal properties of foods can characterize heat transfer mechanisms in different unit operations involving heating or cooling. Specific heat, thermal conductivity, thermal diffusivity, are defined as follows:

2.6.2 Specific heat

This is the quantity of heat needed to raise the temperature of 1kg of material by 1°C. It is the capability of a food product to store heat relative to its ability to conduct (loss or gain) heat. It is strictly depending on how much energy is required and not the rate at which it takes to raise the temperature (Fontana *et al*., 1999). It is dependent on the nature of the process of heat addition, such as a constant pressure process or a constant volume process. The pressure dependence of specific heat for solids and liquids is very small until extremely high pressures are involved. Most of the food processing operations are done at atmospheric pressure (Mohsenin,1980). Therefore, specific heat of food materials is commonly presented at constant pressure. The generally used units are the kJ/ (kg-K), Btu/ (Ib-F) and cal/(g-K). The specific heat of agricultural products is dependent on their moisture content and to a lesser degree on temperature.

An important equation relating specific heat, mass of the sample (M), the quantity of heat that must be added (Q), and the initial and final temperatures of the sample ($T_1$and T_2) may be given by eqn. (2.28)

$$Q = MC_p(T_2 - T_1) \qquad (2.28)$$

2.6.3 Enthalpy

The change in a food's enthalpy can be used to determine the energy that must be added or removed to bring about a temperature change. Above the freezing point, enthalpy comprises of sensible energy; below the freezing point, enthalpy consists of both sensible and latent energy. Enthalpy may be obtained from the definition of constant-pressure specific heat as in eqn. (2.29)

$$c_p = \left(\frac{\partial H}{\partial T}\right)_p \tag{2.29}$$

Where; c_p =is constant pressure specific heat, *H* is enthalpy, and *T* is temperature. Mathematical models for enthalpy may be obtained by integrating expressions of specific heat with respect to temperature.

2.6.4 Thermal conductivity

This is defined as the ability of a material to conduct heat. The significance of thermal conductivity is to predict or control the heat flux in food during processing such as cooking, frying, freezing, sterilization, drying or pasteurization. It is essential in order to ensure the quality of the food product and the efficiency of the equipment. Equation (2.30)s relates the thermal conductivity to the amount of heat that flows through the material per unit of time (dQ/dt), the cross-sectional area of the material through which the heat flows (A), and the temperature difference per unit of length of the conducting material (dT/dx).

$$\frac{dQ}{Dt} = -KA\frac{dT}{dx} \tag{2.30}$$

2.6.5 Thermal diffusivity

This is the ability of products to conduct thermal energy relative to its ability to store thermal energy. It determines how fast heat propagates or diffuses through a material. It helps to evaluate the processing time of canning, heating, cooling, freezing, cooking or frying. Properties like

water content, temperature, composition, and porosity affect thermal diffusivity (Fontana et al., 1999). An object with a higher thermal diffusivity will always heat faster compared to that with a lower thermal diffusivity. Ozişik (1993) reported that the higher the thermal diffusivity, the shorter the time required for the heat to circulate within the solid. It can be estimated indirectly from measured thermal conductivity, density and specific heat. It can also be evaluated from the solution of a one-dimensional steady state heat transfer equation.

The thermal conductivity, thermal diffusivity and specific heat capacity can be measured by several well-established methods (Mohsenin, 1980), however, measuring any three of them would lead to the forth through the relationship in eqn. (2.31)

$$\alpha = \frac{K}{\rho c} \tag{2.31}$$

Where; α is thermal diffusivity, k is thermal conductivity, ρ is density, and c is specific heat. Experimentally determined values of food's thermal diffusivity are scarce. However, thermal diffusivity can be calculated using equation (2.31), with appropriate values of thermal conductivity, specific heat, and density.

2.6.6 Heat of respiration

All living things including living foods respire. During respiration, sugar and oxygen combine to form CO_2, H_2O, and heat as in eqn. (2.32):

$$C_6H_{12}O_6 + 6O_2 \rightarrow 6CO_2 + 6H_2O + 2667KJ \tag{2.32}$$

In most stored plant products, little cell development takes place, and the larger part of respiration energy is released as heat, which must be taken into account when cooling and storing

these living products (Becker et al. 1996a). The rate at which this chemical reaction takes place varies with the type and temperature of the product.

Becker et al. (1996b) developed relationships that connect a commodity's rate of carbon dioxide production to its temperature. Then the rate of carbon dioxide production can be related to the commodity's heat generation rate from respiration. The resulting relationship gives the commodity's respiratory heat generation rate W in W/kg as a function of temperature t in °C as shown in eqn.(2.33)

$$W = \frac{10.7f}{3600}\left[\frac{9t}{5} + 32\right]^{g} \tag{2.33}$$

Where;

f and g are the respiration coefficients for various commodities.

Fruits, vegetables, flowers, bulbs, florists' greens, and nursery stock are storage commodities with substantial heats of respiration. However, dry plant products, such as seeds and nuts, have very low respiration rates. Young, actively growing tissues, such as asparagus, broccoli, and spinach, immature seeds have high rates of respiration. Fast-developing fruits, such as strawberries, raspberries, and blackberries, have much higher respiration rates than fruits that are slow to develop, such as apples, grapes, and citrus fruits. Basically, most vegetables, apart from root crops, have a high initial respiration rate for the first one or two days after harvest. However, within a few days, the respiration rate quickly lowers to the equilibrium rate (Ryall & Lipton 1972).

2.6.7 Mechanical properties of food crops

These are properties connected with the behaviour of agricultural materials under applied forces. The study of mechanical properties is necessary for texture analysis and a better understanding of product quality. Compressive and other engineering properties are required in the design of machines and the analysis of the behavior of the food sample during unit operations such as drying, cleaning, sorting, crushing and milling (Akaaimo & Raji, 2006). Force-deformation testing of agricultural materials can also be used to study damage which arises during harvesting and handling of the products. The knowledge of the behavior of a particular agricultural product from testing or from test data improves the evaluation of its engineering design. One most important consideration in engineering design is to ensure that stresses in components do not surpass the strength of agricultural materials. Damages done to agricultural products during harvesting, handling and transportation can decrease their structural integrity (Mohsenin, 1986). The amount of force necessary to produce a given amount of deformation depends on many factors including the rate at which the force is applied, the previous history of loading, moisture content and the composition of the product (Bahnasawy, 2007).

These factors play vital roles when the qualitative evaluation of the grain's hardness is required during size reduction operations. A number of scholars have investigated the mechanical properties of different agricultural materials and food products. Wang *et al.* (2004) reviewed the firmness detection by excitation dynamic characteristics for peach and observed that impact orientation, detected orientation, impact velocity and impact material did not considerably affect the dominant frequency. Some of the mechanical properties of food crops are:

i. Force deformation characteristics

Agricultural products and food materials deform in response to applied forces. The nature of these responses varies extensively among different materials. The uniaxial compression method

is the most popular technique used for compression tests to determine force deformation characteristics. This method involves trimming of the agricultural produce into a precise geometry to facilitate the measurement of the various forces.

ii. Stress-Strain

According to Stroshine and Hamann (1995) compression test may be conducted on a food sample at different moisture content levels using the Instron Universal Testing Machine (IUTM) controlled by a micro-computer. The sphericity of the test sample and the linear dimensions are measured before the compression test. During the compressive test, the food sample to be tested is placed laterally or axially on the table or platform and compression is done with a motion probe at a constant speed until the specimen is fractured. The data acquisition system produces rupture load and displacement automatically during the compression. The load-displacement curve is used to derive the compressive properties of food samples such as seeds. The maximum compressive load, the load at which the sample fractures is estimated by the ratio of peak load of the displacement curve. Treating the seed as a sphere, the maximum compressive stress, strain, and crushing energy are determined using eqns. (2.34) and (2.35):

$$\delta_{max} = \frac{P_{max}}{dL} \tag{2.34}$$

$$E_c = \frac{P}{2} \text{ x } \Delta D \tag{2.35}$$

δ_{max} is the maximum compressive stress in MPa, P_{max} is the maximum load in N, d is the mean diameter in mm, and L is the mean length in mm, ΔD is the displacement interval in mm, E_c is the crushing energy in J.

iii. Modulus of elasticity

It is defined as the ratio of the stress applied to the strain produced. It could be referred to as the stress required in producing a unit amount of elastic strain (Gupta, 2006). For food and engineering materials, the relationship between stress and strain in the linear region of the stress-strain curve is described using the modulus of elasticity while in the case of biological materials, the apparent modulus of elasticity where stress and strain relationship is nonlinear is used.

iv. Shrinkage

This is defined as the reduction in volume or geometric dimensions during processing operations. When post-processing volume is larger than initial volume, it is called expansion. Two types of shrinkage: isotropic and anisotropic, are usually observed in the case of food products. Isotropic shrinkage is described as the uniform shrinkage of the materials or food samples under all geometric dimensions, whereas anisotropic (or non-uniform) shrinkage develops in different geometric dimensions. The former is common in fruits and vegetables while the latter is usually in animal tissue, such as in fish. Shrinkage occurs due to moisture loss (during drying), ice formation (during freezing), and formation of pores (by drying, puffing, extrusion, and frying). The glass transition theory is one of the conceptions proposed to explain the process of shrinkage, collapse, fissuring, and cracking during material drying. The methods of freeze-drying and hot-air drying can be compared based on this theory.

v. Optical properties of food crops

These are those food properties resulting from physical phenomena occurring when any form of light interacts with the material under consideration. In foods, the foremost optical property considered by consumers in evaluating quality is color, followed by gloss and translucency or

turbidity among other properties. “Color” is the common name applied to all sensations arising from the activity of the retina, and is related to visual appearance of food (shape, size, surface and flesh structure, and defects). Optical properties are related to consumer decision on food appearance and produce some kind of visual effect. Among these, color, gloss and translucency can be defined as follows:

vi. Gloss

This is the name given to light specularly reflected from a plain smooth surface. It can be defined by a goniophotometric curve that usually represents the intensity of light reflected at the surface at different angles of incidence and viewing.

vii. Color

Color is basically a beam of light composed of irregularly dispersed energy emitted at different wavelengths. Depending on the type of illumination, the same material can indicate different light qualities and produce different sensations. Food samples, along with other materials, have color properties, which depend entirely on their composition and structure.

viii. Translucency

This is usually defined using an opaque-to-transparent scale. In liquid food materials, light passing through changes its path randomly (scattered) when interacting with suspended particles. Although light can be transmitted or reflected, the human eye only experiences translucency as a sensory feature distinct from color. Many food materials are neither fully opaque nor fully transparent, but are translucent.

2.6.8 Electrical properties of food crops

The two main electrical properties in food engineering are electrical conductivity and electrical permittivity. Electrical properties are necessary when processing foods involving electric fields, electric current conduction, or heating through electromagnetic waves. These properties are also valuable in the detection of processing conditions or the quality of foods. They are;

i. Electrical conductivity

Electrical conductivity is a measure of how well electric current flows through food of unit cross-sectional area A, unit length L, and resistance R. It is the inverse value of electrical resistivity (a measure of resistance to electric flow) and is expressed in SI unit's S/m in the following relation:

$$\sigma = \mathrm{L}/(\mathrm{AR}) \tag{2.36}$$

ii. Electrical permittivity

This is a dielectric property used to explain the interactions of food materials with electric fields. It describes the interaction of electromagnetic waves with matter and defines the charge density under an electric field. In solids, liquid, and gases the permittivity depends on two values:

- The dielectric constant ε', related to the capacitance of a substance and its ability to store electrical energy; and
- The dielectric loss factor ε", related to energy losses when the food is subjected to an alternating electrical field (i.e., dielectric relaxation and ionic conduction).

The electrical conductivity of foods has been found to rise with temperature (linearly), and with water and ionic content. Mathematical relationships have been developed to predict the electrical conductivity of foods, e.g. for modeling heating rates through electrical conductivity

measurements, or for probability distribution of conductivity through liquid-particle mixtures. It shows different behaviors during ohmic and convective heating. At freezing temperatures, electrical conductivity increases with temperature rise, as ice conducts less well than water. Starch transitions and cell structural changes influence electrical conductivity, and fat content decreases conductivity. As seen in thermal properties, the porosity of the food plays a significant role in the conduction of electrons through the food.

2.7 Water activity

Water activity is a measurement of the availability of water for biological reactions and activities. It determines the capability of micro-organisms to grow. If water activity decreases, the growth of micro-organisms will also decrease. Water activity (a_w) is expressed as the ratio of the vapour pressure in a food (P) to the vapour pressure of pure water (P_0) as shown in eqn. (2.37). It predicts whether water is likely to move from the food product into the cells of micro-organisms that may be present.

$$a_w = P/P_o \tag{2.37}$$

For instance, a water activity of 0.90 means the vapour pressure is 90 per cent of that of pure water. Water activity increases as temperature increases due to changes in the properties of water such as the solubility of solutes (salt and sugar), or the state of the food. Most foods have a water activity above 0.95 and that will provide sufficient moisture to support the growth of bacteria, yeasts, and mold. The amount of available moisture can be decreased to a point that will inhibit the growth of microorganisms. Water activity (a_w) has its utmost application in predicting the growth of bacteria, yeast, and mold. For a food material to have a useful shelf-life without relying on refrigerated storage, it is essential to control either its acidity level (pH) or the level of

water activity (a_w) or a suitable combination of the two. This can efficiently increase the product's stability and make it possible to predict its shelf life under known ambient storage conditions. Food can be made safe to store by decreasing the water activity to a point that will not allow pathogens such as *Clostridium botulinum* and *Staphylococcus aureus* to grow in it.

Knowledge of water activity of food materials is essential when preparing a hazard analysis critical control plan (HACCP). The moisture condition of food materials can be measured as the equilibrium relative humidity (ERH) expressed in percentage or as the water activity expressed as a decimal.

2.7.1 Critical factors affecting water activity

The critical factors that affect water activity are;

- **Drying:** Water activity is decreased by physically removing water.
- **Solutes:** Water activity is decreased by adding solutes such as salt or sugar.
- **Freezing:** Water activity is decreased by freezing (e.g water is removed in the form of ice).
- **Combination:** One or more of the above can be combined for a greater influence on water activity (e.g: salting and drying fish).

Importance of water activity.

The importance of water activity includes:

- Water activity (α_w) is one of the most important factors in determining the quality and safety of foods.

- Water activity affects the shelf life, safety, texture, flavor, and smell of food materials.
- While temperature, pH and several other factors can influence if and how fast organisms will grow in a sample, water activity may be the most significant factor in controlling spoilage.
- Most bacteria do not grow at water activities below 0.91, and most molds cease to grow at water activities below 0.80.
- By measuring water activity, it is possible to predict which microorganisms will and will not be potential sources of spoilage.
- It determines the lower limit of available water for microbial growth. It also plays an important role in determining the activity of enzymes and vitamins in foods and can have a major impact on their color, taste, and aroma.

2.8 Thermal transport modelling

Basically, heat is transferred by three mechanisms: conduction through solids or stationary liquids or gases, convection through flowing fluids, and radiation. However, for conduction and convection, the rate of heat transfer is proportional to the temperature difference, while for radiation it is the difference between the fourth powers of the temperatures. For food materials where conduction is the sole mechanism of heat transfer the temperature profile may be estimated from the partial differential equation:

$$\rho C_p = \nabla(\lambda \nabla T) \tag{2.38}$$

The solution of this equation requires knowledge of the spatial variation, and temperature dependence of the thermal conductivity, λ, the density, ρ, and the specific heat, C_p, of the product. At the edges of the solid or food material, different boundary conditions may apply. The

simplest is constant temperature; however, a heat transfer boundary condition is often essential, in which the flux to the surface is given by a convective heat transfer coefficient, or by radiation. The overall rate of heating of a solid will be dependent on the consecutive processes; heat must move to the product and then within it. The relationship between external and internal thermal transport can be estimated using the Biot number in eqn. 2.39:

$$Bi = \frac{hd}{\lambda} \tag{2.39}$$

Where h is the interfacial heat transfer coefficient and d some characteristic dimension of the body being heated. The higher the Biot number, the greater is the effect of heat transfer coefficient. In practice, a Bi > 10 implies that the slowest heat transfer process will be conduction within the solid particle. For a low Biot number (<0.1) the process is controlled externally, with the solid essentially isothermal. The heating of fluids is more complex because of fluid motion so that both thermal and fluid transport equations must be solved. The solution of the Navier- Stokes equation is required for the flow field. Simplified equation sets are mostly used; for example, in a tubular geometry the partial differential equations describing the heat and momentum transport are (Bird et al., 1964):

Equation of continuity:

$$\frac{1}{r}\frac{\partial}{\partial r}(rv) + \frac{\partial u}{\partial z} = 0 \tag{2.40}$$

Equation of motion:

$$\rho\left(v\frac{\partial u}{\partial r} + u\frac{\partial u}{\partial z}\right) = -\frac{\partial P}{\partial z} + \frac{1}{r}\frac{\partial}{r\,\partial}\left(ru\left(\frac{\partial v}{\partial z} + \frac{\partial u}{\partial r}\right)\right) + 2\frac{\partial}{\partial z}\left(u\frac{\partial u}{\partial z}\right) \tag{2.41}$$

$$\rho\left(v\frac{\partial v}{\partial r} + u\frac{\partial v}{\partial z}\right) = -\frac{\partial P}{\partial r} + \frac{2\,\partial}{r\,\partial}\left(ru\frac{\partial v}{\partial r}\right) + \frac{\partial}{\partial z}\left(\mu\left(\frac{\partial v}{\partial r} + \frac{\partial u}{\partial z}\right)\right) \tag{2.42}$$

$$\rho C_p \left(v \frac{\partial T}{\partial r} + u \frac{\partial T}{\partial z} \right) = \lambda \left\{ \frac{1}{r} \frac{\partial}{\partial r} \left(\frac{\partial T}{\partial r} + \frac{\partial^2}{\partial z^2} \right) \right\} \quad (2.43)$$

The assumptions used in deriving these equations are:

- that the flow is axisymmetric
- there is negligible thermal generation by viscous dissipation
- the effects of natural convection are also negligible
- the liquid is homogeneous
- Constant density, specific heat and thermal conductivity.

The types of boundary conditions generally applied are: for both velocity and temperature, a known profile at the inlet of the heater, with a known temperature profile at the wall of the heater and cooler, with a no-slip boundary for the velocity. In the case where a holding tube is used an adiabatic boundary condition is applied at the wall.

2.9 Blanching

Food quality can be measured by chemical analysis (for instance vitamin C retention) but can also be estimated visually. For yam, browning can be a problem that makes the materials less appealing. Browning in yam is principally caused by the activity of the enzyme polyphenol oxidase (PPO), which catalyzes the reaction between oxygen in the air and phenolic compounds in the product (Akissoe et al. 2005). When yam is cut and the surface is exposed to oxygen in the air, it browns. This type of browning can be stopped by blanching; putting the product in hot water for a short period of time to inactivate the enzyme. It is a common practice before the drying of yam (Akissoe et al. 2005). Vitamin C as an antioxidant can prevent enzymatic browning for some time by inhibiting PPO activity (Evans et al. 2013). This simply means that the valuable vitamin C is used far before it enters the human body, and is lost. It has been

revealed that a blanched product after storage contains more vitamin C than without blanching, despite the degradation of vitamin C due to the heat treatment (Kadam et al. 2005). Blanching should be considered as a way to improve vitamin C and reduce browning of dried or otherwise processed yam.

2.10 Shelf life

Shelf life is the recommended maximum time for which food samples or fresh (harvested) produce can be stored, during which the defined quality of a specified proportion of the goods remains acceptable under expected (or specified) conditions of distribution, storage and display. Shelf life is dependent on the degradation mechanism of the specific product. Most can be influenced by several factors: exposure to light, heat, moisture, transmission of gases, mechanical stresses, and contamination by things such as micro-organisms. Food product quality is often mathematically modelled around a parameter (concentration of a chemical compound, a microbiological index, or moisture content).

2.11 Finite element method

The finite element method (FEM) is a numerical method used to perform finite element analysis (FEA) of any given physical phenomenon. It is required to use mathematics to comprehensively understand and quantify any physical phenomena, such as structural or fluid behavior, thermal transport, wave propagation, and the growth of biological cells. Most of these processes are described using partial differential equations (PDEs). However, for a computer to solve these PDEs, numerical methods have been developed over the last few years and one of the most prominent today is the finite element method.

The principle of minimization of energy forms the principal backbone of the finite element method. In other words, when a particular boundary condition is applied to a body, this can lead to a number of configurations but yet only one particular configuration is realistically possible. Even when the simulation is performed several times, same results prevail. This is governed by the principle of minimization of energy which states that when a boundary condition (like displacement or force) is applied, of the numerous possible configurations that the body can take, only that configuration where the total energy is minimum is the one that is taken (Ajah 2018).

2.11.1 Application of finite element method

The finite element method has a significant promise in the modeling of several mechanical applications related to aerospace and civil engineering. One of the most exciting prospects of finite element method is its application in coupled problems such as fluid-structure interaction, thermo-mechanical, thermo-chemical, thermo-chemo-mechanical problems, biomechanics, biomedical engineering, piezoelectric, ferroelectric, and electromagnetics (Ajah 2018).

2.11.2 Types of finite element method

The traditional FEM technology has revealed shortcomings in modeling problems related to fluid mechanics and wave propagation. Numerous improvements have been made recently to improve the solution process and extend the applicability of finite element analysis to a wide range of problems. Some of the important FEM still in use include:

i. Extended finite element method (XFEM)

Bubnov-Galerkin method entails continuity of displacement across elements. Although problems like contact, fracture, and damage involve discontinuities and jumps that cannot be directly handled by the FEM. To overcome this shortcoming, XFEM was developed in the 1990s. XFEM works through the principle of expansion of the shape functions with Heaviside step functions. Extra degrees of freedom are usually assigned to the nodes around the point of discontinuity so that the jumps can be considered (Ajah 2018).

ii. Generalized finite element method (GFEM)

GFEM was developed around the same time as XFEM in the ’90s. It combines the features of the traditional FEM and meshless methods. Shape functions are primarily defined by the global coordinates and further multiplied by partition-of-unity to create local elemental shape functions. One of the foremost advantages of GFEM is the prevention of re-meshing around singularities (Ajah 2018).

iii. Mixed finite element method

In several problems, like contact or incompressibility, constraints are imposed using Lagrange multipliers. These extra degrees of freedom emanating from Lagrange multipliers are solved independently. The system of equations is solved like a coupled system of equations(Ajah 2018).

iv. The h-method finite element

The h-method usually improves results by using a finer mesh of the same type of element. This method refers to reducing the characteristic length (h) of elements, dividing each existing element into two or more elements without altering the type(s) of elements used (Paul 2016).

v. The p-Finite element method

The p-method improves results by employing the same mesh but increasing the displacement field accuracy in each element used. This method refers to increasing the degree of the highest complete polynomial (p) within an element without altering the number of elements used.

The difference between the h and p-methods lies in how these elements are treated. The h-method employs many simple elements, whereas the p-method uses few complex elements (Paul 2016).

vi. hp-Finite element method

This is a combination of automatic mesh refinement (h-refinement) and an increase in the order of polynomial (p-refinement). This is not the same as doing h- and p- refinements differently. When automatic hp-refinement is employed, and an element is divided into smaller elements (h-refinement), each element can have different polynomial orders as well(Ajah 2018).

vii. Discontinuous Galerkin finite element method (DG-FEM)

DG-FEM has shown important promise for utilizing the idea of finite elements to solve hyperbolic equations, where traditional finite element techniques have been weak. In addition, it has also shown improvements in bending and incompressible problems which are usually observed in most material processes. Here, additional constraints are added to the weak form that

includes a penalty parameter (to prevent interpenetration) and terms for other equilibrium of stresses between the elements (Ajah 2018).

2.11.3 Two-dimensional finite element modelling of food sample drying

Among the numerous numerical methods available in simulation study, two dimensional methods have been generally applied to model heat and mass transfer; the finite difference method and the finite element method. When using Galerkin's method to solve the problem, the weight function (shape function) must be multiplied by the remainder function. The general form of the equation is given by eqn. (2.44)

$$\int_a^b N_i(x)R(x, a_1, a_2, \ldots . a_a)dx = 0 \tag{2.44}$$

The integral on the domain can be divided into M integrals on the element, whose sum also equals the integral as in eqn. (2.45):

$$\sum_{a=1}^{m} N_i(x)R^a\left(x_i T_i T_j\right)dx = 0 \tag{2.45}$$

Numerical simulation of drying process is normally carried out with the assumption that the distribution of moisture and temperature in different zones of the part is uniform. Fick's law of diffusion can be used to model the moisture movement within the drying sample. The general form of the law can be written as eqn. (2.46)

$$\frac{\partial \mathrm{m}}{\partial \mathrm{t}} = \mathrm{D}\left(\frac{\partial^2 \mathrm{m}}{\partial \mathrm{x}^2} + \frac{\partial^2 \mathrm{m}}{\partial \mathrm{y}^2} + \frac{\partial^2 \mathrm{m}}{\partial \mathrm{z}^2}\right) \tag{2.46}$$

This diffusion equation is applied to describe the three-dimensional movement of moisture (M) in a slice of food materials or sample in the Cartesian coordinates with constant diffusivity (D). Therefore, the heat transfer equation can be written as eqn. (2.47).

$$\frac{\partial T}{\partial t} = \alpha\left(\frac{\partial^2 T}{\partial x^2} + \frac{\partial^2 T}{\partial y^2} + \frac{\partial^2 T}{\partial z^2}\right) \tag{2.47}$$

By generalization, the mass transfer problem can be converted to a heat transfer problem. With this approach and using the moisture diffusion coefficient obtained experimentally, the problem can be tackled. To determine the moisture diffusivity, Fick's law is usually applied to a sliced sample with thickness of L. The analytical solution of this equation can then be written as eqn. (2.48).

$$\frac{M - M_e}{M_s - M_e} = 1 - \frac{8}{\pi^2 \exp\left(-\pi D t / L^2\right)} \tag{2.48}$$

2.12 Thermal gravimetric analysis (TGA)

TGA is a method of thermal analysis in which the mass of the food samples is measured against time or temperature while the temperature of the samples is programmed in a controlled atmosphere. This analytical method is normally employed in determining the composition of samples and predicting their thermal stability. From TGA analysis, we can provide information about chemical phenomena and physical phenomena, including chemisorption, dehydration, decomposition, solid-gas reactions (e.g., oxidation or reduction), vaporization, sublimation, absorption, and desorption. In essence, TGA can assess the samples that exhibit weight loss or gain owing to decomposition, oxidation, or dehydration.

Typical applications of TGA include:

- Determining thermal stability: If a material (foods) is thermally stable, there will be no observed mass change.
- Determining oxidative stability: Oxidative mass losses are the most common observable losses in TGA. Thus, it is very essential to analyze the resistance to oxidation in copper alloys.
- Compositional analysis: Temperature and weight change of decomposition reactions can allow quantitative composition analysis.
- Determination of the purity of a mineral, inorganic compound, or organic material.
- Measuring the weight of fiberglass and inorganic fill materials in laminates, plastics, paints and composite materials. s
- Determining water/carbon content or other residual solvents in a material.
- Allowing analysis of reactions with air, oxygen, or other reactive gases.
- Enhancing product formulation processes or ensuring product safety.

2.13 Response surface methodology

Response Surface Methodology (RSM) is a collection of statistical and mathematical techniques useful for developing, improving, and optimizing processes. The most extensive applications of RSM are in particular circumstances where several input variables potentially influence some performance measure or quality characteristic of the process. Thus, performance measure or quality characteristic is called the response. The input variables are at times called independent variables, and they are subject to the control of the scientist or engineer. The field of response surface methodology consists of the experimental strategy for exploring the space of the process or independent variables, empirical statistical modeling to develop a suitable approximating

relationship between the yield and the process variables, and optimization methods for finding the values of the process variables that produce desirable values of the response.

To develop an appropriate approximating model between the response

Y and independent variables $\xi_1 \xi_2 \ldots\ldots \xi_k$

In general, the relationship is:

$$y = f(\xi_1 \xi_2 \ldots\ldots \xi_k) + \varepsilon \quad (2.49)$$

where the form of the true response function f is unknown and perhaps very complicated, and ε is a term that represents other sources of variability not

accounted for in f. Usually, ε includes effects such as measurement error on the response, background noise, the effect of other variables, and so on. Usually, ε is treated as a statistical error, often assuming it to have a normal

distribution with mean zero and variance σ^2. Then

$$E(y) = \eta = E[\xi_1 \xi_2 \ldots\ldots \xi_k)] + E(\varepsilon) = f(\xi_1 \xi_2 \ldots\ldots \xi_k); \quad (2.50)$$

Equation (2.56) is usually called the natural variables, since they are expressed in the natural units of measurement, such as degrees Celsius, pounds per square inch, etc. In much RSM work, it is convenient to transform the natural variables to coded variables $x_1 x_2 \ldots x_k$, which are usually defined to be dimensionless with mean zero and the same standard deviation. In terms of the coded variables, the response function (eqn. 2.50) will be written as

$$\boldsymbol{\eta} = \mathbf{f}(x_1 x_2 \ldots x_k) \quad (2.51)$$

For the case of two independent variables, the first-order model in terms of the coded variables is;

$$\eta = \beta_0 + \beta_1 x_1 + \beta_2 x_2; \quad (2.52)$$

The form of the first-order model in Equation (2.52) is sometimes called a

main effects model, because it includes only the main effects of the two variables $x_1$and x_2. If there is an interaction between these variables, it can be added to the model easily as follows:

$$\eta = \beta_0 + \beta_1 x_1 + \beta_2 x_2 + \beta_{12} x_2 x_2 \quad (2.53)$$

This is the first-order model with interaction. Adding the interaction term introduces curvature into the response function.

For the case of two variables, the second-order model is given by eqn. 2.54,

$$\eta = \beta_0 + \beta_1 x_1 + \beta_2 x_2 + \beta_{11} x_1^2 + \beta_{22} x_2^2 + \beta_{12} x_1 x_2 \quad (2.54)$$

Sobukola et al., (2010) studied the optimization of pre-fry drying of yam slices using response surface methodology. In his study, response surface methodology technique was employed to develop models for the responses as a result of variation in levels of drying temperature (60–80^{o}C), and drying time (1–5°min). The result showed that the response surface regression analysis was significant ($P < 0.05$) and correlated with drying temperature. The optimal drying condition observed was a drying temperature of 70–75C for about 3–4 min. However, Aneke et al., (2018) used response surface methodology to investigate the effects of temperature, thickness and time on the drying of water yam slices and to determine the optimum conditions for hot air drying. It was observed that falling rate drying regime was predominant. Experiments were

performed at air temperature of 60, 70 and 80^{o}C, slice thickness of 4, 6 and 8mm and drying times of 60, 165 and 270 min. The optimum conditions for water yam drying were found to be 70^{o}C, 74.9^{o}C, slice thickness 6mm, 6.6mm and drying time 165, 116.1min. for untreated and treated water yam respectively. The predicted responses for drying rate were 0.000345kg/m2s, 0.000358kg/m2s respectively.

Lihua et al, (2014) worked on optimization of hot air drying of purple sweet potato using response surface methodology. The optimization factors considered were slice thickness (2-6mm), air velocity(1-2m/s) and temperature(45-55^{o}C. The best values of factors were found to be slice thickness of 5.11mm with air velocity of 1.88m/s and temperature of 55^{o}C.

2.14. Review of related works

2.14.1 Review of related work on aerial yam drying

Sanful et al., (2015) investigated the air drying characteristics of aerial yam in a fabricated air dryer within a temperature range of 50 to 70°C. Before drying, the sample was divided into two portions; one part was blanched at 100°C for 20 min and the other part was left unblanched. The drying data were fitted to twelve well-known thin layer drying models. Amongst the models used, the Midilli *et al.*,Verma *et al*., Diffusion Approach, Wang and Singh, Parabolic and Simplified Fick's Diffusion models were found to be the best models to predict the moisture ratio values during the drying process with high capability. The effective moisture diffusivity was found to vary between the range of 1.401 ×10-10 m^2/s to 6.720 x 10-10 m^2/s for the unblanched yam slabs and 7.223 x 10-11 m^2/s and 2.306 x 10-10 m^2/s for the blanched yam slabs over the temperature range of 50 to 70°C. The activation energy values were 28.42kJ/mol, 30.33kJ/mol for the unblanched yam samples of thicknesses of 0.5cm and 1cm respectively,

whereas that for blanched yam were 6.77kJ/mol and 15.37kJ/mol for slabs of 1cm and 0.5cm thicknesses respectively.

Sanful et al., (2013) studied the effects of pre-treatment and drying on the functional properties of the aerial yam. In the study, aerial yam flourwas got by subjecting the yam to diverse processing methods (grating, steaming and boiling) oven/solar drying, milling and sieving. The resulting flours were evaluated for their functional composition. Between these two drying methods, the flour samples had functional properties ranging from 200.41 to 303% water binding capacity, 14.82 to 22.01% solubility, 9.34 to 10.09% swelling index and pH varying between 5.90 and 7.25%. However, Kayode et al., (2017) examined the physicochemical properties of processed aerial yam and sensory properties of paste (amala) prepared with cassava flour. This was done by washing, sorting, peeling, slicing and blanching the aerial yam in hot water at 80ºC for 10min. The blanched yam samples were divided into four portions. The first two portions were fermented for 48hr and sun (BFSUD) and solar (BFSOD) dried. The other two blanched portions were also sun (BSUD) and solar (BSOD) dried respectively. The dried sliced samples were milled, sieved and used for proximate, functional and phytochemical analysis. Proximate composition of aerial yam flour was found to be as follows; moisture content (7.66-10.60%), total ash (0.05-1.76%), crude protein (4.42-5.07%), crude fibre (0.56-0.69%), crude fat (3.42-3.82%), and carbohydrate (79.28-82.37%). The phytochemical constituent included alkaloid, steroids, saponin and fl avonoid. The bulk density, water absorption capacity and dispersibility all fall within the range of 0.52-0.54g/ml, 56.50-66.00g/g and 4.47-5.75% respectively.

Jacques et al., (2016), studied the physicochemical properties and anti-nutritional factors of aerial yam flour. The samples were analyzed for proximate composition, mineral, organic acid content and levels of anti-nutritional factors by standard analytical methods. The moisture

content of the yam flour was 6.22 ± 0.87 % dw. The aerial yam (cultivar yellow) had low fat (2.36± 0.87 % dw), protein (8.12 ± 0.02% dw) ash (3.44± 0.05% dw) and cellulose (0.91 ± 0.08% dw) but higher levels of carbohydrate (79.86± 0.09% dw) and energy (373.16 kcal/100g). The most predominant mineral was potassium (847mg/100g). The major organic acids were oxalic acid (486 ± 0.03 mg/100g) and citric acid (365.4 ± 0.5 mg/100g). The result revealed that the high anti-nutritional factors (total phenol 558 ± 3.46 mg/100g, oxalate 320 ± 2.65 mg/100g, phytate 469.33 ± 2.08 mg/100g) could pose a serious problem to human health.

Ayo et al., (2018) worked on the proximate, functional properties and phytochemical composition of pre-treated aerial yam flour. This was done by dividing the aerial yam sample into four equal parts and pre-treating differently (roasting, boiling, soaking), while the fourth part not treated served as control. Some quality evaluation such as proximate, functional properties and phytochemical composition were carried out. The results showed that the roasted-dried aerial yam flour had the highest values for crude fibre (1.82%) and carbohydrate (80.07%). The roasted-dried sample had the highest values in loose bulk density, water absorption capacity and swelling capacity (0.50 g/cm3, 4.91 g/cm3 and 1.34 g/cm3, respectively), while the soaked-dried sample has the highest values for packed bulk density and emulsion stability with values of 0.5647 g/cm3 and 0.56 g/cm3, respectively. The soaked sample showed the highest value for peak and trough (148.13 and 142.92 RVU, respectively), while roasted sample showed highest values for breakdown, final viscosity and set back (7.21, 186.00 and 45.08 RVU, respectively).

Afiukwa and Igwe., (2015) evaluated and compared the nutritional and antinutritional profiles of aerial and underground tubers ofair potato. The result revealed that Oxalate, tannins and phenols were significantly higher in the underground tubers while the bulbils were richer in alkaloids,

HCN saponins and flavonoids. It also indicated the presence of some mineral elements such as K, Na, Ca, Mg, Fe, Zn, Cu, P and Mn and the absence of heavy metals like Cd, Pb, Cr, Ni, Se and Co.

However, Ogbuagu (2008) investigated the Nutritive and Anti-Nutritive Composition of the Wild (In-Edible) Species of aerial yam and *Dioscorea dumentorum* (Bitter Yam). The evaluation of the nutritive and anti-nutritive principles in the uncooked and cooked wild species of aerial yamand *Dioscorea dumentorum* revealed that the wild yams contain all the food nutrients within the reported and acceptable values for root and tuber crops. The result further revealed that cooking of these yam species decreased the concentration of oxalate, alkaloids and tannins to values that may earn the wild yams consideration as food for human consumption.

2.14.2 Review of related works on water yam drying

Oko and Famurewa., (2014) investigated five commonly cultivated varieties of water yam *(D. purpurea*, *D. atropurpurea*, *D. liliopsida* (purple yam), *D. vilgaris,* and *D. villosa)* to estimate the proximate, mineral and starch characteristics. The results indicated that the varieties have moisture content 9.20-10.30%, ash content 2.48-3.53%, fiber content 3.31-3.53%, fat content 1.62-2.41%, protein content 8.40-10.46%, and carbohydrate content 70.88-73.90%. The result further revealed significant differences ($P<.05$) in the proximate compositions within the varieties. The ranges of minerals in mg per kg (dry weight) were Na 16.38- 24.84, K 97.78-141.14, Ca 79.99-269.75, Mg 18.55-31.53, P 114.65-211.63, Fe 15.18-30.86. The results showed that the protein and fiber contents of *water yam* varieties estimated in the study were high. It was

however concluded that the yam varieties are good sources of protein nutrient and suitable staple food for the diabetics.

Ramiro et al., (2012) investigated the evaluation of the kinetics and the drying conditions of two yam varieties (*Dioscorea alata* 9506-021 and *Dioscorea alata* 9506-027) at the temperature range of 40 to 70 °C and the air speed of 0.7 m s^{-1}. The experimental data were fitted appropriately to Fick, Page, and Logarithmic models. Mass transfer in the yam slices was described by using Fick's diffusion model, which was the best fitted model. The result showed that the drying occurred mostly in the decline phase. Arrhenius described appropriately the dependency of the moisture diffusivity with temperature. Amongst the temperature range evaluated, moisture diffusivities varied from 1.70 x 10^{-9} to 6.84 x 10^{-10} m^2/s and 1.33 x 10^{-9} to 6.30 x 10^{-10} m^2/s for the D. alata 9506-21 and 9506-27, respectively. The drying activation energy for D. alata 9506-21 and 9506-27 varied from 23.19 to 25.72, and 16.03 to 17.82 kJ/mol, respectively.

Ogidi et al., (2017) worked on the evaluation of some nutritional properties of fourteen water yam cultivars. The investigation revealed that moisture content ranged from 76.08% to 55.10% with a mean value of 63.03%, ash from 3.54% to 0.34% and mean result 1.81%, protein from 9.87% to 4.54% with the mean 7.89%, lipid from 1.86% to 0.86% with an average of 1.46%, fibre from 4.64% to 1.66% and mean 2.60%, dry matter from 44.90% to 23..92% and mean 36.97%, carbohydrate from 88.22mg/100g to 80.71mg/100g, average value of 86.17mg/100g. The result also revealed the presence of K, Na, Ca, Mg, Fe, Zn, Cu, P and Mn in a significant amount.

Uyigue and Achadu, (2018) examined the measurement and modeling of the thin layer drying properties of water yam and white yam assisted by hot-water blanching. The yam samples were blanched at 70 and 80 ^{o}C at varied cooking time of 5, 10 and 15 mins using method of cook and shock and thereafter dried in a hot air oven dryer operating at constant air velocity of 4 m/s and at two oven drying temperatures:30 and 50 ^{o}C each for 6 hr drying period. The results obtained indicated that the drying curves of the sliced yam samples followed the falling rate period and that the moisture ratio, moisture absorption capacity and effective diffusivity of the blanched sliced yam samples were highly enhanced relative to the not-blanched. Optimum blanching condition for the sliced yam samples was recommended for 70 ^{o}C at 5 mins. The Wang and Singh model and the Logarithmic model were also found to be more accurate drying models for fitting the drying properties of blanched sliced yam samples dried at 30 and 50 ^{o}C respectively.

2.14.3 Review of related works on other agricultural product

Adesola, (2017) studied the kinetics of gelatinized white yam (*Dioscorea rotundata*, Poir) during convective drying. He used a convective dryer at a temperature of 40, 50, 60 and 70^{o}C to dry a gelatinized white yam cubes, having a moisture content of 196% dry basis. The drying data obtained were fitted to five thin layer drying model and the goodness of fit of the models were calculated by comparing the percent mean relative deviation modulus (E%), RMSE, χ 2 and R^2 between their experimental and predicted moisture ratio. The result showed that there was no constant rate period throughout the whole drying period as drying took place entirely through a falling rate period. The effect of temperature was more evident than that of relative humidity. The Binomial approximation of Fick's diffusion equation gave the best fit to the drying data as the highest values of R^2 and the lowest values of, χ 2 and RMSE were consistently obtained with the Binomial model equation.

Fatima et al., (2017) investigated solar energy dryer kinetics using flat-plate finned collector and forced convention for potato drying. The research was aimed at obtaining the drying kinetics model of potato using indirect solar dryer (ISD) with flat plate-finned collector and forced convention, and the result then compared to open sun drying method (OSD). The findings revealed that the best result was obtained from the sample size of 1 cm thickness using ISD method with an average drying rate of 0.018 kg H_2O per kg dry-weight.hour and the water content was constant at 5.01% in 21 hours of drying time. The result also revealed page model to be the best model. The result showed that better quality potato drying was achieved using ISD.

Ajala., et al., (2012) worked on the drying characteristics and mathematical modelling of cassava chips. Cassava chips with dimension 5x2x0.4cm were dried at 60^0C, 70^0C and 80^0C in a laboratory tunnel dryer. Kinetics of drying was studied using Fick's second law. Drying pattern was seen to be in the falling rate period. The experimental data were fitted to non-linear regression analysis and the coefficient of determination was found to be greater than 0.97 for all the models. The values of R^2, RMSE, MBE and reduced chi-square showed that Logarithm model best described the drying behaviour of the samples. The activation energy value was found to be 30kJ/mol.

Gharehbeglou et al (2014) carried out an investigation on the drying process of turnip and drying rate curves at different temperatures (55, 70 and 85°C) with air flow rate of 1.5 m/s. The data were fitted into Newton, Page, Modified Page, Henderson and Pabis, Logarithmic, Two-term, Two-term exponential, Wang and Singh, Simplified Fick's diffusion, Modified Page –II, Verma, Midilli–Kucuk, Hii, Law and Cloke, Approximation of diffusion, Modified Henderson and Pabis models. The result showed that the effective diffusivity varied between 5.471×10^{-10} and 8.966×10^{-10} in the range of (55°C to 85°C). The value of activation energy was found to be

16.013 kJ/mol. Modified Henderson and Pabis in 85°C and Hii, Law and Cloke in 55°C and 70°C with highest R^2 and lowest MBE, $\chi 2$ and RMSE were selected to better describe the drying curves.

Meenakshi et al (2014) performed an **e**xperimental study to determine the drying characteristics of pea pods in a laboratory scale tray dryer at a constant air velocity of 0.5m/s and temperature of 70°C. The results indicated that maximum drying took place in the falling rate period. Three different thin layer drying models were compared with respect to their coefficient of determination (R^2). The reduced chi-square and root mean square error (RMSE) was selected to better estimate the drying curves. The entire models showed a good fit to the drying data. However, the Page model showed a better fit to the experiment data among other models.

Olabinjo et al (2017) conducted an experiment on thin layer drying characteristics of fermented cocoa beans in open sun and indirect natural convection solar dryer. The drying curves obtained from the experimental data were fitted to thirteen different thin layer mathematical models. The various models were compared based on three evaluation parameters (R^2, RMSE and χ^2). The results showed that increasing drying air temperature resulted to shorter drying times. The Vermal et al. model was found to be the most suitable for describing the drying curve of the convective indirect solar drying process of cocoa beans with R^2 = 0.9562, χ^2=0.0069 and RMSE=0.0067; while, the Midilli and Kucuk model, best described the drying curve of fermented cocoa beans under open sun with R^2 = 0.9866, χ^2=0.0024 and RMSE=0.0023.

Amin et al., (2011) investigated thin-layer drying kinetics of tomato in a pilot scale convective dryer at 40, 60, and 80ºC and at three relative humidity of 20%, 40% and 60% and constant air velocity of 2.0 m/s. Different thin layer drying models were fitted to experimental data. The high values of coefficient of determination and the low values of reduced sum square errors and root

mean square error indicated that the Midilli et al. model could adequately describe the drying curve of tomato at the three different relative humidity with R^2, SSE and RMSE value of 0.9997, 0.22662, 0.0040912; 0.99946, 0.46702, 0.0051192; and 0.99952, 0.438982, 0.0050188 for 20%, 40% and 60% relative humidity, respectively.

Olawale and Omole., (2012) carried out a study on thin layer drying of sweet potato slices in three different dimensions and between 50^{o}C and 80^{o}C in tray dryer using hot air at a flow rate of 2.5 m/s and 10% relative humidity. Eight thin-layer drying kinetic models were evaluated on blanched and unblanched sweet potato slices presented in three different dimensions. The drying rate was observed to decrease with thickness and mass of sample at a constant drying temperature. Similarly, the drying rate was found to increase with temperature and the blanched slices dried faster than unblanched slices. The eight models investigated fitted the experimental data of the six sweet potato samples between 50^{o}C and 80^{o}C adequately. However, Page model was found to be the best for all the samples.

Masud Alam et al., (2014) carried out a study on the kinetics of drying of summer onion. Drying was done in a mechanical dryer at constant air flow using blanched and unblanched onion with variable temperature (52, 60 and 68^{0}C) and thickness (3, 5 and 7 mm). The result indicated that drying rate increased with increase of temperature and decreased with the increase in thickness in both the blanched and unblanched onion. Blanched onion showed higher drying rate than unblanched onion. The influence of temperature on diffusion co-efficient follows an Arrhenius type relationship. The activation energy for the diffusion of water was found to be 5.781 Kcal/g-mole for unblanched and 2.46 Kcal/g-mole for blanched onion.

Ndukwu and Nwabuisi (2011) investigated the drying kinetics of cocoyam corm slice with heated and unheated air. Two thin layer drying equations were used to investigate the drying kinetics of cocoyam corm slice with heated and unheated air. The result revealed that the drying process followed a falling rate period. The entire tested equations showed high R^2 value with low $\chi 2$ and RMSE error with Lewis equation showing a lower $\chi 2$ and RSME value at the same temperature than Henderson and Parbis equation. The R^2 values of the two models ranged from 0.98 - 0.99, the $\chi 2$ value ranged from 0.00130 – 0.01553 while the RMSE ranged from 0.10188-0.3524, for the sun drying. The effective diffusivity value ranged from 1.4977×10^{-9} to $1.4021 \times 10^{-8} m^2/s$. These values of effective diffusivity were found to increase with temperature.

Leonell (2017) carried out a study on the drying kinetics of sweet potato chips in a forced convection tray-type dryer. The experimental conditions are temperatures of the drying air (40, 50 and 60 °C), air blower velocity (14.336 m/sec, 15.724 m/sec, and 17.212 m/sec), and slice thickness of 1.5 mm. the experimental data were fitted to five thin layers drying. The quality of the models fit was evaluated using the determination correlation coefficient (R^2), the reduced chi-square ($\chi 2$) and the root mean square error (RMSE). The result showed that all the drying process occurred in the falling rate period. Among the models considered, the Page and Modified models were the most adequate in describing the drying processes of sweet potato chips under the experimental conditions studied with R^2 above 0.99616. However, both Henderson and Diffusion models gave comparatively higher R^2 values in all cases considered, whereas the $\chi 2$ and RMSE values were lower; the highest value of R^2 (0.99974) and the lowest values of $\chi 2$ (0.000020) and RMSE (0.004242) were observed for 15.724 m/sec velocity and drying air temperature of 40°C. Thus, these models may be assumed to describe the drying behavior of sweet potato chips in a forced convection tray-type dryer within the experimental study range.

Afolabi et al., (2015) investigated the effect of pretreatment and drying temperature on the drying kinetics and quality of cocoyam. In the study, cocoyam slices were pretreated by water blanching (WB) and soaking in sodium metabisulphite (SM) and dried in a hot air oven at temperatures of 50, 60 and 70 °C while untreated samples were sun dried. The experimental data were fitted into exponential, generalized exponential, Page, logarithmic, parabolic, Wang and Singh and two-term models and selection was done based on model with highest correlation coefficient (R^2), and lowest reduced chi-square (χ^2), sum square error (SSE) and root mean square error (RMSE) respectively. The Logarithmic and Parabolic model was found to best describe the oven and sun drying of cocoyam respectively.

Jafari et al., (2016) carried out investigation onmodeling the drying kinetics of green bell pepper in a heat pump assisted fluidized bed dryer. In this research, green bell pepper was dried in a pilot plant fluidized bed dryerequipped with a heat pump humidifier using three temperatures of 40, 50 and60 ^{o}C and two airflow velocities of 2 and 3 m/s in constant air moisture. Threemodeling (nonlinear regression technique, fuzzy logic andartificial neural networks) were applied to investigate drying kinetics for thesample. Midilli model with R^2= 0.9998 and rootmean square error (RMSE) = 0.00451 showed the best fit with experimental data among the models investigated.Feed-forward-back-propagation network with Levenberg–Marquardt trainingalgorithm, hyperbolic tangent sigmoid transfer function, training cycle of 1,000 epoch and 2-5-1 topology, deserving R^2 = 0.99828 and mean square error (MSE) = 5.5E-05, was determined as the best neural model. Overall, neural networks method was much more precise than two other methods in prediction of drying kinetics and control of drying parameters for green bell pepper.

Ronoh et al., (2010) investigated thin layer drying kinetics of amaranth (*Amaranthus cruentus*) grains in a natural convection solar tent dryer. This was carried out on a drying rack having two layers; top and bottom. The ambient temperature and relative humidity ranged from 22.6–30.4^{o}C and 25–52%, respectively, while the inside temperature and relative humidity in the solar dryer ranged from 31.2–54.7^{o}C and 22–34%, respectively. A non-linear regression analysis was employed to evaluate six thin layer drying models (Newton, Page, Modified Page, Henderson & Pabis, Logarithmic and Wang & Singh) for amaranth grains. The results showed that drying of amaranth grains was best described by the Page model satisfactorily with R^2 of 0.9980, $\chi 2$ of 0.00016 and RMSE of 0.01175 for bottom layer and R^2 of 0.9996, $\chi 2$ of 0.00003 and RMSE of 0.00550 for top layer of the drying rack. The water transport during dehydration was described by applying the Fick's diffusion model. The effective moisture diffusivity for solar tent drying of amaranth grains was found to be 5.88×10^{-12} m^2/s at the bottom layer and 6.20×10^{-12} m^2/s at the top layer. High temperatures developed at the top layer of the dryer resulted in high effective moisture diffusivity and this showed that temperature strongly influences the mechanism of moisture removal from the grains.

Umar et al., (2015) studied the effect of blanching treatment (98 °C for 3 and 6 min) and air-drying temperature of 40, 50 and 60 °C on the thin layer drying characteristics such as drying time, drying rate constant, effective moisture diffusivity and activation energy, as well as on anthocyanin content of black carrot shreds. They observed that the drying temperature affected the drying rate but blanching did not have an effect on drying time. The drying data were fitted to Page, Lewis and Henderson-Pabis models. The goodness of these models was determined based on the coefficient of determination (R^2), root mean square error, reduced chi-square ($\chi 2$) and standard error. Page model was found to best describe the experimental data. The activation

energy of 37.5, 26.0 and 34.6 kJ/(mol·K) of the control samples and samples blanched for 3 and 6 min respectively was determined from the Arrhenius plot.

Nwajinka, Okpala and Benjamine, (2014) worked on the thin layer drying characteristics of cocoyam corm slices using hot air convective dryer. The experiment was carried out at five different drying temperatures of 65, 70, 75, 80 and 85ºC, at air velocity of 2 m/s with relative humidity of 50, 40, 39.5, 33.8 and 22.2% respectively. The data were fitted to Newton, Page, Henderson and Pabis and Logarithmic models. The drying kinetic parameters were found to be best described by Logarithmic model with high values of coefficient of determination of 0.973, 0.988, 0.991, 0.999 and 0.99. The moisture diffusivities result varied from 2.53 x 10–5 m2/s to 1.09 x 10–5 m2/s.

2.14.4 Summary of the literature review and research gap

Review of literature shows that there was scanty work on the drying of water yam and aerial yam using hot air dryer and solar dryer. The literature also revealed that determination of the engineering properties of both water yam and aerial yam has not been reported. Equally, instrumental analysis such as scanning electron microscopy (SEM), thermo-gravimetric analysis (TGA) and Fourier transform Infra-Red (FTIR) on these yams have not been reported. Detailed work on the kinetics and drying characteristics of the two yam species have not been reported. Only Aneke et al, (2018) carried out optimization of hot air drying of water yam using RSM, but no work has been reportedon aerial yam. To the best of the knowledge of the researcher, no work has beenreported on the sensory test and numerical finite element analysis of both water yam and aerial yam.

Therefore, in this research, detailed work on drying kinetics and characteristics, thermal treatment, engineering properties, sensory test analysis, proximate analysis, phytochemicals analysis, instrumental analysis, finite element modelling and optimization of the drying process of the yams will be studied.

CHAPTER THREE

MATERIALS AND METHODS

3.1. Material collection and preparation

3.1.1. Collection and preparation of aerial yam and water yam sample

The aerial yam sample was sourced from Afor Opi market in Nsukka local government area of Enugu state, while the water yam was sourced from Eke Awka market, Awka Anambra state. The aerial yam and water yam were identified in the Crop Science Department of Nnamdi Azikiwe University, Awka. The yams (Figs. 3.1a and 3.1b) were washed with clean water and spread in open air to avoid spoilage. The water yam was peeled and cut into desired size while the aerial yam was cut without peeling because peeling tends to remove the mesocarp of the yam which is known to be medicinal.

Fig.3.1a Aerial Yam

Fig.3.1b Water yam

3.2 Instrumentation characterization

The instrumental analyses in this work were done at the Department of Chemical Engineering laboratory, Ahmadu Bello University, Zaria Kaduna state.

i. The functional groups present in the sample was determined using a Fourier transform infra-red (FTIR) machine, Cary 630 model from Agilent Technologies,U.S.A.

ii. The surface morphology of the sample was analyzed by scanning electron microscopy (SEM) machine, ProX model from Phenom World,Eindhoven Netherlands.

iii. The thermal stability of the sample was analyzed using Thermo Gravimetric Analysis (TGA) machine, TGA 4000 model from PerkinElmer.

3.3 Moisture content determination

The determination of the moisture content was carried out by the oven method in accordance with AOAC (2000) at a temperature of 103^{o}C for 10 hours at the Department of Chemical

Engineering laboratory, Nnamdi Azikiwe University Awka. Equation 3.1 was employed for moisture content determination of both water yam and aerial yam.

$$\chi = \frac{M_1 - M_2}{M_1} \, x \, 100 = M_{db} \qquad (3.1)$$

Where; χ is the moisture content of the sample after drying.M_1 is the initial mass before drying and M_2 is the mass after oven drying.

For any weight of the sample at any time, the moisture content at that weight was determined from eqn. (3.2), (Onu, et al., 2017).

$$M_{t(db)} = M_o(db) - \left(\frac{100(W_o - W_t)}{(1 - M_{o(wb)})W_o}\right) \qquad (3.2)$$

Where; $M_{t(db)}$ = Moisture content at any time %(db), M_o (db) = initial moisture content % (db), M_o(wb) = initial moisture content % (wb), W_t = weight of sample at any time, g and W_o = initial weight of sample, g

3.3.1Convective hot-air drying

The convective hot air dryer (Fig 3.2) is made up of an oven-like body consisting of blower (for air circulation), heating element (for heat supply), airspeed regulator, thermocouple, temperature control knob and trays. Hot air is forced through the material with the help of fan or blower and which aid the moisture diffusion process that results in the drying. This experiment was carried out at the Chemical Engineering laboratory, Nnamdi Azikiwe University Awka. The method employed in convective hot air drying was according to Daniel et al., (2017). The two samples (Water yam and Aerial yam) were dried with convective hot-air dryer (Fig. 3.2) at the following conditions: temperature (40, 50, 60 and 70^{o}C), air speed (2.0, 2.5, 3.0, 3.5 and 4.0 m/s) and

sample thickness (2.0, 4.0 and 6.0mm). 2.0 mm of the samples was cut and 100g each of the samples weighed with an electronic weighing scale (Model TDUB-63V09, from Netzgerat) into the dryer tray. The temperature and air speed of the dryer was set at 40^{o}C and 2.0 m/s, respectively. The losses in weight of the samples were taken at an interval of 5, 10, 20, 30, 60, 90 mins. and so on, until there was no significant change in the weight of the sample. The experiments were repeated for various temperatures while keeping air speed and thickness constant and thereafter repeated for various air speeds with temperature and slice thickness kept constant. Also, the thicknesses of the samples were varied with temperature and air speed kept constant. The moisture contents of the sample at time t, was calculated using equation (3.1).

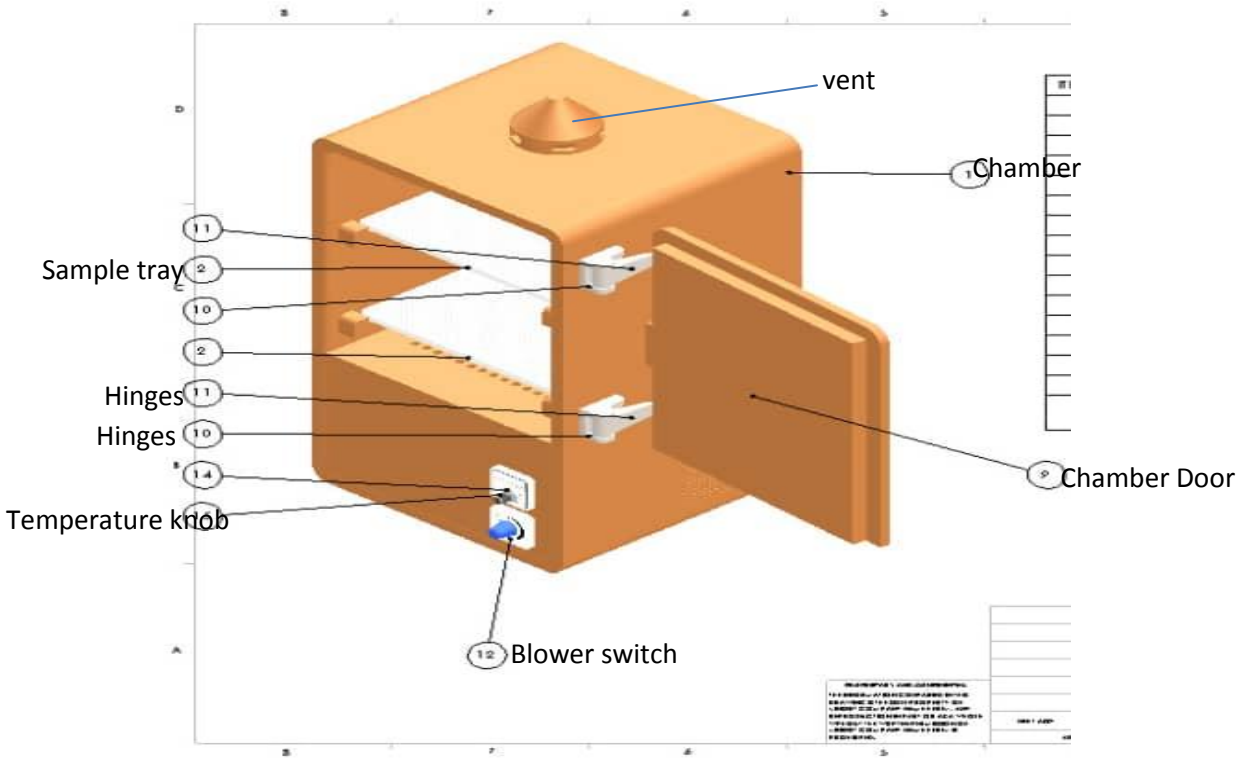

Fig 3.2: A Schematic diagram of convective hot air dryer used

3.3.2 Solar Drying

The solar dryer (Fig 3.3) is made up of drying chamber, trays, concentrator, fan or blower, vents, and metal supports. The airflow into the dryer can be generated by forcing preheated air into the drying chamber with the help of the attached fan or blower. This experiment was carried out at the Chemical Engineering laboratory, Nnamdi Azikiwe University Awka. Following Fauziah et al., (2013) methods, the experiments were conducted at five different airspeed (0.5, 1.0, 1.5, 2.0 and 2.5m/s), and three different sample thickness (2, 4 and 6mm). The samples (water yam and Aerial yam) were cut to different sizes (2, 4 and 6mm), and 100g each of the samples weighed with electronic weighing scale (Model TDUB-63V09, from Netzgerat) and placed into the drying tray. The airspeed was set at 0.5m/s using anemometer. The loss in weight was recorded at an interval of 5, 10, 20, 30, 60, and 90 mins. until there was no significant change in weight of the samples. Hygro-thermometer (Model TH029) was used to measure the wet and dry bulb temperatures of the surrounding as well as the relative humidity of the surrounding. The experiments were repeated for different speed of fan and sizes of samples. The solar radiation of the surroundings at the department of Chemical Engineering laboeratory, Nnamdi Azikiwe University, Awka, was taken using a radiometer (Model *QED-100*)between the hours of 8AM-4PM on 1^{st}, 10^{th}, 15^{th}, 20^{th} and 28^{th} of the months examined.The moisture contents of the sample at time, t was calculated usingequation(3. 2).

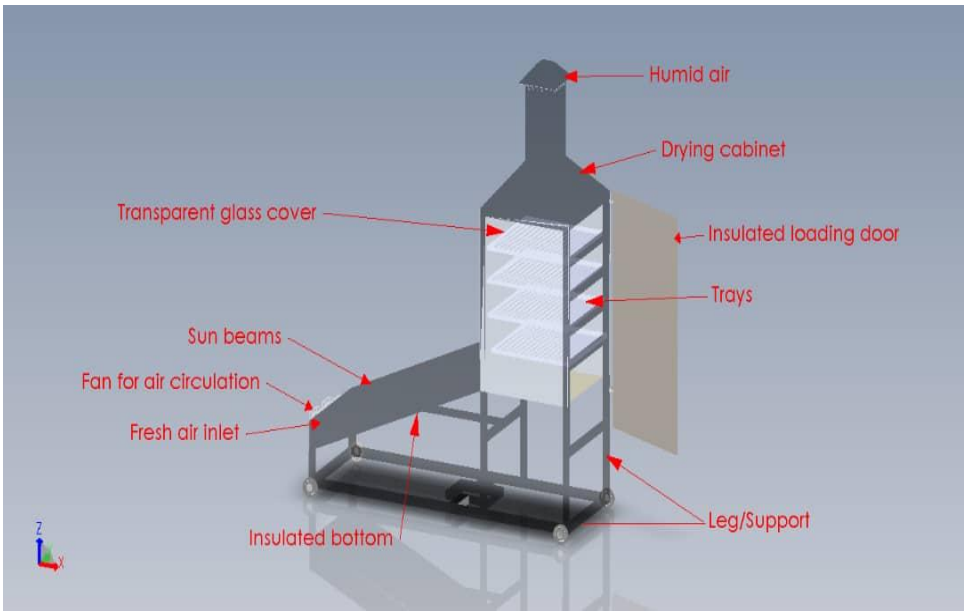

Fig 3.3: A Schematic diagram of solar dryer used

3.3.3 Blanching of the Samples

This experiment was carried out at the Chemical Engineering laboratory, Nnamdi Azikiwe University Awka. In blanching for both convective hot air dryer and solar dryer, 2.0 mm of the sample was cut and 100g of the sample weighed into a bowel containing boiled water at 80^{o}C. The sample was left in the hot water for 10 minutes. The water was removed and the new weight of the sample taken. The samplewas put in the dryer (convective and solar) and allowed to dry to constant weight with the weight taken at interval as done with unblanched samples.

3.3.4 Determination of drying rate (D_r)

The drying rate of the yam species was determined using equation (3.3) (Akpinar et al., 2003);

$$D_r = \frac{M_{t+dt} - M_t}{dt} \quad (3.3)$$

Where;D_r is the drying rate (q_{water} /$q_{dry\ matter}$), M_t and M_{t+dt} are the moisture contentsat t and t+dt, respectively, and t is the drying time.

3.4 Phytochemical analysis

3.4.1 Preparation of sample of water yam and aerial yam extract

All the phytochemical analyses were carried out at the Material, Energy and Techonology Laboratory, Project Development Institute, Enugu state. The two different species of yam samples were prepared for qualitative phytochemical analysis as described by Harbone, (1998). The crude extracts of the samples were prepared using standard procedure (Falope etal.. 1999). The fresh yam samples were peeled with a sharp stainless knife. The yams were cut into 5mm diameter and pounded with a ceramic mortar and pestle. This was done to increase the surface area and reduce the size. About 5 g of each sample was weighed into four different 250ml conical flasks. 100ml of four different solvents was added to the samples (ethanol, water, butanol and hexane). The mixture was agitated at room temperature with a vibrator shaker at 500rpm. Each of the mixtures was filtered with a Whatman filter paper I at room temperature. Then, the extract was collected into sample bottles and kept in the refrigerator for further analysis.

(i) Test for alkaloids:

1mL of 1% HCl(V/V) was pipetted into a test tube containing 3mL of the extract. The mixture was heated gently for 10 minutes in a water bath at 60^0C. Itwas then cooled and filtered. 1mL of the filtrate was pipetted into a test tube, 0.5mL of Wagner's reagent was added immediately. Reddish brown colouration confirmed the presence of alkaloid.

(ii) Test for flavonoids:

3mL of the extract was pipetted into a test tube, then 10mL of distilled water was added. The solution was shaken and 1mL of 10% Na0H solution was added. A yellow (pale yellow) coloration confirmed the presence of flavonoids.

(iii) Test for tannin:

2mL of extract was pipette into a test tube and boiled gently. 2mL of 10% ferric chloride was added. The presence of tannin was confirmed by green colour, green precipitation or bluish green colouration.

(iv) Test for glycosides:

1mL of extract was pipetted into a test tube, 1mL of 2% 3,5-dinitrosalicyclic acid (DNS) in methanol was added. This was followed by 5% aqueous sodium hydroxide.Bright orange coloration indicated the presence of cyanogenic glycoside. The mixture was heated in boiling water to obtain a brick red coloration. This indicates cardiac glycoside.

(v) **Test for Saponin**:

(a) Frothing Test: 2mL of extract was pipetted into a test tube, 2mL of distilled water was introduced. The solution was shaken vigorously. A persistent mass of bubbles movement indicated the presence of saponin.

(b) Emulsion Test: 2mL of extract was pipetted into a test tube and 5 drops of olive oil were added. Emulsification was observed. These are thick liquid drops which are very distributed.

(vi) **Test for steroid:**

In a test tube, 2mL of extract was treated with 0.5mL of acetic acid, 0.5mL of chloroform and 1mL of concentrated sulphuric acid were added. A reddish-brown ring indicated the presence of steroid.

(vii) Test for Phenol/Polyphenol:

In a test tube containing 2mL of extract, 5mL of distilled water was added and heated gently in a water bath at 60^0C for 10 minutes. Then, 1mL of 10% potassium ferricyanide was added tothe mixture. The formationof a green-blue coloration indicated the presence of polyphenol.

3.4.2 Proximate analysis

1. **Determination of moisture content in yam**

All the proximate analyses were carried out at theMaterial, Energy and Techonology Laboratory, Project Development Institute, Enugu. The method used in this is according to AOAC (2000). 2g of the pounded sample was weighed into a previously washed, dried, cooled and weighed petri-dish. It was transferred into a drying oven set at 102^oC and allowed for 3 hours. After this, it was cooled in a desiccator and weighed with an electronic weighing balance and recorded asW_3. The percentage moisture content was determined using equation (3.4).

$$\text{Percentage moisture content} = \frac{W_2 - W_3}{W_2 - W_1} \text{ x } \frac{100}{1} \quad (3.4)$$

Where; W_1 is the weight of empty petri-dish,W_2 is the weight of dish + sample before drying and W_3 is the weight of dish + dried sample.

2. **Determination of ash content in yam**

Ash content was determined according to AOAC (2000). A silica dish or crucible was washed and dried in an oven at 80^oC for 10 minutes. The silica dish was collected from the oven with a tong into a desiccator to cool for 10 minutes. The silica dish was weighed with an electronic weighing balance and recorded as W_1. The weight of the crucible was neglected on a weighing balance. 2g of the sample was scooped into the crucible on an electronic weighing balance and the weight was recorded as W_2. The crucible + content was transferred onto a bunsen burner with

a blue flame. The organic component was allowed to be driven off. The sample was ashed to grey colour. On completion of the incineration, the crucible + ash was transferred into a desiccator to cool. The weight was taken and recorded as W_3 and the % ash content was calculated using equation (3.5)

$$\% \text{ ash content} = \frac{W_3 - W_1}{W_2 - W_1} \; x \; \frac{100}{1} \qquad (3.5)$$

Where; W_1 is the weight of crucible,W_2 is the weight of crucible + ash, and W_3 is the weight of ashed sample + crucible.

3. **Determination of crude fiber in yam sample**

The method employed was in accordance with AOAC (2000). 2 g of the sample was weighed into a 250 mL conical flask and soaked with 200 mL of 1.25% H_2SO_4 for about 10 minutes. The mixture was heated for 30 minutes at 90^{o}C in a water bath. The mixture was brought to a work bench and filtered. The filtrate was discarded and the residue from the filter paper was washed off with distilled water severally. This was done until the residue was no longer acidic by testing with a pH meter. The residue was further treated with 200 mL of 1.25 % NaOH. On completion, it was filtered onto a filter paper. The residue on the filter paper was dried at 80^{o}C for 15 minutes in the drying oven. The filter paper + residue was cooled, weighed and recorded as W_2. The weighed content was placed inside a weighed crucible and transferred onto a Bunsen burner and incinerated to ash or grey colour. It was then cooled in a desiccator. After cooling, it was weighed and recorded as W_3, and the % crude fibre was calculated using equation (3.6).

Crude fiber determination is divided into three:

(a) **Sample treatment**:

W_1 is the weight of empty filter paper, W_2 is the weight of filter paper + residue after drying and W_3 is the weight of residue

Thus; $W_3 = W_2 - W_1$

(b) **Crucible treatment:**

W_4 is the weight of empty crucible, W_5 is the weight of crucible + ash, and W_6 is the weight of ash.

Thus; $W_6 = W_5 - W_4$

(c) Fibre treatment:

W_7 = weight of fibre

$W_7 = W_3 - W_6$

Note: W_6 must be less than W_6 meaning thatW_3.

Therefore,

$$\% \text{ Fibre} = \frac{W_7}{\text{weight of sample treated}} \; x \; \frac{100}{1} \qquad (3.6)$$

4. **Determination of protein content in yam**

There are five stages in determination of protein contents of a sample.

(i) Digestion

The protein content in the yam samples was determined according to Kirk and Sawyer (1991). 1 g of the sample was weighed and transferred into micro Kjeldahl flask. 10 g of Na_2SO_4 and 1

$gCuSO_4$ was added into the Kjeldahl flask, respectively followed by addition of 20 mL of H_2SO_4. The mixture was shaken and placed on a Bunsen burner at angle 60^o. It was heated gently and then vigorously until there was a colour change (green).

(ii) Solidification

After the colour change, the sample was removed from the Bunsen burner and placed in a desiccator to cool and solidify. Before solidification, there was a colour change in the sample (green) on cooling which later turned white.

(iii) Neutralization.

200 mL of distilled water was measured with a measuring cylinder and transferred into the micro Kjeldahl flask holding the sample and agitated till the solidified sample dissolves. It was transferred into a flat bottom flask. 60 mL of 40 % NaOH was added to the flat bottom flask. 4 pieces of zinc metal were added to the flat bottom flask containing the sample. The mixture turned faint blue and on addition of 60 mL of NaOH, it turned black and then back to faint blue.

(iv) Distillation

After neutralization stage, the flat bottom flask containing the mixture was placed on a heating mantle. 100 mL of 4 % H_3BO_3 was transferred into a conical flask and 3 drops of screened methyl red added to it causing the mixture to turn faint pink. It was placed at the receiving end of the distillation unit. The mixture was boiled on a heating mantle. The ammonia from the mixture was trapped into the methylated boric acid which is the absorber (when this happened, there was a formation of ammonium borate). It turned the methylated boric acid colourless at 200 mL.

Back titration

0.1N H_2SO_4 was poured into the burette and the ammonium borate was back titrated to get the original colour change (faint pink).

(v) Determination of fat and oil

This was done in accordance with AOAC (2000) method. The sample was ground using mortar and pestle. This was carried out to increase the surface area and reduce the size. About 5 g of each sample was weighed into a washed test tube. 50 mL of n-Hexane was pipetted into the sample. The mixture was mixed thoroughly. The test tubes were covered with masking tape to prevent the evaporation of the solvent. The mixture was allowed to stand for 24 hours at room temperature. On completion of the settling, the supernatant was decanted into a previously weighed beaker. The weight of the beaker was recorded asW_1. The mixture was heated on a hot plate set at 60^{o}C until the solvent was completely removed. Then the beaker containing the lipid was transferred into a desiccator and allowed to cool for 10 minutes. The beaker containing the lipid was weighed and recorded as W_2. Therefore, the % lipids was calculated using equation (3.7).

$$\% \text{ Lipid} = \frac{W_2 - W_1}{W_3} \text{ x } \frac{100}{1} \qquad (3.7)$$

Where;W_1 is the weight of empty beaker (g), W_2 is the weight of beaker + lipid and W_3 is the weight of the sample tested.

(v) Carbohydrate determination: (Differential method)

% Carbohydrate = 100 - (%Protein + % Moisture + %Ash + %Fat + %Fibre) (3.8

3.5 Engineering properties

3.5.1 Mechanical properties

All themechanical properties analyses in this work were carried out at the Department of Civil Engineering Laboratory, University of Nigeria, Nsukka, Enugu state, following Huerta et al (2010) method.

i. Shear test (for shear force and shear strength):

The shear test was performed using the Tensometer which is a universal testing machine (UTM) in accordance with Huerta et al (2010) method. The shear spindle of the machine was fixed to the shear accessory of the UTM (Model SN-8889 Monsanto tensometer from England). The test sample was fixed into the shear chamber of the UTM and the revolving graph was attached to the graph drum of the UTM. The working fluid (mercury) was zeroed and a continuous but gradual load was applied to the sample until the working fluid returns back to zero. The corresponding load recorded on the graph (which serves as the shear force) was recorded and the shear strength was determined using the area of the shear spindle and the shear force recorded.

ii. Brinnel hardness test.

The testing chamber was replaced by the brinnel hardness bulb tester (indenter bulb) of 5 mm diameter. A constant load for which all the samples must be subjected to was chosen, and the depth of indentation produced on the sample as recorded by the machine graph was measured. The brinnel hardness number (HBN) formulae (eqn 3.9) was then used to calculate the hardness strength.

$$\text{HBN} = \frac{2P}{\pi D\left(D-\sqrt{D^2-d^2}\right)} \tag{3.9}$$

Where; **P** is the constant axial load, **d** is the impression diameter (2mm), **D** is the depth of indentation (5mm), and **HBN** is the Brinned hardeness strength.

iii. Bio-yield and energy.

The sample was placed on the compressive chamber of the testing machine and the graph was fixed on the graph drum. Appropriate load spring was selected and the load was applied gradually while the movement of the working fluid was carefully monitored for the point of first failure (the point the working fluid purses back and after about 30 seconds it continues to move upwards again). The force on the graph drum (this serves as the bio yield force) was recorded. The energy is a function of the maximum force the sample can withstand before failure and its average deformation at same point. This was also measured on the fixed machine graph.

iv. Compressive test: (Elasticity, deformation at brake, compressive force and strength).

The sample was placed in the compressive chamber (measurement of the chamber 40*40mm was ensured). The sample to be tested was fixed into the appropriate chamber and the working fluid was returned to zero load/deformation. Gradual load was applied to the test sample, while monitoring the movement of the working fluid with the aid of an attached microscope. At a choseninterval, the pin button was pushed down to the slider to make the load/deformation graph of the material. When failure occurs, the working fluid was automatically returned to zero. The required parameters were then calculated from the plotted graph.

v. Gummness (separating force):

The sample wasprepared into colloidal form and pasted into the separating wooden buds. The joined wooden buds were placed into the tensile chamber for bio materials on the UTM. Loads were applied to the test piece and the loads that separate the pastes on the wooden buds were recorded. The value of the corresponding force on the machine graph was recorded.

3.5.2 Thermal properties

i. Specific heat capacity

The specific heat capacity of the sample was determined using equation (3.10) as given by Luther et al, (2003).

$$C_p = 1.42X_c + 1.549X_p + 1.675X_f + 0.837X_a + 4.187X_w \quad (3.10)$$

Where; C_p is the Specific heat capacity (KJ/kgK) and X_c, X_p, X_f, X_a,and X_w are the respective mass fractions of carbohydrate, protein, fat, ash and water obtained from the proximate analysis.

ii. Thermal conductivity

The thermal conductivity of the samples was determined according to Nwabanne, (2009) using equation (3.11).

$$k = 0.25X_c + 0.155X_p + 0.16X_f + 0.135X_a + 0.58X_w \quad (3.11)$$

Where; k is thermal conductivity of sample (W/m K) and X_c, X_p, X_f, X_a,and X_w are the respective mass fractions of carbohydrate, protein, fat, ash and water present in each cultivar.

iii. Thermal diffusivity

The thermal diffusivity of the samples was determined according to Luther et al, (2003) as given by equation (3.12).

$$\alpha = k/\rho C_p \quad (3.12)$$

where; $C_p$is the Specific heat capacity, k is the thermal conductivity

3.5.3 Determination of effective moisture diffusivity

The effective moisture diffusivity in the sample was determined in accordance with Mohsen (2016) using equation (3.13)

$$\ln M_R = \ln\frac{8}{\pi^2} - \left(\frac{\pi}{2H}\right)^2 D_{eff}\, t \quad (3.13)$$

Where;M_R is the moisture ratio at time, t, H is half thickness of the slice (mm)

3.6 Determination of drying kinetic model

Moisture ratio of samples during drying is expressed by equation (3.15) (Deepak & Gattumane, 2015).

$$M_R = \frac{M_t - M_e}{M_o - M_e} \quad (3.15)$$

where; M_R is the dimensionless moisture ratio,

M_t = moisture content at time t; M_o = initial moisture content,; Me = equilibrium moisture content

Moisture ratio data obtained with Equations (3.15) for each sample was fitted to eleven thin layer drying equations (Table 3.1) to assess their suitability as models for thin layer drying kinetics of water yam and aerial yam slices in both solar and convective hot air dryer. Coefficient of determination (R^2) was used to determine the appropriateness of the model while the accuracy of fits was assessed using sum square of error (SSE) and root mean square error (RMSE). For quality fit, R^2 value should be close to one while SSE and RMSE values should be close to zero.

Table 3. 1:Some thin-layer drying models used

S/N	Model	Mathematical function	Reference
1	Wang and Singh	$M_R = at^2 + bt + c$	Wang and Singh (1978)
2	Verma e*t al*.	M_R=a exp(-kt)+(1-a)exp(-gt)	Motevali *et al*. (2010)
3	Henderson and Pabis	M_R=a exp(-kt)	Motevali *et al*. (2010)
4	Logaritmic	M_R=a exp(-kt)+c	Dandamrongrak *et al*. (2002)
5	Modified page	$M_R = \exp(-(kt)^n$	Wang *et al.* (2007)
6	Two term	M_R= a exp$(k_o t) + b$ exp$(-k_1)$	Diamente and Munro (1991)
7	Approx. of diffusion	M_R= a exp(-kt)+(1-a)exp(-kbt)	Ertekin and Yaldiz (2004)
8	Page	$M_R = \exp(-kt^n)$	Motevali *et al*. (2010)
9	Modified Henderson &Pabis	M_R= a exp(-kt)+b exp(-gt)+c exp(-ht)	Sharma *et al*. (2005)
11	Midilli *et al.*	M_R= a exp$(-kt^n)$+bt	Midilli *et al*. (2002)
12	Two term exponential	M_R=a exp(-kt)+(1-a)exp(-kat)	Motevali *et al*. (2010)

3.7 Experimental procedure of finite element analysis

The experimental procedure for finite element analysis was carried out at the chemical engineering laboratory, Nnamdi Azikiwe University, Awka.For finite element analysis of aerial yam and water yam drying by convective hot air dryer, 30 x 20 x 4mm (Fig 3.4) sizes of the samples were cut. This was done with a sharp mold fabricated for the purpose. The initial moisture content of the samples was determined by drying 10 g of the fresh samples at 103 °C until constant weight. Prior to each experiment, the samples were left at room temperature for 2 h to reach thermal equilibrium with the environment.

For each drying experiment, 12 pieces of the cut samples were placed in a small wire gauze with a known weigh inside the drying tray. The remaining samples were spread in the drying tray inside the drying chamber. The airspeed of the fan was kept constant at 4 m/s throughout the experiment while the air inlet temperature was set at 40 ^{o}C in the first instance. The samples were left to dry to a constant weight. The loss in weight of the sample in the wire gauze was taken at an interval of 10 minutes, and the shrinkage rates were determined at the same time by inserting a piece of the sample taken from the drying tray into a 100 mL measuring cylinder containing toluene at a known level. The volume of toluene displaced was measured. The experiments were replicated twice and the average values were used. The tests were repeated at the air inlet temperatures of

50 ^{o}C, 60 ^{o}C, and 70 ^{o}C.

The sample mass was monitored by a digital balance with accuracy of 0.001 g and the instantaneous moisture content was calculated using Eqn. (3.16) (Torki-Harchegani, et al., 2015)

$$\chi = \left(\frac{(\chi_o + 1)\,\mathrm{w}}{\mathrm{W_o}} - 1\right) \tag{3.16}$$

Where χ and χ_o are the moisture content at any given time ($\mathrm{Kg_{water}}/\mathrm{Kg_{dry\ matter}}$), and the initial moisture content ($\mathrm{Kg_{water}}/\mathrm{Kg_{dry\ matter}}$), respectively and w and $\mathrm{W_o}$ are the mass of samples at any given time(g) and the initial mass of fresh samples (g), respectively.

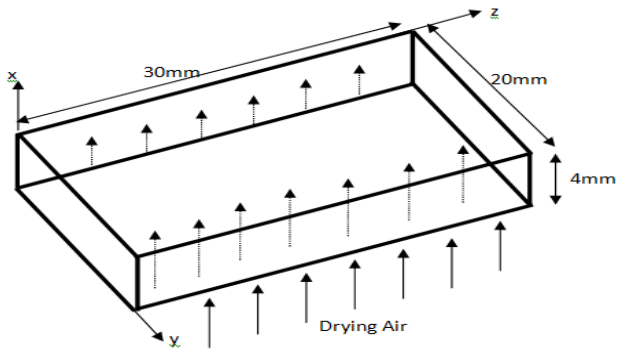

Fig. 3.4: Heat flow direction on the yam slice

3.7.1 Finite Element Formulation

Drying as a mass transfer process is governed by the parabolic partial differential equation (PDE)

$$\frac{\partial \chi}{\partial t} = \text{Div}\left[D_{eff}\,\text{grad}(\chi)\right] \tag{3.17}$$

For 2-D case where effective diffusivity is not considered a function of position then eqn. (3.17) becomes;

$$\frac{\partial \chi}{\partial t} = D_{eff}\left(\frac{\partial^2 \chi}{\partial x^2} + \frac{\partial^2 \chi}{\partial y^2}\right) \tag{3.18}$$

The initial condition

$$\chi(t = 0) = \chi_0 \tag{3.19}$$

and the Neumann boundary condition is given as

$$D_{eff}\,\frac{\partial \chi}{\partial n} + h_m \chi_{surf} = h_m \chi_{eq} \tag{3.20}$$

where χ_{surf} is the moisture content at the surface of the sample and χ_{eq} is the equilibrium moisture content. The Galerkin approach of weighted residual is adopted for solution of this parabolic problem. The method requires analysis of the integration problem

$$\iint \varphi D_{eff}\left(\frac{\partial^2 \chi}{\partial x^2} + \frac{\partial^2 \chi}{\partial y^2}\right) dA - \iint \varphi \frac{\partial \chi}{\partial t}\, dA = 0 \tag{3.21}$$

where the weight function $\varphi(x,y)$, which is a virtual moisture content, is constructed from the same basis as the field function χ. This is re-written as

$$\iint D_{eff}\left[\frac{\partial}{\partial x}\left(\varphi\frac{\partial\chi}{\partial x}\right)-\frac{\partial\varphi}{\partial x}\frac{\partial\chi}{\partial x}\right]dA+\iint D_{eff}\left[\frac{\partial}{\partial y}\left(\varphi\frac{\partial\chi}{\partial y}\right)-\frac{\partial\varphi}{\partial y}\frac{\partial\chi}{\partial y}\right]dA-\iint\varphi\frac{\partial\chi}{\partial t}dA=0 \qquad (3.22)$$

This can become

$$\iint D_{eff}\left[\frac{\partial}{\partial x}\left(\varphi\frac{\partial\chi}{\partial x}\right)+\frac{\partial}{\partial y}\left(\varphi\frac{\partial\chi}{\partial y}\right)\right]dA-\iint D_{eff}\left[\frac{\partial\varphi}{\partial x}\frac{\partial\chi}{\partial x}+\frac{\partial\varphi}{\partial y}\frac{\partial\chi}{\partial y}\right]dA-\iint\varphi\frac{\partial\chi}{\partial t}dA=0 \qquad (3.23)$$

Applying the divergence theorem on the first term in the right-hand-side of equation (3.23) gives

$$\int D_{eff}\left[\varphi\frac{\partial\chi}{\partial x}n_x+\varphi\frac{\partial\chi}{\partial y}n_y\right]d\Omega-\iint D_{eff}\left[\frac{\partial\varphi}{\partial x}\frac{\partial\chi}{\partial x}+\frac{\partial\varphi}{\partial y}\frac{\partial\chi}{\partial y}\right]dA-\iint\varphi\frac{\partial\chi}{\partial t}dA=0 \qquad (3.24)$$

where n_x and n_y are the direction cosines of unit normal to the boundary, then

$$\int D_{eff}\left[\varphi\frac{\partial\chi}{\partial n}\right]d\Omega-\iint D_{eff}\left[\frac{\partial\varphi}{\partial x}\frac{\partial\chi}{\partial x}+\frac{\partial\varphi}{\partial y}\frac{\partial\chi}{\partial y}\right]dA-\iint\varphi\frac{\partial\chi}{\partial t}dA=0 \qquad (3.25)$$

At this point, the isoparametric relations for the triangular element are introduced. They are $\chi=\mathbf{N}\boldsymbol{\chi}^{(\mathrm{e})}$, $\varphi=\mathbf{N}\boldsymbol{\varphi}$ and

$$\begin{Bmatrix}\frac{\partial\chi}{\partial x}\\ \frac{\partial\chi}{\partial y}\end{Bmatrix}=\frac{1}{\det\mathbf{J}}\begin{Bmatrix}y_{23} & y_{31} & y_{12}\\ x_{32} & x_{13} & x_{21}\end{Bmatrix}\begin{Bmatrix}\chi_1\\ \chi_2\\ \chi_3\end{Bmatrix}=\boldsymbol{B}_T\boldsymbol{\chi}^{(\mathrm{e})} \qquad (3.26)$$

where $\mathbf{J}=\begin{bmatrix}x_{13} & y_{13}\\ x_{23} & y_{23}\end{bmatrix}$is a Jacobean matrix and $x_{ij}=x_i-x_j$. Similarly

$$\begin{Bmatrix}\frac{\partial\varphi}{\partial x}\\ \frac{\partial\varphi}{\partial y}\end{Bmatrix}=\boldsymbol{B}_T\boldsymbol{\varphi} \qquad (3.27)$$

Inserting the isoparametric relations and the boundary condition in equation (3.25) gives

$$\int\varphi h_m\left(\chi_{eq}-\chi_{surf}\right)d\Omega-\iint D_{eff}\left[\frac{\partial\varphi}{\partial x}\frac{\partial\chi}{\partial x}+\frac{\partial\varphi}{\partial y}\frac{\partial\chi}{\partial y}\right]dA-\iint\varphi\frac{\partial\chi}{\partial t}dA=0 \qquad (3.28)$$

which on execution of the integrals on element-by-element basis and approximating $\frac{\partial\chi}{\partial t}$ with forward difference formula give

$$\sum_e \boldsymbol{\varphi}^{\mathrm{T}}\mathbf{h}_T\,\mathbf{r}_{eq} - \sum_e \boldsymbol{\varphi}^{\mathrm{T}}\mathbf{h}_T\,\boldsymbol{\chi}^{(\mathrm{e})}_{surf,i} - \sum_e \boldsymbol{\varphi}^{\mathrm{T}}\mathbf{k}_T\,\boldsymbol{\chi}^{(\mathrm{e})}_{i} - \sum_e \boldsymbol{\varphi}^{\mathrm{T}}\mathbf{m}_T\,\boldsymbol{\chi}^{(\mathrm{e})}_{i+1} + \sum_e \boldsymbol{\varphi}^{\mathrm{T}}\mathbf{m}_T\,\boldsymbol{\chi}^{(\mathrm{e})}_{i} = 0 \quad (3.29)$$

Where;

$$\mathbf{r}_{eq} = \frac{h_m \chi_{eq}\, l_{2-3}}{2}\begin{Bmatrix}0\\1\\1\end{Bmatrix} \quad (3.30)$$

$$\mathbf{h}_T = \frac{h_m\, l_{2-3}}{6}\begin{bmatrix}0 & 0 & 0\\0 & 2 & 1\\0 & 1 & 2\end{bmatrix} \quad (3.31)$$

$$\mathbf{k}_T = D_{eff}\,\boldsymbol{\varphi}^{\mathrm{T}}\mathbf{B}_{\mathrm{T}}^{\mathrm{T}}\boldsymbol{B}_T \quad (3.32)$$

$$\mathbf{m}_T = \frac{A_e}{3\Delta \mathrm{t}}\begin{Bmatrix}1\\1\\1\end{Bmatrix} \quad (3.33)$$

The l_{2-3} is the length of a boundary element edge between nodes "2" and "3". If all the nodal moisture content values are arranged in a global moisture content vector then equation (3.27) becomes

$$\boldsymbol{\chi}_{i+1} = (\mathbf{M}_T)^{-1}(\mathbf{M}_T - \mathbf{K}_T - \mathbf{H}_T)\boldsymbol{\chi}_i + (\mathbf{M}_T)^{-1}\mathbf{H}_T\mathbf{R}_{eq} \quad (3.34)$$

The time steps "i" range from the initial condition at which $i = 0$ to the end of a drying run $i = n$. At $i = 0$, the solution is known; the initial moisture content which is assumed to be uniform. The rest of the solution are gotten iteratively, for example, at time step "2" and the scripts are shown in Appendix

$$\boldsymbol{\chi}_{i+2} = (\mathbf{M}_T)^{-1}(\mathbf{M}_T - \mathbf{K}_T - \mathbf{H}_T)\boldsymbol{\chi}_{i+1} + (\mathbf{M}_T)^{-1}\mathbf{H}_T\mathbf{R}_{eq} \quad (3.35)$$

3.7.2 Determination of mass transfer coefficient (h_m)

The mass transfer coefficient (h_m) of the samples were determined using equation (3.36);

$$h_m = \frac{S_h D}{L} \quad (3.36)$$

where; S_h is the sherwood number, D is the thermal diffusivity of the sample and L is the diameter of the dryer. The Sherwood number was determined from the relation in equation (3.37);

$$S_h = 0.023 * R_e^{0.83} * S_c^{0.44} \quad (3.37)$$

where , R_e is the Reynold number and S_c is the schmidt number determined from the corresponding air temperature in the steam table. The schmidt number was determined from equation (3.38);

$$S_c = \frac{\mu}{\rho * D} \quad (3.38)$$

Where; μ is the air viscosity at temperature (T ^{o}C), ρ is the density of air at (T ^{o}C) and D is the thermal diffusivity. The Reynold number R_e was determined from the relation in equation (3.39)

$$R_e = \frac{\rho v L}{\mu} \quad (3.39)$$

Where; v is the air velocity and L is the diameter of the dryer.

3.8 Experimental Design

In this study, RSM via central composite design (CCD) was utilized for the experimental design of the drying process. CCD was chosen because it could eliminate the time-consuming phase which cannot be achieved using the one-factor-at-a-time approach. Besides, the CCD is well suited for fitting a quadratic surface, which usually works well for the process optimization, and it requires a minimum number of experiments to be carried out. By using CCD, linear, quadratic, cubic and cross-product effects of operating condition variables on the drying efficiency (moisture contents) were investigated. The drying temperature, air speed and the slice thickness were identified as the set of three independent process variables for convective hot air dryer, while mass of sample, airspeed and slice thickness were identified as the set of independent variables for solar dryer. The influence of these independent variables on the output variable (moisture content) was investigated. The CCD

method was adopted to decide the number of experiments to be performed for optimization of the process variables. Design Expert Version.11.0.3 software was used to optimize the drying process. Tables 3.1 and 3.2 show the CCD design matrix of convective hot air dryer and solar dryer, respectively.

Table 3. 2:Factor level for convective hot air dryer

Factor	$-\alpha$	Low level (-)	Medium level (0)	High level (+)	$+\alpha$
Temperature(^{o}C)	47.5	50	55	60	62
Slice thickness(mm)	1.5	2	3	4	4.5
Airspeed(m/s)	1.75	2	2.5	3	3.25

Table 3. 3:Factor level for solar dryer

Factor	$-\alpha$	Low level (-)	Medium level (0)	High level (+)	$+\alpha$
Mass (g)	59.0192	70	85	100	110.981
Slice thickness(mm)	1.2679	2	2	4	4.73205
Airspeed(m/s)	1.1339	2	3	2.866	4.73205

3.8.1 Artificial Neural Network

A total of 12 (60%) of experimental results were used to train the network, 5 (25%) of the experimental result was used to validate the training while the remaining 3 (15%) was used for testing.

After the selection of the hidden number of neurons, a number of training runs were performed to look out for the best possible weights in error back propagation framework. The architectural framework of the ANN for convective hot air dryer and solar dryer are shown in Figs. 3.5a and 3.5b respectively.

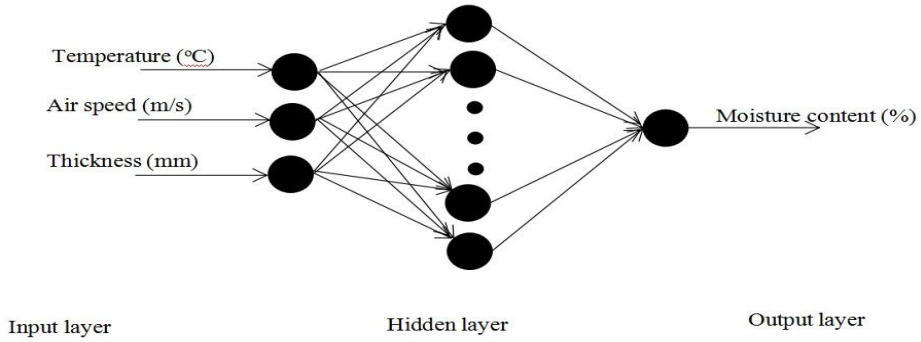

Figure 3.5a: ANN frame work of convective hot air dryer

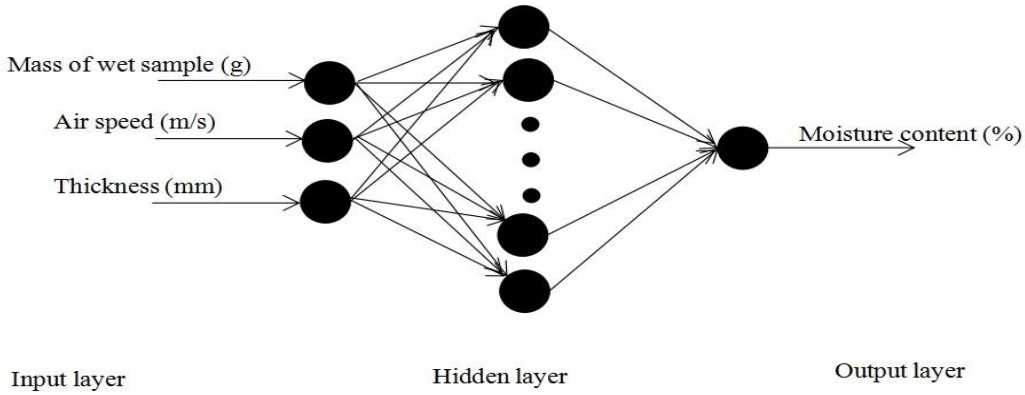

Figure 3.5b: ANN frame work of solar dryer

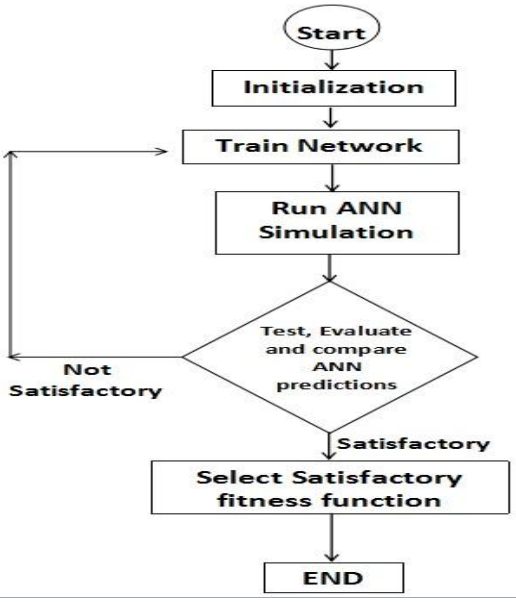

Fig 3.6: ANN schematic diagram

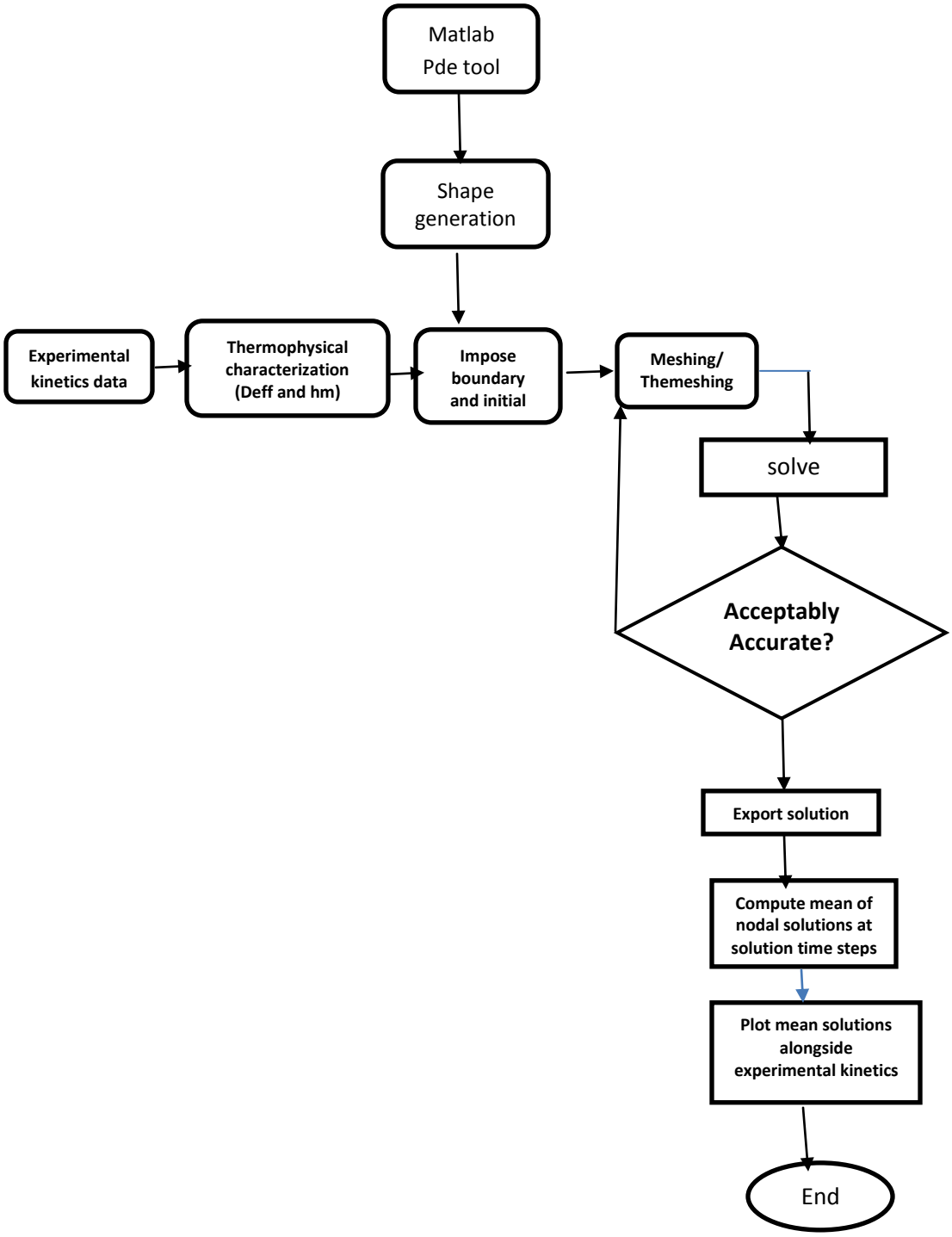

Fig. 3.5c: Flowchart for MATLAB Simulation of Finite Element Analysis of Aerial& Water Yam

3.9 Hedonic sensory analysis

The hedonic scale may be used to determine degree of acceptability of one or more products. This scale is a category-type scale with an odd number (five to nine) of categories ranging from "dislike extremely" to "like extremely". A neutral midpoint (neither like nor dislike) is included. Consumers rate the product on the scale based on their response. The hedonic test was done according to Munoz and King (2007) methods, by distributing 30 questionnaires and the flour samples to different people who use flour for different purposes. Each individual was given enough time to complete the test. The sensory tests conducted were; colour of the sample, general appearance, texture of the sample and Aroma. The analysis was later done using statistical package for social science (SPSS) software.

9-Hedonic scale ranking: The hedonic scale ranking employed in the analysis of the samples were: Like extremely, Like very much, Like moderately, Like slightly, Neither like nor dislike, Dislike slightly, Dislike moderately, Dislike very much, Dislike extremely.

CHAPTER FOUR

RESULTS AND DISCUSSION

4.1 Phytochemical analysis

The result of the qualitative phytochemical analysis of the two yam speciesis given in Tables 4.1 and 4.2. The result shows that Flavonoids, Tannin and polyphenol are absent in water yam sample irrespective of the solvent. Glycoside, Alkaloids, Steroid and Saponin are found to be present in the different solvents used though in varying concentrations. In aerial yam analysis, Glycoside was found to be present in different concentrations in all the solvents. Saponin and Tannin were moderately abundant in water solvent while Steroids were insignificantly present in the solvents.

Flavonoids have been reported to affect the heart and circulatory system, and are used as spasmodytics and diuretic (Schavenberg & Paris, 1977). Also, some traditional crops and plants are known for the management of diabetes mellitus. It is also known that the medicinal properties of crop and plant samples have been attributed to the active ingredients present in the phytochemical analysis of the samples. The flavonoids and polyphenols are well-known oxidants (Tiwari & Rao. 2002). In terms of the phytochemical analysis, aerial yam is considered to be of more importance because of the presence of flavonoids, polyphenols and tannin among others.

Table 4. 1:Phytochemical constituents of Water Yam

S/N	PARAMETER	ETHANOL	WATER	BUTANOL	HEXANE
1	Alkaloids	+	-	++	+++
2	Flavonoids	-	-	-	-
3	Tannin	-	-	-	-
4	Glycoside:Cyanogenic	+++	+++	+	+
	Cardiac	++	-	++	-
5	Steroid	-	-	+	-
6	Polyphenol	-	-	-	-
7	Saponin:	+	+++	-	-
		+	+++	-	-

KEY: -: Absent, +: Insignificantly present**,** ++: Moderately present**,** +++: Abundantly present.

Table 4. 2:Phytochemical constituents of Aerial Yam

S/N	PARAMETER	ETHANOL	WATER	BUTANOL	HEXANE
1	Alkaloids	+	-	+	+++
2	Flavonoids	+	++	+	-
3	Tannin	-	+++	-	++
4	Glycoside:	++	+++	+	+
	Cyanogenic	+++	+	+	-
	Cardiac				
5	Steroid	-	-	+	+
6	Polyphenol	++	-	+	+
7	Saponin:	-	+++	-	-
	Frothing	+	+	-	-
	Emulsion				

KEY:-: Absent, +: Insignificantly present**,** ++: Moderately present**,** +++: Abundantly present.

4.2 Proximate Analysis

The proximate analysis of the food samples was done to determine their different compositions. As expected, the moisture content of the raw water yam was highest with 68.25% (Tables 4.3). Water yam is a food sample that is known to contain large quantities of water. The moisture content of the samples decreased drastically after drying. This is expected because the major aim of drying is to reduce the moisture content which will subsequently increase the shelf life (Onu et al, 2017).

The ash content is the inorganic component remaining after the removal of water and incineration of organic compounds. The ash content of water yam was 7.50% while that of the

aerial water was 1.75%. The ash content was relatively unchanged after drying especially for water yam. The ash content of the aerial yam increased from 1.75 to 3.75%.

The crude fibre is the indigestible part of the main food sample. The crude fibre of both water yam and aerial yam decreased after drying from 4.25 and 5.25 to 2.50 and 1.50 respectively. Nwabanne (2009) in the analysis of fermented ground cassava reported fibre content values ranging from 5.10 to 5.40.

All the samples have low fats and protein content which is in agreement with the results reported by Luther et al (2003) for different food samples. While the fat content increased after drying, the protein content decreased after the drying. The aerial yam had more carbohydrate content than water yam.

The carbohydrate content increased the most after drying for both water yam and aerial yam.Nwabanne (2009) explains that the difference in drying rates of food samples is as a result of the difference in the chemical compositions of the samples.

Table 4. 3:Proximate analysis of the yam samples

Sample	**Water**	**Ash**	**Crude**	**Fats**	**Protein**	**Carbohydr**

	Content	Content	fibre	content	content	ate content
Raw water yam	68.25±0.35	7.25± 1.06	2.50± 0.71	2.40± 0.28	1.71± 0.18	16.21 ± 0.93
Raw aerial yam	62.25± .35	3.75± 1.06	1.50 ± 0.00	3.10± 0.14	0.83± 0.18	27.29 ± 0.13
Dry water yam	7.25 ± 0.35	7.50± 1.41	4.25±0.35	0.60± 0.28	3.20± 0.06	78.89 ± 0.95
Dry aerial yam	9.75 ± 0.35	1.75± 0.35	5.25± 0.35	0.30± 0.14	3.16±0.36	81.07 ± 0.66

The percentage change in the compositions between the raw and dried samples was equally evaluated. The percentage change was calculated on wet basis in accordance with Luther et al, (2003) and shown in Table 4.4.For water yam, the moisture content showed a percentage decrease of 89.38% after drying. A similar trend was obtained in the ash content, crude fibre and protein contents. However, an increase was observed in protein and carbohydrate contents with 300 % and 386.67 % respectively.

For aerial yam, the moisture content, crude fibre and protein showed a decrease of 84.42, 71.43 and 73.73 % respectively. However, ash content showed an increase of 117.14%.

Table 4. 4:Percentage differences between the raw and dried samples

Sample	Water Content (%)	Ash Content (%)	Crude fibre (%)	Fats content (%)	Protein content (%)	Carbohydrate content (%)

Water yam	89.38	3.33	41.18	-300	46.56	-386.67
Aerial yam	84.42	-117.14	71.43	-933.33	73.73	-197.07

4.2.1 Statistical analysis of the proximate analysis

The one-way analysis of variance (ANOVA) was evaluated to determine whether the changes obtained in the mean values of the proximate analysis between the raw and dried yam samples were statistically significant. The p-value was set at 0.05 that is, at 95% confidence level. The results were given in Tables 4.5 and 4.6.

For the water yam in Table 4.5, the variations observed in the mean values of moisture content, fats, protein and carbohydrate of both raw and dried samples were not statistically significant since their significant values of 0.00, 0.024, 0.008 and 0.00 respectively are all less than 0.05. This means that these compositions were affected by the drying process. However, the changes observed in mean values of the ash content and crude fiber are not statistically significant since their significant values of 0.860 and 0.089 respectively are all greater than 0.05, the *p*-value. This implies that the changes in their mean values were not affected by the drying process.

The one-way ANOVA of the aerial yam is shown in Table 4.5. The changes observed in the mean values of moisture content, crude fiber, fats, protein and carbohydrate of the raw and dried sample of aerial yam were not statistically significant since their significant values of 0.00, 0.004, 0.003, 0.015 and 0.000 respectively were all less than 0.05. This means that these compositions were affected by the modification of the samples. However, the change in the mean value of the ash content is not statistically significant since its significant value of 0.127 is

greater than the p-value. This implies that the change in its mean value was not affected by the drying process.

It is concluded that the drying process caused changes in the proximate parameters of the yam samples which resulted in an appreciable change in their nutritive and calorific values

Table 4. 5:One-way ANOVA for water yam

Parameter	Sum of squares	Df	Mean square	F value	p-value
Moisture content	3721.00	1	3721.00	29768.00	0.000
Ash content	0.63	1	0.63	0.04	0.860
Crude fibre	3.06	1	3.06	9.80	0.089
Fats	3.24	1	3.24	40.50	0.224
protein	2.21	1	2.21	116.52	0.008
carbohydrate	3929.41	1	3929.41	4475.79	0.000

Table 4. 6:One-way ANOVA for aerial yam

Parameter	Sum of squares	df	Mean square	F value	p-value
Moisture content	1756.25.25	1	1756.25.25	22050.00	0.000
Ash content	4.00	1	4.00	6.40	0.127
Crude fibre	14.063	1	14.063	225.00	0.004
Fats	7.840	1	7.840	392.00	0.003
protein	5.406	1	5.406	65.98	0.015
carbohydrate	22891.75	1	22891.75	12576.93	0.000

4.3 Instrumental Analysis

4.3.1 Thermo Gravimetric Analysis

Thermo-Gravimetric Analysis (TGA) is based on mass measurement of mass loss of material as a function of temperature. The loss of weight could result from chemical reaction (decomposition, combustion) and physitransition (evaporation, desorption, drying) (Vyazovkin 2012). The TGA curves of the water yam and aerial yam are presented in Figures 4.1 and 4.2. The TGA profile of the raw samples (water yam and aerial yam) clearly gives an approximation about the weight loss with respect to temperature due to the release of surface bounded water, volatile matter, hemicellulose, cellulose and lignin present in the samples. The TGA of water yam consisted of two regions (I and II). As can be seen from the TGA profile of water yam (Figure 4.1), the initial step (Region I) shows weight loss of 2.9% in the temperature range of 10^{o}C to 290^{o}C, this might have resulted from the release of moisture and volatile matter. The second region shows steep weight loss of 82.474 % at the temperature range from 300^{o}C to 480^{o}C. Region II was related to the thermal degradation of hemicellulose which completes its decomposition at temperature intervals of 300 to 480^{o}C (Emilio et al., 2015).

However, the TGA of aerial yam consisted of three regions (Figure 4.2). Region I shows a weight loss of 4-5% in the temperature range of 5-300^{o}C, which might have resulted from the release of moisture and volatile matter (Emilio et al., 2015). The second region shows a consistent steep weight loss of 88.42% at the temperature region of 300-520^{o}C, related to the thermal degradation of hemicellulose. The final stage of the profile exhibited weight loss of 2.01 % at a temperature range of 520^{o}C to 888^{o}C resulting from the decomposition of lignin (Wyasu et al., 2016).

Differential thermo gravimetric analysis (DTA) curves were performed in order to identify the temperatures at which the maximum thermal degradation rates of each sample occurred (Figures 4.3 and 4.4). The decomposition temperature reflects the maximum rate of mass loss, and

occurred at 389.5 °C in the water yam and at 432.7 °C in the aerial yam, indicating that the thermal stability was higher in aerial yam than in water yam.

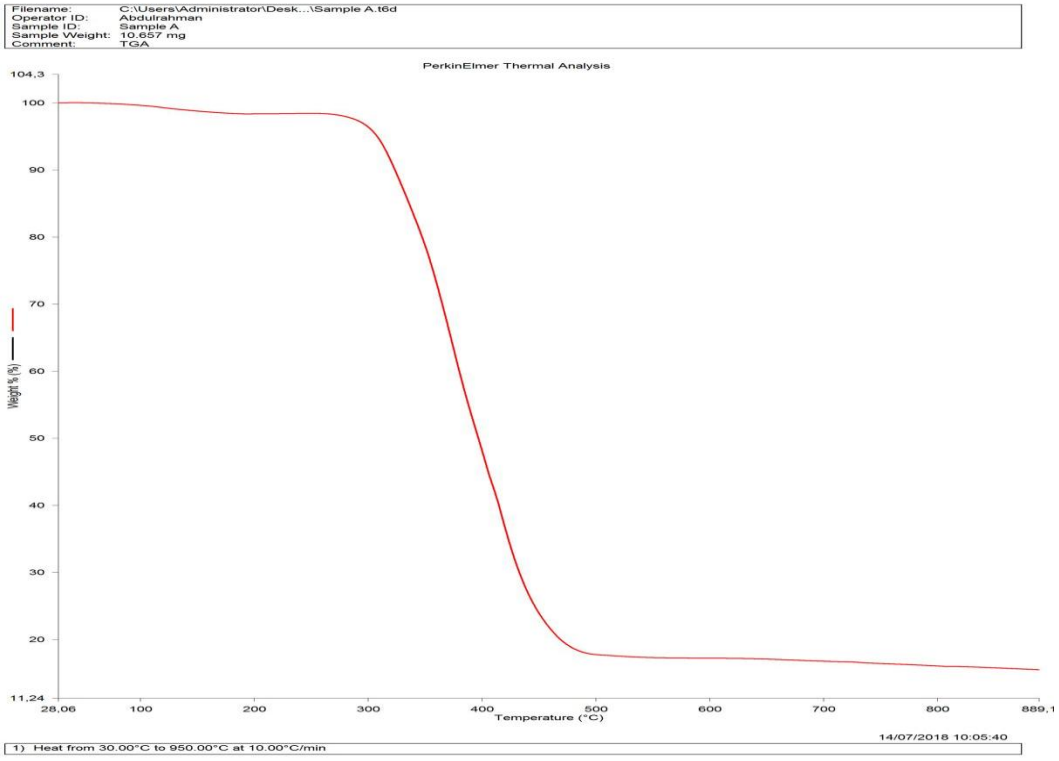

Figure 4. 1: Graph of Thermo-Gravimetric Analysis of water yam

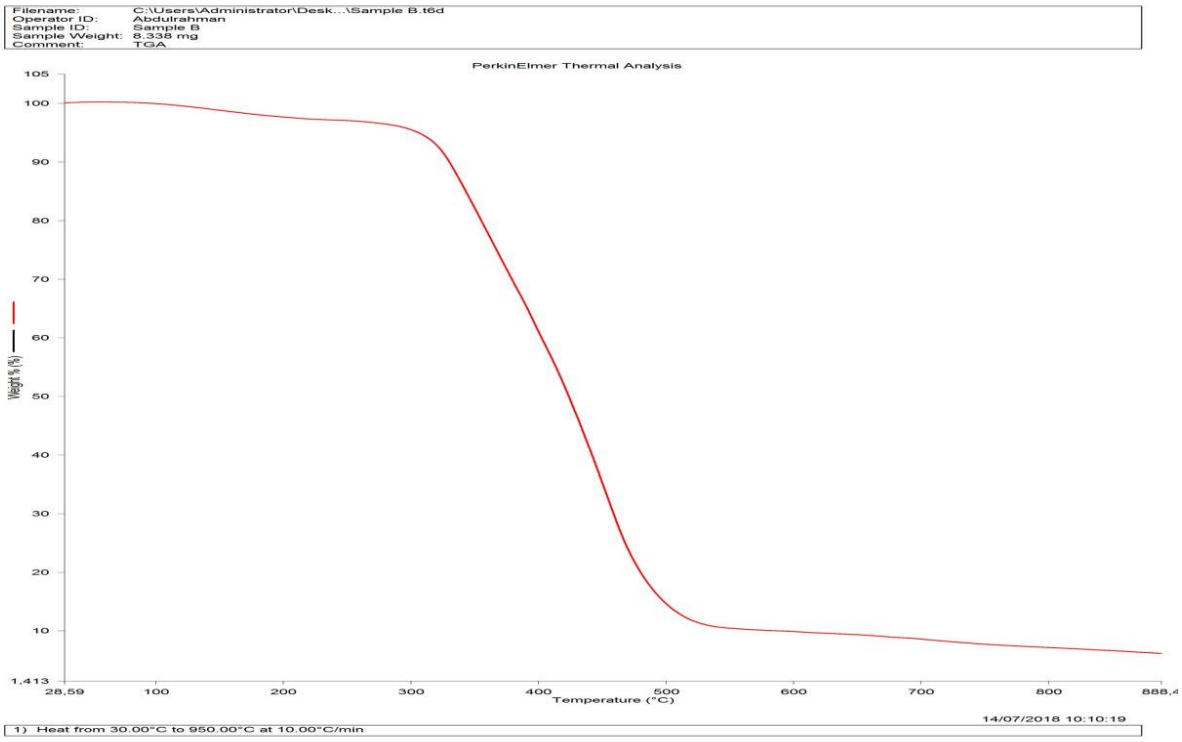

Figure 4. 2: Graph of Thermo-Gravimetric Analysis of aerial yam

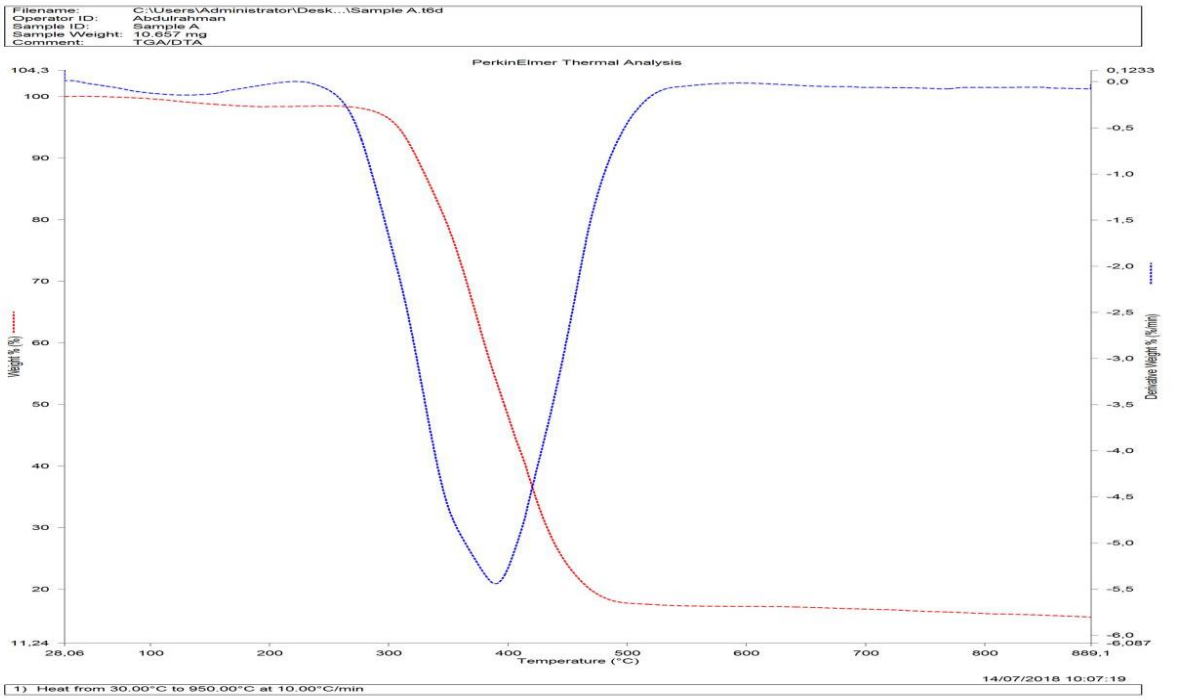

Figure 4. 3:Graph of Differential thermo gravimetric analysis of water yam

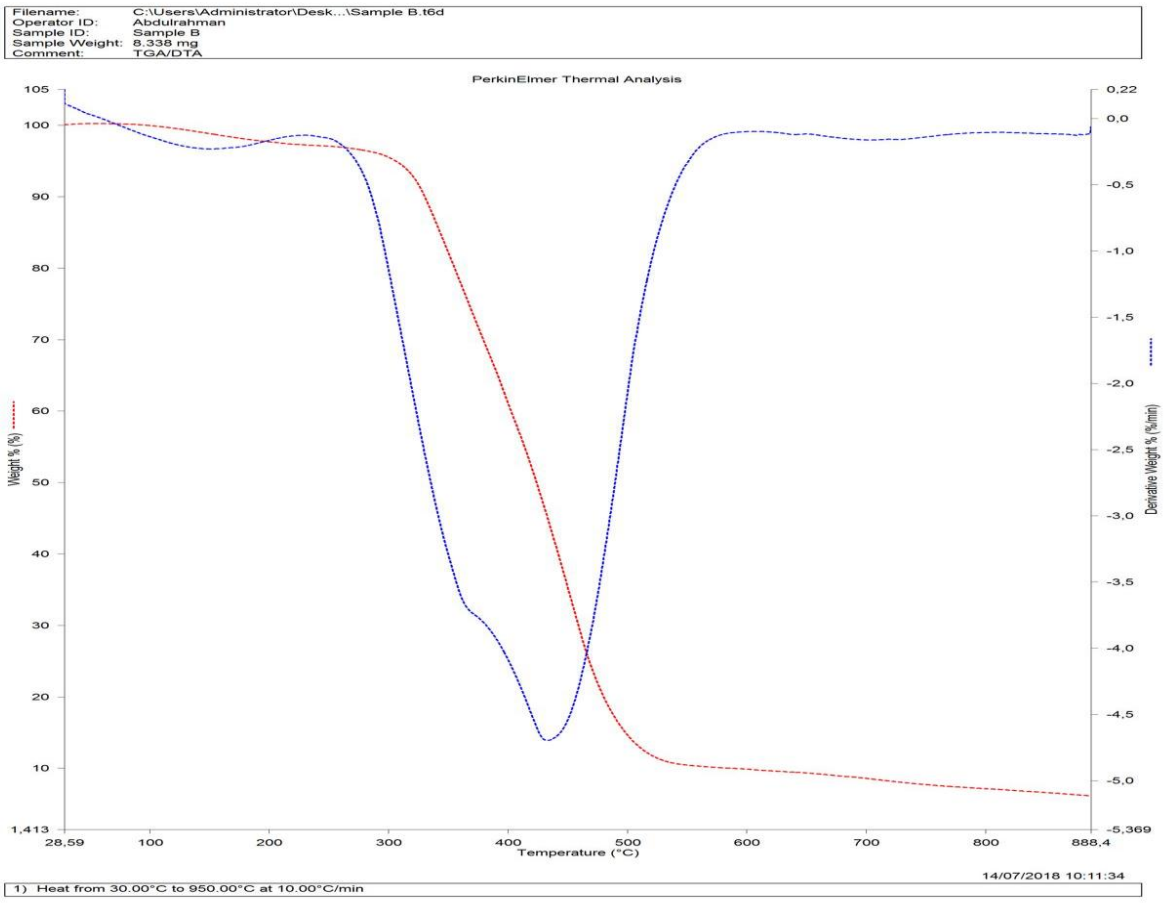

Figure 4. 4:Graph of Differential thermo gravimetric analysis of aerial yam

TGA/DTA of the water yam and aerial yam were compared as shown in Table 4.7. The result showed that aerial yam required higher temperature (454.39 ^{o}C) to be degraded while water yam required lower temperature (454.05 ^{o}C) to be degraded. Equally, aerial yam gave higher weight loss of 51.19 % while water yam gave a weight loss of 49.29 %. Also, aerial yam gave higher derivative weight loss of -0.92 %/min while water yam gave lower derivative weight loss of -1.02 %/min. T-test analysis showed significant difference in weight percent and derivative weight between aerial yam and water yam ($p<0.05$). There was no significant difference in temperature requirement between aerial yam and water yam ($p>0.05$).

Table 4. 7TGA/DTA comparison between aerial yam and water yam

Sample	**Temperature (^{o}C)**	**Weight percent (%)**	**Derivative weight (%/min)**
Aerial yam	454.39±245.875	51.19±37.803	-0.92±1.625
Water yam	454.05±245.49	49.29±40.936	-1.02±1.505
p-value	0.942	0.011	0.001

4.3.2 Fourier Transform Infra-Red Spectroscopy

Figure 4.5 shows FTIR spectrum of raw aerial yam. The absorption bands in the 3500-2500 cm^{-1} is due to O-H stretching of carboxylic acids group; in the region of 2140-2100 $cm^{-1}$is due to C≡C stretching of alkynes group; in the region of 1655-1590 cm^{-1} is due to N-H bending of amides group while in the region of 1050-1035 cm^{-1} is due to C-O stretching of alcohols group.

However, Figure 4.6 shows FTIR spectrum of aerial yam dried at 50^{o}C. The absorption bands in the 3500-2500 cm^{-1} is due to O-H stretch of carboxylic acids group; alkanes and alkyls occurred in the 3000-2850 cm^{-1} region of C-H stretching; amides occurred in the 1655-1590 cm^{-1} region of N-H bending; alkyl halides occurred in the 1350-1000 cm^{-1} and 850-750 cm^{-1} regions of C-F and C-Cl stretching; arenes occurred in the 885-860 cm^{-1} region; alcohols occurred in the 1260-1035 cm^{-1} region of C-O stretching while alkenes occurred in the 990-910 cm^{-1} region of =C-H bending. Fig. 4.6 showed that some functional groups became more visible in the dried sample. It showed that alkanes, alkyl, alkyl halide and alkenes were all very visible after Heating. This added compounds where more likely been masked by high moisture content in raw aerial yam (Fig. 4.5), and thereby provide excellent nutrition for both adults and young ones so that the process of preservation for continued availability has been achieved.

Figure 4.7 shows the FTIR spectrum of raw Water yam. The absorption bands in the 3500-2500 cm^{-1} is due to O-H stretching of carboxylic acids group; in the region of 1655-1590 cm^{-1} is due to N-H bend of amides group; in the region of 1205-1125 cm^{-1} is due to C-O stretching of alcohols group while in the region of 1350-1000 cm^{-1} is due to C-F stretching of alkyl halides group. However**,** Figure 4.8 shows FTIR spectrum of Water dried at 50^{o}C. The absorption bands in the 3500-2500 cm^{-1} is due to O-H stretch of carboxylic acids group; esters occurred in the 1750-1725 cm^{-1} region of C=O stretching; amides occurred in the 1655-1590 cm^{-1} region of N-H bending; nitro compounds occurred in the ~1370 cm^{-1} region; ethers occurred in the 1150-1085 cm^{-1} region of C-O-C stretching while alkyl halides occurred in the 1350-1000 cm^{-1} and 850-750 cm^{-1} regions of C-F and C-Cl stretching. Comparing the FTIR result of raw water yam (Fig4..7) and the dried water yam (Fig.4. 8), it shows that other compounds like Esters, Ethers and Nitro Compounds were more visible to the UV, after heating to 50^{o}C. These may be due to the high moisture content in Water yam which masked the presence of these compounds in the raw sample. The visibility of these compounds adds to excellent nutrition to a variety of humans, including old and young. It also shows that drying at this temperature does not alter the nutrient components of this variety of yam which is one of the goals of food preservations and processing.

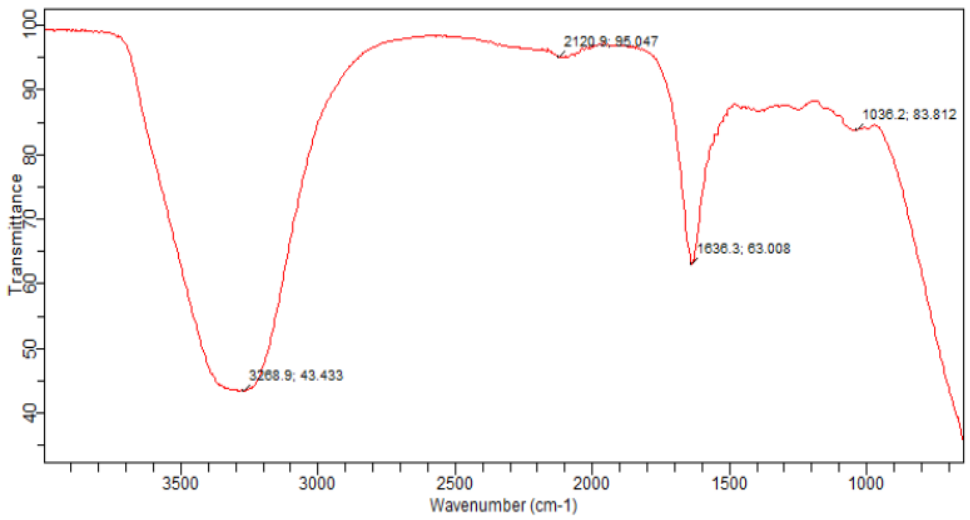

Figure 4. 5:FTIR spectrum of raw aerial yam

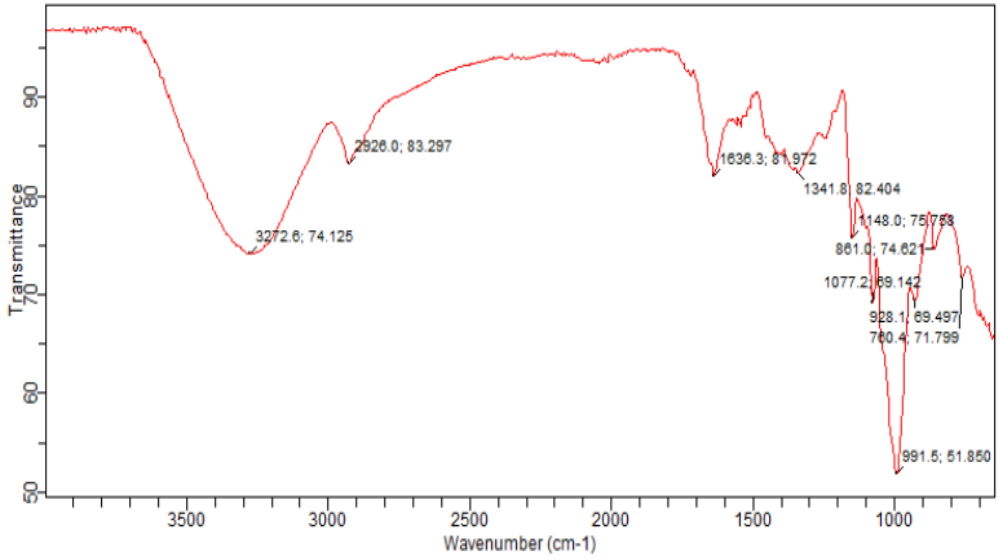

Figure 4. 6:FTIR spectrum of dried aerial yam

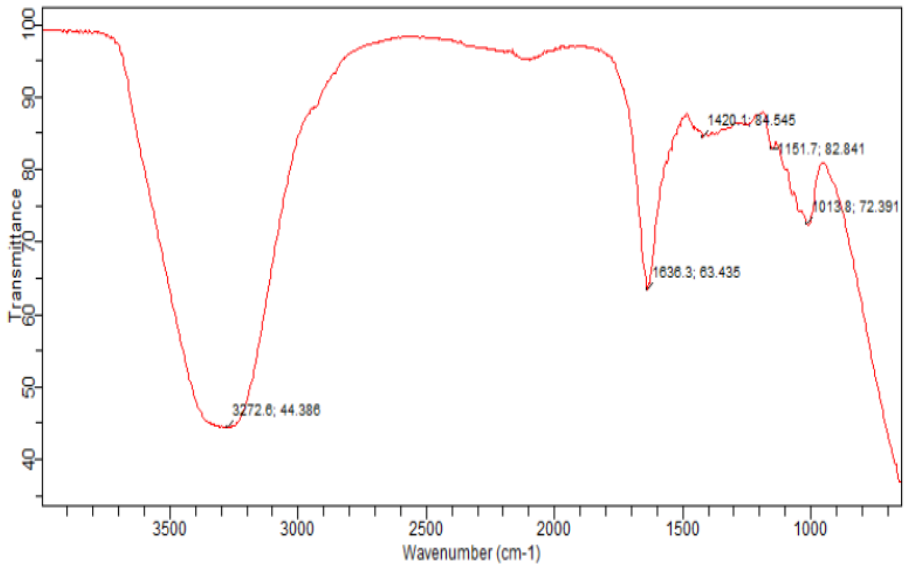

Figure 4. 7: FTIR spectrum of raw Water yam

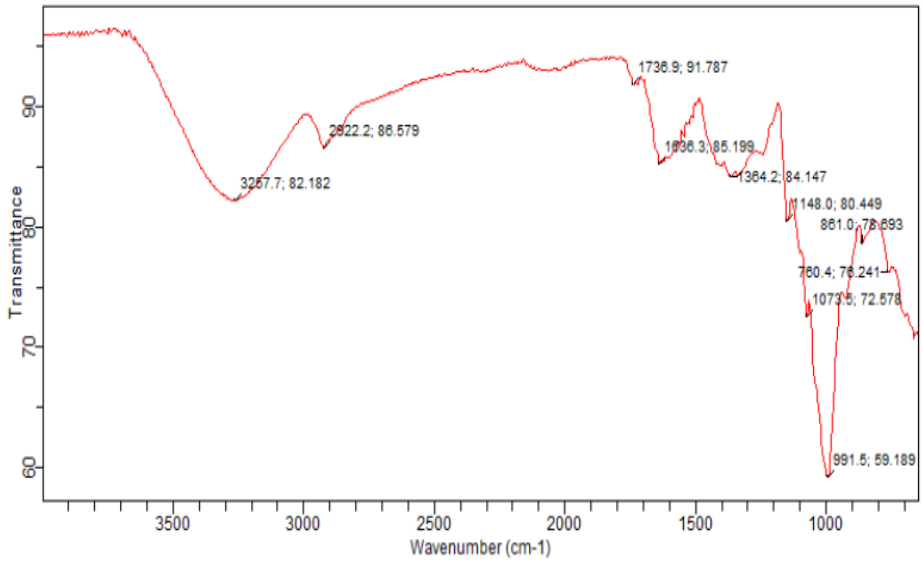

Figure 4. 8: FTIR spectrum of dried Water yam

4.3.3 Scanning electron microscopy of the yam samples.

Plate 4.1 shows the SEM micrograph of raw aerial yam sample. It shows well arranged microtubule, parenchyma and sclerenchyma in its micro structure. Plate 4.2, shows that the tuber was highly degraded leaving the cells with just sheets of parenchyma and sclerenchyma cells, fiber was seen evidently remaining after the drying process was completed, the micro tubules were seen disintegrated and fallen apart by the effect of drying, and relapse of cells were clearly seen, these could be as a result of intensive heat or a chemical reaction as a result of heating, the major role of the micro tubules was for water and electron transport. However, excessive heat leads to the denaturing and fallen apart of these cells as clearly seen in plate 4.2.

Plate 4.3 shows the SEM micrograph of the fresh sample of water yam. It shows beautifully arranged cells, the micro tubules were all seen intact and visible without any form of deformation, the vascular bundle were seen radially arranged and the epidermis and endodermis were over lapping against the other. This radial longitudinal section shows it is a clear monocotyledonous plant with fresh, fleshy and succulent mesoderm. However, plate 4.4 shows the SEM image of dried water yam sample. It shows relapse and degradation as a result of heating, denatured xylem and phloem which is the prominent cell in the vascular bundle is believed to show that effect on the micrograph of the plant tuber.

The Phloem and the xylem, comprise the major part of Anatomy in tuberous plant, with little patches of plasmodesma which explains why tuberous plant contains a lot of fluid in them. These core part of the anatomy of this plant plays a vital role in electron and water transport when tuberous plant like yam are heated or dried, this cell denature and exposes the sieve tubes with sheets of parenchyma and sclerenchyma cells exposed to the surface of the stem. The SEM image of this sample from plate 4.2 and4. 4 shows that the dominant remnant after exposure to

heat is the sieve elements, the definitive callus disintegrates and this account for weight and water loss of about 50% of the initial weight before processing. The fiber which is always ever present remain in small quantity, thermal degradation have little action on the fiber content in yam.

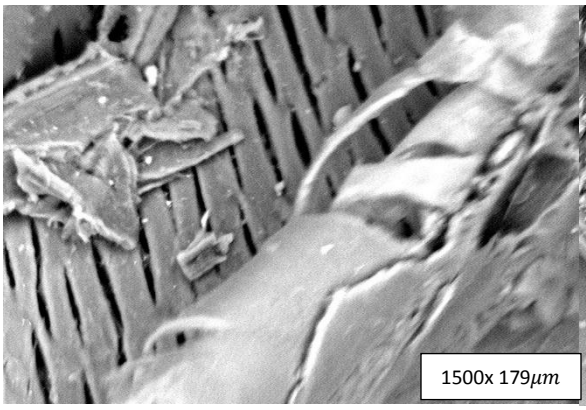

Plate 4. 1:SEM image of raw aerial yam

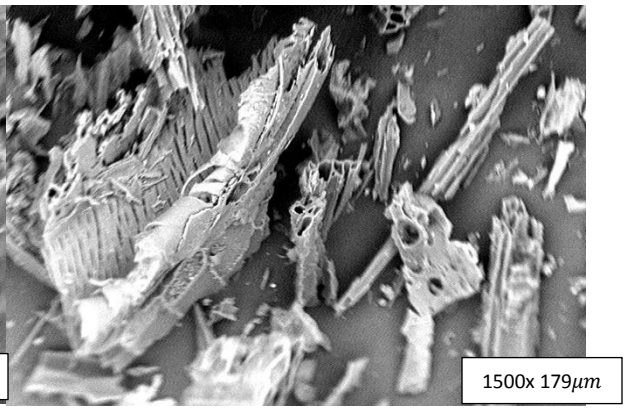

Plate 4. 2: SEM image of dried aerial yam

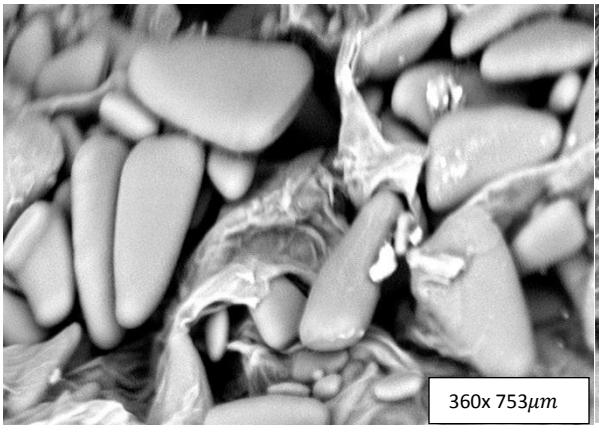

Plate 4.3: SEM image of raw water yam

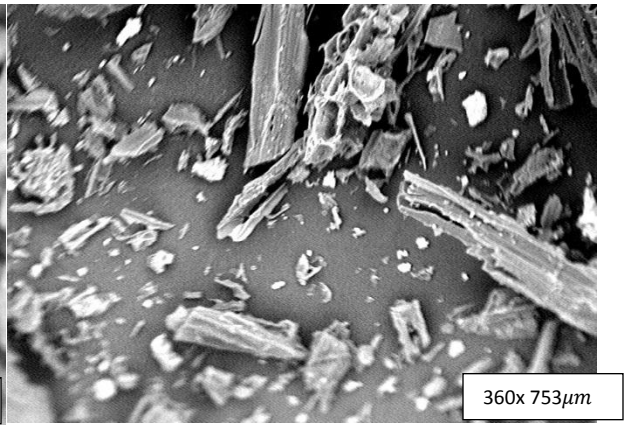

Plate 4.4: SEM image of dried water yam

4.4Engineering Properties of the yams

4.4.1 Mechanical properties of the samples

The shear strength indicates the resistance of the material to the applied load and it is an indicator of the toughness of the product when consumed in the rehydrated state (Markowski & Zielinska, 2013). The toughness indicates the energy absorbed by the material prior to rupture. Figures 4.9 and 4.10 are the plots of the sample dried by hot air and solar dryers respectively, while the numerical data are presented in Tables 4.8 and 4.9. It was observed that for hot air dryer, the raw water yam (RWY) recorded the highest shear strength followed by the blanched water yam (BWY) with the unblanched water yam (UWY) recording the lowest value. For aerial yam, blanched aerial yam (BAY) Unblanched aerial yam (UAY) had then the same numerical values. For the solar dried samples, the water yam follows the same trend as that of the hot air dryer but in the case of the aerial yam, BAY recorded the highest values (4.86N/mm^2), followed by UAY (4.74N/mm^2), with RAY (4.21N/mm^2) recording the list.

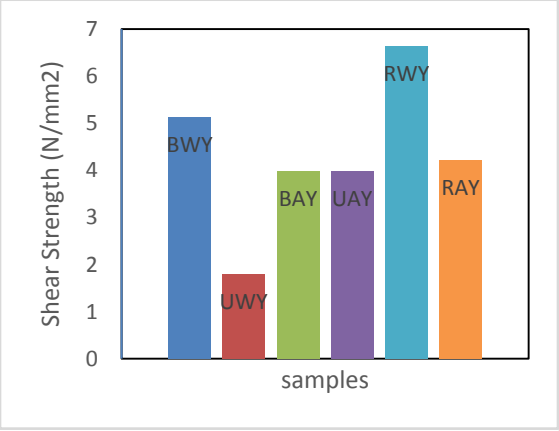

Figure 4. 9:Shear strength for Hot air dryer

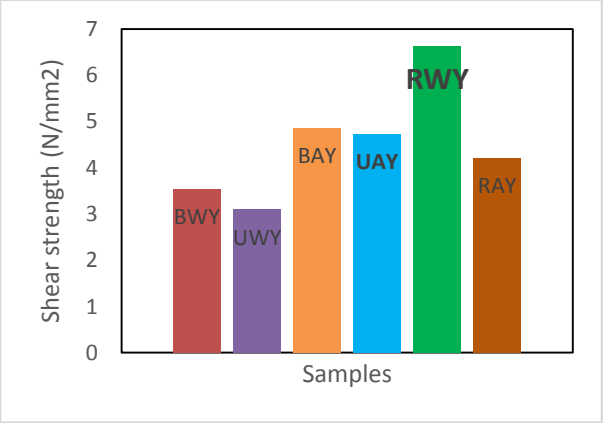

Figure 4. 10:Shear strength for solar dryer

Key: BWY=Blanched water yam, UWY= Unblanched water yam, BAY= Blanched aerial yam, UAY= Unblanched aerial yam, RWY= Raw water yam, RAY= Raw aerial yam.

Hardness is a measure of food crops ability to resist localized plastic deformation and is determined using an indentation test. It is estimated by the magnitude of the reaction force or by the depth of indentation and can be correlated to other mechanical properties, such as ultimate strength and Young's modulus (Callister, 2004). According to Figure 4.11, BWY, UWY, BAY and UAY have HBN values of 31.73, 18.55, 31.98 and 15.58, respectively showing that blanching before drying increases hardness using Hot air dryer. This could be as a result of some structural changes resulting from blanching. Blanching tends to alter the structural arrangement of the materials by weakening some bonds which bind free water so that after drying the blanched materials tend to have lower moisture contents than the unblanched. Figure4.11 also showed that RWY (15.58) and RAY (17.91) have lower value of hardness than both the blanched and unblanched dried samples. However, the values obtained for solar dryer (Figure 4.12) were BWY, UWY, BAY, and UAY; 29.37, 30.06, 24.73 and 30.06 , respectively showing that the unblanched products have a slightly higher value that the blanched products. It could be observed that hot air convective dryer had a higher value of hardness compared to the solar dryer. The high degree of internal heating, which occurs during convective hot air drying results in the formation of significant concentration gradients, thereby causing rapid moisture loss. This differences could also be attributed to the fact that the drying using solar dryer was achieved at ambient temperature while that of hot air drying was done at a much higher temperature that the solar.The low values of hardness for all the dried samples (blanched and unblanched) for both hot air and solar dryer show that water yam and aerial yam had tolerable properties appropriate for efficient industrial and food processing application.

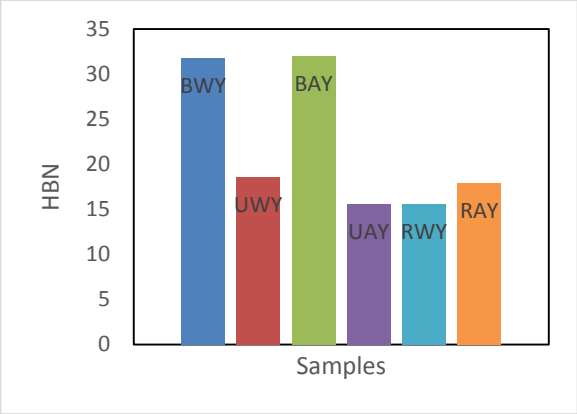

Figure 4. 11: HBN for Hot air dryer

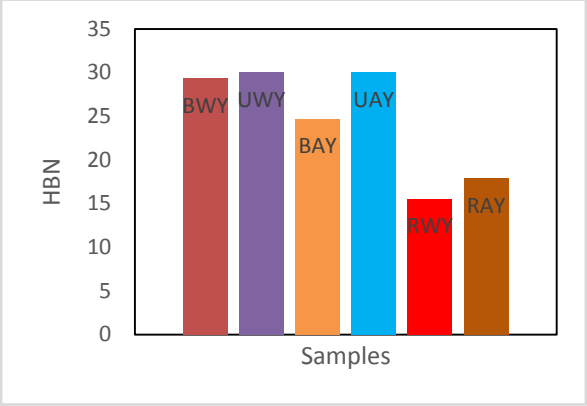

Figure 4. 12: HBN for solar dryer

The bioyield strength is taken as the stress at which the material failed in its internal cellular structure (Mamman, et all 2012). The variation of bio yield force of blanched and unblanched water yam and aerial yam dried with hot air dryer and solar dryer when subjected to compressive loading at the lateral orientation is represented in the Figures 4.13 and 4.14 respectively using the data of Tables 4.8 and 4.9, respectively. The bio yield force increased with blanching with BAY (615N) exhibiting the highest values and the UWY (225.5 N) showing the lowest values for hot air convective dryer. However, UAY (443.5N) exhibited the highest value for solar dryer with BAY (231.5N) showing the least. The minimum bioyield force was obtained for the RAY (87.5N). Overall the convective hot air dryer presented the highest value of bio yield with BAY having a value of 615N. This is because the hot air dryer was operated at a higher temperature range (40-70^{0}C) than of the solar drier which was done at ambient temperature (27-32^{0}C).This is in agreement with the report by Ramana, et al, (1992) that increase in temperature reduces the cellular integrity of biomaterials due to enhanced depolymerization.

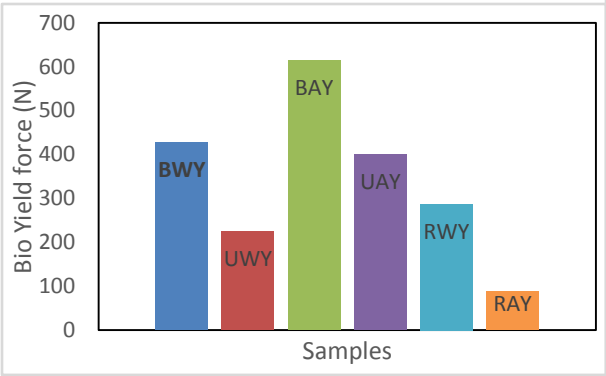

Figure 4. 13:Bio-Yield for Hot air dryer

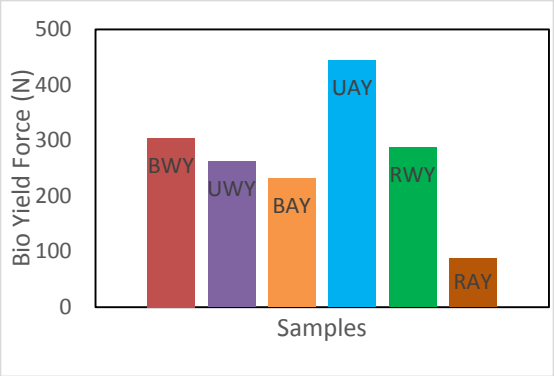

Figure 4. 14:Bio-Yield for solar dryer

For rupture energy, it could be seen from Figure 4.15, that the energy absorbed by the BWY, UWY, BAY, UAY, RWY and RAY before initiating its rupture in the case of hot air convective dryers were 2.73, 1.64, 1.38, 4.70, 2.91 and 1.26 J, respectively indicating that UAY needs more energy to get ruptured while RAY needs the least amount of energy to get ruptured. Similarly, the amount of energy needed by BWY, UWY,BAY, UAY, RWY and RAY in the case of solar dryer (Figure 4.16) were 1.25, 1.72, 1.20, 6.41, 2.91 and 1.26J, respectively which also show that UAY requires the highest amount of energy to rupture. The results showed that the UAY is more flexible and is more resistant to rupturing on the application of loads as compared to the others in both hot air dryer and solar dryer.

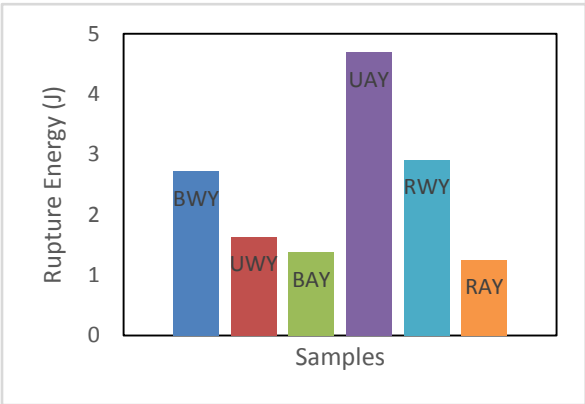

Figure 4. 15:Rupture energy for hot air dryer

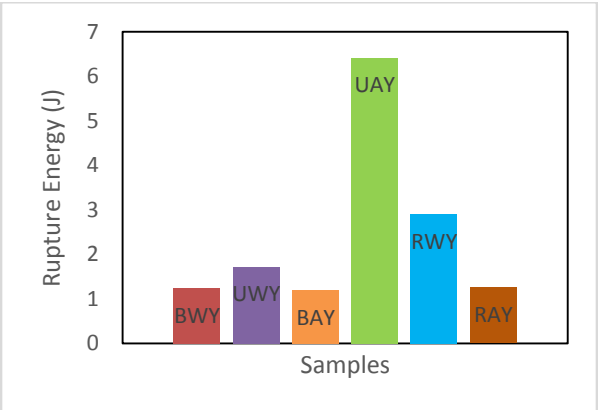

Figure 4. 16:Rupture energy for solar dryer

The modulus of elasticity is defined as a quantity that measures an object or substance's resistance to being deformed elastically when a stress is applied to it. Figures. 4.17 and 4.18 show the modulus of elasticity of samples dried with hot air dryer and solar dryer, respectively. According to Table 4.8, the values of the modulus of elasticity for hot air convective dryer is given as 22.64, 31.72, 36.83, 21.69, 4.53 and 2.78 N/mm^2, respectively for BWY, UWY, BAY, UAY, RWY, RAY. It could be seen that BAY had the highest elastic modulus among other samples which shows that it is stiffer. A stiffer material will have higher elastic modulus. However, for solar dryer, UWY (20.13 N/mm^2) presented higher value (Table 4.9) of elastic modulus than BWY (11.23), BAY (12.78), UAY (13.29), RWY (4.53) and RAY(2.79 N/mm^2). The results show that drying increases the stiffness of materials as the two raw samples (RWY and RAY) had the least elastic modulus. However, the sample dried with hot air convective dryer had higher values of elastic modulus compared to that from solar dryer. It shows that the hot air convective dryer is more efficient in the removal of moisture from the samples than the solar dryer.

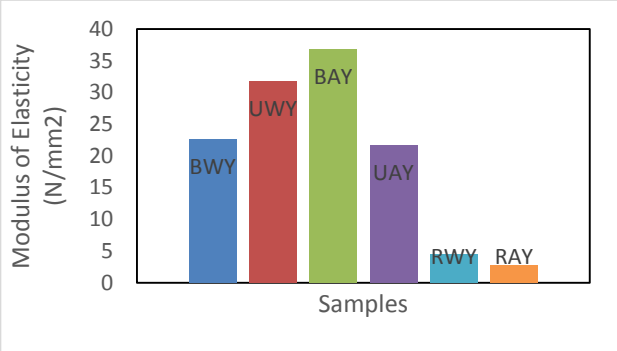

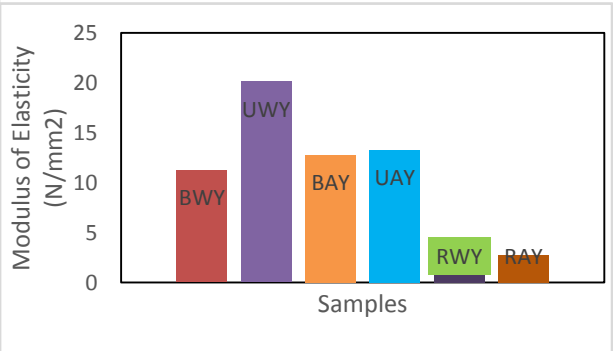

Fig. 4. 17:Modulus of elasticity for solar dryer Fig. 4. 18:Modulus of elasticity for Hot air dryer

Deformation is the change in shape or size of an object that occurs due to the action of an applied force or a change in temperature. Figures 4.19 and 4.20 show the plot of deformation at break for convective hot air dryer and solar dryer. For Figure 4.19, the value of BWY, UWY, BAY, UAY, RWY and RAY were 3.25, 2.25, 1.815, 4.375, 7.5 and 6.275mm, respectively for convective hot air dried samples. This result shows that the raw samples presented higher values of deformation at break for samples dried with convective hot air dryer. Figure 4.20 also shows the values of BWY, UWY, BAY, UAY, RWY and RAY to be 3.125, 2.75, 2.875, 6.5, 7.5 and 6.275 mm, respectively for solar dried samples. This also showed that the raw samples (RWY, RAY) had higher values of deformation at break than the dried samples.

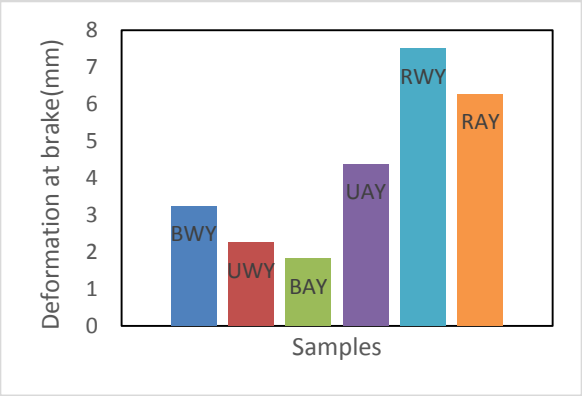

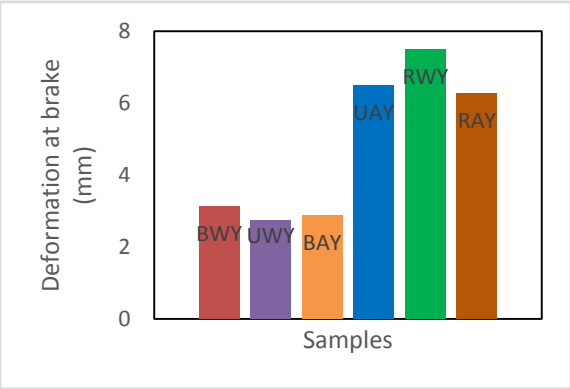

Fig. 4.19:Deformation at break for Hot air dryer Fig. 4.20:Deformation at break for solar dryer

Compressive strength shows how much the sample will deform under applied compressive loading before plastic deformation occurs. The variation of compressive strength of BWY, UWY, BAY, UAY, RWY and RAY when subjected to compressive loading are presented in Figures 4.21 and 4.22, respectively for hot air dryer and solar dryer. According to Figure 4.21 for hot air convective dryer, UAY had the highest compressive strength (2.69 N/mm^2) and closely

followed by BWY, BAY and UWY with values of 2.09, 1.91, 1.81 N/mm^2, respectively. The result also shows that the two raw sample (RWY, RAY) had lower value of compressive strength, which could be as a result of the presence of much moisture in the raw sample. However, the values of compressive strength obtained from the sample when using solar dryer are much smaller than that obtained from hot air dryer though UAY (2.47 N/mm^2) for solar is almost equal to UAY from hot air dried sample (2.69 N/mm^2). The values of BWY (0.94), UWY (1.23) and BAY (1.05 N/mm^2) for solar is much smaller when compared to that for hot air dryer. This shows that convective hot air dryer is more efficient in the removal of moisture from the aerial yam and water yam since the presence of moisture indicates low compressive strength (Aviara et al., 2013).

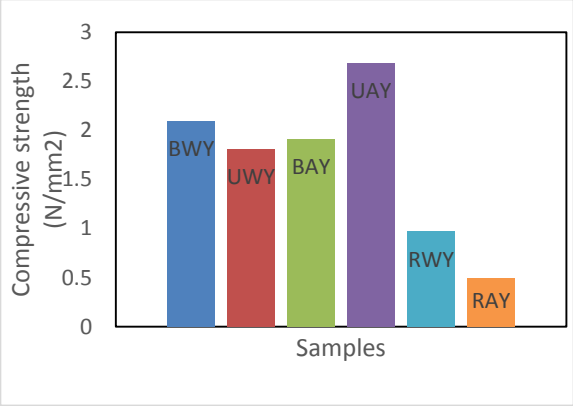

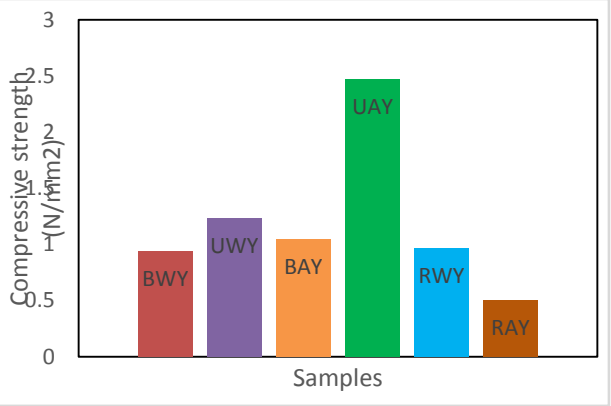

Fig. 4. 21:Compressive strength for Hot air dryer Fig. 4. 22:Compressive strength for solar dryer

Gumminess is seen as a parameter derived from hardness × cohesiveness (Al-Hinai *et al.* 2013); therefore, anything that affects hardness will also affect gumminess in the same way. When the temperature rose, stickiness levels increased as well (Özge et al., 2018). Gumminess is a characteristic of semisolid foods with a low degree of hardness and a high degree of cohesiveness. From Figures 4.23 and 4.24, it was observed that drying generally reduces gumminess for both hot air and solar dried water yam and aerial yam. This is because drying

reduces moisture that bounds the particles together, thus reducing cohesiveness. It could also be seen that the blanched samples (BWY, BAY) for both hot air and solar dryers were higher that the unblanched samples (UWY, UAY). This could be as a result of the distortion in water starch bond that occurs during blanching which enhances starch to starch bond. Also during drying, blanched samples lose more moisture than the unblanched samples thus, resulting in more starch concentration.

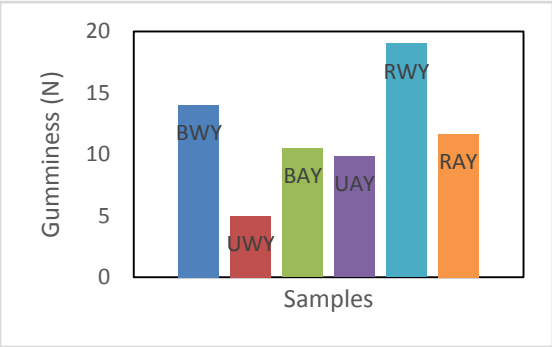

Figure 4. 23:Gumminess for Hot air dryer

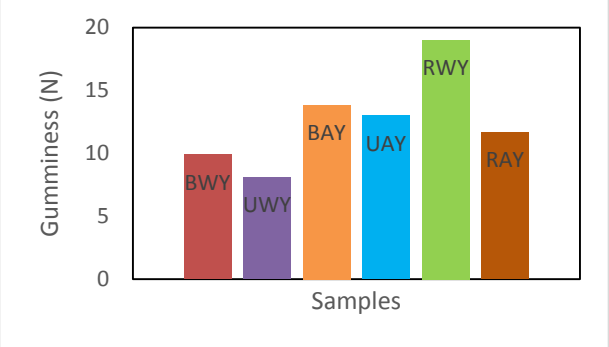

Figure 4. 24:Gumminess for solar dryer

Table 4. 8: Mechanical properties of hot air dried water yam and aerial yam

properties	units	BWY	UWY	BAY	UAY	RWY	RAY
shear force	N	145	51	112.5	112.5	187.5	119
shear strength	N/mm^2	5.127	1.8035	3.978	3.978	6.63	4.208
HBN	---	31.728	18.554	31.977	15.582	15.582	17.908
Bio-yield	N	428.125	225	615	400	287.5	87.5
Energy	J	2.729	1.6375	1.383	4.6995	2.9125	1.2559
Elasticity	N/mm^2	22.638	31.719	36.8285	21.686	4.5315	2.7875
Deformation at brake	mm	3.25	2.25	1.815	4.375	7.5	6.275
compressive force	N	837.75	725	762.5	1075.25	387.5	200
compressive strength	N/mm^2	2.0945	1.8125	1.9065	2.6875	0.969	0.5005
Gumminess	N	14	4.975	10.5	9.85	19	11.65

Table 4. 9:Mechanical properties of solar air dried water yam and aerial yam

properties	units	BWY	UWY	BAY	UAY	RWY	RAY
shear force	N	100	87.5	137.5	134	187.5	119
shear strength	N/mm^2	3.536	3.094	4.86	4.7385	6.63	4.208
HBN	---	29.37393	30.06378	24.72843	30.06378	15.58241	17.90803
Bio-yield	N	304.5	262.5	231.5	443.5	287.5	87.5
Energy	J	1.2495	1.7265	1.204	6.419	2.9125	1.2559
Elasticity	N/mm^2	11.2315	20.125	12.784	13.2935	4.5315	2.7875
Deformation at brake	mm	3.125	2.75	2.875	6.5	7.5	6.275
compressive force	N	400.25	627.5	419	987.5	387.5	200
compressive strength	N/mm^2	0.938	1.2315	1.048	2.469	0.969	0.5005
Gumminess	N	9.9	8.1	13.85	12.99	19	11.65

4.4.2 Thermal Properties

Thermal properties of food products include their specific heat capacity, thermal conductivity and diffusivity. The knowledge of these thermal properties of food materials is very important in the design of industrial dryers for drying them.

i. Specific Heat capacity

The specific heat capacities of the yam samples were calculated according to eqn. (3.10) using the method outlined by Luther et al, (2003) and shown in Figure 4.25.

The specific heat capacity of the samples decreased after drying for both water yam and aerial yam. The specific heat capacity of decreased from 3.21 to 1.55 KJ/kgK as the water yam was dried while it decreased from 3.06 to 1.66 as the aerial yam was dried. This is relatively high due to the fact that both water yam and aerial yam contain high moisture content since water has the greatest effect upon specific heat capacity among other constituents (Luther et al, 2003). Ademiliyu et al (2006) reported values of ranging from 1.085 to 1.284 KJ/KgK for specific heat capacity of bone dry fermented ground cassava cultivars. The specific heat capacity of water is higher than that of aerial yam as expected because it contains higher water content since water has the greatest effect upon specific heat capacity among other constituents (Luther et al, 2003).

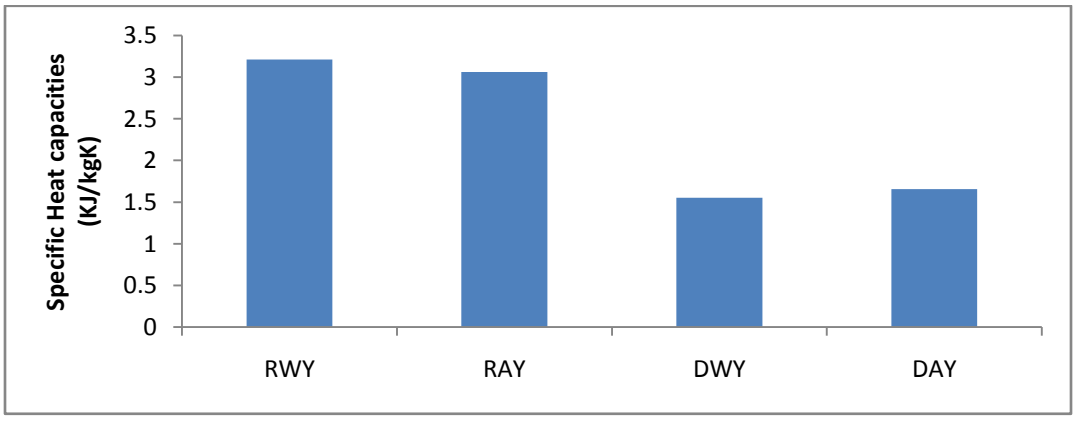

Figure 4. 25: Specific heat capacities of the yam samples

ii. Thermal conductivity

The variation of the thermal conductivity on the yam samples were calculated according to eqn. (3.11) and are shown in Figure 4.26. The values ranged from 0.452 to 0.256 W/mK for water yam and 0.437 to 0.271 W/mK for aerial yam. Thermal conductivity deals with the ease with which heat flows through a material. The thermal conductivity decreased for dried products. It is strongly influenced by a material's water content. In drying of cassava, Nwabanne (2009) reported thermal conductivity values of 0.24 W/mK. It was reported by Luther et al (2003) that the thermal conductivity of most food materials is in the range of 0.2 to 0.5 W/mK.

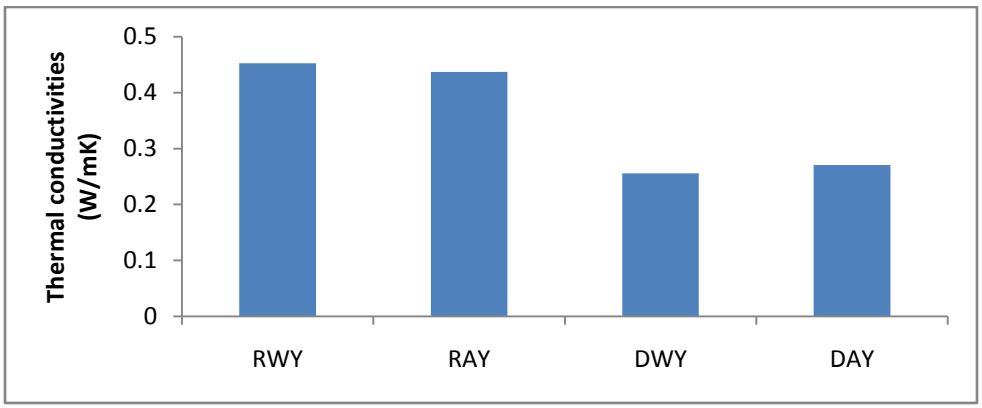

Figure 4. 26: Thermal conductivities of the yam samples

iii. Thermal diffusivity

Thermal diffusivity is a measure of how fast heat propagates or diffuses through a material. Thermal diffusivity is very relevant in transient heat transfer where temperature varies with time and location and it is a combination of three basic thermal properties namely; thermal

conductivity, density and specific heat capacity (Luther et al, 2003). The thermal diffusivities of the yam samples were calculated according to eqn. (3.12) using the method of Luther et al, (2003). Figure 4.27 shows the thermal diffusivities of the yam samples. The thermal diffusivity increased with drying for the products ranging from 1.28 x 10^{-4} to 1.5 x 10^{-4} m^2/s for water yam and from 1.3 x 10^{-4} to 1.49 x 10^{-4} m^2/s for aerial yam. The Thermal diffusivity of ground cassava has been reported to be between 9.0 x 10^{-4} to 2.0 x 10^{-4} (Nwabanne, 2009).

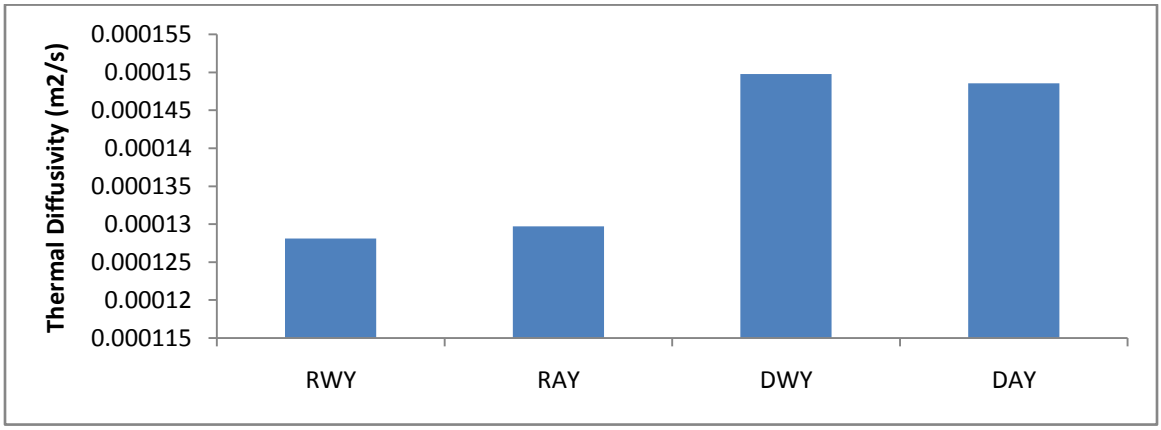

Figure 4. 27:Thermal Diffusivities of the yam samples

4.5 Batch Studies on Moisture Content Variation

The effects of process parameters such as temperature, air speed, slice thickness, time on the moisture content were investigated using both the solar dryer and the convective dryer. Equally, the experiment was done to determine if there is any effect on blanching. The blanching was done by soaking the yam samples in hot water for 20 minutes. The average maximum temperature, minimum temperature and average solar radiation of the surroundings of the Department of Chemical Engineering Laboratory, Nnamdi Azikiwe University, Awka were measured and the results are presented in table A.31 in Appendix.

4.5.1 Effect of slice thickness on moisture content

Slice thickness is one of the main factors affecting the drying characteristics of food materials. The variation of the slice thickness with the moisture content was evaluated by drying different slice thicknessesof the yam samples as shown in Figures 4.28 to 4.35 at constant air speed. The numerical data is shown in Tables A.29-A.33 The slice thicknesses used were 2.0mm, 4.0mm and 6.0mm for both solar and convective dryer. The rate of moisture content decrease was found to be dependent on the thickness of the sample. This is because, after the same time interval, the moisture content of the 2.0mm samples was found to be much smaller than the moisture content of 4.0mm and the 6.0mm samples. Hence, the rate of moisture content removal decreased as the slice thickness increased. This is because, at low slice thicknesses, the free moisture can be easily removed from the surface. The thicker the slice, the slower the approach to equilibrium moisture content and the slower the drying rate (Etoamaihe & Ibeawuchi, 2010).

The convective dryer was found to be faster in reducing the moisture content of the yam samples. This is probably because of the additional heat that is supplied by the dryer. In addition, Mohammad et al, (2013) reported that at fixed temperature, the drying time of a product increases as the product becomes thicker mainly because the moisture dissipation inside the product and finally its departure from the product would face more resistance, hence prolonging the drying time. Aremu et al (2013) when investigating the effect of slice thickness on drying kinetics of mango reported that the drying time increased as the slice thickness increase. This is in agreement with the findings of Etoamaihe and Ibeawuchi (2010) in drying different slices of cassava.

It was found out that the effect of the blanching was minimal and almost negligible. Though blanching caused the initial moisture content of the yam sample to increase, yet it took almost the same time of 300 minutes for both the blanched and unblanched yam samples to reach

equilibrium moisture content. The moisture content was seen to decrease with time as expected because drying removes the water molecules in the food samples (John et al, 2008). With the 2mm thick slices, drying of yam samples attained equilibrium moisture content at 270 minutes while for the 4mm thick slice, a time of 390 minutes was needed to attain equilibrium moisture content. When a bigger slice thickness of 6mm was used, it took a time of about 510 minutes to achieve equilibrium moisture content.

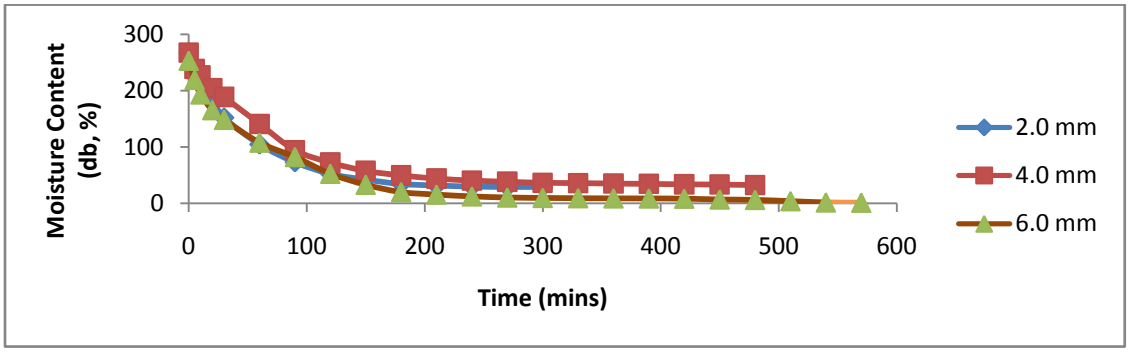

Figure 4. 28:Effect of slice thickness on moisture content for drying of unblanched water yam using the convective dryer

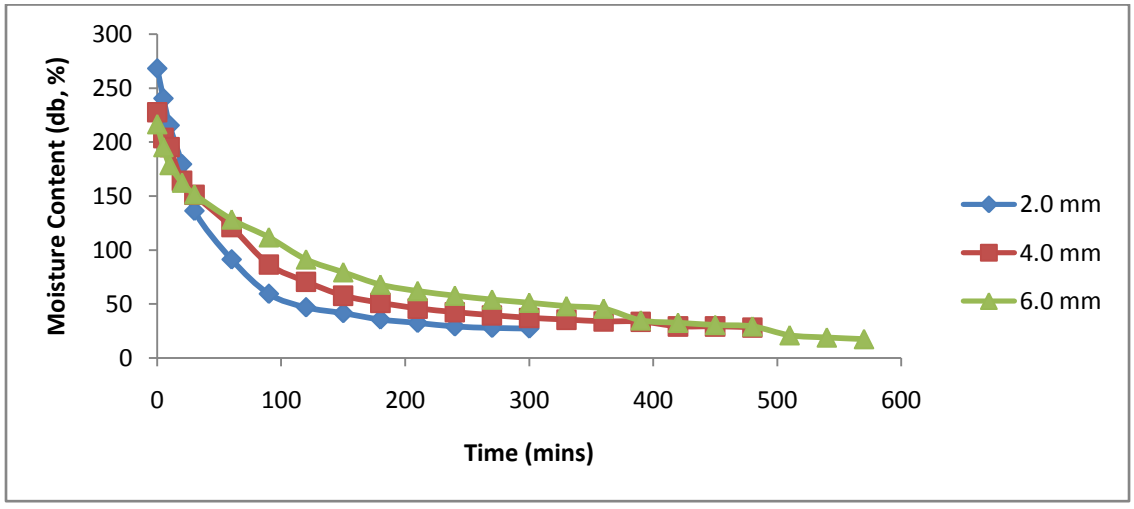

Figure 4. 29: Effect of slice thickness on moisture content for drying of unblanched aerial yam using the convective dryer

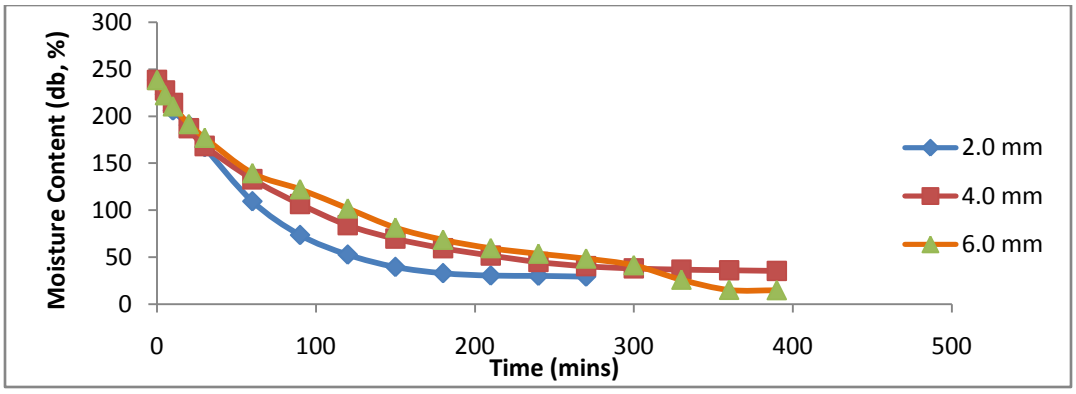

Figure 4. 30: Effect of slice thickness on moisture content for drying of blanched water yam using the convective dryer

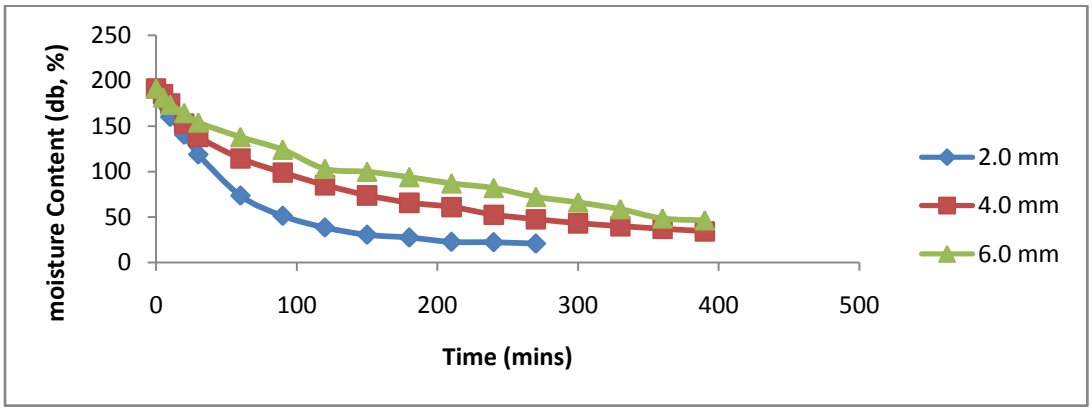

Figure 4. 31:Effect of slice thickness on moisture content for drying of blanched aerial yam using the convective dryer

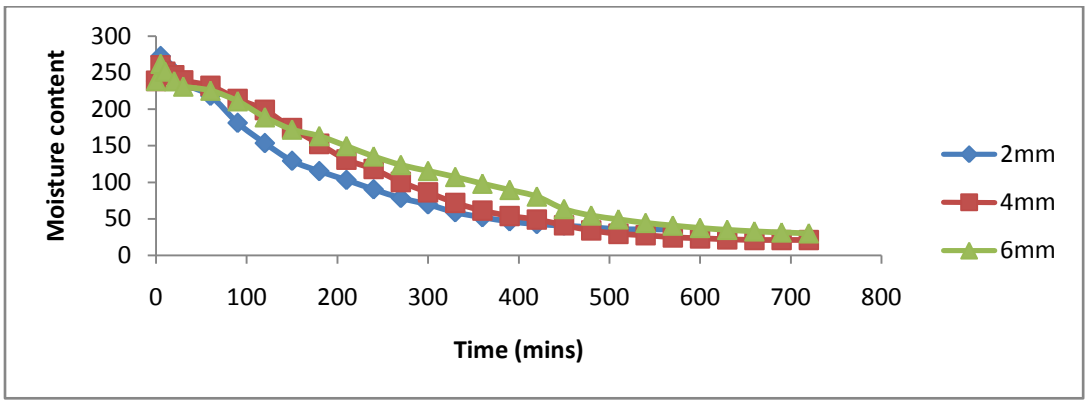

Figure 4. 32: Effect of slice thickness on moisture content for drying of unblanched water yam using the solar dryer

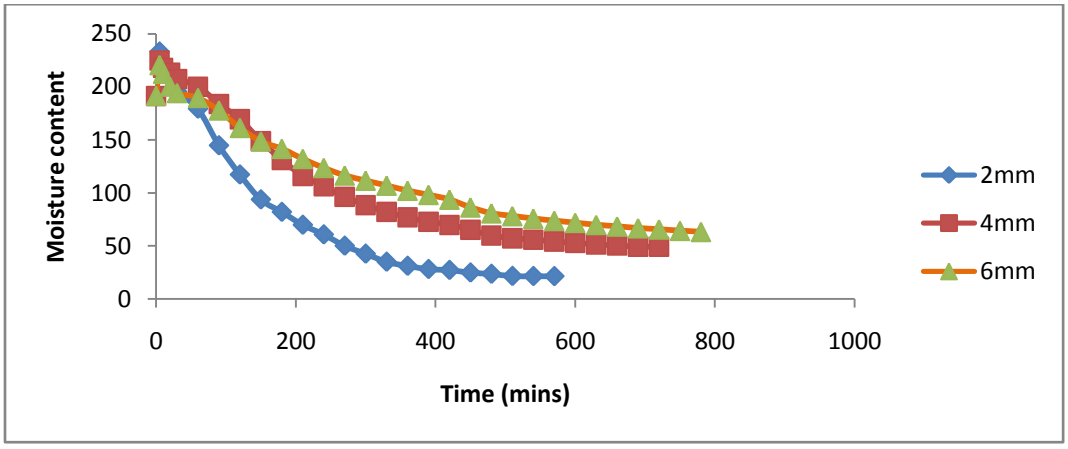

Figure 4. 33: Effect of slice thickness on moisture content for drying of unblanched aerial yam using the sola r dryer

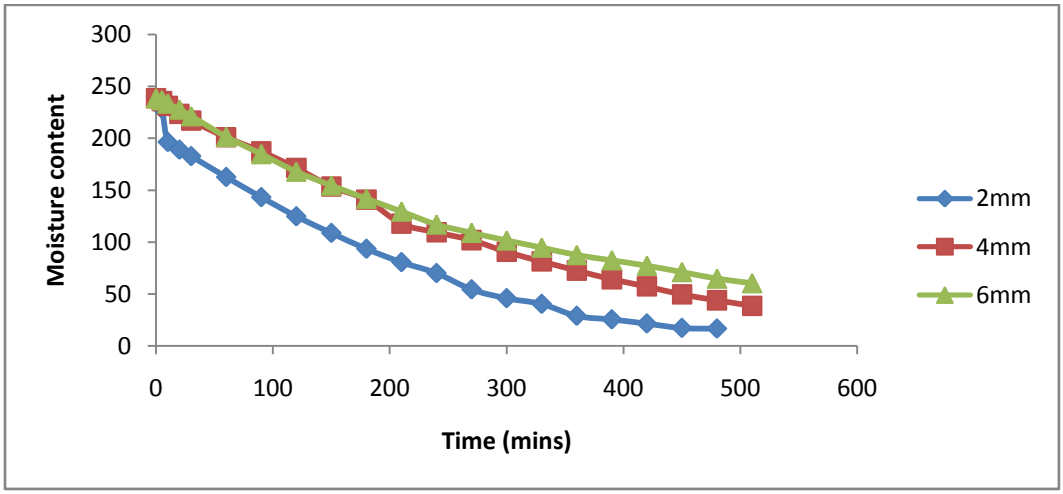

Figure 4. 34: Effect of slice thickness on moisture content for drying of blanched water yam using the solar dryer

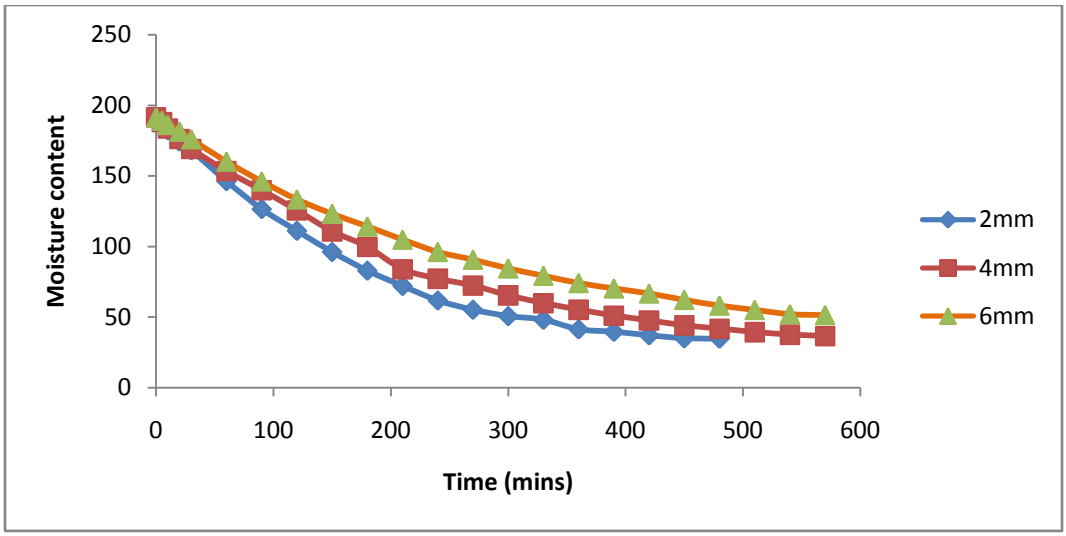

Figure 4. 35: Effect of slice thickness on moisture content for drying of blanched aerial yam using the solar dryer

4.5.2 Effect of Drying Air Speed on Moisture Content

Different air speeds were used to study the effect of air speed on the drying characteristics of the yam samples as given in figure 4.36 to 4.43 at constant slice thickness (2.0mm). The tabular data is shown in Tables A.27, A.28, A.34. The air speeds used were 2.0, 2.5, 3.0, 3.5 and 4.0 m/s for convective dryer and 0.5m/s, 1.0m/s, 1.5m/s, 2.0m/s and 2.5m/s for solar dryer at 2.0 mm constant thickness.

A decrease in the drying time and increase in the drying rate of the yam samples was observed as the air speed was increased. This is because one of the requirements for drying is that the air must be moving. When the hot dry air absorbs water from the surface of the drying product, it needs to be quickly moved on so that another set of air can repeat the process. The faster this process, the higher the drying rate will be. Hence, it is seen that the drying time is decreased as the air speed increased.

Though smaller drying speed was used in the solar dryer, it was discovered that the time to attain equilibrium moisture content was almost the same. With an air speed of 2m/s in convective

dryers, a drying time of 300 minutes was required in other to attain equilibrium moisture content while for drying with an air speed of 4m/s, a drying time of 270 minutes was required. When the air speed was increased to 4 m/s, a lower drying time of 240 minutes was required to achieve equilibrium moisture content.

There was an insignificant difference in the time to attain equilibrium moisture content for both the blanched and unbalanced yam samples. The blanched yam samples have higher initial moisture content hence, it dried much faster than the unbalanced yam samples. In thin layer drying model, the rate of change in material moisture content in the falling rate drying period is proportional to the instantaneous difference between material moisture content and the expected moisture content when it comes into equilibrium with the drying air (Mohammad et al, 2013). The combination of higher temperature, movement of the air and lower humidity in a solar dryer increases the rate of drying. The moisture content decreases continuously with drying time (Wankhade et al, 2012).

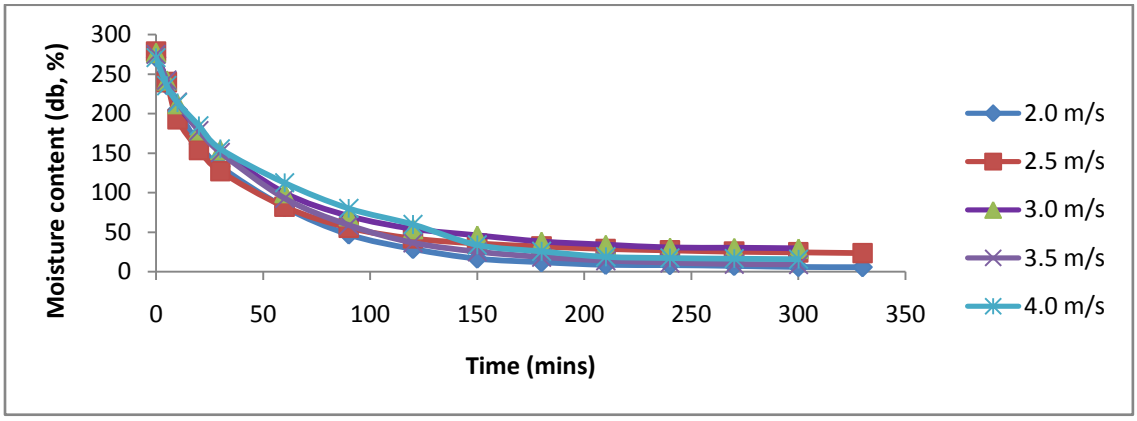

Figure 4. 36: Effect of drying air speed on moisture content for drying of unblanched water yam using the convective dryer

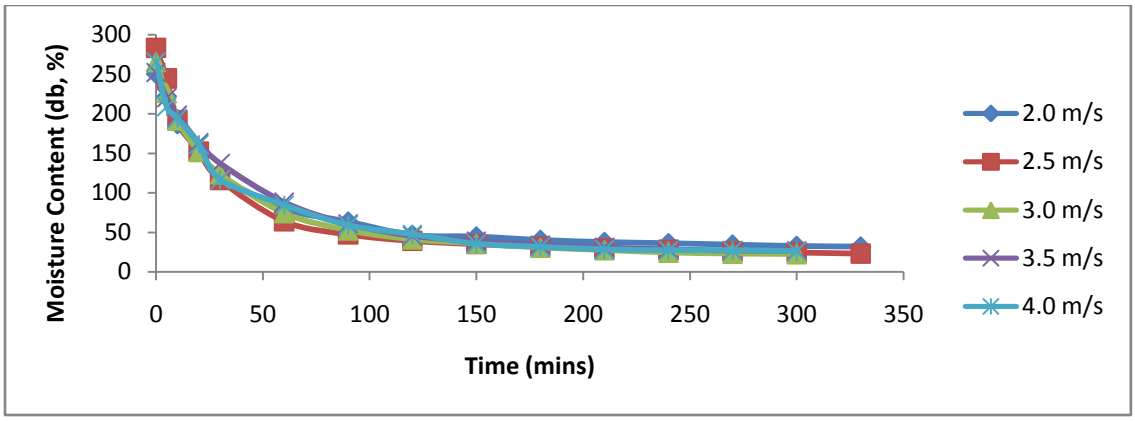

Figure 4. 37: Effect of drying air speed on moisture content for drying of unblanched aerial yam using the convective dryer

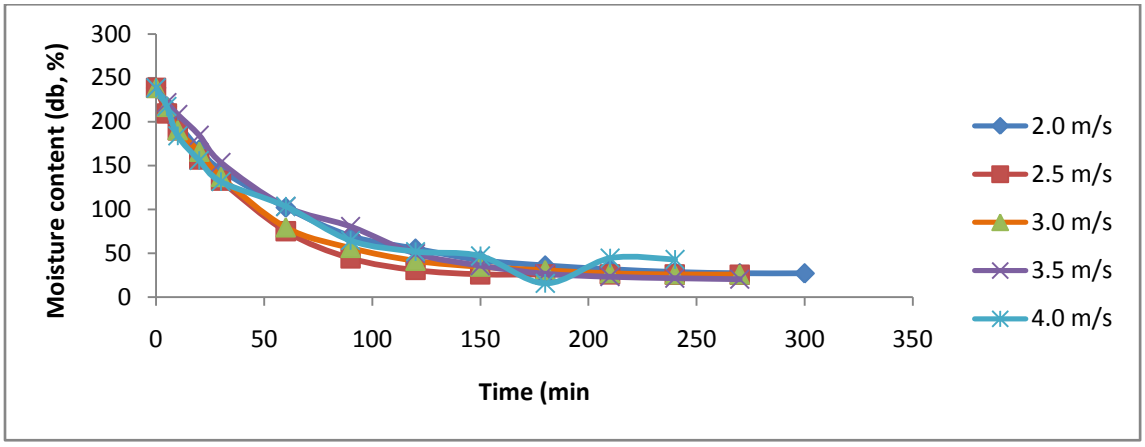

Figure 4. 38:Effect of drying air speed on moisture content for drying of blanched water yam using the convective dryer

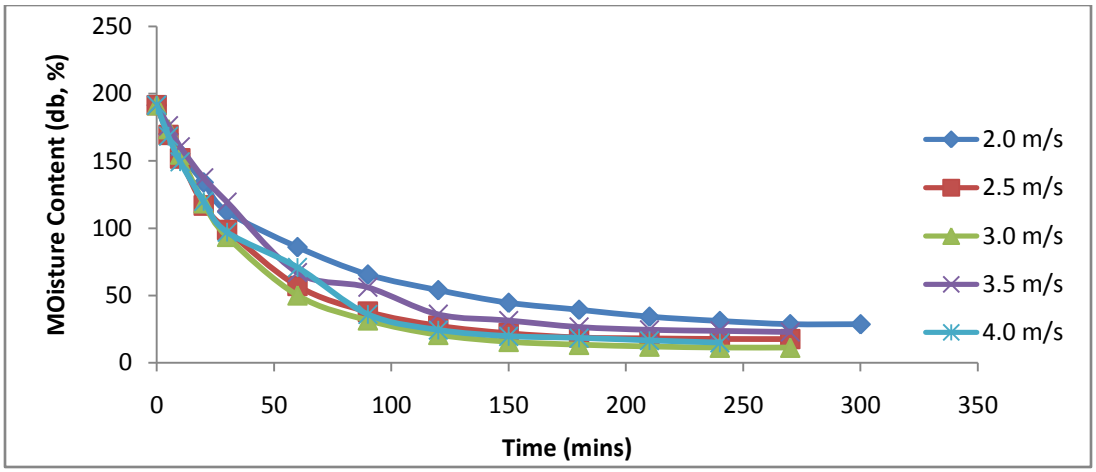

Figure 4. 39: Effect of drying air speed on moisture content for drying of blanched aerial yam using the convective dryer

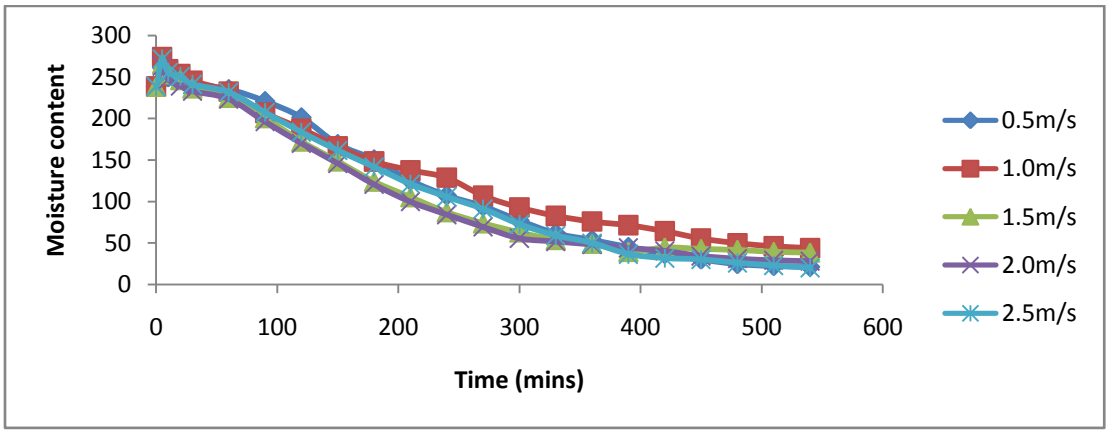

Figure 4. 40: Effect of drying air speed on moisture content for drying of unblanched water yam using the solar dryer

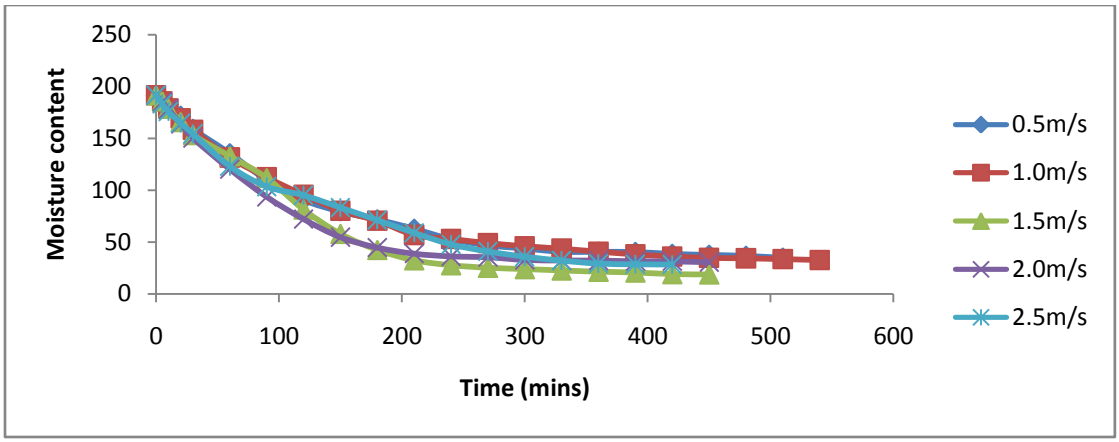

Figure 4. 41: Effect of drying air speed on moisture content for drying of unblanched aerial yam using the solar dryer

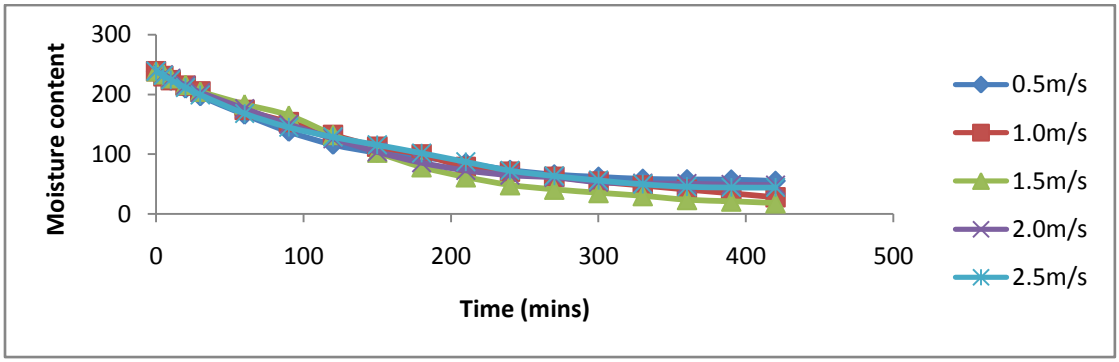

Figure 4. 42:Effect of drying air speed on moisture content for drying of blanched water yam using the solar dryer

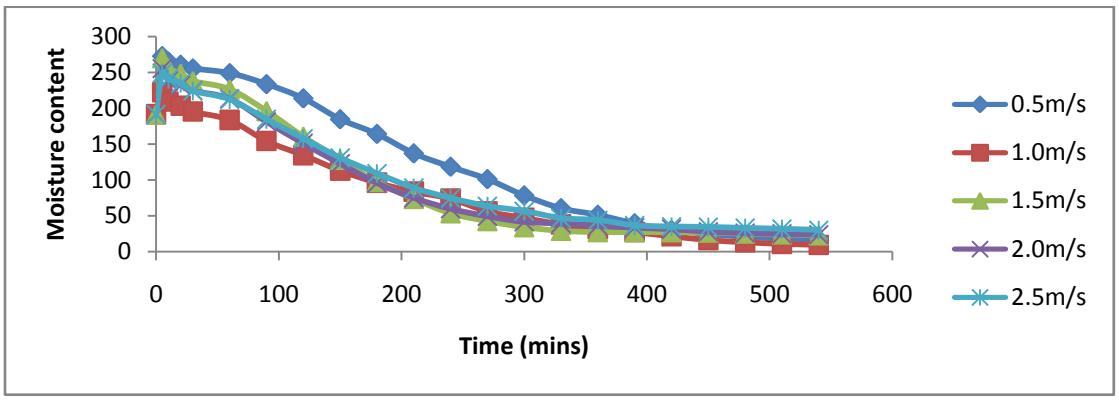

Figure 4. 43:Effect of drying air speed on moisture content for drying of blanched aerial yam using the solar dryer

4.5.3 Effect of Temperature on Moisture Content

The effect of changes in the drying temperature of the convective dryer on the moisture content was investigated using different temperature at constant slice thickness of 2mm and constant air speed of 2.5 m/s and the results are presented in Figures 4.44 to 4.47. The tabular data is shown in Tables A.1-A.8. The temperatures used were 40, 50, 60 and 70 ^{o}C. These ranges of temperatures were used because using a very high temperature may cause the food item to be hardened on the surface (Adu et al, 2012).

The effect of the blanching was significant in the effect of temperature because the plots indicated that the blanched yam samples dried faster than the unbalanced yam samples.

The results showed that as the temperature increased, the drying time to attain equilibrium moisture content was decreased. Using drying temperature of 40 ^{o}C, a drying time of 420 minutes was required to reach equilibrium moisture content while a temperature of 50 ^{o}C gave a drying time of 300 minutes. When a temperature of 70 ^{o}C is used a drying time of just 210 minutes was needed to achieve equilibrium moisture content.

This is due to the fact that as the temperature increased, the average kinetic energy of the moisture increases making it easier for the moisture to diffuse out of the products. It was seen that drying at higher temperature affected the drying time as would have been expected.

Wankhade et al (2012) and Saeed et al (2008) reported that air temperature had a significant effect on the moisture content of samples. Increasing the temperature brings about a decrease in drying time because both the thermal gradient inside the object and the evaporation rate of the product increase (Mohammad et al, 2013).

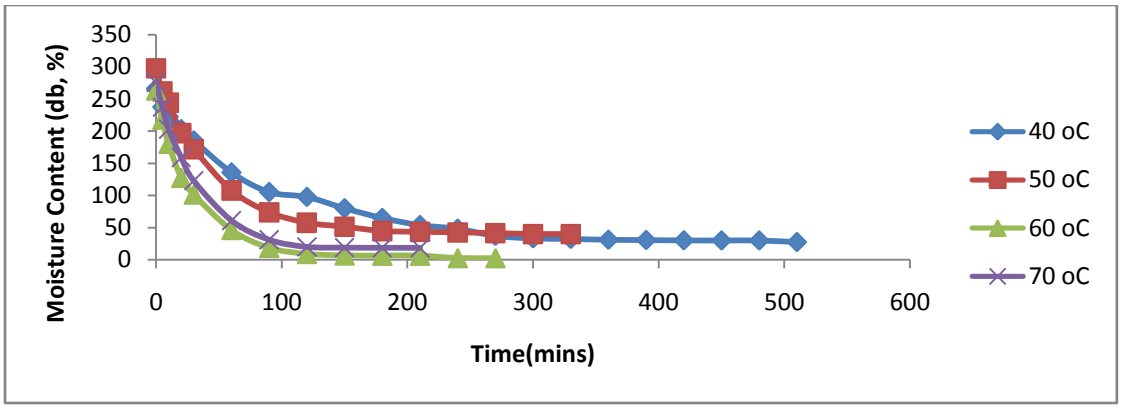

Figure 4. 44: Effect of inlet air Temperature on moisture content for drying of unblanched water yam using convective dryer

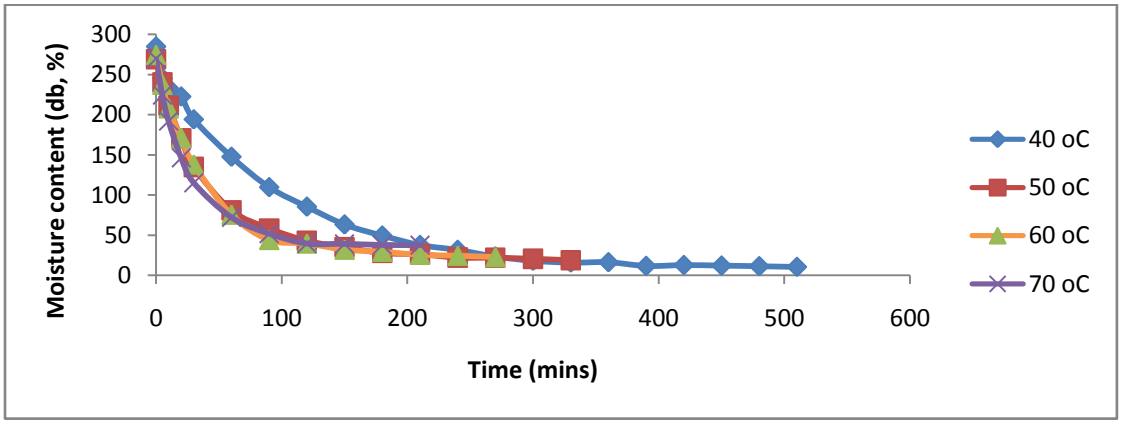

Figure 4. 45:Effect of inlet air Temperature on moisture content for drying of unblanched aerial yam using the convective dryer

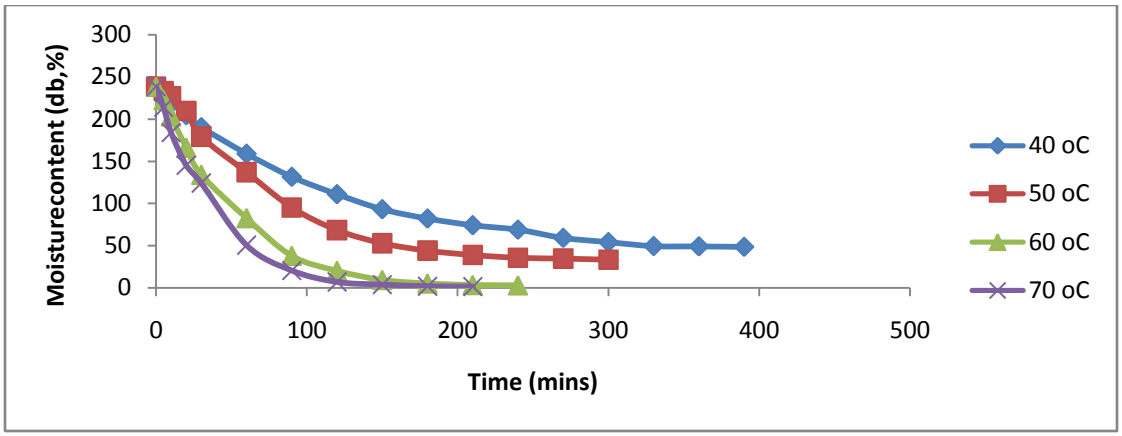

Figure 4. 46: Effect of inlet air Temperature on moisture content for drying of blanched water yam using the convective dryer

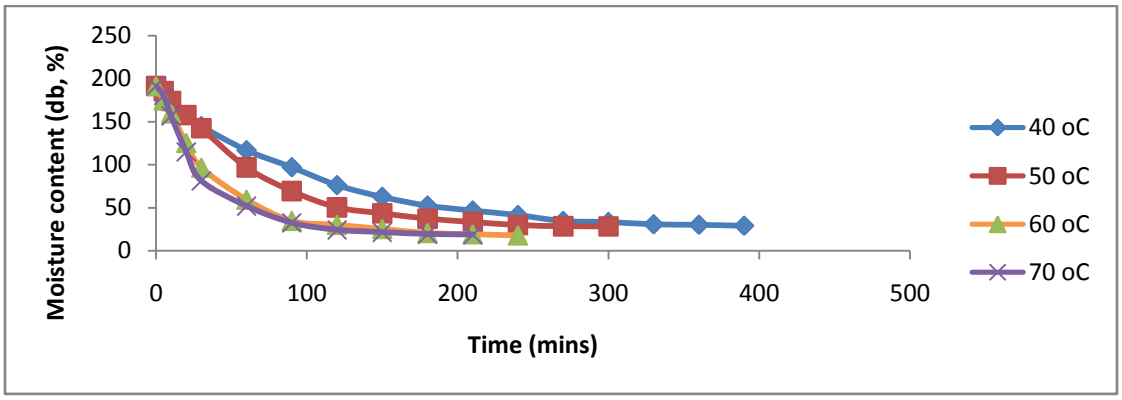

Figure 4. 47:Effect of inlet air Temperature on moisture content for drying of blanched aerial yam using the convective dryer

4.6 Drying rate

The drying rate is the amount of moisture content removed per unit time. It shows the rate at which the sample is being dried. The drying rate was evaluated as the decrease of the water concentration during the time interval between two subsequent measurements divided by the time interval (Anna et al, 2014). This was done for both convective and solar dryers. Slice thickness, drying temperature and drying air speed were discovered to affect the drying rate.

4.6.1 Effect of slice thickness on drying rate

The main factor that controls the drying rate is the rate at which moisture can move from the interior of a piece of food to the surface. Therefore the shorter the distance that moisture has to travel, the faster the drying rate will be. Different slice thickness of 2mm, 4mm and 6mm were used to investigate the effect of slice thickness on the drying rate of the yam samples as shown in Figures 4.48to 4.55 at constant airs speed and temperature of 2.5 m/s and 50 ^{o}C, respectively. The numerical data is shown in Table A.19-A.24.

The drying rate of the convective dryer was higher than the drying rate of the solar dryer. The drying rate gradually decreased as the slice thickness increased. After 90 minutes of drying, the drying rate of the 2 mm slice thickness was 0.353 g/g.min for drying of water yam while for 4 mm and 6 mm slice thickness, the drying rate were 0.261 and 0.169 g/g.min.

The drying rate was less for the unblanched yam samples. Reducing the slice thickness increases the surface area of the food in relation to the volume of the pieces which increases the rate at which water can be evaporated from the food. During the initial period, drying rate is high. This is due to the fact that the energy required to evaporate the surface moisture is low (Sajith & Muraleedharan, 2014). With moisture content, the drying rate decreases as the moisture content decrease. This is probably because the amount of moisture removed depends on the quantity of moisture in the product.

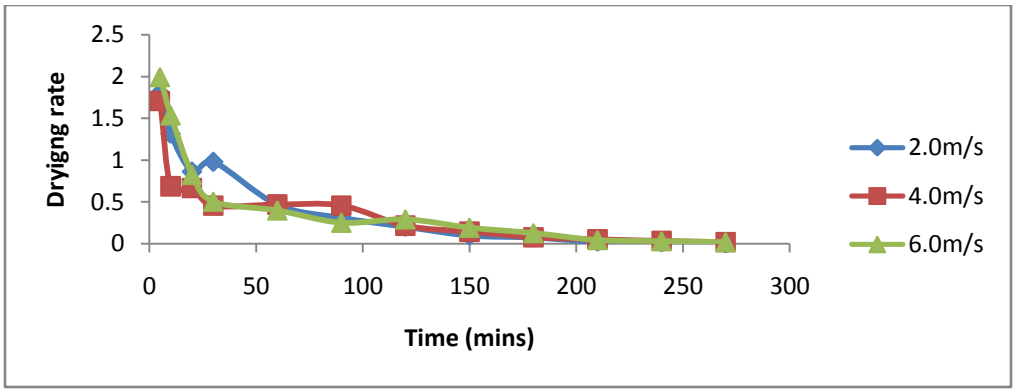

Figure 4. 48:Plot of drying rate against time at different slice thicknesses for drying of unblanched water yam using convective dryer

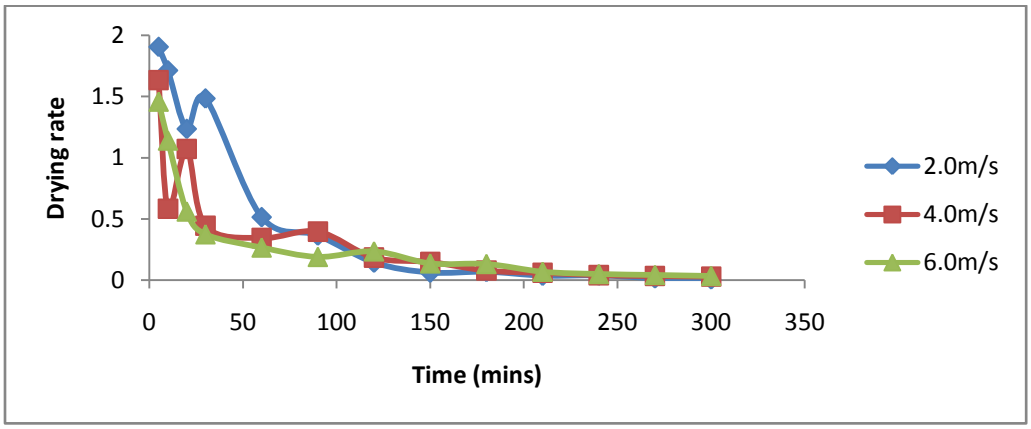

Figure 4. 49:Plot of drying rateagainst time at different slice thicknesses for drying of unblanched aerial yam using convective dryer

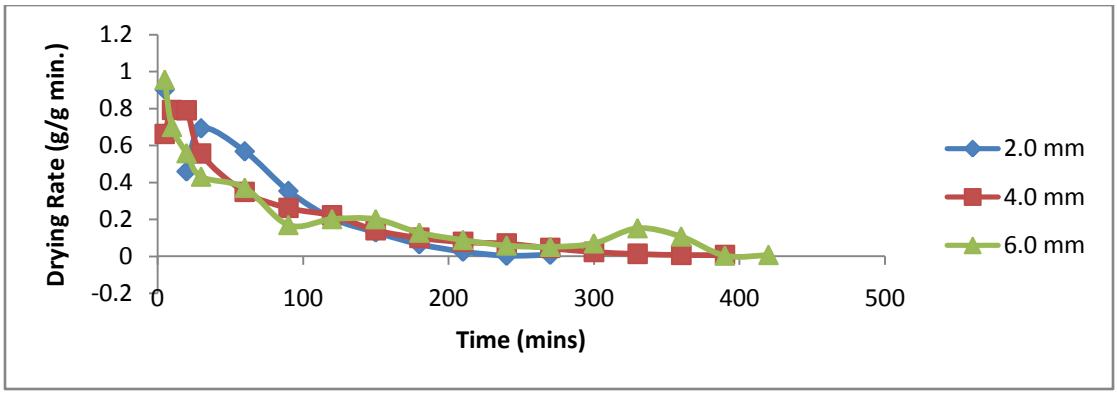

Figure 4. 50: Plot of drying rate against time at different slice thicknesses for drying of blanched water yam using convective dryer

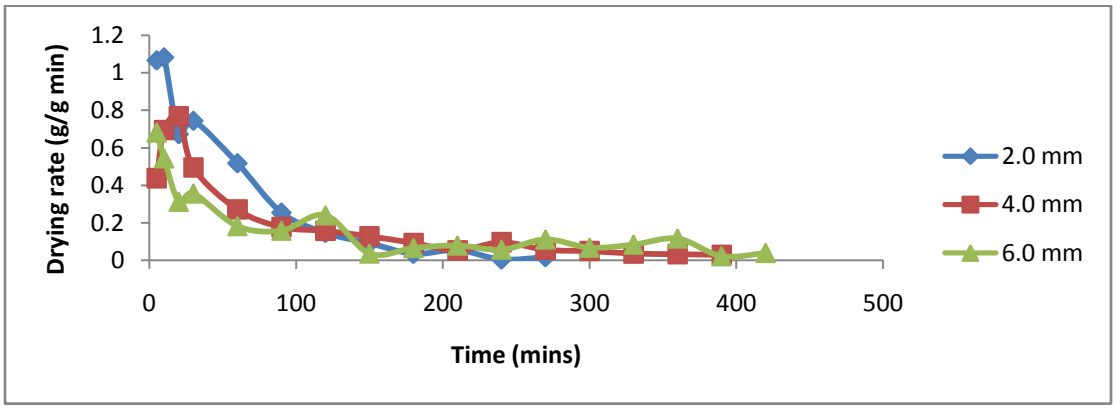

Figure 4. 51:Plot of drying rate against time at different slice thicknesses for drying of blanched aerial yam using convective dryer

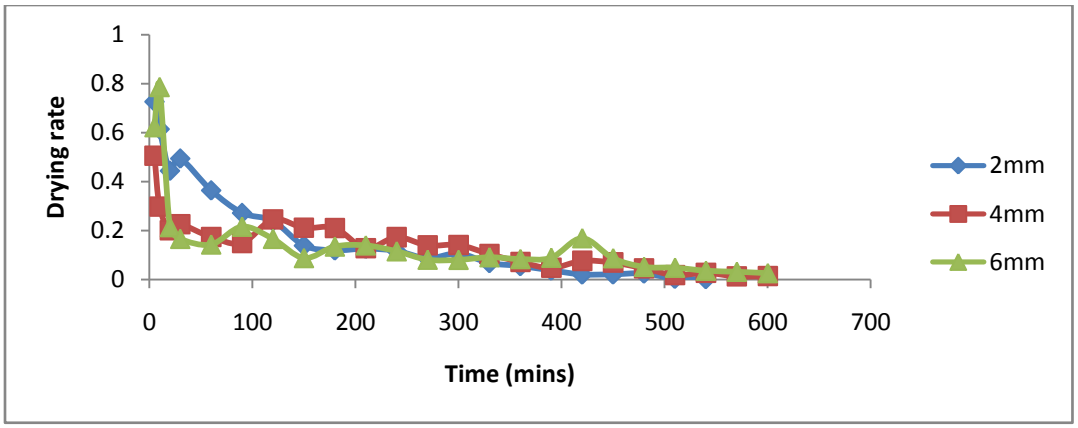

Figure 4. 52:Plot of drying rate against time at different slice thicknesses for drying of unblanched water yam using solar dryer

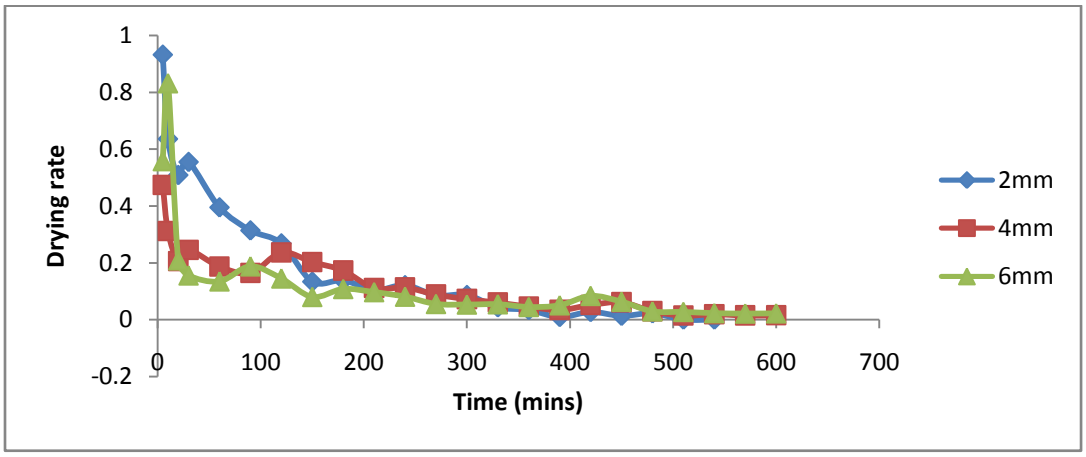

Figure 4. 53: Plot of drying rate against time at different slice thicknesses for drying of unblanched aerial yam using solar dryer

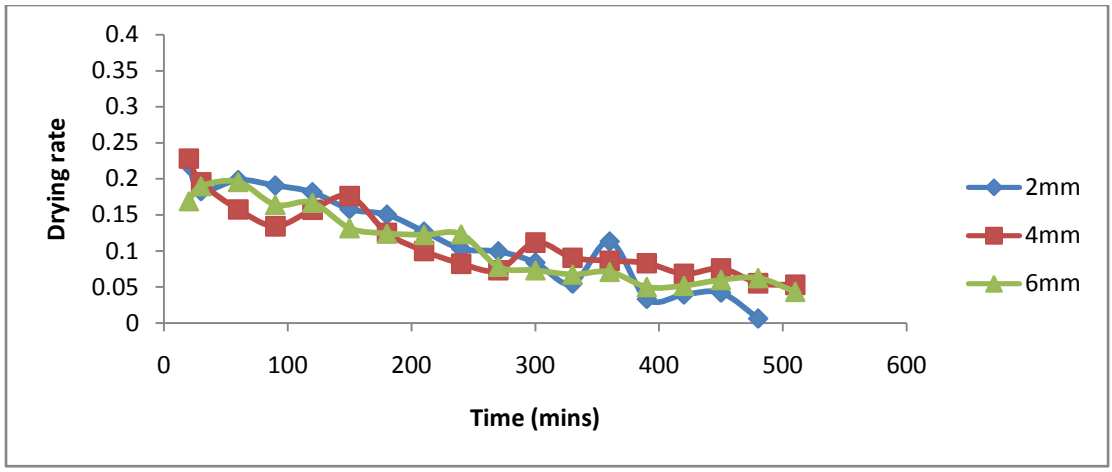

Figure 4. 54: Plot of drying rate against time at different slice thicknesses for drying of blanched water yam using solar dryer

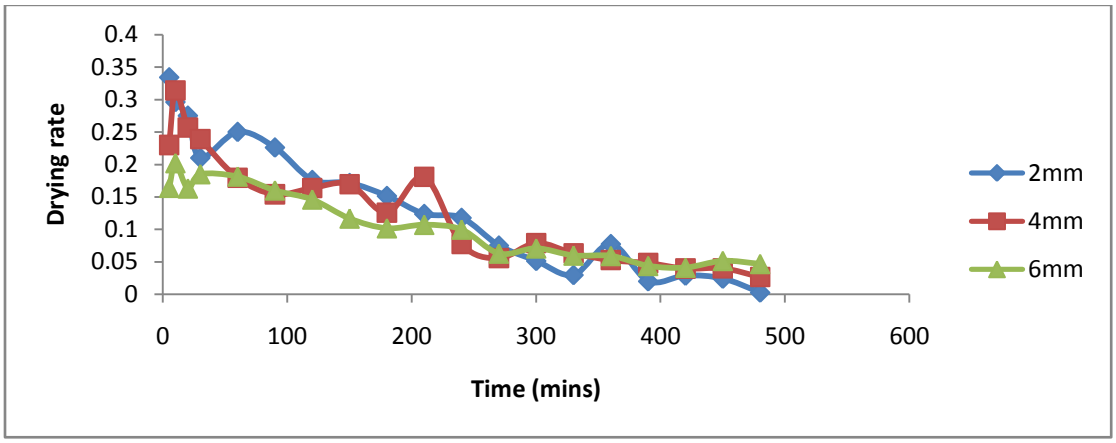

Figure 4. 55: Plot of drying rate against time at different slice thicknesses for drying of blanched aerial yam using solar dryer

4.6.2 Effect of Drying Air Speed on the Drying Rate

Various air speeds of 2.5m/s, 3.0m/s, 3.5m/s and 4.0m/s at constant thickness were used to study the effects of drying sir speed on the drying rate as given in Figures 4.56 to 4.63. The numerical data is shown in Table A.9-A.18. It was seen that increase in air speed leads to a relative increase in the drying rate at the initial time of drying before decreasing for both balanced and unbalanced yam samples. After a drying time of 60 minutes, the drying rate was seen to be 0.566, 0.565,

0.494 and 0.277 g/g.min for drying air speeds of 2.5, 3.0, 3.5 and 4.0 m/s respectively. Nicholas (2012) reported an increase in drying rate as air speed increases from 1.8 to 3.8 m/s. Mirzaee et al (2009) reported a similar trend.

It is apparent that the drying rate is higher at the beginning of the drying process and decreases continuously with the drying time for both the convective dryer and the solar dryer. Mirazaee et al, (2009) reported the same trend. According to Wankhade et al (2012), the drying rate goes on decreasing witha decrease in moisture content. The rate of drying also has an important effect on the quality of dried food products.

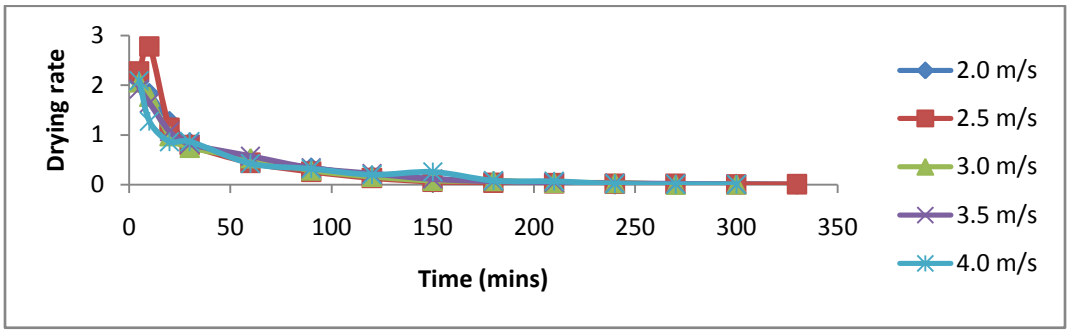

Figure 4. 56:Variation of drying rateat different air speeds for drying unblanched water yam using convective dryer

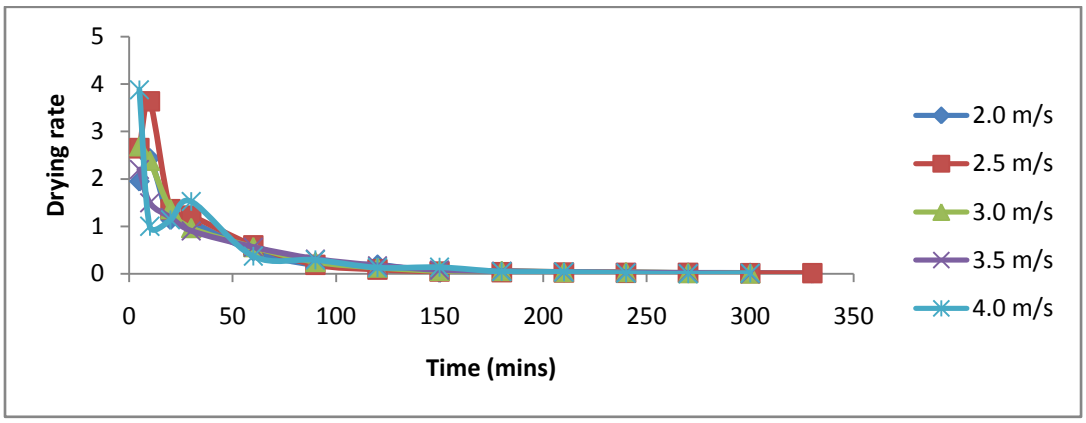

Figure 4. 57:Plot of drying rateagainst time at different air speeds for drying of unblanched aerial yam using convective dryer

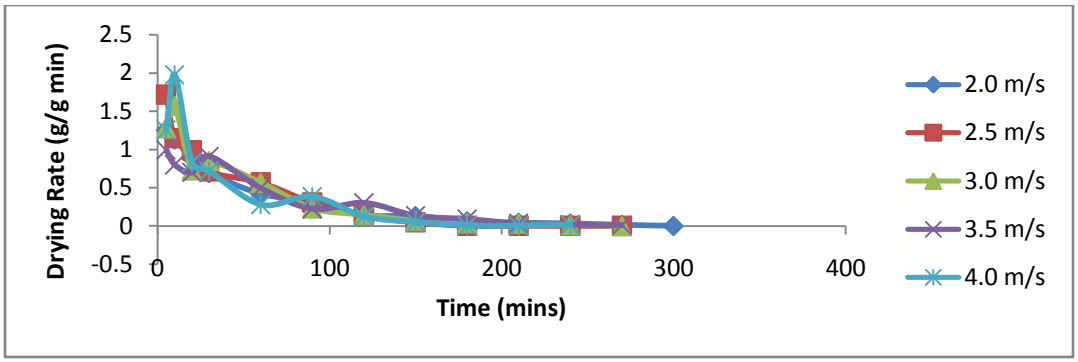

Figure 4. 58:Plot of drying rate against time at different air speeds for drying of blanched water yam using convective dryer

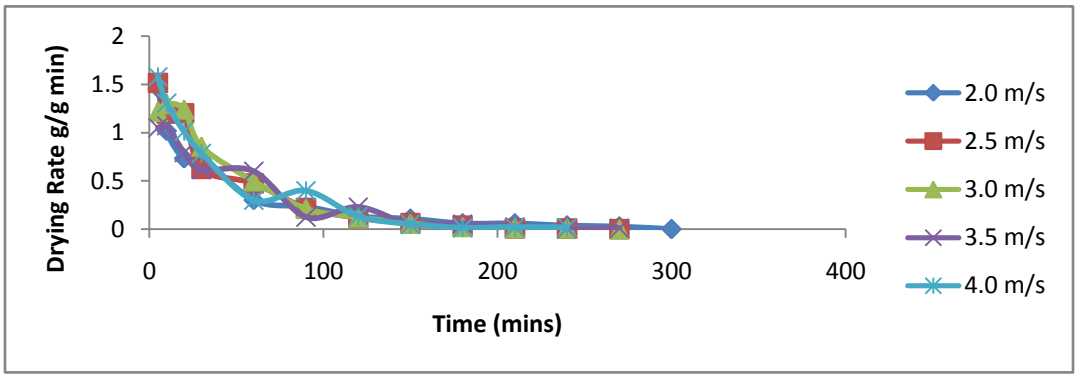

Figure 4. 59: Plot of drying rate against time at different air speeds for drying of blanched aerial yam using convective dryer

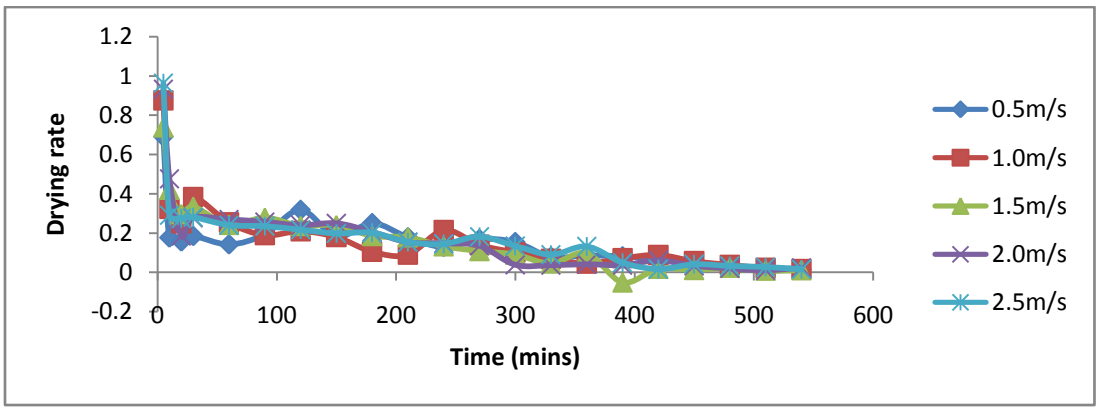

Figure 4. 60: Plot of drying rate against time at different air speeds for drying of unblanched water yam using solar dryer

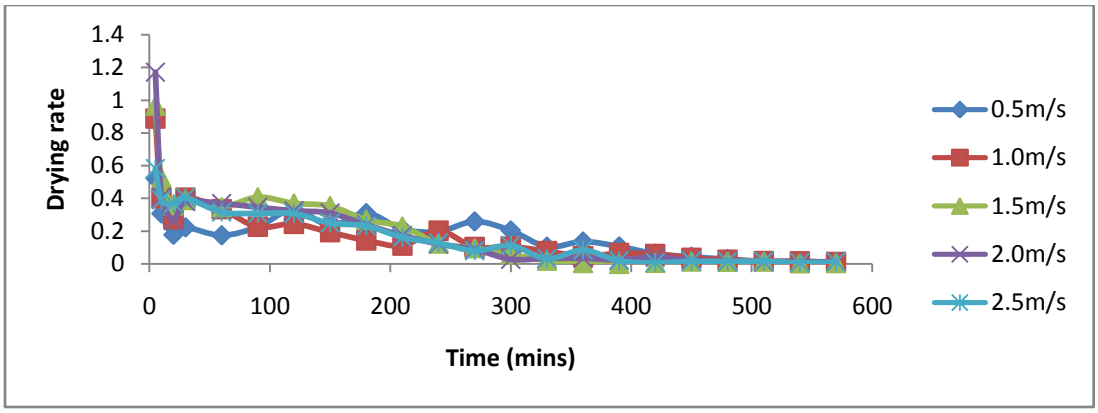

Figure 4. 61:Plot of drying rate against time at different air speeds for drying of unblanched aerial yam using solar dryer

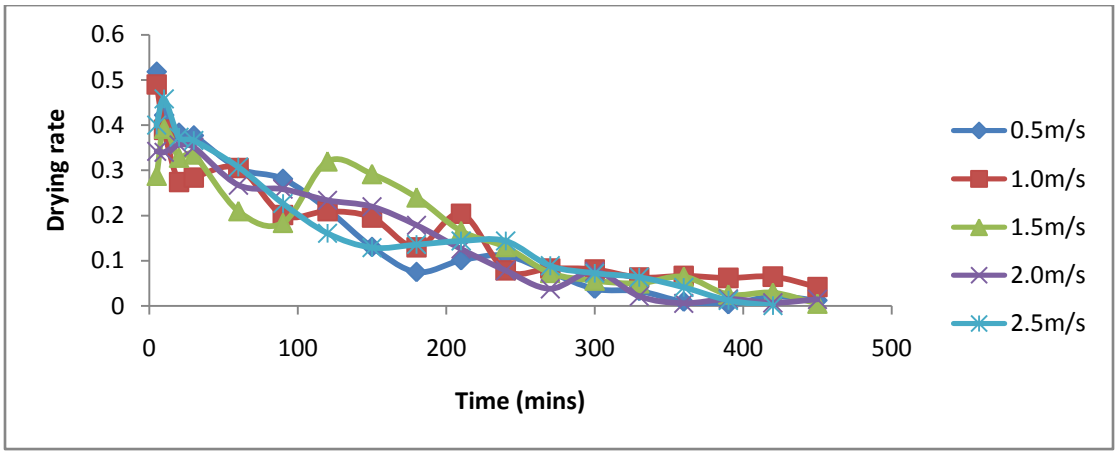

Figure 4. 62:Plot of drying rate against time at different air speeds for drying of blanched water yam using solar dryer

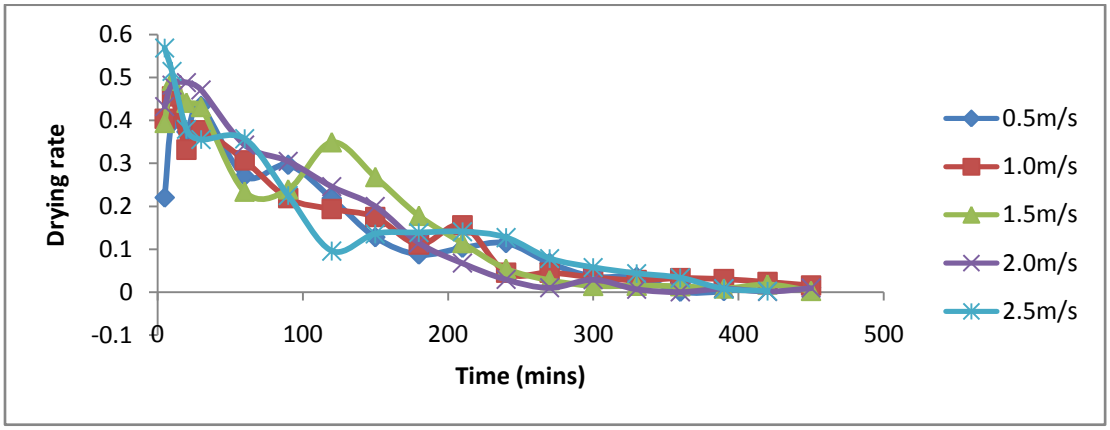

Figure 4. 63:Plot of drying rate against time at different air speeds for drying of blanched aerial yam using solar dryer

4.6.3 Effect of Temperature on Drying Rate

Temperature is one of the factors that affect the drying rate. Various temperatures of 40, 50, 60 and 70 ^{o}C were used to investigate the effect of temperature on the drying rate for convective dryer at constant airspeed and slice thickness of 2.5 m/s and 2.0 mm, respectively. The effects of temperature on the drying rate were given in Figures 4.64 to 4.67, and the numerical data is shown in Table A.1-A.8. It is seen that increase in temperature increases the rate of drying. This is attributed to increased evaporation of water both on the surface and in the products due to the increased temperature (Junling et al, 2008). As the drying process continues, less free water on the surface of the product is available and hence, the drying rate starts to decrease for both the blanched and unblanched yam samples. The high drying rate at high drying temperature could be due to more heating energy which speeds up the movement of water molecules and results in higher moisture diffusivity within the yam samples (Junling et al, 2008).

The curve of the drying rate did not give a perfect curve probably because of the nature of the drying products and the diffusion mechanism inside the products as the drying progresses. Divine et al (2013) obtained similar drying rate curve against temperature.

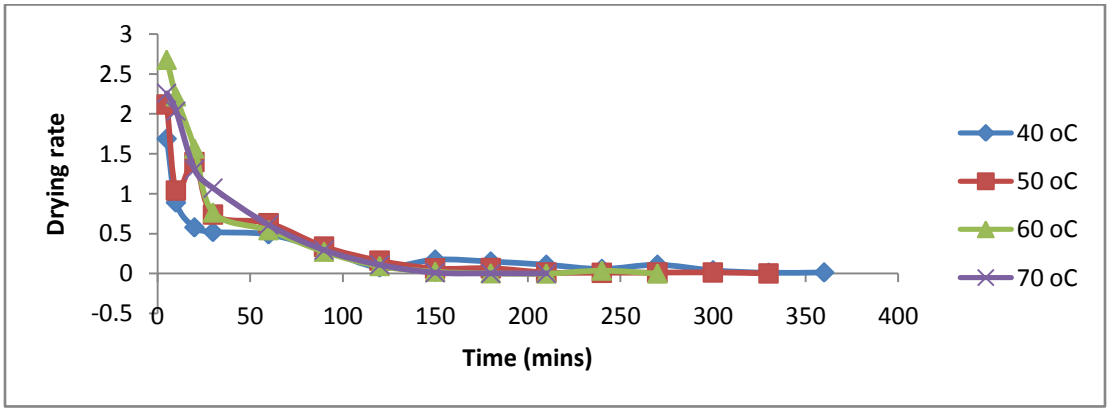

Figure 4. 64: Effect of temperature on drying rate for drying of unblanched water yam using convective dryer

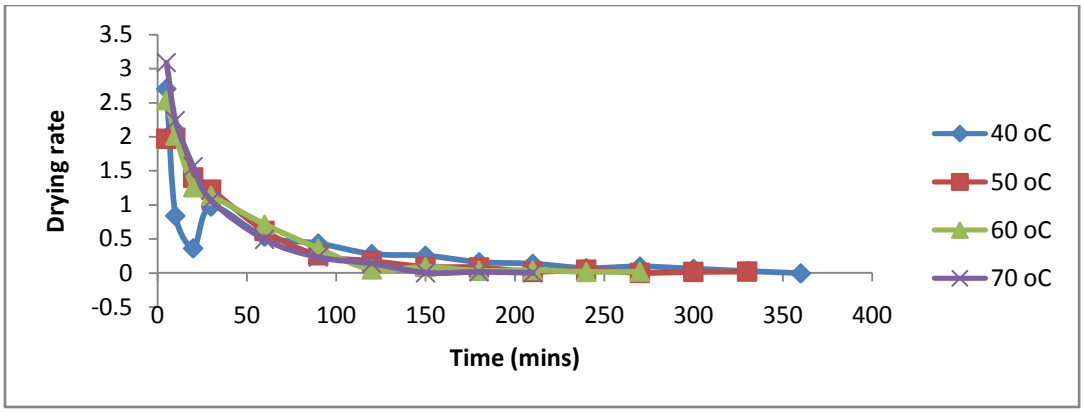

Figure 4. 65:Effect of temperature on drying rate for drying of unblanched aerial yam using convective dryer

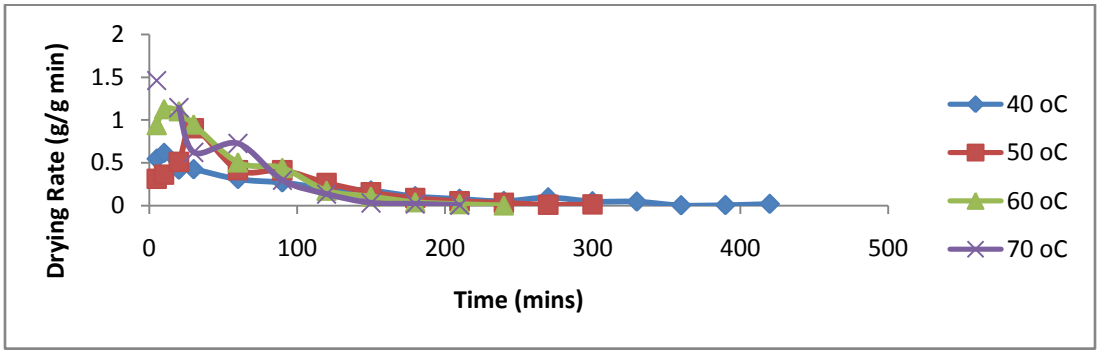

Figure 4. 66: Effect of temperature on drying rate for drying of blanched water yam using convective dryer

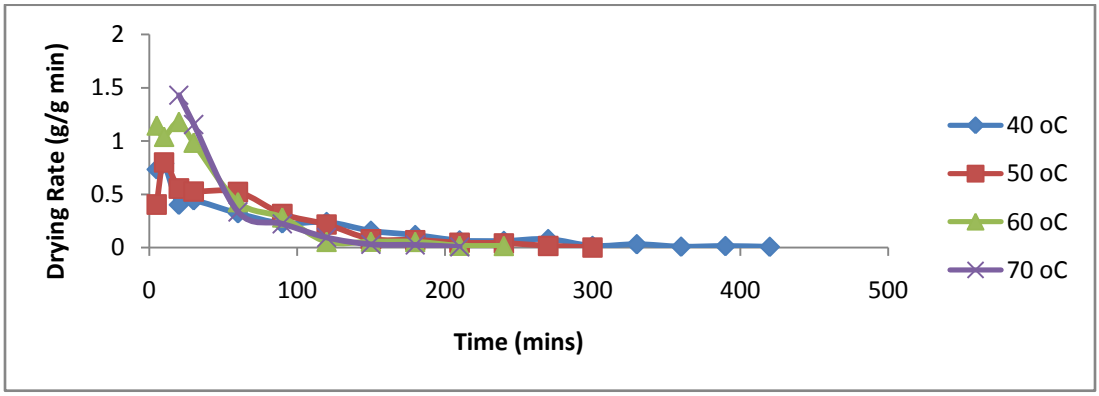

Figure 4. 67: Effect of temperature on drying rate for drying of blanched aerial yam using convective dryer.

4.7Drying Kinetic Models

Seven moisture ratio kinetic models were tested using regression methods for both water yam and aerial yam as presented in Tables 4.10 and 4.11. The acceptability of the drying models was determined by the correlation coefficient first and then by the root mean square error (RMSE) and the others. To select the best model for describing the drying curve, the criteria is that the value of correlation coefficient (R^2) should be high while the RMSE should be low.

It was seen from the statistical error indices in Table 4.10 and the plotted graphs (Figs. 4.68 and 4.69) that the best model for the water yam under the given drying conditions was the Logarithmic model with correlation coefficient of 0.9995. This is followed by Page/ Weibull models.

For the aerial yam, it was observed from the statistical error indices in Table 4.11 and the plotted graphs that the best model for the aerial yam under the given drying conditions was the Logarithmic model with correlation coefficient of 0.9991. This was followed by Page models. This time, the Weibull model performed badly. Therefore, only the Logarithmic model plots are presented in Figures 4.68a and 4.68b. The plots of other kinetic models are given in appendix C.

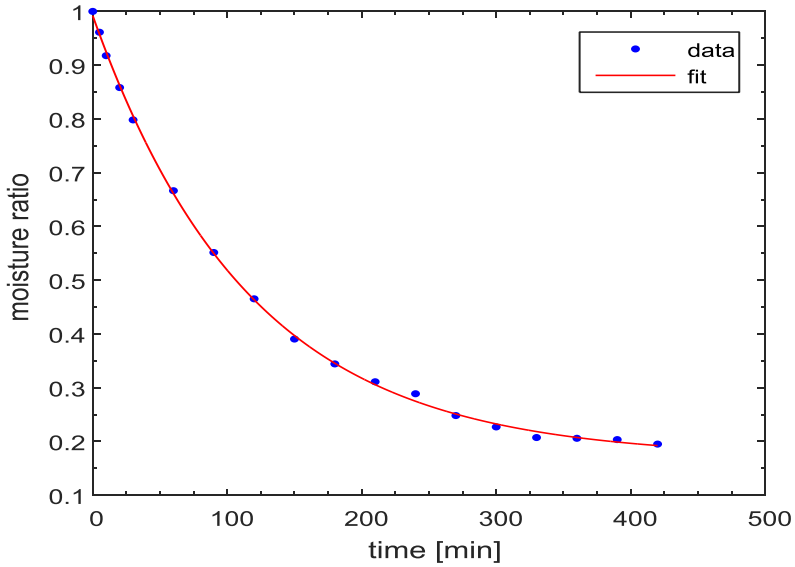

Figure 4. 68a: Variation of experimental and Logarithmic model based predicted moisture ratio with time for drying of water yam

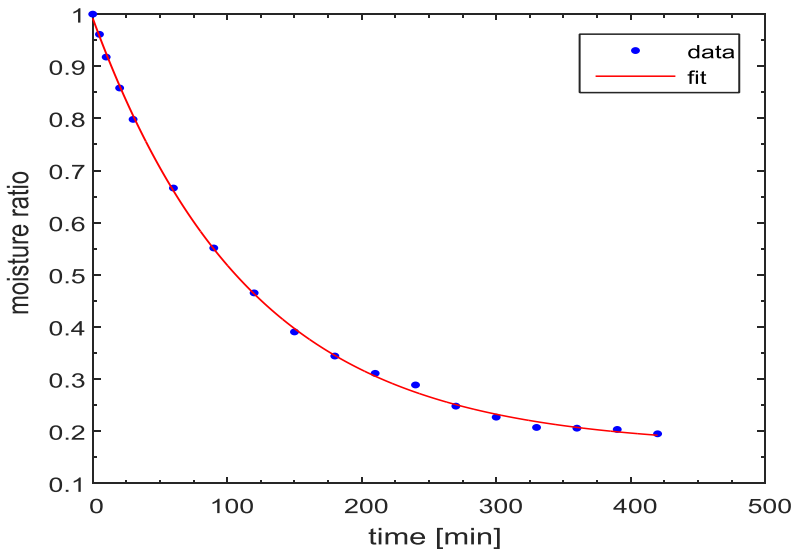

Figure 4. 68b: Variation of experimental and Logarithmic model based predicted moisture ratio with time for drying of aerial yam

Table 4. 10: The Kinetic models and their Statistical Error indicators for the unblanched Water Yam dried at heater temp of 40 ^{o}C

Model	Model Name	Coeffs.	R^2	RMSE	MBE	MABE	Corr.

							Coef.
$\chi = \exp(-kt)$	Newton	k=0.005442	0.9719	0.0482	0.0024	0.0413	0.9925
$\chi = \exp(-kt^n)$	Page	k = 0.01804 n = 0.771	0.9943	0.0218	-0.0042	0.0179	0.9973
$\chi = \exp[-(\kappa t)^n]$	Page modified	κ=0.0055 n = 0.771	0.9943	0.0218	-0.0042	0.0179	0.9973
$\chi = a\exp(-kt)$	Henderson et Pabis	a = 0.9492 k = 0.005074	0.9791	0.0416	-0.0066	0.0351	0.9905
$\chi = 1 + at + bt^2$	Wang et Singh	a = -0.005025 b = 7.735e-06	0.9819	0.0387	0.0125	0.0336	0.9944
$\chi = a\exp(-kt) + c$	Logarithmic	a =0.8222 c =0.1699 k =0.008579	0.9995	0.0062	-0.0000	0.0052	0.9998
$\chi = \exp\left[-\left(\frac{t}{\beta}\right)^{\alpha}\right]$	Weibull	α = 0.771 β =182.7	0.9943	0.0218	-0.0042	0.0179	0.9973

Table 4. 11:The Kinetic models and their Statistical Error indicators for the Unblanched Aerial Yam dried at heater temp of 40 ^{o}C

Model	Model Name	Coeffs.	R^2	RMSE	MBE	MABE	Corr. Coef.
$\chi = \exp(-kt)$	Newton	k=0.006789	0.974	0.0486	-0.0006	0.0421	0.9945

$\chi = \exp(-kt^n)$	Page	k =0.02171 n =0.7709	0.9949	0.0215	- 0.0038	0.0178	0.9975
$\chi = \exp[-(\kappa t)^n]$	Page modified	κ=0.0070 n =0.7709	0.9949	0.0215	- 0.0038	0.0178	0.9975
$\chi = a\exp(-kt)$	Henderson et Pabis	a = 0.942 k = -0.00627	0.9819	0.0406	- 0.0089	0.0339	0.9922
$\chi = 1 + at + bt^2$	Wang et Singh	a = - 0.005648 b =9.049e-06	0.9716	0.0508	0.0181	0.0446	0.9924
$\chi = a\exp(-kt) + c$	Logarithmic	a =0.8521 c =0.1286 k =0.009626	0.9991	0.0093	0.0000	0.0069	0.9995
$\chi = \exp\left[-\left(\frac{t}{\beta}\right)^{\alpha}\right]$	Weibull	α = 9.375 β =1.152	- 1.5340	0.4806	- 0.3864	0.3864	0.4483

Since the Logarithmic Kinetic models best correlated the experimental data, it was selected for modeling the moisture ratio kinetics of the rest of the experimental data at different temperatures. The Logarithmic Kinetic models at different temperatures were evaluated and presented in Table 4.12a. For the unblanched yam samples (Table 4.12a), the best correlation coefficient (0.9991) was obtained at 40^{o}C for both water yam and aerial yam. For blanched samples (Table 4.12b),

the best correlation coefficient (0.9993) for drying water yam was obtained at 50^{o}C while for drying aerial yam, 0.9989 was obtained at 60^{o}C.

Table 4. 12:TheLogarithmic Kinetic models and their Statistical Error indicators for the unblanched Yams dried at different heater temp.

	Temp [^{o}]	Coeffs.	R^2	RMSE	MBE	MABE	Corr. Coef.
	40	a =0.8521 c =0.1286 k =0.009626	0.9991	0.0093	0.0000	0.0069	0.9995

Water Yam	50	a =0.9465 c =0.09586 k =0.01228	0.9957	0.0224	0.0000	0.0184	0.9978
	60	a =1.029 c =-0.01255 k =0.0188	0.9988	0.0132	0.0000	0.0115	0.9994
	a = 0.0088T + 0.5, c = - 0.00038T^2 + 0.031T - 0.5, k = 1.9e-05T^2 - 0.0015T + 0.038						
Arial Yam	40	a =0.8521 c =0.1286 k =0.009626	0.9991	0.0093	0.0000	0.0069	0.9995
	50	a =0.903 c =0.1252 k =0.01425	0.9979	0.0149	0.0000	0.0106	0.9990
	60	a =0.9153 c =0.09962 k =0.02521	0.9985	0.0130	0.0000	0.0110	0.9992
	a= - 0.00019T^2 + 0.022T + 0.26, c = - 0.00011T^2 + 0.0096T - 0.08, k = 3.2e-05T^2- 0.0024T + 0.054						

Table 4. 13:TheLogarithmic Kinetic models and their Statistical Error indicators for the Blanched Yams dried at different heater temp.

Water	Temp [^{o}]	Coeffs.	R^2	RMSE	MBE	MABE	Corr. Coef.
Yam	40	a =0.8381 c =0.1057 k =0.01086	0.9952	0.0200	0.0000	0.0150	0.9976
	50	a =0.9483	0.9993	0.0088	0.0000	0.0064	0.9997

		c =0.1539 k =0.02254					
	60	a =0.9488 c =0.02008 k =0.03371	0.9981	0.0146	0.0000	0.0112	0.9991
	a = - 0.00055T^2 + 0.06T - 0.7, c = - 0.00091T^2 + 0.087T - 1.9, k= 0.0011T - 0.035						
Arial Yam	40	a =1.353 c =0.04775 k =0.01052	0.9973	0.0245	0.0000	0.0139	0.9986
	50	a =1.262 c =0.1252 k =0.02413	0.9980	0.0200	0.0000	0.0171	0.9990
	60	a =1.277 c =0.1332 k =0.02656	0.9989	0.0150	0.0000	0.0132	0.9995
	a = 0.00053T^2 - 0.057T + 2.8, c = - 0.00035T^2 + 0.039T - 0.96 k= - 5.6e-05T^2 + 0.0064T - 0.16						

4.8 Finite Element Analysis

4.8.1 The Effective Diffusivity

The effective diffusivity for the finite element analysis was considered for convective air dryer only. Crank's series solution for moisture ratio kinetics of infinite slab is given as

$$\chi^* = \frac{8}{\pi^2}\sum_{n=0}^{\infty}\frac{1}{(2n+1)^2}\exp\left(\frac{(2n+1)^2\pi^2 D_{eff}\, t}{4H^2}\right) \quad (4.1)$$

where D_{eff} is effective diffusivity [m^2s^{-1}] and H is half thickness of the samples [m]. For long drying periods, the first term alone can give reasonably accurate results such that

$$\chi^* = \frac{8}{\pi^2}\exp\left(\frac{\pi^2 D_{eff}\, t}{4H^2}\right) \tag{4.2}$$

Equation (4.1) can be put in linear form by taking natural logarithm of both sides to give

$$\ln(\chi^*) = \ln\left(\frac{8}{\pi^2}\right) - \frac{\pi^2 D_{eff}}{4H^2}t \tag{4.2a}$$

This can be re-written as

$$y = \frac{4H^2}{\pi^2}\ln\left(\frac{8}{\chi^*\pi^2}\right) = D_{eff}\, t \tag{4.2b}$$

It can be seen from the last equation that D_{eff} is the slope of a plot of $\frac{4H^2}{\pi^2}\ln\left(\frac{8}{\chi^*\pi^2}\right)$ against time. When this is done for drying data at heater temperature of 110^{o}C or air temperature of $T_a = 14.5306 + 0.6014 \times 110 - 0.0010 \times 110^2 = 68.58^oC$ as shown in Figure 4.70a, the effective diffusivity becomes $D_{eff} = 2.5487 \times 10^{-10}$[$m^2s^{-1}$] while when this is done for drying data at heater temperature of 90^{o}C or air temperature of $T_a = 14.5306 + 0.6014 \times 90 - 0.0010 \times 90^2 = 60.56^oC$ as shown in Figure 4.70b, the effective diffusivity becomes $D_{eff} = 2.0809 \times 10^{-10}$[$m^2s^{-1}$].

Doing the same on the drying data of aerial yam at heater temperature of 110^{o}C or air temperature of 68.58^{o}C as shown in Figures 4.70c and 4.70d, the effective diffusivity becomes $D_{eff} = 1.4381 \times 10^{-10}$[$m^2s^{-1}$] while at heater temperature of 90^{o}C or air temperature of 60.56^{o}C, the effective diffusivity becomes $D_{eff} = 1.2241 \times 10^{-10}$[$m^2s^{-1}$].

4.8.2 The Convective Mass Transfer Coefficient for Water Yam

Convective mass transfer coefficient can be given as eqn. (4.3) (Mohsen, 2017)

$$h_m = \frac{S}{At}\ln(\chi) \tag{4.3}$$

The kinetics of samples volume V and area A for convective drying at heater temperature of 110^{o}C or air temperature of 68.58 ^{o}C are shown in Table 4.14. They are used according to equation (4.3) to generate the values in Table 4.14 which quadratically correlate with drying time according to equation 4.4

$$h_m = 3.368 \times 10^{-16} t^2 - 4.22 \times 10^{-12} t + 1.488 \times 10^{-8} \quad (4.4)$$

The statistical error indices obtained were R^2= 0.9749, RMSE=0.0000 and r = 0.9874. The high value of R^2 and r together with the very low value of RMSE indicates high accuracy of the quadratic correlation. The corresponding correlation for the case when the heater temperature of 90^{o}C or air temperature of 60.56 ^{o}C were used in equation 4.5 to generate the values in Table 4.14.

$$h_m = 2.463 \times 10^{-16} t^2 - 3.78 \times 10^{-12} t + 1.545 \times 10^{-8} \quad (4.5)$$

The statistical error indices were R^2= 0.9329, RMSE=0.0000 and r = 0.9659. Again, The high value of R^2 and r together with the very low value of RMSE indicates high accuracy of the quadratic correlation for convective mass transfer coefficient.

Table 4. 12:Thermophysical data for Water yam at Temp: 68.58^{o}C.

	time	Mass of sample[g]		$\chi = \frac{M-M_d}{M_d}$ [dry basis]	$\chi^* = \frac{\chi - \chi_{eq}}{\chi_0 - \chi_{eq}}$	V×10^4[m^3]	A[m]	$h_m \times 10^7 = \frac{S}{At}\ln(\chi) \times 10^7$	K= $\frac{-Lnx^*}{t}$ [Min^{-1}]	Biot No.
0	0	61.409	59.328	1.7291	1.0000	0.2880	0.0192	-	-	-
1	10	57.002	52.383	1.4725	0.819499	0.2312	0.0166	0.1363	0.019906	0.0751
2	20	53.672	48.494	1.3094	0.704769	0.1951	0.0148	0.0960	0.017494	0.0500
3	30	49.702	45.708	1.1566	0.597285	0.1614	0.0130	0.0759	0.017179	0.0371
4	40	44.412	43.236	0.9812	0.473903	0.1226	0.0109	0.0628	0.018669	0.0280
5	50	41.978	41.156	0.8792	0.402153	0.1000	0.0095	0.0512	0.018218	0.0213

6	60	39.844	39.074	0.7839	0.335115	0.0789	0.0081	0.0423	0.018221	0.0163
7	70	38.150	37.250	0.7043	0.279122	0.0613	0.0068	0.0351	0.01823	0.0124
8	80	36.232	35.540	0.6223	0.221441	0.0432	0.0074	0.0287	0.018845	0.0090
9	90	34.798	34.023	0.5556	0.174522	0.0284	0.0061	0.0230	0.019397	0.0063
10	100	33.310	32.835	0.4951	0.131964	0.0150	0.0057	0.0173	0.020252	0.0038
11	110	32.180	31.909	0.4487	0.099325	0.0121	0.0042	0.0109	0.020994	0.0016
12	120	30.850	31.174	0.4020	0.066474	0.0112	0.0039	0.0103	0.022591	0.0012
13	130	30.300	30.464	0.3735	0.046427	0.0107	0.0034	0.0099	0.023614	0.0009
14	140	29.731	30.001	0.3502	0.030037	0.0103	0.0031	0.0091	0.025038	0.0007
15	150	29.322	29.763	0.3356	0.019766	0.0097	0.0027	0.0074	0.026158	0.0006
16	160	29.017	29.640	0.3259	0.012943	0.0092	0.0024	0.0063	0.02717	0.0002
17	170	28.908	29.567	0.3218	0.010059	0.0087	0.0020	0.0056	0.027055	0.00009
18	180	28.882	29.498	0.3196	0.008512	0.0086	0.0017	0.0051	0.02648	0.00005
19	190	28.850	29.442	0.3176	0.007105	0.0075	0.0015	0.0043	0.026037	0.00004
20	200	28.759	29.419	0.3151	0.005346	0.0058	0.0013	0.0038	0.026157	0.00002
21	210	28.750	29.414	0.3147	0.005065	0.0041	0.0010	0.0021	0.025169	0.00001

Table 4. 13:Thermophysical data for Water yam at Temp: 60.56^{o}C.

S/N	time	Mass of sample [g]		$\chi = \frac{M-M_d}{M_d}$ [dry basis]	$\chi^* = \frac{\chi - \chi_{eq}}{\chi_0 - \chi_{eq}}$	V×10^4[m^3]	A[m]	$h_m \times 10^7 = \frac{S}{At}\ln(\chi) \times 10^7$	K=$\frac{-Lnx^*}{t}$ [Min^{-1}]	Biot No.
0	0	60.598	58.713	1.6969	1.000	0.2880	0.0192	-	-	-
1	10	55.867	54.528	1.4954	0.852662	0.2434	0.0172	0.1265	0.015939	0.0862

2	20	52.212	49.122	1.2906	0.70291	0.1981	0.0150	0.1043	0.017626	0.0664
3	30	49.115	47.690	1.1882	0.628035	0.1755	0.0138	0.0790	0.015505	0.0483
4	40	46.704	43.029	1.0283	0.511114	0.1401	0.0119	0.0666	0.016779	0.0378
5	50	44.446	39.789	0.9040	0.420225	0.1126	0.0103	0.0556	0.017339	0.0293
6	60	42.753	37.772	0.8202	0.35895	0.0941	0.0091	0.0465	0.017076	0.0231
7	70	41.215	36.840	0.7644	0.318149	0.0817	0.0083	0.0396	0.016361	0.0188
8	80	39.850	34.407	0.6785	0.255338	0.0627	0.0070	0.0335	0.017065	0.0145
9	90	38.572	32.987	0.6175	0.210734	0.0492	0.0059	0.0285	0.017302	0.0114
10	100	37.346	31.892	0.5651	0.172419	0.0376	0.0049	0.0241	0.017578	0.0088
11	110	36.227	30.819	0.5155	0.136151	0.0267	0.0039	0.0200	0.018127	0.0065
12	12	35.264	29.940	0.4739	0.105733	0.0175	0.0030	0.1628	0.018724	0.0461
13	130	34.571	29.758	0.4541	0.091255	0.0131	0.0024	0.0138	0.018416	0.0035
14	140	33.754	28.749	0.4128	0.061056	0.0120	0.0021	0.0088	0.019971	0.0015
15	150	33.246	28.568	0.3972	0.049649			0.0072	0.020019	0.0004

						0.0170	0.0020			
16	160	31.912	28.364	0.3625	0.024276	0.0110	0.0019	0.0067	0.023239	0.000091
17	170	32.552	28.148	0.3721	0.031296	0.0070	0.0017	0.0061	0.020378	0.000077
18	180	32.259	27.993	0.3619	0.023837	0.0050	0.0013	0.0050	0.020758	0.000071
19	190	32.049	27.935	0.3559	0.01945	0.0040	0.0011	0.0046	0.020736	0.000059
20	200	31.853	27.925	0.3512	0.016013	0.0020	0.0010	0.0039	0.020672	0.000042
21	210	31.707	27.914	0.3477	0.013454	0.0010	0.0009	0.0034	0.020516	0.000040
22	220	31.569	27.897	0.3442	0.010895	0.0009	0.0009	0.0029	0.020543	0.000035
23	230	31.520	27.982	0.3450	0.01148	0.0007	0.0007	0.0025	0.019422	0.000033
24	240	31.488	27.974	0.3441	0.010822	0.0007	0.0006	0.0021	0.018859	0.000031
25	250	31.421	27.629	0.3348	0.004022	0.0005	0.0006	0.0013	0.022064	0.000026
26	260	31.356	27.618	0.3330	0.002705	0.0003	0.0004	0.0012	0.02274	0.000019
27	270	31.350	27.611	0.3328	0.002559	0.0001	0.0004	0.0008	0.022104	0.000016

4.8.3. The Convective Mass Transfer Coefficient for aerial yam

Applying regression analysis to the aerial yam data in at temperature of 68.56 ^{o}C gives the convective mass transfer coefficient as a function of time as in equation 4.6

$$h_m = 4.612 \times 10^{-17} t^2 - 1.024 \times 10^{-12} t + 6.448 \times 10^{-9} \quad (4.6)$$

The results obtained were as expressed in Table 4.16. The statistical error indices of the quadratic correlation are R^2=0.9446, RMSE=0.0000 and r = 0.9719, indicating high accuracy. The convective mass transfer coefficient at the heater temperature of 90^{o}C or air temperature of 60.56^{o}C becomes

$$h_m = 4.075 \times 10^{-17} t^2 - 9.73 \times 10^{-13} t + 6.391 \times 10^{-9} \quad (4.7)$$

The results gotten were presented in Table 4.17. The R^2=0.8763, RMSE=0.0000 and r = 0.9361 all suggested good correlation.

Table 4. 14:Thermophysical data for Aerial yam at Temp: 68.58^{o}C.

S/N	time	M		$\chi = \frac{M-M_d}{M_d}$ [dry basis]	$\chi^* = \frac{\chi - \chi$	V×10^4[m^3]	A[m]	$h_m \times 10^8 = \frac{S}{At}\ln(\chi) \times 10^8$	K= $\frac{-Lnx^*}{t}$ [Min^{-1}]	Biot No.
0	0	52.330	53.486	0.8742	1.000	0.2880	0.0192	-	-	-
1	10	49.786	48.221	0.7359	0.821249	0.2490	0.0174	0.6867	0.019693	0.0682
2	20	46.307	44.750	0.6128	0.662143	0.2142	0.0158	0.5762	0.020614	0.0545
3	30	44.323	42.154	0.5317	0.557322	0.1913	0.0146	0.4650	0.019487	0.0423
4	40	43.000	41.498	0.4966	0.511956	0.1814	0.0141	0.3713	0.016738	0.0332
5	50	41.894	38.848	0.4301	0.426005	0.1626	0.0131	0.3265	0.017066	0.0281
6	60	40.977	37.680	0.3931	0.378183	0.1522	0.0126	0.2835	0.016206	0.0239
7	70	40.016	36.920	0.3627	0.338891	0.1436	0.0121	0.2500	0.015458	0.0207

8	80	39.135	35.838	0.3279	0.293912	0.1338	0.0115	0.2248	0.015306	0.0182
9	90	38.345	34.959	0.2983	0.255655	0.1254	0.0110	0.2036	0.015155	0.0161
10	100	37.648	34.199	0.2725	0.222308	0.1182	0.0106	0.1857	0.015037	0.0144
11	110	36.959	33.656	0.2507	0.194132	0.1120	0.0102	0.1703	0.014902	0.0130
12	12	35.755	33.157	0.2205	0.155099	0.1035	0.0097	0.1575	0.015531	0.0117
13	130	35.906	32.584	0.2131	0.145534	0.1014	0.0096	0.1456	0.014826	0.0107
14	140	34.944	32.552	0.1955	0.122787	0.0964	0.0093	0.1355	0.014981	0.0098
15	150	34.193	32.466	0.1806	0.103528	0.0922	0.0090	0.1266	0.015119	0.0090
16	160	33.433	32.334	0.1648	0.083107	0.0878	0.0087	0.1187	0.015548	0.0083
17	170	32.612	32.183	0.1476	0.060876	0.0829	0.0084	0.1115	0.016464	0.0077
18	180	32.062	32.094	0.1363	0.046271	0.0797	0.0082	0.1051	0.017074	0.0071
19	190	31.550	32.008	0.1257	0.032571	0.0767	0.0079	0.0993	0.018023	0.0067
20	200	31.118	31.819	0.1147	0.018353	0.0736	0.0077	0.0941	0.01999	0.0062
21	210	30.817	31.737	0.1079	0.009564	0.0717	0.0076	0.0894	0.022141	0.0059
22	220	30.541	31.680	0.1020	0.001939	0.0700	0.0075	0.0851	0.02839	0.0055
23	230	30.539	31.645	0.1014	0.001163	0.0698	0.0075	0.0814	0.029376	0.0053
24	240	30.532	31.640	0.1012	0.000905	0.0698	0.0075	0.0780	0.029199	0.0051

Table 4. 15: Thermophysical data for Aerial yam at Temp: 60.56^{o}C.

S/N	time	M	$\chi = \frac{M-M_d}{M_d}$ [dry basis]	$\chi^* = \frac{\chi - \chi_{eq}}{\chi_0 - \chi_{eq}}$	V×10^4[m^3]	A	$h_m \times 10^7 = \frac{S}{At}\ln(\chi) \times 10^8$	K= $\frac{-Lnx^*}{t}$ (Min^{-1})	Biot No.

0	0	54.487	56.116	0.9590	1.00000	0.2880	0.0192	-	-	-
1	10	49.600	51.596	0.7923	0.770259	0.2410	0.0170	0.8027	0.026103	0.0927
2	20	46.845	49.541	0.7072	0.652977	0.2169	0.0159	0.5588	0.021311	0.0623
3	30	45.004	48.024	0.6477	0.570976	0.2001	0.0151	0.4347	0.01868	0.0472
4	40	43.599	46.794	0.6010	0.506615	0.1869	0.0144	0.3581	0.017	0.0380
5	50	42.360	45.907	0.5634	0.454796	0.1763	0.0138	0.3049	0.015758	0.0317
6	60	40.978	44.916	0.5213	0.396775	0.1645	0.0132	0.2693	0.015406	0.0274
7	70	39.875	44.382	0.4923	0.356808	0.1563	0.0128	0.2388	0.014722	0.0239
8	80	39.082	43.751	0.4671	0.322078	0.1491	0.0124	0.2144	0.014162	0.0211
9	90	38.275	43.116	0.4416	0.286935	0.1419	0.0120	0.1950	0.013872	0.0189
10	100	37.531	42.615	0.4195	0.256477	0.1357	0.0116	0.1786	0.013607	0.0170
11	110	36.937	42.130	0.4004	0.230154	0.1303	0.0113	0.1645	0.013355	0.0155
12	12	36.389	41.703	0.3831	0.206312	0.1254	0.0110	0.1524	0.013153	0.0142
13	130	35.706	41.290		0.179576	0.1200		0.1421	0.013209	0.0130

				0.3637			0.0107			
14	140	35.216	40.909	0.3483	0.158352	0.1156	0.0104	0.1329	0.013164	0.0120
15	150	34.880	40.569	0.3363	0.141814	0.1122	0.0102	0.1246	0.013022	0.0111
16	160	34.510	39.864	0.3173	0.115628	0.1069	0.0099	0.1175	0.013484	0.0103
17	170	34.276	39.654	0.3094	0.104741	0.1046	0.0098	0.1108	0.013272	0.0097
18	180	34.031	39.499	0.3023	0.094956	0.1026	0.0097	0.1048	0.01308	0.0091
19	190	33.863	39.210	0.2942	0.083793	0.1003	0.0095	0.0995	0.01305	0.0086
20	200	33.722	39.022	0.2884	0.075799	0.0987	0.0094	0.0946	0.012898	0.0081
21	210	33.495	38.792	0.2803	0.064636	0.0964	0.0093	0.0902	0.013043	0.0077
22	220	33.306	38.370	0.2695	0.049752	0.0934	0.0091	0.0861	0.01364	0.0073
23	230	33.186	38.162	0.2637	0.041759	0.0917	0.0090	0.0824	0.013808	0.0069
24	240	33.118	37.971	0.2591	0.035419	0.0904	0.0089	0.0790	0.013919	0.0066
25	250	32.997	37.767	0.2533	0.027426	0.0888	0.0088	0.0758	0.014385	0.0063
26	260	32.975	37.756	0.2528	0.026736	0.0886	0.0088	0.0729	0.01393	0.0060

27	270	32.972	37.749	0.2526	0.026461	0.0886	0.0087	0.0702	0.013452	0.0058

4.8.4 Finite Element Predictions

The finite element analysis was considered for convective air dryer onlyThe above thermo-physical parameters were introduced into the finite element model for prediction of moisture content using equation (3.35) . A sample discretization applied is presented as Figure 4.69. It is a two-dimensional triangular discretization of a transverse section of the sample. Nodal values of water content were averaged to get the mean water content which is compared with the experimental water content values. Inserting the relevant values of D_{eff} and h_m and solving the finite element/difference scheme presented in equation (3.35) gave the time step solutions. The finite element prediction of moisture content of water yam at air temperature of 68.58^{o}C is given in Figure 4.70. The results are given in comparison to the experimentally measured moisture content. A good agreement is seen between the predictions and the measurements. These agreements were quantified with some statistical indicators of goodness of fit like coefficient of determination (R^2-value), root mean square error (RMSE) and correlation coefficient (r). The values are R^2-value =0.9021, RMSE=0.1295 and r = 0.9964. The values indicate a highly reliable prediction. Figure 4.71 shows the finite element prediction of water content variation with time for water yam at air temperature of 60.56^{o}C. A very good level of agreement is again recorded. The statistical fitness indices were; R^2-value =0.9240, RMSE=0.1048 and r = 0.9943, which indicate very reliable results. In Figure 4.72, the Finite element prediction of water content variation with time for

aerial yam at air temperature of 68.58 ^{o}C is given. In comparing the predicted and the experimental measurements, R^2-value = 0.7663, RMSE=0.1000 and r = 0.9780 were computed to quantify the reliable agreement of the predictions with measurements. The validity of the finite elements predictions for the case of aerial yam dried at air temperature of 60.56 ^{o}C is verified with the R^2-value = 0.7155, RMSE=0.0955 and r = 0.9829. The results are presented in Figure 4.73.

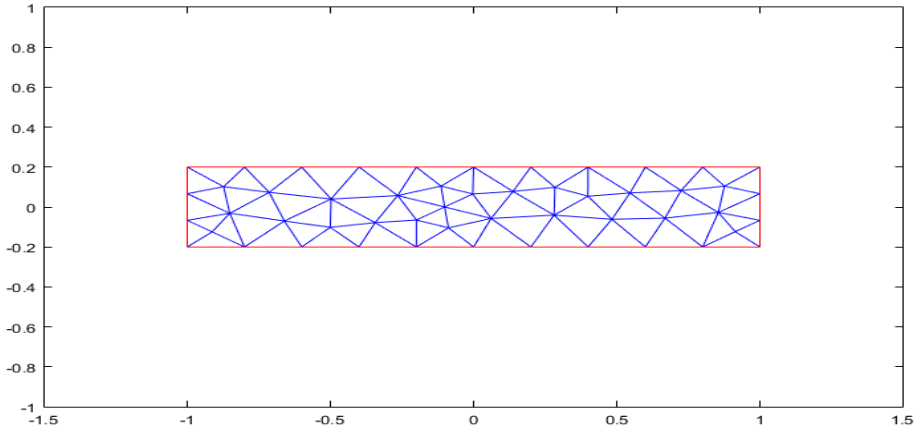

Figure 4. 69:Two dimensional discretization of sample transverse section

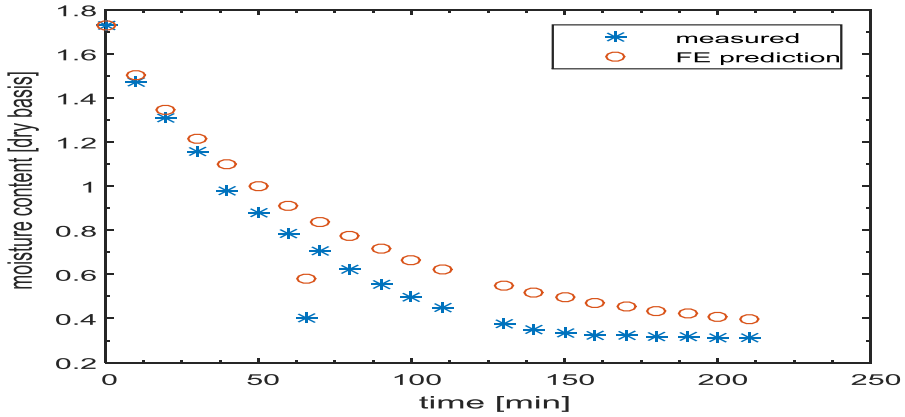

Figure 4. 70:Finite element prediction of water content variation with time for Water yam at air temperature of 68.58^{o}C.

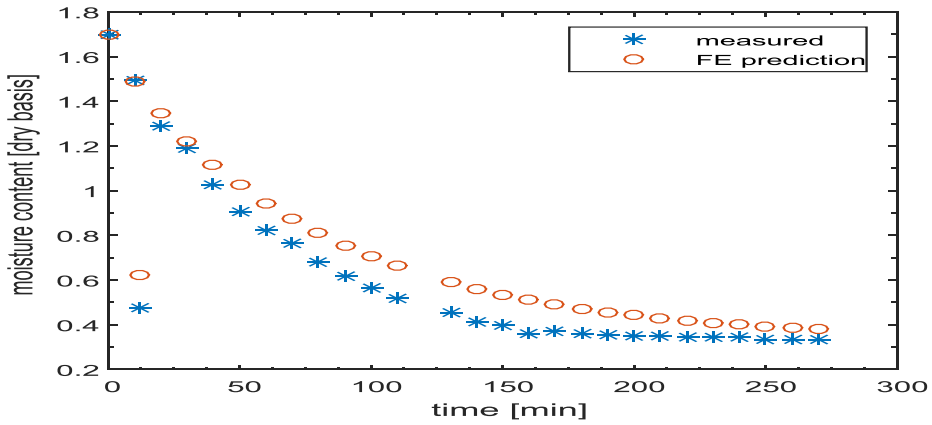

Figure 4. 71:Finite element prediction of water content variation with time for Water yam at air temperature of 60.56^{o}C.

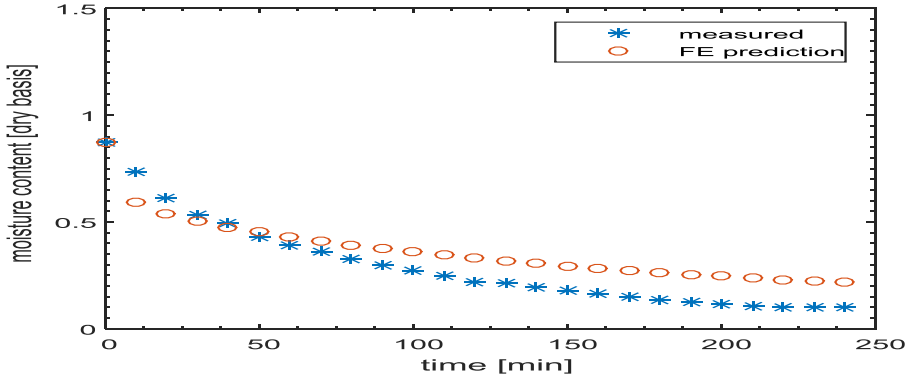

Figure 4. 72:Finite element prediction of water content variation with time for aerial yam at air temperature of 68.58 ^{o}C.

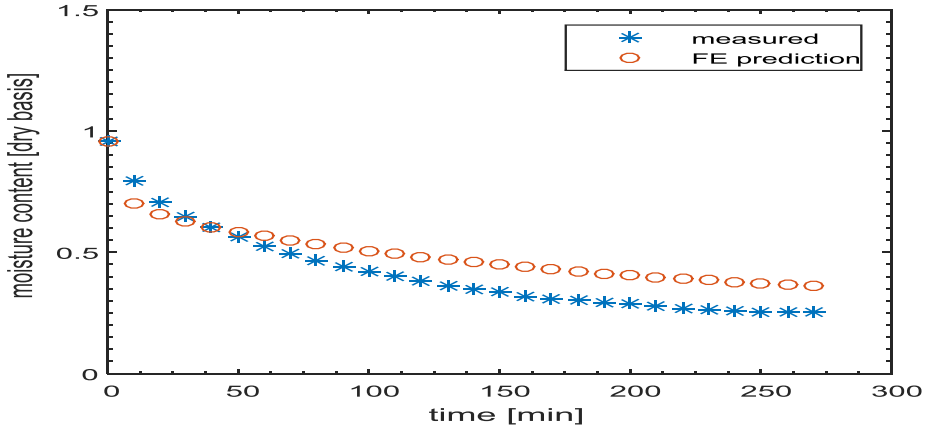

Figure 4. 73:Finite element prediction of water content variation with time for aerial yam at air temperature of 60.56 ^{o}C

4.9Optimization of drying process using convective dryer

The responses obtained from different experimental runs carried out by combinations of the three variables (Drying Temp., Thickness and Air speed) are tabulated on the response column of Table 4.18 for Water Yam(WY) and Aerial Yam(AY). The three-experimental variable interaction gave a total of 20 experimental runs comprising of 14 distinct runs and 6 repeated runs usually called the centre points. The responses obtained from various runs are significantly exceptional which implies that each of the factors hasa substantial effect on the response.

Table 4. 18:The CCD matrix along with the experimental responses for moisture removal from blanched WY and AY using convective drying

	Temp.(Deg C)	Thickness (cm)	AirSpeed (m/s)	χfor W.Y(%)	χfor A.Y(%)
1	50	2	2	31.72	41.75
2	60	2	2	28.51	32.13
3	50	4	2	25.62	49.30
4	60	4	2	30.82	33.36
5	50	2	3	34.39	30.57
6	60	2	3	39.4	41.7
7	50	4	3	44.8	50.67
8	60	4	3	43.97	45.01
9	47.5	3	2.5	40.54	41.3
10	62.5	3	2.5	31.97	34.8
11	55	1.5	2.5	37.02	38.84
12	55	4.5	2.5	39.86	40.08
13	55	3	1.75	34.39	44.64

14	55	3	3.25	32.76	47.2
15	55	3	2.5	34.87	47.93
16	55	3	2.5	36.87	46.54
17	55	3	2.5	33.87	48.54
18	55	3	2.5	30.07	47.19
19	55	3	2.5	34.89	44.54
20	55	3	2.5	35.87	45.54

4.9.1 ANOVA analysis and model fitting

The adequacy of the models was evaluated by applying the lack-of-fit test. This test is used in the numerator in an f-test of the null hypothesis and indicates that a proposed model fits well or not. The test for lack-of-fit compares the variation around the model with pure variation within replicated observations. This test measures the adequacy of the different models based on response surface analysis (Lee *et al.,* 2006). As shown in Table D1 and D2 in the appendix section, there was a significant difference (F-value = 38.93 and 46.18) of lack of fit for Linear and 2FI models, and (F-value = 108.68 and 37.08) for water yam (WY) and aerial yam (AY) respectively. However, the test was not significant in quadratic model (F-value = 2.4 and 0.78) for AY and WY respectively. The significant results of lack of fit for linear and 2FI models showed that these models are not adequate to use. The results of tables for regression model summary and model summary statistics (Tables D3, D4, D5, and D6) show that the quadratic model can well describe the convective drying of blanched WY and AY for moisture content removal, respectively. The R-squared, adjusted R-squared and the predicted R-squared values for the quadratic models show a high value of 0.9742, 0.9509, 0.8475 respectively for the W.Y and

0.9936, 0.9878, 0.9742 respectively for the AY, when compared to other models (cubic, 2FI and linear) as shown in TablesD5 and D6. The measure of how efficient the variability in the actual response values can be explained by the experimental variables and their interactions is given by the R-Squared value.

The higher the R^2 value, the better the model predicts the response. Adjusted-R^2 is a measure of the amount of variation around the mean explained by the model, adjusted for the number of terms in the model. The adjusted-R^2 decreases as the number of terms in the model increases, if those additional terms don't add value to the model. Predicted-R^2 is a measure of the amount of variation in new data explained by the model. The predicted-R^2 and the adjusted-R^2 should be within 0.20 of each other. Otherwise, there may be a problem with either the data or the model, (Taran and Aghaie, 2015). Based on these results, the effect of each parameter was evaluated using quadratic model as shown on ANOVA for Response Surface quadratic model.

Table 4. 19:ANOVA for Response Surface Reduced Quadratic model for moisture content removal from blanched W.Y

Source	Sum of Squares	Df	Mean Square	F Value	p-value Prob > F	
Model	3605.57	9	400.62	41.93	< 0.0001	significant
X_1-Temp.	54.06	1	54.06	5.66	0.0387	
X_2-Thickness	903.3	1	903.3	94.54	< 0.0001	
X_3-Air Speed	339.41	1	339.41	35.52	0.0001	
X_1X_2	198.8	1	198.8	20.81	0.001	
X_1X_3	119.2	1	119.2	12.48	0.0054	
X_2X_3	7.84	1	7.84	0.82	0.3863	
X_1^2	1327.47	1	1327.47	138.93	< 0.0001	
X_2^2	535.64	1	535.64	56.06	< 0.0001	
X_3^2	69.81	1	69.81	7.31	0.0222	
Residual	95.55	10	9.55			
Lack of Fit	67.8	5	13.56	2.44	0.1747	not significant
Pure Error	27.75	5	5.55			
Cor Total	3701.12	19				
Std. Dev.	3.09	R-Squared		0.9742		
Mean	27.29	Adj R-Squared		0.9509		
C.V. %	9.32	Pred R-Squared		0.8475		

PRESS	564.25	Adeq Precision	20.64

Table 4. 20:ANOVA for Response Surface Reduced Quadratic model for moisture removal from blanched A.Y

Source	**Sum of Squares**	**Df**	**Mean Square**	**F Value**	**p-value Prob > F**	
Model	3077.42	9	341.94	172.3	< 0.0001	significant
X_1-Temp.	32.06	1	32.06	16.16	0.0024	
X_2-Thickness	356.23	1	356.23	179.5	< 0.0001	
X_3-Air Speed	26.12	1	26.12	13.16	0.0046	
X_1X_2	448.95	1	448.95	226.22	< 0.0001	
X_1X_3	878.85	1	878.85	442.84	< 0.0001	
X_2X_3	680.99	1	680.99	343.14	< 0.0001	
X_1^2	145.1	1	145.1	73.12	<0.0001	
X_2^2	491.15	1	491.15	247.48	< 0.0001	
X_3^2	5.04	1	5.04	2.54	0.1423	
Residual	19.85	10	1.98			
Lack of Fit	8.67	5	1.73	0.78	0.6062	not significant
Pure Error	11.17	5	2.23			
Cor Total	3097.27	19				

Std. Dev.	1.41	R-Squared	0.9936
Mean	39.77	Adj R-Squared	0.9878
C.V. %	3.54	Pred R-Squared	0.9742

PRESS	79.9	Adeq Precision	47.07

The independent variables in the specified model and the effect of each variable were evaluated. For this reason and in order to evaluate the adequacy of the selected model several appraisal techniques were used. The coefficient of determination (R^2), the adjusted determination coefficient (adjusted R^2) and coefficient of variation (CV) were used to weigh the adequacy of the model as used by other researchers (Chen *et al.,* 2010; Wang *et al.,*2007). The high model F-values from both ANOVA estimations show that the quadratic model term is significant. Hence the reduced quadratic has$\mathbf{X_1, X_2, X_3, X_1X_2, X_1X_3, X_2X_3, X_1^2, X_2^2, X_3^2}$as significant model terms. The low f-values for lack of fit depicts its insignificance relative to pure error. Non-significant lack of fit is desirable because it means the model will produce a good fit. Model reduction eliminates insignificant terms, hence improving the model prediction accuracy and the model reproducibility. The f-value for effect of yam thickness shows that its effect on the moisture content was significantly high. The coefficient of variation (CV) which is defined as the ratio of the standard deviation of estimate to the mean value of the observed responses. It is also a measure of reproducibility and repeatability of the model (Chen *et al.,* 2010; Chen *et al.,* 2011). The results obtained from the CV of both processes are below 10% indicating that the models can reasonably reproduce the output of the drying process (Chen *et al.,* 2011). The signal to noise ratio which is given as the value of the adequacy precision indicates that an adequate relationship of signal to noise ratio exists.

The selected model in terms of the actual values are given in the equations 4.8 and 4.9;

$$\chi_{W.Y} = 1850.57 - 57.204X_1 - 84.640X_2 - 120.612X_3 + 0.997\,X_1X_2 + 1.544X_1X_3 - 1.980X_2X_3 + 0.453X_1^2 + 7.209X_2^2 + 10.410X_3^2 \quad (4.8)$$

$$\chi_{A.Y} = 24.741 + 10.203X_1 + 83.031X_2 - 269.074X_3 - 1.498X_1X_2 +$$

$$4.192X_1X_3 + 18.452X_2X_3 - 0.150X_1^2 - 6.903X_2^2 - 2.796X_3^2 \quad (4.9)$$

Where χ is the moisture content.

The equation in terms of actual factors can be used to make predictions about the response for given levels of each factor. Here, the levels are to be specified in the original units for each factor. The response values obtained by inserting the independent values are the predicted values of the model. These values are compared to the actual and experimental values. The result of this comparison is shown in Figure 4.75 - 4.78. Figs. 4.75 and 4.76 show the comparison for convective drying of unblanched aerial yam and water yam, while Figs. 4.77 and 4.78 show the predicted and actual correlation for convective drying blanched aerial and water respectively. The linear correlation for the blanched samples depicts a confidently distributed relationship between the predicted and the actual values which is attributed to the enhanced drying resulting from thermal treatment (blanching).

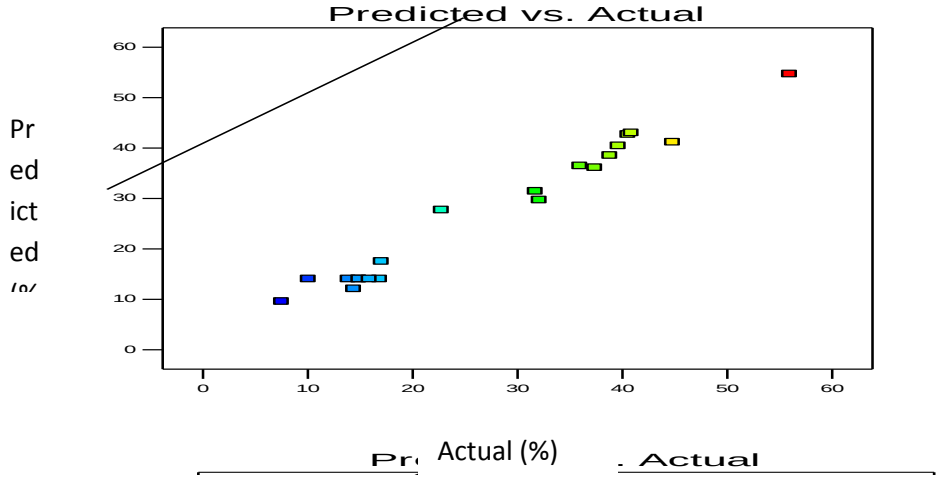

Figure 4. 69:Linear correlation between predicted vs. actual values for moisture removal of unblanched AY convective drying

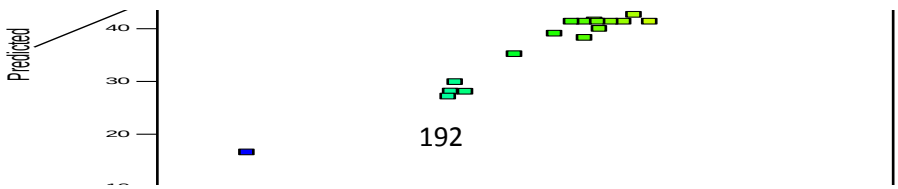

Figure 4. 70:Linear correlation between predicted vs. actual values for moisture removal of unblanched WY convective drying

Pre
dic
ted
(%)

Actual (%)

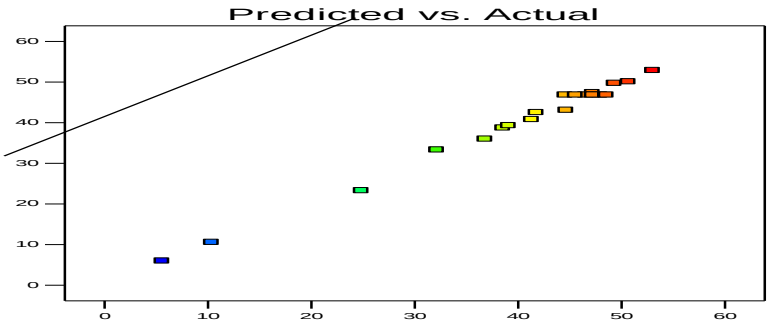

Pre
dic
ted
(%)

Actual (%)

Figure 4. 71:Linear correlation between predicted vs. actual values for moisture removal of blanched AY convective drying

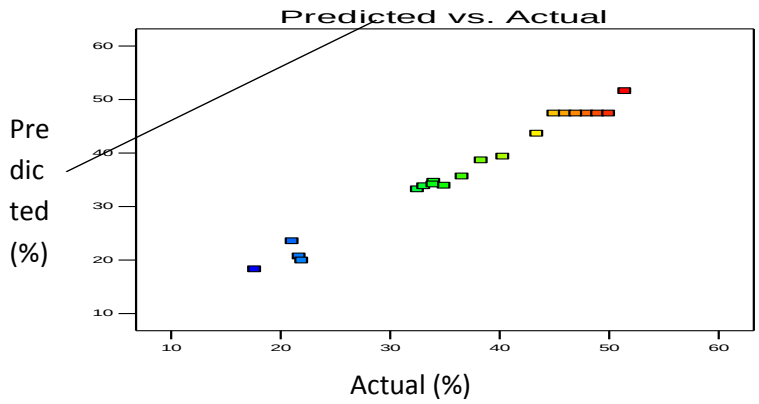

Figure 4. 72:Linear correlation between predicted vs. actual values for moisture removal of blanched WY convective drying

This relationship is desirable for optimisation step because the predicted optimal result will produce an insignificant deviation from the experimental value.

4.9.2 3D surface and interaction plots

In order to visualize the relationship between the experimental variables and the responses, and to study single and interaction effects of all the factors, response surface and interaction plots were generated from the quadratic model. The results are displayed in Figures 4.79 – 4.82. These plots illustrate the response of different experimental variables and can be used to identify the major interactions between the variables.

4.9.3 Effect of drying temperature and thickness

The effect of sample thickness and drying temperature for the convective drying of blanched AY and WY are displayed in Figures 4.79 and 4.80 respectively.

At all levels of sample geometry, the moisture content decreased steadily with increase in drying temperature as shown in Figures 4.79a and 4.80a. The rate of moisture removal was rapid at small sample sizes and quite minimal at increased thickness.

At drying temperature lower than 58^0C, more than 25% moisture removal was recorded as seen in Figures. 4.79b and 4.80b. At low sample sizes, there was an observable accelerated rate of moisture content removal for both AY and WY.

The results for the effect of drying temperature and thickness on moisture content for unblanched AY and WY are displayed on Figures 4.81 and 4.82 respectively. The unblanched samples recorded an enhanced rate of moisture removal with an increased rate at low values of sample thickness and drying temperature.

The reduced moisture content observed at increased temperature for both blanched and unblanched samples is attributed to high kinetic energy associated with increased temperature (Surija et al., 2016).

Also, unlike other drying techniques, convective drying enables some unique characteristics such as high drying rate, lower oxygen medium which will ensure high quality and nutritive dried food products (Wu et al., 2007). The increased rate of moisture loss at low sizes is as a result of higher steam and liquid diffusion rates considering the fact that water moves from the interior part of the substance to the surface. This movement is instigated by concentration gradient and temperature differences. Similar observation was made by Correia *et al.*, (2015) during the study to determine the effect of temperature, time and food material thickness on the dehydration process of WY.

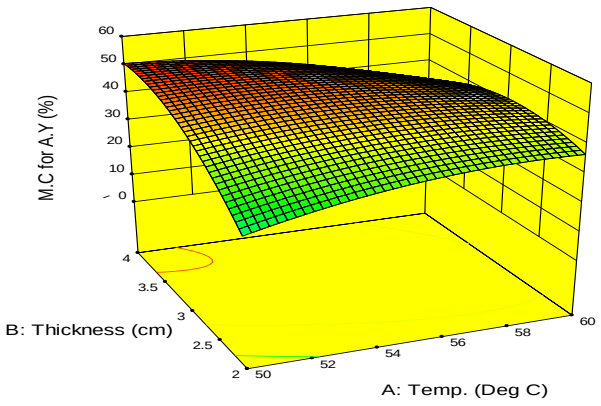

Figure 4. 73a:3D surface plot for the effect of sample thickness and temperature on moisture content of blanched AY using convective drying

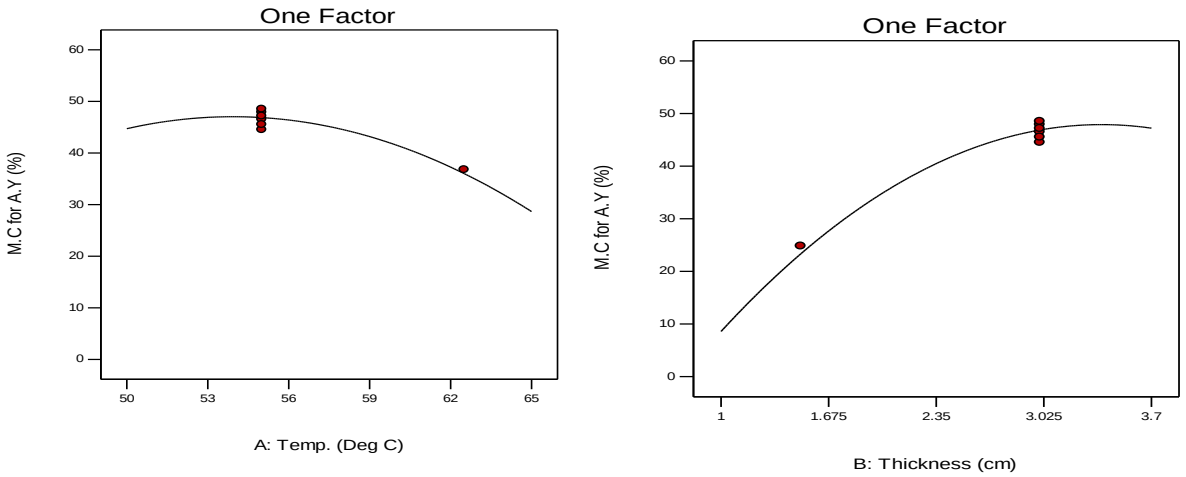

Fig. 4.79c - Single effect plot for the effect of thickness on moisture content of blanched AY using convective drying

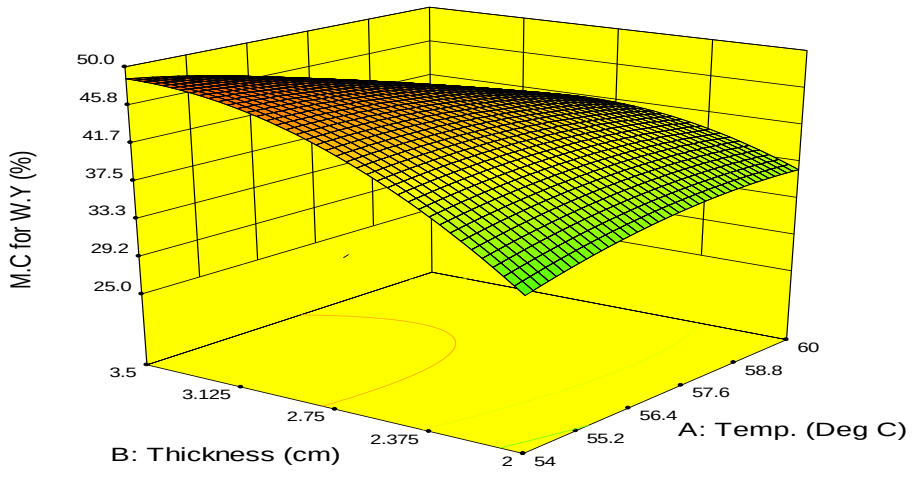

Figure 4. 74a:3D surface plot for the effect of sample thickness and temperature on moisture content of blanched WY using convective drying

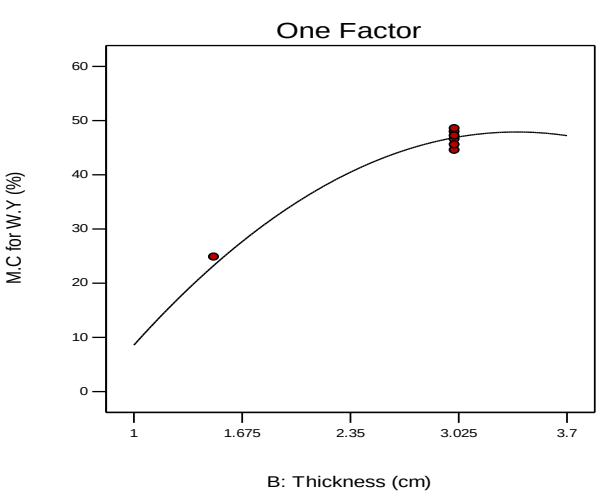

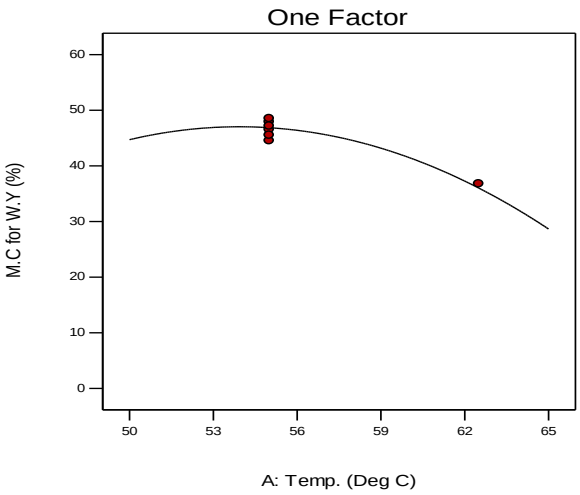

Fig. 4.80b - Single effect plot for the effect of thickness on moisture content of blanched WY using convective drying

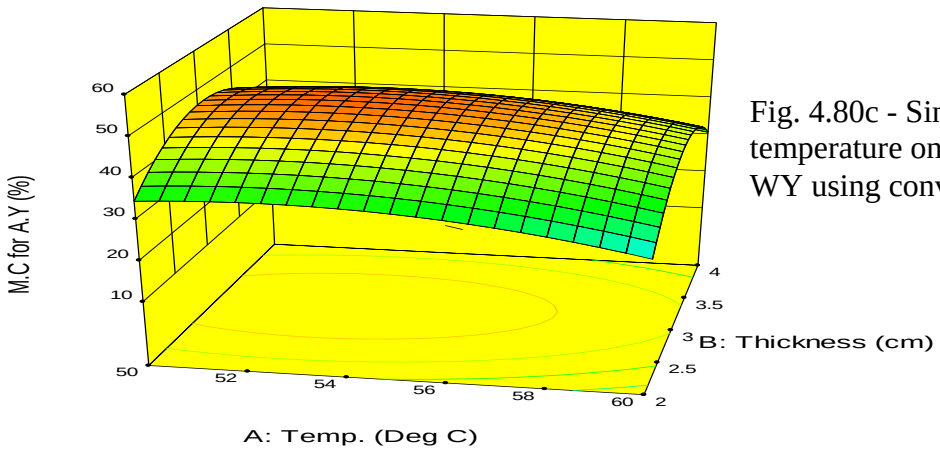

Fig. 4.80c - Single effect plot for the effect of temperature on moisture content of blanched WY using convective drying

Figure 4. 75a:- 3D surface plot for the effect of sample thickness and temperature on moisture content of unblanched AY using convective drying

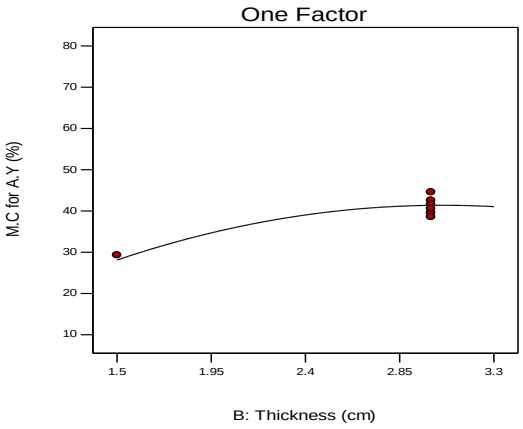

Fig. 4.81b - Single effect plot for the effect of sample thickness on moisture content of unblanched AY using convective drying

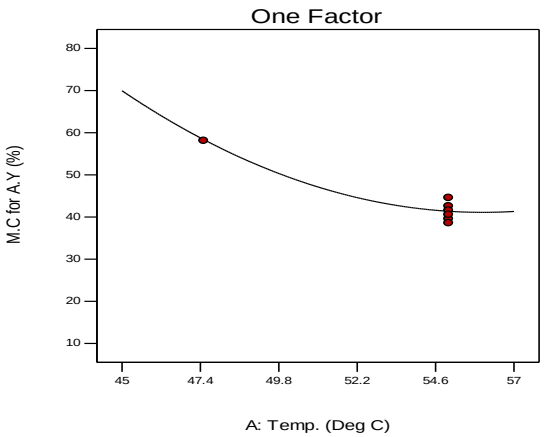

Fig. 4.81c - Single effect plot for the effect of sample temperature on moisture content of unblanched AY using convective drying

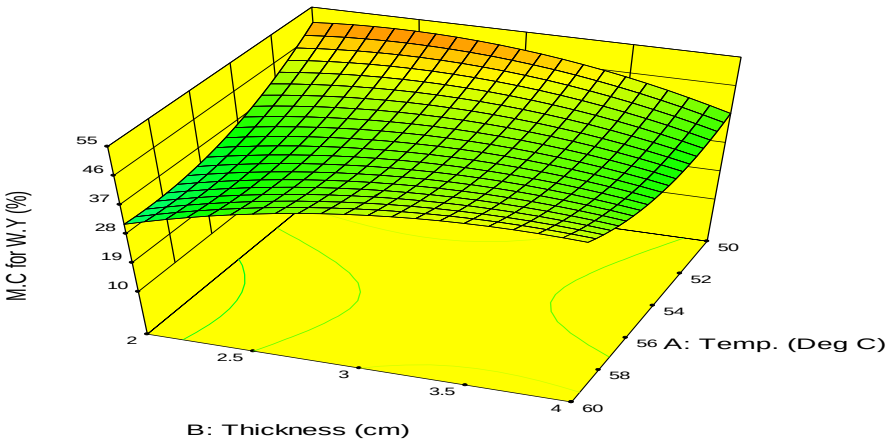

Figure 4. 76a:3D surface plot for the effect of sample thickness and temperature on moisture content of unblanched WY using convective drying

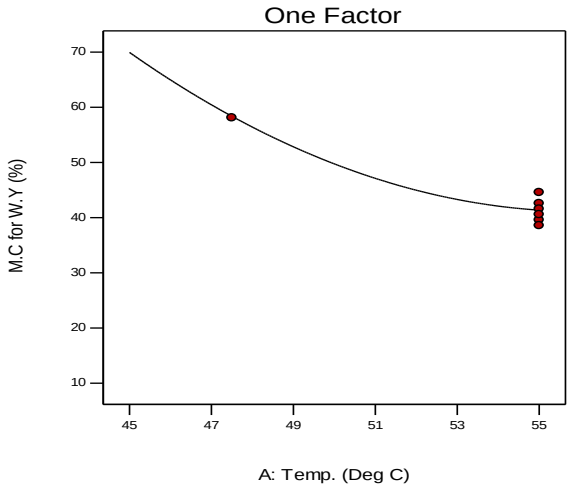

Fig. 4.82b - Single effect plot for the effect of sample temperature on moisture content of unblanched WY using convective drying

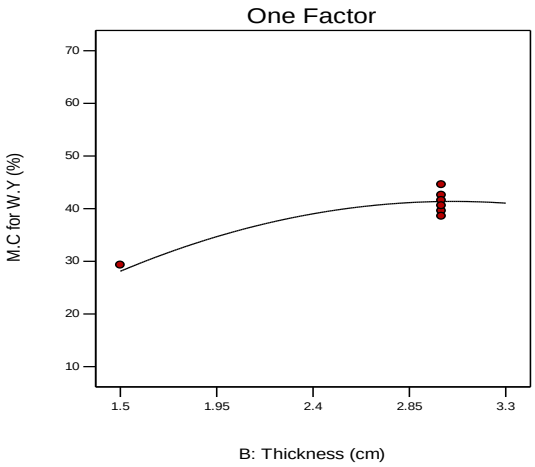

Figure 4.82c - Single effect plot for the effect of sample thickness on moisture content of unblanched WY using convective dry

4.9.4 Optimization using Solar dryer

Table 4.21 is the result of the optimization of the drying of the two yam samples using solar dryer.

Table 4. 21:The CCD matrix along with the experimental responses for moisture removal from blanched and unblanched WY and AY using solar drying at average ambient temp. of 29.7^{o}C.

No. of runs Num.	**Air speed (m/s)**	**Thickness (mm)**	**Mass wet sample (g)**	**χ for Blanched samples**		**χfor Unblanched Samples**	
				W.Y (%)	**A.Y (%)**	**W.Y (%)**	**A.Y (%)**
1	1.5	2	70	21.54	21.66	28.5	31.09
2	2.5	2	70	33.8	38.03	34.59	41.21
3	1.5	4	70	18.07	23.03	27.89	27.24
4	2.5	4	70	34.36	43.51	36.65	48.7
5	1.5	2	100	42.09	38.19	45.64	45.52
6	2.5	2	100	28.22	32.6	39.54	37.06
7	1.5	4	100	32.66	22.79	40.22	28.41

8	2.5	4	100	38.84	43.44	46.33	45.36
9	1.1	3	85	31.87	32.39	34.69	37.01
10	2.9	3	85	31.1	30.12	38.05	36.23
11	2	1	85	35.23	29.75	45.43	38.81
12	2	5	85	54.15	60.59	56.38	68.24
13	2	3	59	22.27	24.13	25.77	31.18
14	2	3	111	52.84	55.66	57.29	65.71
15	2	3	85	36.97	37.71	38.04	55.06
16	2	3	85	39.97	42.52	43.04	55.15
17	2	3	85	52.97	56.66	53.04	57.65
18	2	3	85	55.97	57.66	59.04	59.06
19	2	3	85	42.97	62.66	46.09	65.06
20	2	3	85	43.02	47.61	47.52	56.05

4.9.5 ANOVA analysis and model fitting

Lack-of-fit test was applied in weighing the fitness of the generated models based on response surface analysis (Lee *et al.*, 2006). This test compares the variation around the model with pure variation within replicated observations. Tables 4.22 to 4.25 in the appendix section show that there was a significant difference of lack of fit for Linear and 2FI models for both WY and AY respectively. However, the test was not significant in quadratic modelfor AY and WY respectively. The significant results of lack of fit show that the linear and 2FI model are not adequate to use for response prediction. Similarly, the regression analysis result further affirms

the superiority of the quadratic model over other models as seen in Table D11 - D14. The R-squared, adjusted R-squared and the predicted R-squared values for the quadratic models show a high value of R^2> 0.95 for both AY and WY when compared to other models. The measure of how efficient the variability in the actual response values can be explained by the experimental variables and their interactions is given by the R-Squared value.

The higher the R^2 value, the better the model predicts the response. Adjusted-R^2 is a measure of the amount of variation around the mean explained by the model, adjusted for the number of terms in the model. The adjusted-R^2 decreases as the number of terms in the model increases, if those additional terms don't add value to the model. Predicted-R^2 is a measure of the amount of variation in new data explained by the model. The predicted-R^2 and the adjusted-R^2 should be within 0.20 of each other. Otherwise there may be a problem with either the data or the model, (Taran and Aghaie, 2015). Based to these results, the effect of each parameter was evaluated using quadratic model as shown on ANOVA for response surface quadratic model.

Table 4. 22:ANOVA for Response Surface Reduced Quadratic model for moisture removal from unblanched W.Y using solar drying

Source	Sum of Squares	df	Mean Square	FValue	p-value Prob> F	Remarks
Model	23761.12	9	2640.12	988.28	< 0.0001	significant
X_1-Airspeed	14420.37	1	14420.37	5397.96	< 0.0001	
X_2-Thickness	554.78	1	554.78	207.67	< 0.0001	
X_3-Mass	1316.38	1	1316.38	492.76	< 0.0001	
X_1X_2	311	1	311	116.42	< 0.0001	
X_1X_3	971.52	1	971.52	363.67	< 0.0001	

X_2X_3	466.35	1	466.35	174.57	< 0.0001	
X_1^2	4.41	1	4.41	1.65	0.2276	
X_2^2	4798.57	1	4798.57	1796.24	< 0.0001	
X_3^2	1229.46	1	1229.46	460.22	< 0.0001	
Residual	26.71	10	2.67			
Lack of Fit	4	5	0.8	0.18	0.9602	not significant
Pure Error	22.71	5	4.54			
Cor Total	23787.83	19				

Std. Dev.	1.63	R-Squared	0.9989
Mean	69.54	Adj R-Squared	0.9979
C.V. %	2.35	Pred R-Squared	0.9973
PRESS	64.28	AdeqPrecision	107.453
-2 Log Likelihood	62.55	BIC	92.5

Table 4. 23:ANOVA for Response Surface Reduced Quadratic model for moisture removal from unblanched A.Y using solar drying

Source	**Sum of Squares**	**df**	**Mean Square**	**F Value**	**p-value Prob> F**	
Model	13429.87	9	1492.21	1186.03	< 0.0001	significant
X_1-Air speed	9654.44	1	9654.44	7673.47	< 0.0001	
X_2-Thickness	33.11	1	33.11	26.32	0.0004	
X_3-Mass	980.14	1	980.14	779.03	< 0.0001	
X_1X_2	39.38	1	39.38	31.3	0.0002	

X_1X_3	720.29	1	720.29	572.5	< 0.0001	
X_2X_3	194.54	1	194.54	154.62	< 0.0001	
X_1^2	48.51	1	48.51	38.56	0.0001	
X_2^2	739.99	1	739.99	588.15	< 0.0001	
X_3^2	1073.84	1	1073.84	853.5	< 0.0001	
Residual	12.58	10	1.26			
Lack of Fit	7.13	5	1.43	1.31	0.3878	not significant
Pure Error	5.45	5	1.09			
Cor Total	13442.45	19				

Std. Dev.	1.12	R-Squared	0.9991
Mean	46.23	Adj R-Squared	0.9982
C.V. %	2.43	Pred R-Squared	0.9954
PRESS	62.22	Adeq Precision	122.397
-2 Log Likelihood	47.49	BIC	77.44

Table 4.24:ANOVA for Response Surface Reduced Quadratic model for moisture removal from blanched W.Y using solar drying

Source	**Sum of Squares**	**df**	**Mean Square**	**F Value**	**p-value Prob> F**	
Model	10793.4	9	1199.27	50.85	< 0.0001	Significant
X_1-Air speed	7345.43	1	7345.43	311.46	< 0.0001	
X_2-Thickness	436.5	1	436.5	18.51	0.0016	
X_3-Mass	614.34	1	614.34	26.05	0.0005	
X_1X_2	821.75	1	821.75	34.84	0.0002	

X_1X_3	46.27	1	46.27	1.96	0.1916	
X_2X_3	44.65	1	44.65	1.89	0.1989	
X_1^2	1.86E-03	1	1.86E-03	7.89E-05	0.9931	
X_2^2	1046.88	1	1046.88	44.39	< 0.0001	
X_3^2	296.45	1	296.45	12.57	0.0053	
Residual	235.84	10	23.58			
Lack of Fit	173.19	5	34.64	2.76	0.1444	not significant
Pure Error	62.65	5	12.53			
Cor Total	11029.24	19				

Std. Dev.	4.86	R-Squared	0.9786
Mean	67.55	Adj R-Squared	0.9594
C.V. %	7.19	Pred R-Squared	0.8722
PRESS	1409.44	Adeq Precision	23.564
-2 Log Likelihood	106.11	BIC	136.06

Table 4.25:ANOVA for Response Surface Reduced Quadratic model for moisture removal from blanched A.Y using solar drying

Source	**Sum of Squares**	**df**	**Mean Square**	**F Value**	**p-value Prob> F**	
Model	10015.48	9	1112.83	60.75	< 0.0001	significant
X_1-Air speed	6841.82	1	6841.82	373.52	< 0.0001	
X_2-Thickness	142.3	1	142.3	7.77	0.0192	

X_3-Mass	504.65	1	504.65	27.55	0.0004	
X_1X_2	827.23	1	827.23	45.16	< 0.0001	
X_1X_3	79.44	1	79.44	4.34	0.0639	
X_2X_3	13.55	1	13.55	0.74	0.41	
X_1^2	228.77	1	228.77	12.49	0.0054	
X_2^2	1135.75	1	1135.75	62.01	< 0.0001	
X_3^2	179.27	1	179.27	9.79	0.0107	
Residual	183.17	10	18.32			
Lack of Fit	133.76	5	26.75	2.71	0.1492	not significant
Pure Error	49.41	5	9.88			
Cor Total	10198.65	19				

Std. Dev.	4.28	R-Squared	0.9828
Mean	43.89	Adj R-Squared	0.9659
C.V. %	9.75	Pred R-Squared	0.8932
PRESS	1088.73	Adeq Precision	25.539
-2 Log Likelihood	101.05	BIC	131.01

The coefficient of determination (R^2), the adjusted determination coefficient (Adj R-Squared), the predicted -R^2 and coefficient of variance (CV) were used to weigh the adequacy of the model (Chen et al., 2010; Wang et al., 2007). The high regression values associated with these terms show that the produced models are easily reproducible with negligible errors. The results

obtained from the coefficient of variance (CV) indicates that all values are <10%, which certifies the reproducibility accuracy of the models in predicting experimental values (Chen et al., 2011). Model reduction was used to eliminate insignificant model terms for better prediction accuracy. Therefore, the significant model terms are X_1, X_2, X_3, X_1X_2, X_1X_3, X_2X_3, X_1^2, X_2^2 and X_3^2. The f value is used to measure the contribution of each term to the overall model output and performance. The low f-value for lack of fit depicts its insignificance relative to pure error. Non-significant lack of fit is desirable because it means the model will produce a good fit. The f-value for the effect of air speed shows that it has the highest effect on the overall performance of the solar drying process.

The selected model in terms of the actual values are given in the equations 4.10 to 4.13;

Final Equations in terms of Actual Factors:

$$\chi_{\text{blanched W.Y}} = -92.507 + 14.661X_1 - 78.778X_2 + 4.7576X_3 + 19.690X_1X_2 - 0.3147X_1X_3 - 0.1501X_2X_3 + 0.0447X_1^2 + 7.9142X_2^2 - 0.0191X_3^2 \quad (4.10)$$

$$\chi_{\text{blanched A.Y}} = 117.0176 - 111.497X_1 - 84.239X_2 + 2.341X_3 + 19.756X_1X_2 + 0.412X_1X_3 - 0.083X_2X_3 + 15.682X_1^2 + 8.243X_2^2 - 0.015X_3^2 \quad (4.11)$$

$$\chi_{\text{unblanched W.Y}} = -339.083 - 102.333X_1 + 123.157X_2 + 5.802X_3 + 12.113X_1X_2 + 1.442X_1X_3 - 0.485X_2X_3 + 2.179X_1^2 - 16.944X_2^2 - 0.0389X_3^2 \quad (4.12)$$

$$\chi_{\text{blanched W.Y}} = -235.357 - 94.213X_1 + 58.785X_2 + 5.175X_3 + 4.311X_1X_2 + 1.242X_1X_3 - 0.313X_2X_3 + 7.222X_1^2 - 6.654X_2^2 - 0.0363X_3^2 \quad (4.13)$$

Where χ is the moisture content of the sample

The equation in terms of actual factors can be used to make predictions about the response for given levels of each factor. Here, the levels are to be specified in the original units for each factor. The response values obtained by inserting the independent values are the predicted values of the model. These values are compared to the actual and experimental values. The result of this comparison is shown in Figure 4.83 - 4.86. Figs. 4.83 and 4.84 show the comparison for solar drying of unblanched aerial yam and water yam, while Figs. 4.85 and 4.86 show the predicted and actual correlation for solar drying of blanched aerial and water respectively. The data points were well distributed showing a good agreement between the experimental and predicted response values for all the blanched samples. These values appeared in a very good agreement between the predicted and actual data. Since it can be seen from Figs. 4.85-4.86 that the points wereclosely distributed closely to the straight line of the plot, it confirms the good relationship between the actual values and the predicted values of the response

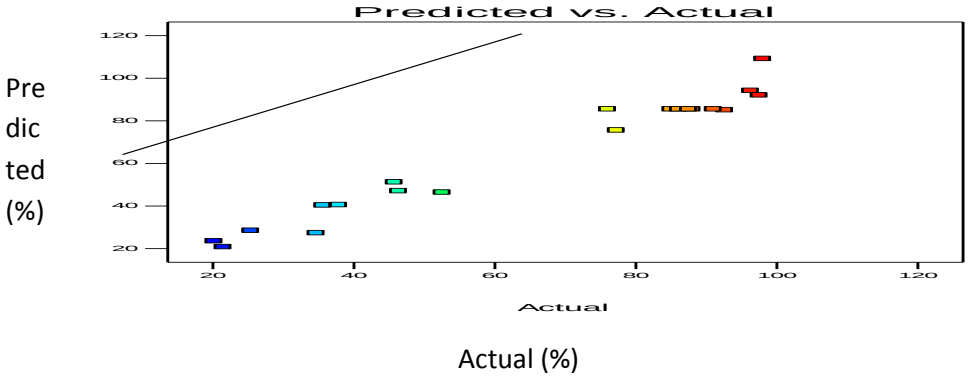

Figure 4. 77:Linear correlation between predicted vs. actual values for moisture removal of unblanched WY by solar drying

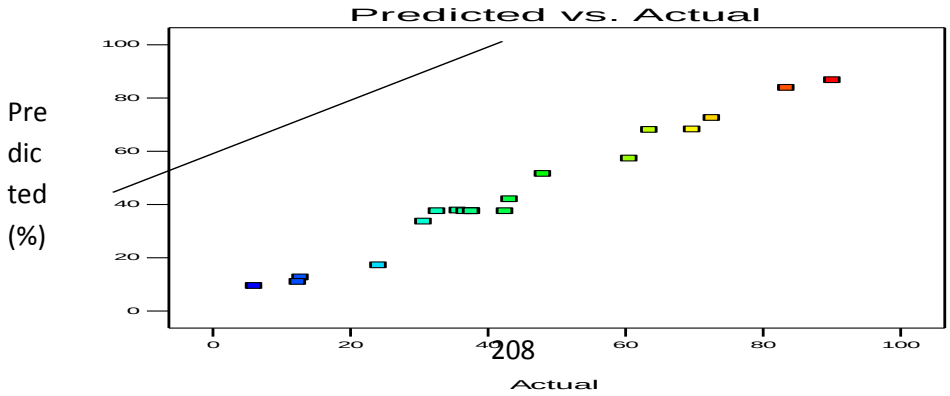

Figure 4. 78:Linear correlation between predicted vs. actual values for moisture removal of blanched WY by solar drying

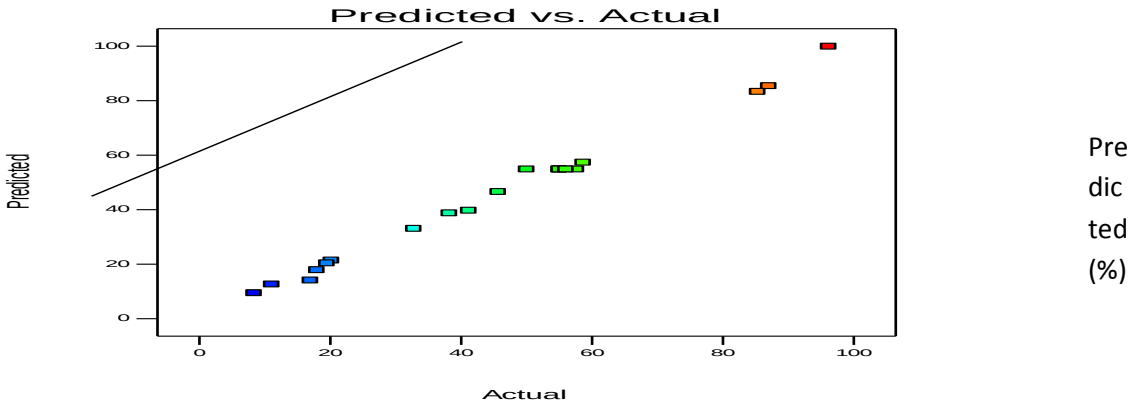

Figure 4. 79: Linear correlation between predicted vs. actual values for moisture removal of unblanched AY by solar drying

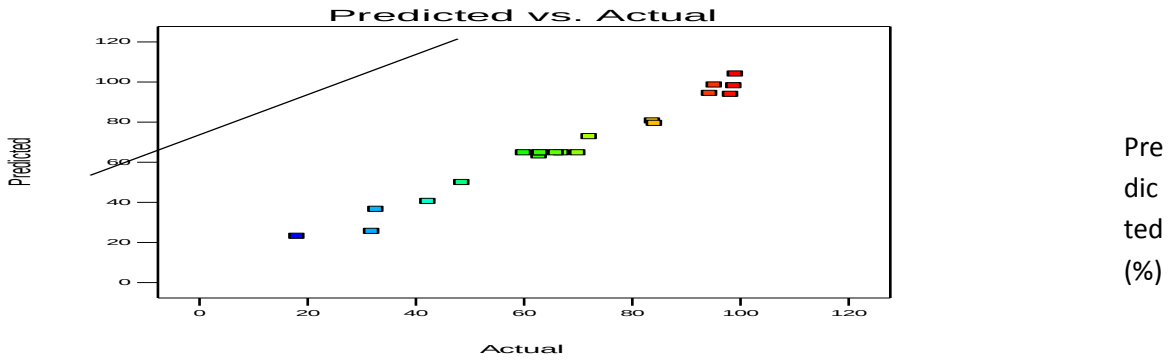

Figure 4. 80:Linear correlation between predicted vs. actual values for moisture removal of blanched AY by solar drying

4.9.6Combined effect of process parameters

The results of all process parameters are presented in Figures 4.87 to 4.90 using 3D surface and single effect plots. The responses and the graphical representations were generated from the experimental quadratic models (eq. 4.3 - eq.4.6)

i. Effect of slice thickness,drying air velocity and mass of samples

The statistical and data analysis show that the thickness and air drying velocity have very significant effects ($p < 0.02$) on the moisture content of both blanched and unblanchedAY and

WY. The effect of the process parameters is displayed on Figures 4.87 to 4.91 for unblanchedand blanched samples.

For both varieties, moisture removal accelerated with increase in drying air velocity. This effect did not display any quadratic character throughout the study. The effect of material thickness showed different trends for the blanched and unblanched samples. For the unblanched samples, increasing the sample thickness from 2mm-3mm resulted in improved removal of moisture (Figs. 87a and 88a). However, bigger sample thickness beyond 3mm declined the rate of moisture content removal as seen in Figures 4.87a and 4.88a.

The effect of sample thickness for the blanched sample is displayed in Figures. 4.87b and 4.88b.It could be observed that the drying rate was slow at thin slices and got to the lowest point of 2% and 6.2% for WY and AY respectively for 3mm slice. Beyond this size, the rate of moisture removal increased steadily with increase in slice thickness. The increase in moisture removal resulting from increase in air drying velocity is as a result of rapid movement of dry air molecules across the drying chamber.

The sample mass had a substantial effect on the moisture removal efficiency. The rate of moisture loss was accelerated with an increase in sample mass as depicted in Figs 4.89b and 4.91 for blanched water yam and aerial yam respectively. From Figures 89a – 91, there was an enhanced rate of moisture removal between 70 g – 90 g mass, for both blanched and unblanched yam samples. Beyond 90 g, the rate of moisture removal attained equilibrium and produced a negligible amount of moisture loss when compared to the result obtained for 100 g mass sample. The particle mass is proportional to the amount of moisture contained in each of the samples.

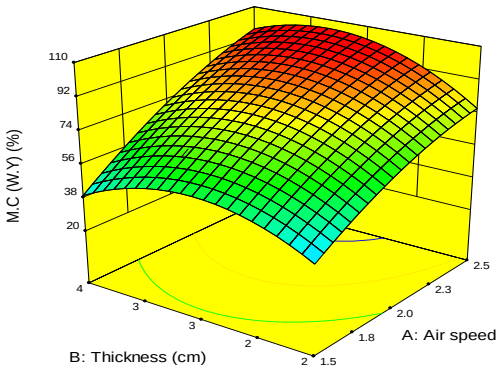

Figure 4. 87a:3D surface plot for the effect of slice thickness and air velocity on moisture content of unblanched WY using solar

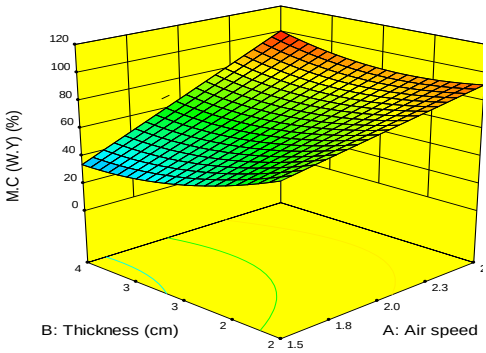

Figure 4. 87b:3D surface plot for the effect of slice thickness and air velocity on moisture content of blanched WY using solar drying

M.C (A.Y) (%)

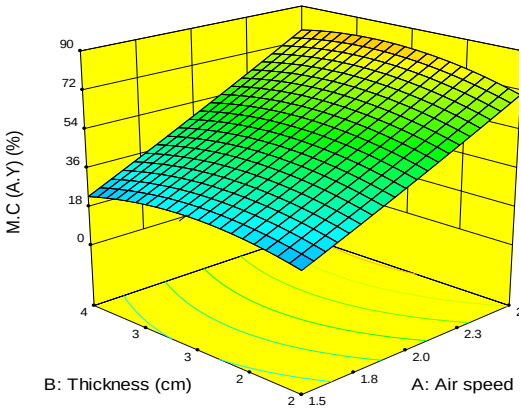

Figure 4. 88a:- 3D surface plot for the effect of slice thickness and air velocity on moisture content of unblanched AY using solar drying

Figure 4. 88b:3D surface plot for the effect of slice thickness and air velocity on moisture content of blanched AY using solar drying

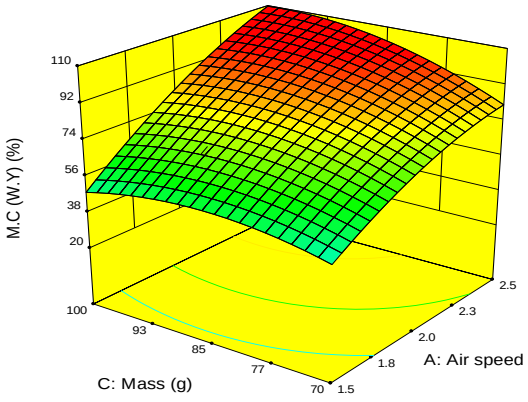

Figure 4. 89a:3D surface plot for the effect of mass of sample and air speed on moisture content of unblanched WY using solar drying

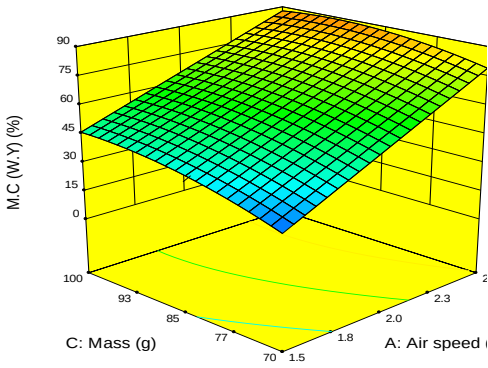

Figure 4. 89b:3D surface plot for the effect of mass of sample and air speed on moisture content of blanched WY using solar drying

Figure 4. 90:3D surface plot for the effect of mass of sample and air speed on moisture conte[illegible] AY using solar dry[illegible]

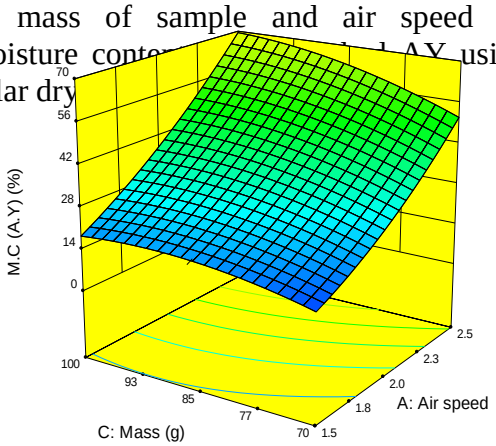

Figure 4. 91:3D surface plot for the effect of mass of sam[illegible] air speed on mois[illegible]ing solar[illegible]

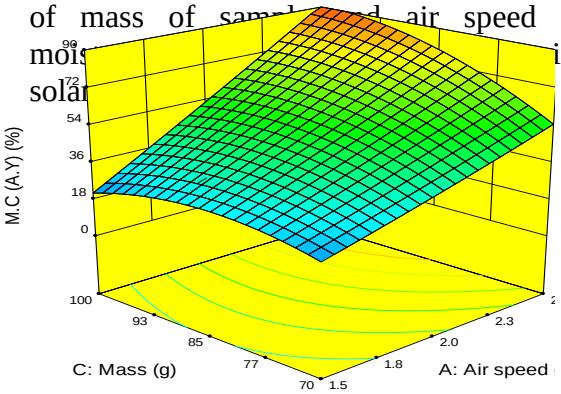

4.10 Artificial Neural Network modelling

Artificial neural networks (ANN's) are inspired by biological neural systems. In this approach weighted sum of inputs arriving at each neuron is passed through an activation function (generally nonlinear) to generate an output signal (Manpreet *et al.,* 2011). Interest in using artificial neural networks (ANNs) for predicting the responses of nonlinear systems has led to a tremendous surge in research activities in the past two decades (Omid *et al.,* 2009; Aghbashlo *et al.,* 2011). They can also be configured in various arrangements to perform a range of tasks including classification, pattern recognition, data mining and process modelling. In the multi-layer perception (MLP) networks, error minimization can be obtained by a number of procedures including gradient descent (GD), Leuenberger–Marquardt (LM), and conjugate gradient (CG). MLPs are normally trained with error back-propagation (BP) algorithm. It is a general method for iteratively solving for weights and biases (Heshmatollah*et al.,* 2014).

4.10.1 Network training

Matlab R2015a was used in this program. A total of 12 (60%) of experimental results were used to train the network, 5 (25%) of the experimental result was used to validate the training while the remaining 3 (15%) was used for testing.

After the selection of the hidden number of neurons, a number of training runs were performed to look out for the best possible weights in error back propagation framework.

4.10.2 Comparison of RSM and ANN

In order to validate the nonlinear nature of the present system and to assess the superiority of either technique in capturing the quadratic nature, a couple of methods are applied. These include;

1) Absolute average relative deviation (AARD) observed for both models;

2) Coefficient of determination for both models.

The AARD observed for both models give an indication of how accurate the model predictions can be. (Josh *et al.*, 2014).

$$\text{AARD (\%)} = \left(\frac{1}{n}\sum_{i=1}^{n}\left\{\frac{\left(R_{art\ .pred} - R_{art\ .exp}\right)}{R_{art\ .exp}}\right\}\right) x\ 100 \qquad (4.14)$$

where n is the number of sample points, $R_{art,pred}$ the predicted value and $R_{art,exp}$ the experimentally determined value. (Josh *et al.*, 2014).

The results of this analysis are tabulated in Tables 4.27 and 4.28 for convective and solar drying respectively, while the model predictions are tabulated in appendix-A. The model comparison and appraisal plots are displayedin Figures 4.92 to 4.107.

Although the results of the RSM and ANN are in reasonable agreement (validating the quadratic nature of the present system), the AARD and regression coefficient (R-SQRD) values suggest that the ANN performed better in capturing the nonlinearity of the system than the RSM. However, RSM performed better in data prediction accuracy for all convective drying processes except the drying of unblanched water yam species.

Table 4. 27:Convective drying parameters for model comparison

Sample	Regression Coefficient (R-SQURD)		Absolute Average Relative Deviation (%)	
	ANN	RSM	ANN	RSM
Blanched Water Yam	0.9371	0.9743	14.16	9.27
Blanched Aerial Yam	0.8817	0.9936	11.95	2.41
unblanched Water Yam	0.9955	0.9694	3.74	4.35
unblanched Aerial Yam	0.9726	0.9839	5.00	3.24

Table 4. 28: Solar drying parameters for model comparison

sample	Regression Coefficient (R-SQURD)		Absolute Average Relative Deviation (%)	
	ANN	RSM	ANN	RSM
Blanched Water Yam	0.9482	0.9786	3.91	5.90
Blanched Aerial Yam	0.9762	0.982	8.62	9.59
Unblanched Water Yam	0.9681	0.9665	7.65	8.39
Unblanched Aerial Yam	0.9941	0.9941	2.17	4.49

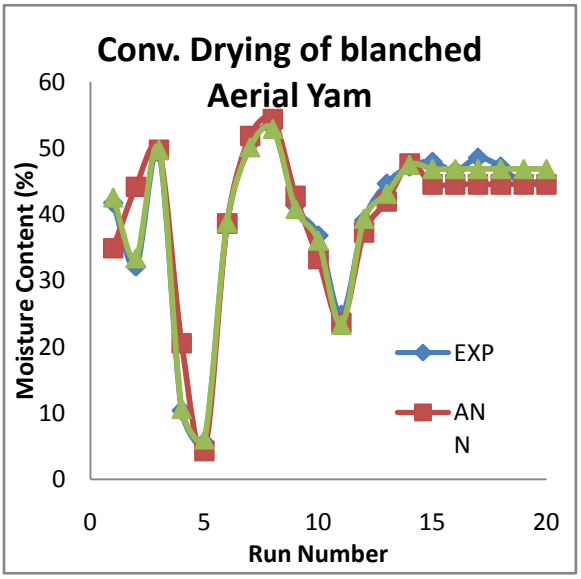

Figure 4. 92:RSM and ANN comparative parity plot for the convective drying of Blanched Aerial Yam.

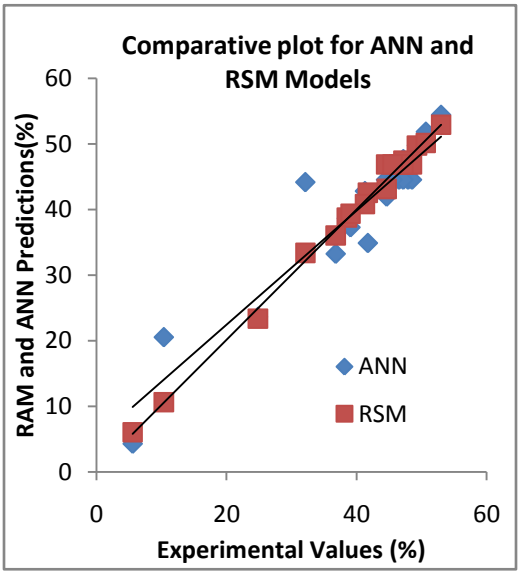

Figure 4.93:RSM and ANN model appraisal plot for the convective drying of Blanched Aerial Yam.

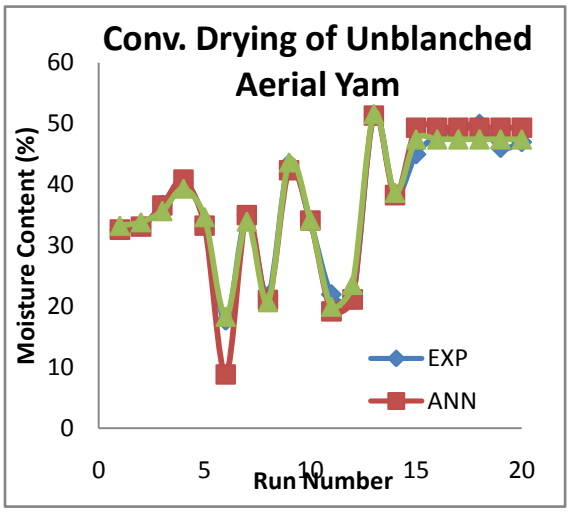

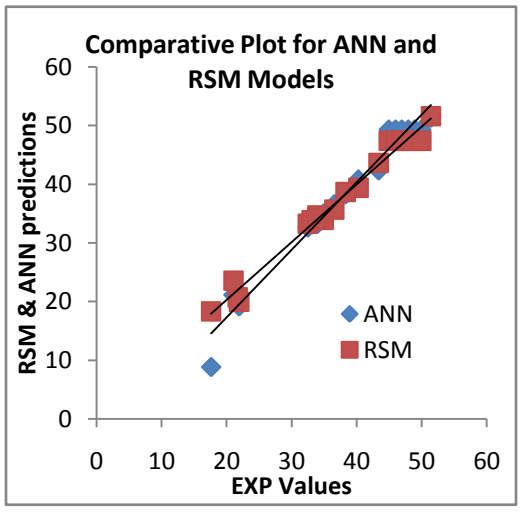

Figu Figure 4.95:RSM and ANN model pari appraisal plot for the convective drying Unl of Unlanched Aerial Yam.

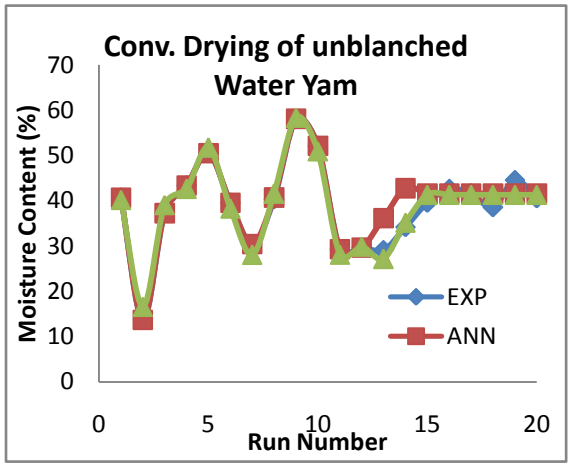

Figure 4.96:RSM and ANN comparative parity plot for the convective drying of Unblanched Water Yam.

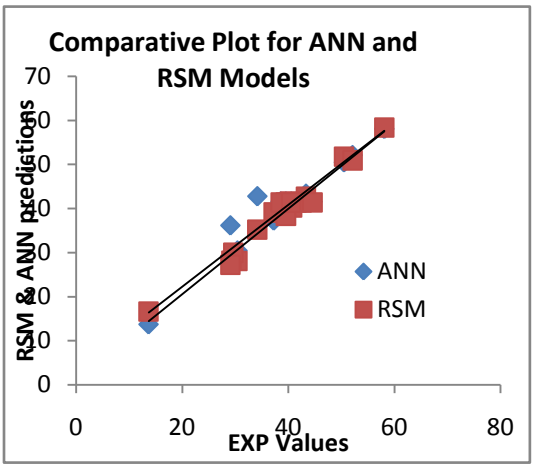

Figure 4. 97:RSM and ANN model appraisal plot for the convective drying of Unblanched Water Yam.

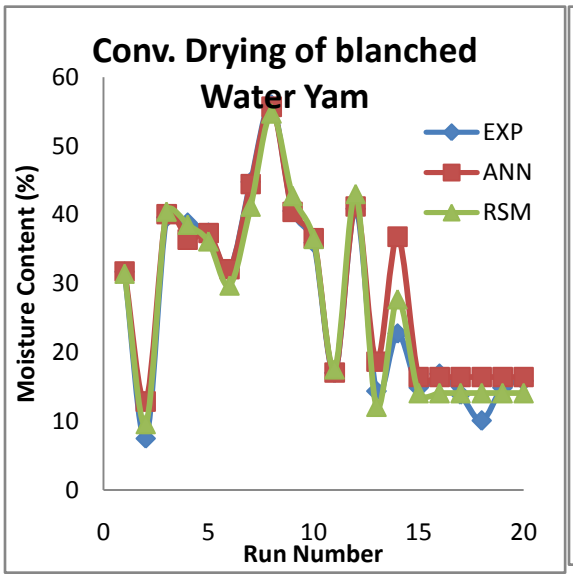

Figure 4.98:RSM and ANN comparative parity plot for the convective drying of Blanched Water Yam.

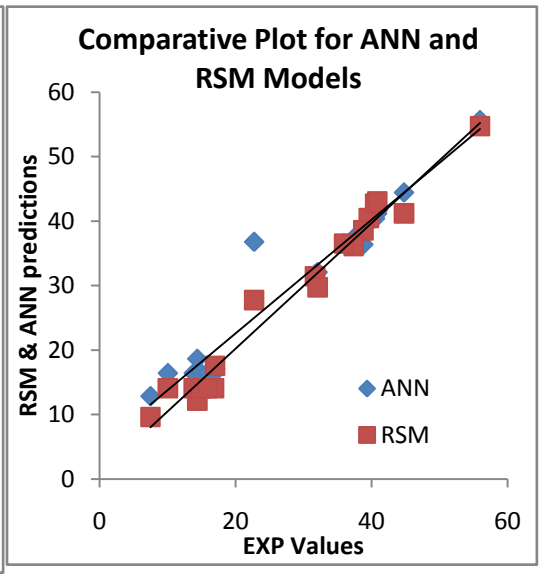

Figure 4.99: RSM appraisal plot f drying of Blanche

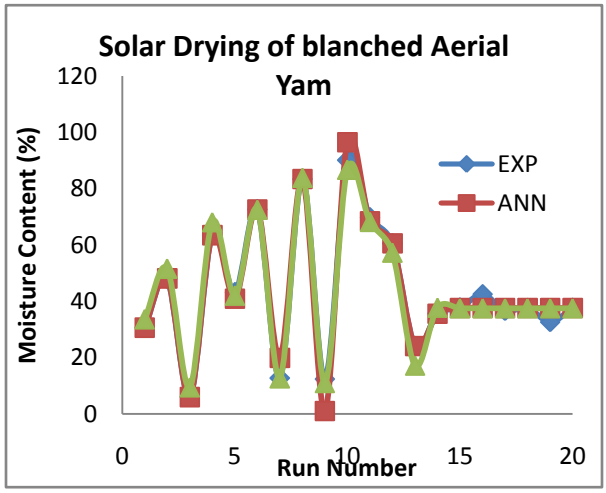

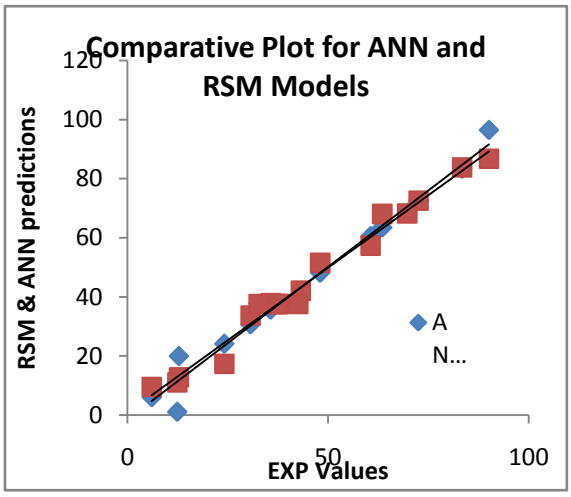

Figure 4.100: RSM and ANN comparative parity plot for the solar drying of Blanched Aerial Yam.

Figure 4.1
appraisal
Blanched

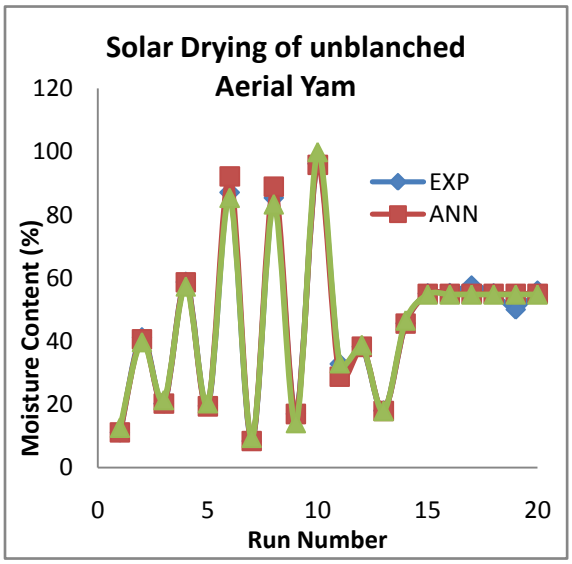

Figure 4.102: RSM and ANN comparative parity plot for the solar drying of Unblanched Aerial Yam.

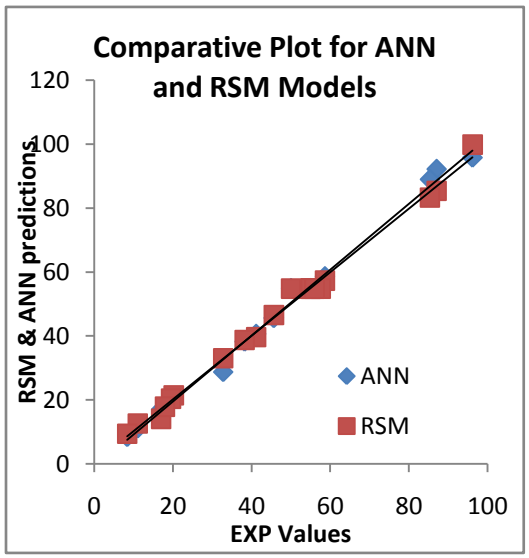

Figure 4.103: RSM and ANN model appraisal plot for the solar drying of Unblanched Aerial Yam

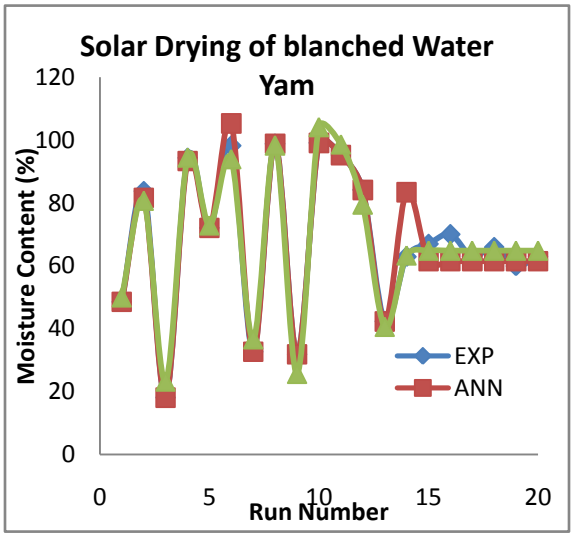

Figure 4.104: RSM and ANN comparative parity plot for the solar drying of Blanched Water Yam.

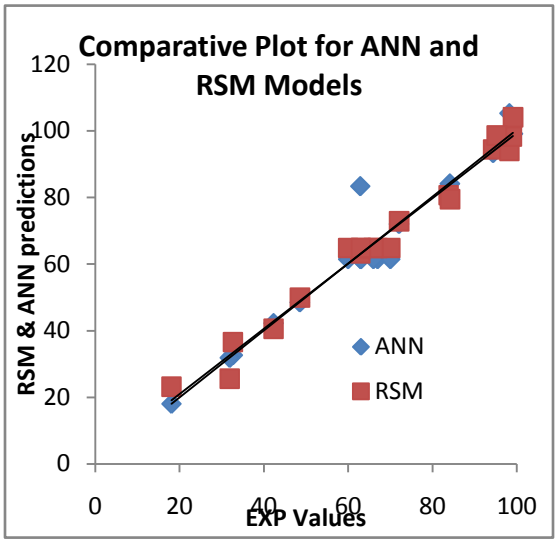

Figure 4.105 RSM and ANN model appraisal plot for the solar drying of Blanched Water Yam.

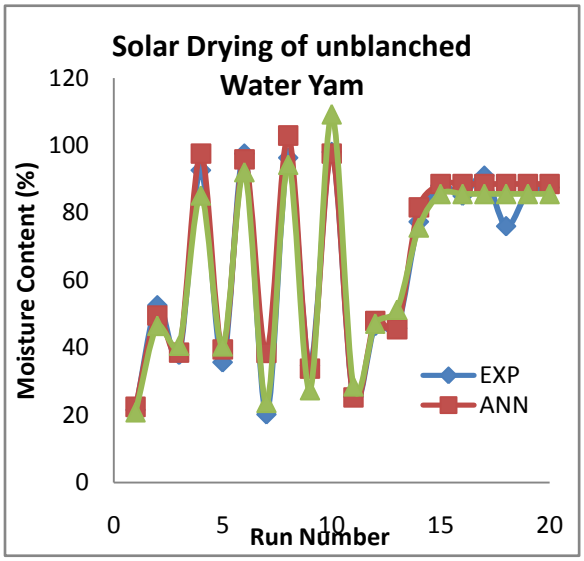

Figure 4.106: RSM and ANN comparative parity plot for the solar drying of Unlanched Water Yam.

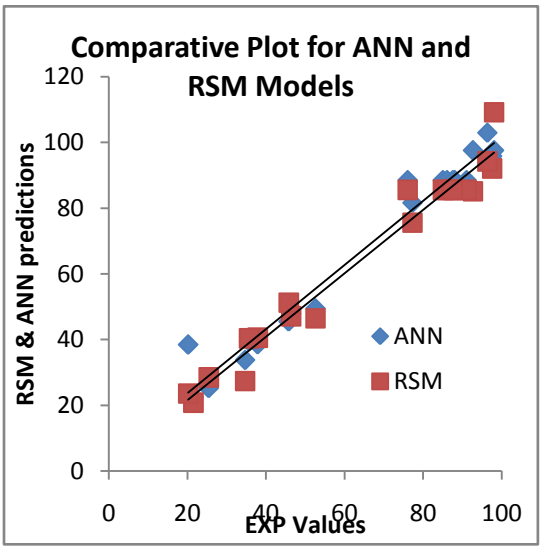

4.9 Process Optimization

Using the numerical optimization technique which is a feature of CCD in the design expert software, a combination of factors that concurrently satisfy the requirements placed on each of the responses and factors could be determined by the software. In choosing the goal for each factor of the numerical optimization, a number of considerations were made. The significance of each of the factors on the final response was the most important consideration. The goal of all other factors was set 'in range', while the moisture content was set at a minimum level.

Based on these, the software predicted optimum reaction conditions (with a desirability level > 85%) and are tabulated in Table 4.29.

Table 4.29:Table of optimal parameters

Sample	Convective Drying Method				
	Temp. (^{o}C)	Thickness(mm)	Air speed (m/s)	MC for WY(%)	MC for AY(%)
Blanched	60^{0}C	3.5mm	2.0	26.0	24.0
Unblanched	60^{0}C	2.0mm	2.4	31.5	30.0
Sample	Solar Drying Method				
	Mass	Thickness	Air speed	MC for WY	MC for AY
Blanched	71g	3.2mm	1.5	28.8	12.3
Unblanched	70g	3.0mm	1.5	33.8	18.0

4.11Sensory evaluation

The dried water yam and aerial yam were milled into flour which was used in carrying out the hedonic analysis to determine the sensory attributes of the flour produced.Fifty (50) questionnaires were administered to respondents (mainly bakers) who serve as the panelists. They completed the questionnaires based on the flour samples presented to them. The flour samples were coded as follows

Flour A: Blanched Water yam for convectivehot air dryer

Flour B: Un-blanched Water yam for convectivehot air dryer

Flour C: Blanched Aerial yam forconvective hot air dryer

Flour D: Un-blanched Aerial yam forconvective hot air dryer

Flour E: Blanched Water yam for solar dryer

Flour F: Un-blanched Water yam for solar dryer

Flour G: Blanched Aerial yam for solar dryer

Flour H: Un-blanched Aerial yam for solar dryer

The questionnaire was based on 9-point Hedonic Rating on Water Yam and Aerial Yam Flour. The rating was summarized in overall like and dislike disposition. To enable the ratings of the like and dislike to be made in a continuous manner, it was constructed as a bipolar scale with neutral in the centre. This makes the positive and negative descriptors to be statistically symmetrical around the neutral hence, agreeing in general with other affective scales (Guest et al, 2007). The 50 panelists used were made of 34 females and 16 males. Majority of them (76%) were in the age bracket of 20 – 40 years and were people who work with flour.

The result of the sensory attributes of the flour produced from cocoyam and potato is as shown in Table 4.29. As shown in Figure 4.107 to 4.111, the overall best score in all the tested categories indicated that the flours obtained from the blanched products were more acceptable than other

flours obtained from unblanched products. The flour obtained from blanched water yam was the most acceptable followed by that obtained from blanched aerial yam. In terms of the drying method, the flours obtained from the hot air dryer was more acceptable than the flours obtained from solar dryer. This may be due to the combination of speed and temperature that was employed which resulted in the lowest drying time and the distorted colour of the products.

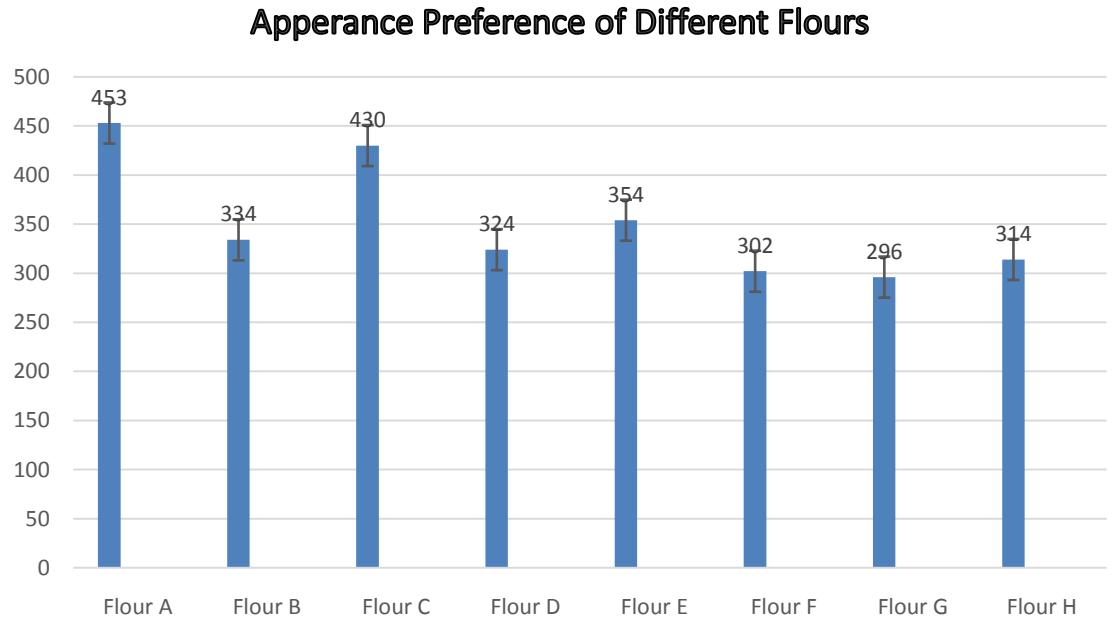

Figure 4.107: Appearance preference of the different flours

From the chart above, Flour A has the highest preference of 453, followed by Flour C with total preference of 430, whereas Flour G has the least preference of 296.

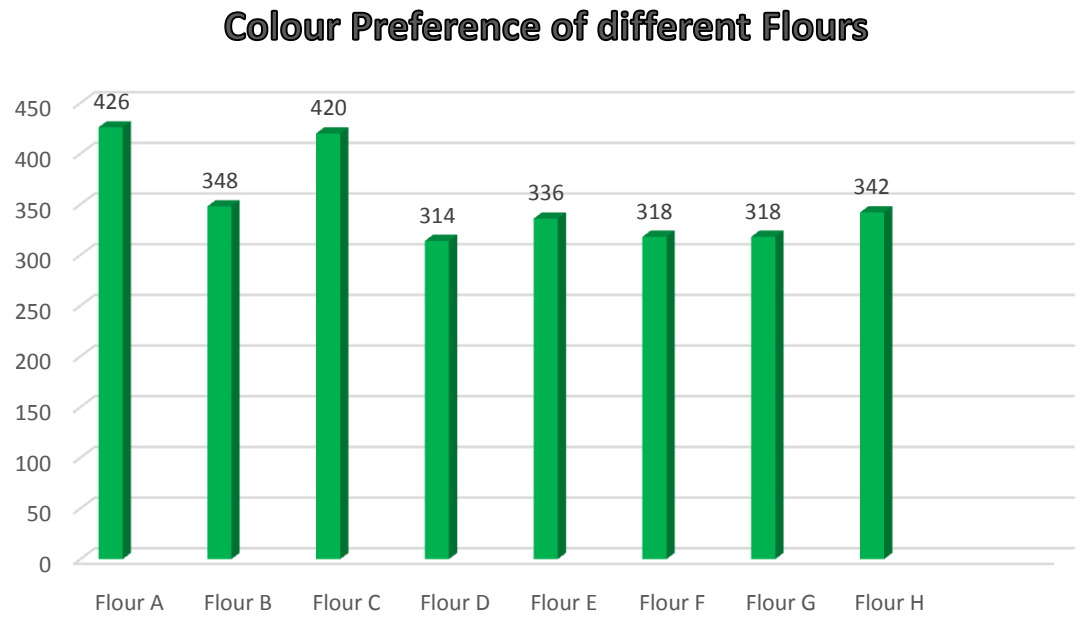

Figure 4.108: Colour preference of the different flours

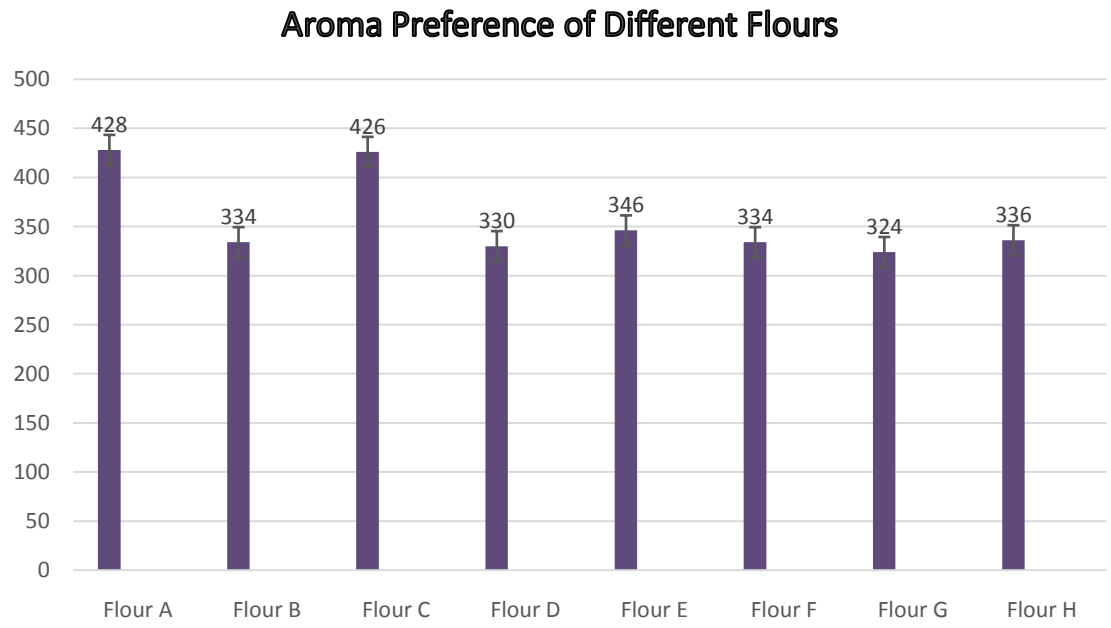

Figure 4.109: Aroma preference of the different flours

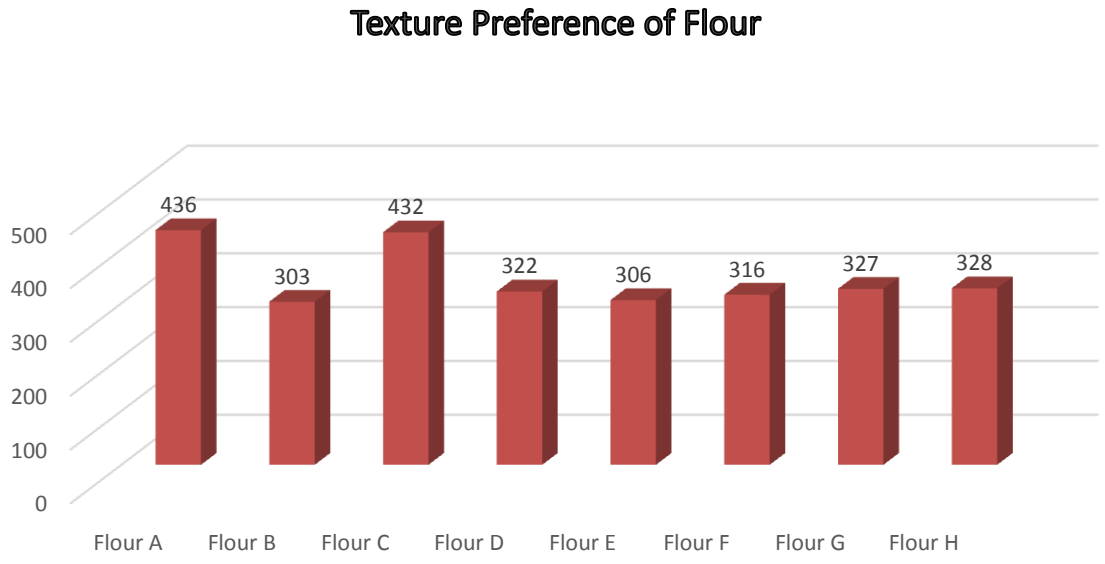

Figure 4.110: Texture preference of the different flours

From the Chart above, Flour A has the highest Texture preference, followed by Flour D, whereas Flour B has the lowest Texture preference.

A combination of the factors that contribute to the preference of flour is presented in the chart below:

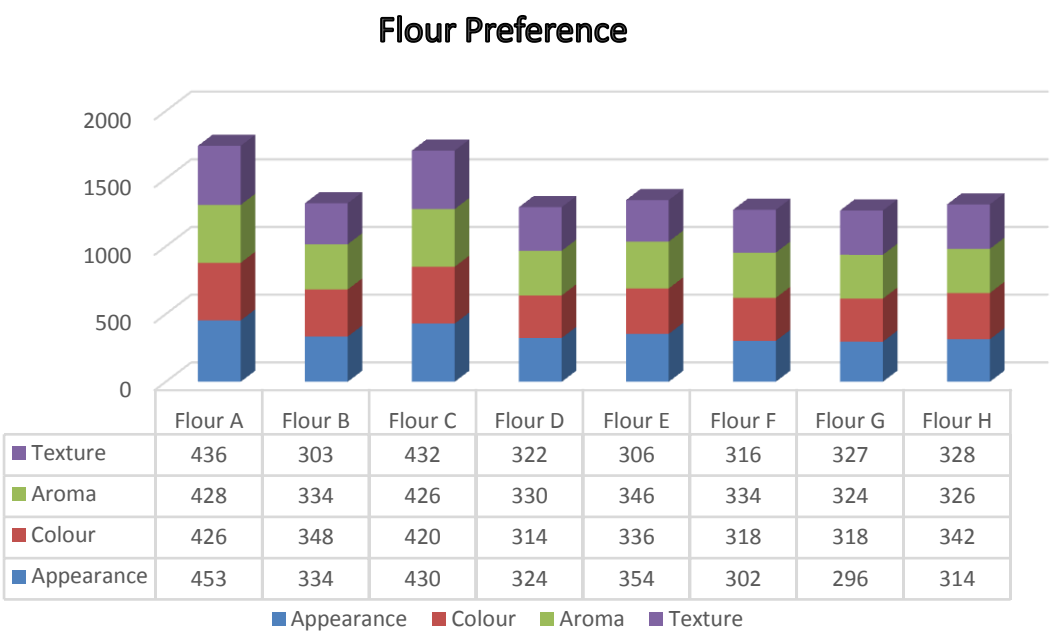

Figure 4.111: Overall flour preference of the different flours

From the chart above, Flour A and Flour C have the highest preference.

Analysis of Variance Test was used to test the difference between the mean of the different flours, to know whether there is a significant difference.

The result is presented in Table 4.29:

Table 4. 16: Descriptive Statistics of the flour samples

Flour Samples	Mean	Std. Deviation	Minimum	Maximum
Flour A	435.75	12.28	426.00	453.00
Flour B	329.75	19.02	303.00	348.00
Flour C	427.00	5.29	420.00	432.00
Flour D	322.50	6.61	314.00	330.00
Flour E	335.50	21.00	306.00	354.00
Flour F	317.50	13.10	302.00	334.00
Flour G	316.25	14.01	296.00	327.00
Flour H	327.50	11.47	314.00	342.00
Total	**351.47**	**48.84**	**296.00**	**453.00**

From the Table above, Flour A has a mean of 435.75, Flour B has a mean of 329.75, Flour C has a mean of 427.00, Flour D has a mean of 335.50, Flour F has a mean of 317.50, Flour G has a mean of 316.25 and Flour H has a mean of 327.50.

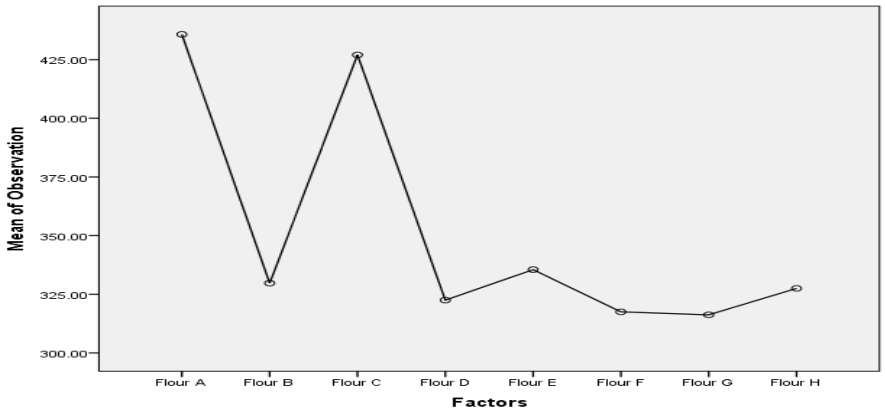

Figure 4.112: Mean Plot of the different Flours.

From the Means plot (Figure 4.112), one can carefully see that Flour A has the highest mean of 435.75, followed by Flour C with a mean of 427.00. Flour G has the least mean of 316.27.

Thus generally we can say that Flour A (Blanched Water yam for hot air dryer) is more preferred in terms of its Appearance, Colour, Aroma and Texture, followed by Flour C (Blanched Aerial yam for hot air dryer). Flour G (Blanched Aerial yam for Solar dryer) is less preferred.

CHAPTER FIVE

CONCLUSION AND RECOMMENDATIONS

5.1 Conclusions

The following conclusions were drawn from the research;

- The result indicated the presence of flavonoids, tannin and polyphenol in water yam irrespective of solvent used. Glycoside, alkaloids, steroids and saponin were found to be present in the different solvents used in varying concentrations. It also showed the presence of flavonoid, glycoside and tannin in aerial yam.
- The proximate analysis confirms that water yam (68.5%) and aerial yam (62.25 %) contains a lot of water in its raw forms. It also showed that other proximate compositions are present in varying quantities.
- The TGA result showed that the curves for water yam and aerial yam have two and three regions, respectively. The DTA results showed that the thermal degradation temperature of water yam and aerial yam were 389.5 °C and 432.7 °C, respectively, indicating that the thermal stability was higher in aerial yam than in water yam. The FTIR and SEM results showed that that drying at the various temperature did not alter the important functional groups or nutrient components of this variety of yams which is one of the goals of food preservations and processing.
- The information on engineering properties of water yam and aerial yam showed that the shear stress, hardness, bio-yield, rupture energy, modulus of elasticity, deformation at break, compressive strength and gumminess were all significantly influenced by the drying process. The thermal properties showed that the specific heat capacity and

thermal conductivity of the samples decreased on drying. However, the thermal diffusivity of the samples increased on drying. These parameters obtained are of importance in designing equipment for processing and handling operations of these important agro-products.

- Logarithmic model was the best model that described the drying process of water yam (R^2=0.9995), and aerial yam (R^2=0.9991)

- The kinetics results showed that for water yam, the effective diffusivity was obtained as2.5487×10^{-10}[m^2s^{-1}] and 2.0809×10^{-10}[m^2s^{-1}] at air temperatures of 68.58^{o}C and 60.56^{o}C respectively while for aerial yam, effective diffusivity was obtained as1.4381×10^{-10}[m^2s^{-1}] and 1.2241×10^{-10}[m^2s^{-1}]at the same respective air temperatures.
- The Hedonic test results showed wide acceptability of the colour, aroma, texture and general appearance of both blanched and unblanched samples of the yam species. However, the blanched yam species dried with convective hot air dryer were more acceptable than the solar dried samples.
- The RSM results showed that the regression model equations were successfully developed to efficiently predict quality parameters of convective air drying and solar drying of aerial yam and water yam at any given drying time. The optimum drying conditions obtained for convective hot air dryer are 2.0 m/s, 60^{o}C and 3.5 mm, and 2.4 m/s, 60^{o}C and 2.1 mm forair speed, drying temperature and thickness of samples, respectively for blanched and unblanched samples. The optimum drying conditions obtained for solar dryer are 1.5 m/s 71 g and 3.2 mm for air speed, mass of sample and

slice thickness respectively. The optimum parameters for unblanched sample dried by solar are 1.5 m/s, 3.0 mm and 70 g for airspeed, slice thickness and mass of sample

- A 2-Dimensional finite element/finite difference model based on triangular elements was successfully developed for drying processes of rectangular samples of the yam species. The results showed a good agreement between the predictions and the measurements indicating that a highly reliable finite element model was developed. Therefore, the costly case-by-case experimental drying kinetics needed for handling, storage and distribution/exportation of yam can be replaced with finite element/difference based computer simulations, saving costs.

5.2 Recommendations

The following recommendations are made for practical application of the results of this work and for future research and development.

1. The costly case-by-case experimental/empirical drying kinetics needed for making decisions on the handling, storage and distribution/exportation of yam should be replaced with finite element/difference based computer simulations for industrial saving costs.
2. In this work, the finite element/difference prediction of drying kinetics was limited to convective hot-air electrically-driven drying. It is recommended that the research be extended to natural and hot-air solar drying. This is because drying is historically driven by solar in Africa, especially open-air drying.
3. It will be good to replicate the methodology of this work over a wider range of seasons and post-harvest age of yam samples. This is because the thermophysical properties of

the studied yam species are expected to vary over seasons of the year and post-harvest age of the yam species.

4. The economic and technological benefits of the presented methodology, especially computer based finite element modelling, should be extended to other yam species and food crops in Nigeria. A food crop that should be accorded great importance is yam since it is widely and mainly produced in Nigeria for domestic consumption and the most important step in the processing of yam is drying. Therefore, simulation-based prediction of its drying will amount to enormous national economic gains.

4.3 Contributions to knowledge

i. This work successfully carried out study on mechanical and thermal properties of water yam and aerial yam. The results revealed water yam and aerial yam had tolerable properties appropriate for efficient industrial and food processing application. Application of the conditions obtained in this work can help in the design of processing equipment for postharvest processing of the two yam species.

ii. The work also carried out detailed instrumental analysis (TGA, FTIR and SEM) of the two yam species which to the best of my knowledge has not been reported anywhere. It showed that aerial yam is more stable than water yam and that both should not be dried at a temperature above the optimum (60^{o}C) to avoid denaturation and destabilization of the nutrient components.

iii. The work established the best drying temperature for convective hot air dryer to be 60^{o}C. The optimum operating conditions (temperature, airspeed and sample thickness) obtained in this work has been verified and adopted by aerial yam floor producing company.

iv. The work also successfully developed a numerical finite element modelsfor the drying of water yam and aerial yam.It also provided data from thermo physical properties which will help in design of dryers and industrial processing of the two agro- products.

v. The sensory analysis of both yam samples to determine its acceptability by the people is further contribution of this work.

REFERENCES

Abasse, A. B., Olorunda, A. O. Asiedu, R., & Bokanga, M. (2003). Effect of age of yam tuber at harvest on the qualities of yam foods. In Root Crops: The Small Processor and Development of Local Food Industries for Market Economy. Proceedings of the 8th Triennial Symposium of the *International Society for Tropical Root Crops Africa Branch* (ISTRC-AB), Ibadan, Akoroda, M.O. (ed) pp. 131-138.

Adejumo, B., Okundare, R., Afolayan, O., Balogun, S. (2013). Quality attributes of yam flour (Elubo) as affected by blanching water temperature and soaking time. *Int J Eng Sci*. 2(1):216-21.

Adesola, A. S. (2017). Kinetics of Gelatinized White Yam (*Dioscorea Rotundata*, Poir) During Convective Drying. *FUOYE Journal of Engineering and Technology*, 2(2), 2579-0617.

Adesuyi, J.A., & Mackenzie, J.A. (1973). The Inhibition of Sprouting in Stored Yams Dioscorea rotundata Poir by Gamma Radiation and Chemicals. Radiation Preservation of Foods. *International Atomic Energy Agency (IAEA) Bulletin*, 127-136.

Adewale, O., Omolola, A.I., Jideani, O., & Kapila, K.F. (2015).Drying kinetics of banana (Musaspp.). *Asociación Interciencia Caracas, Venezuela* VOL. 40 (6). 374-380.

Adu, E. A., Bodunde, A. A., Awagu, E. F. and Olayemi F. F. (2012) Design, Construction and Performance Evaluation of a solar Agricultural Drying Tent. International journal of engineering research and technology. 1, (10) : 1 – 12.

Afiukwa C. A., & Igwe D. O. (2015). Comparative Nutritional and Phytochemical Evaluation of the Aerial and Underground Tubers of Air Potato (*Dioscorea bulbifera*) Available in Abakaliki, Ebonyi State, Nigeria, *British Journal of Applied Science & Technology 11(4): 1-7,*

Afolabi, T. J., Tunde-Akintunde, T. Y., & Adeyanju, J. A. (2015). Mathematical modeling of drying kinetics of untreated and pretreated cocoyam slices.*Journal of Food Sci Technol*; 52(5): 2731–2740.

Afolabi, T. J., & Agarry, S. E. (2014). Thin Layer Drying Kinetics and Modelling of Okra (Abelmoschus Esculentus (L.) Moench) Slices under Natural and Forced Convective Air Drying. *Food Science and Quality Management*. 28: 35-49.

Aghbashlo, M., Kianmehr, M.H., Nazghelichi, T., & Rafiee, S. (2011). Optimization of an artificial neural network topology for predicting drying kinetics of carrot cubes using combined response surface and genetic algorithm. *Drying Technology*, 29, 770–779.

Agwu, A., Avoaja, A.G.I. (2012). Nutritional Assessments Of Musa Paradisiacal (Plantain) And Dioscorea Alata (Water Yam) Harvested Within Abia State Of Nigeria. *International journal of academic research in progressive and development*, 1(2), 193-198.

Aidoo, K. (1993). Post-harvest storage and preservation of tropical crops. *International Biodeterioration & Biodegradation* 32(1-3):161-173. DOI: 10.1016/0964-8305(93)90048-7

Ajah, H. (2018). Finite element method – what is it? FEM and FEA explained, From J. T. Oden, Finite elements: An introduction, in Handbook of Numerical Analysis II, Finite element methods (Part I), North-Holland, Amsterdam, pp. 3-12.

Ajala, A.S., Aboiye, A.O., Popoola, J.O., & Adeyanju, J.A. (2012). Drying Characteristics and Mathematical Modelling of Cassava Chips. *Chemical and Process Engineering Research*, Vol 4. 213-223.

Akissoe, N., Mestres,C., Hounhouigan, J., & Nago, M. (2005). "Biochemical Origin of Browning during the Processing of Fresh Yam (Dioscorea spp.) into Dried Product." *Journal of Agricultural and Food Chemistry*,53(7): 2552-2557.

Akissoe, N., D.J. Hounhouigan, N. Bricas, P. Vernier, C.M. Nago and A. Olorunda, (2001). Physical, chemical and sensory evaluation of dried yam (*Dioscorea rotundata*) tubers, flour and amala a flour derived product. Trop. Sci., 41: 151-155.

Akaaimo,D. I. & Raji,A. O. (2006). Some physical and engineering properties of Prosopis Africana seed. *Biosystems Engineering*.95(2): 197-205.

Akpinar, E.K., Bicer, Y., & Yildiz, C., (2003). Thin layer drying of red pepper. *Journal of Food Engineering*, 59, 99–104

Al-Hinai K.Z., Guizani N., Singh V., Rahman M.S., Al-Subhi L. (2013): Instrumental texture profile analysis of date-tamarind fruit leather with different types of hydrocolloids. Food Science and Technology Research, 19: 531–538.

Amin T.G., Shahin, R., & Alireza, K. (2011). Mathematical Modeling of Thin Layer Drying Kinetics of Tomato Influence of Air Dryer Conditions. *International Transaction Journal of Engineering, Management, & Applied Sciences & Technologies*. Volume 2 No.2, 147-150.

Aneke, N.A.G., Mbah, G.O. and Edeani, N. J. (2018). Response Surface Methodology For optimisation of hot air drying of water yam slices. *International Journal of Scientific and Research Publications*, 8 (8), 248-259.

Anna, H., Iva, K., Rithy, C., Petra, C. and Jan, B. (2014) Development of solar drying model for selected Cambodian Fish species. The scientific word journal, 4, 1-10.

AOAC. (2000) Official methods of analysis of AOAC. *International 17th edition; Gaithersburg, MD, USA Association of Analytical Communities.*

Aremu, A. K., Adedokun, A. J. and Abdulganiy, O. R. (2013) Effects of slice thickness and temperature on the drying kinetics of mango. International journal of research and reviews in applied sciences. 15, (1) :41-50.

Arinze, E. A. (1987). Solar energy for crop drying in developing countries. In Solar drying in Africa, proceedings of a workshop in Dakar, Senegal.

Asiru, W. B., Raji, A. O., Igbeka, J. C., & Elemo, G. N. (2015). Mathematical Modelling of Thin Layer Dried Cashew Kernels. *Nigeria Food Journal*, Elsevier. 31(2): 106-112.

Asumadu-Sarkodie, S., & Owusu, P.A. (2016). The Potential and Economic Viability of Wind Farms in Ghana. Energy Sources, Part A: Recovery, Utilization, and Environmental Effects, 38, 695-701.

Aviara1, N.A., Edward, M.Y., & Ojediran, J.O. (2013). Effect of moisture content and processing parameters on the strength properties of *Brachystegia Eurycoma* seed, *Global journal of engineering, design and technology, **2(1), 8-20***

Ayo, J. A., Ojo, M., & Obike, J., (2018). Proximate composition, functional and phytochemical properties of pre-heated aerial yam flour. *Research Journal of Food Science and nutrition* vol. 3, page 1-8.

Ayoola, G.A., Coker, H.A.B., Adesegun, S.A., Adepoju-Bello, A.A., Obaweya, K., & Ezennia, E.C. (2008). Phytochemical Screening and antioxidant activities of some Selected Medicinal Plant used for malaria therapy in South-western Nigeria. *Tropical Journal of Pharmaceutical Research*, 7(3):1019-1014.

Azadbakht, M., Darvishi, H., Rezaeiasl, A. & Asghari, A. (2012). Thin layer drying characteristics and modeling of melon slices (Cucumismelo). *Journal of Agricultural Technology*. 8(6): 1867-1880.

Bahnasawy, A.H. (2007). Some physical and mechanical properties of garlic. *International Journal of Food Engineering*. 3(5):51-87.

Becker, B.R. &Fricke, B.A. (1996a.) Transpiration and respiration of fruits and vegetables. In New Developments in Refrigeration for Food Safetyand Quality. *International Institute of Refrigeration, Paris, and American Society of Agricultural Engineers, St. Joseph, MI.* pp. 110-121.

Becker, B.R., Misra, A, & Fricke, B.A. (1996b). Bulk refrigeration of fruits and vegetables, Part I: Theoretical considerations of heat and mass transfer. *International Journal of HVAC&R Research* (now *HVAC&R Research*) 2(2):122-134.

Bird, R.b., Stewart, W.E., Lightfoot, E.W. (1964). Transport Phenomena. John Wiley & Sons, Inc.

Black, T. (2014). A Review on the Rooibos Tea Industry and Thin-layer Drying Literature. Available on: http://efwe.ukzn.ac.za/Libraries/ResearchSeminars/Black_T.sflb.ashx (Accessed on 16 December 2018).

Bonner, I. J. & Kenney, K. L. (2012). Effect of Mechanical Conditioning on Thin-Layer Drying of Energy Sorghum (Sorghum bicolor (L.) Moench). National Conference: Science for Biomass Feedstock Production & Utilization, Idaho USA.

Callister WD. 2004. Fundamentals of Materials Science and Engineering: An integrated approach. Second. New York: John Wiley & Sons.

Camargo, J., Ebinuma, C.D., & Cardoso, S. (2003). A mathematical model for direct evaporative cooling air conditioning system, *Eng. Term*. 4, 30–34

Cao, R.L., Sun, Z.Y., Wang, Z.D., & Yin, X.Z. (1957). The investigation of Chinese medicine decoction anti-fungal activity in vitro. *Chinese journal of dermatology,* 5:286-292.

Chen, G., Xiong, K., Peng. J., & Chen, J. (2010). Optimization of combined mechanical activation roasting parameters of titania slag using response surface methodology. *Advanced powder technology,* 21(3), 331-335.

Chen, J., Chen, C., Srinivasakannan, L., & Peng, J. (2011). Application of response surface methodology for optimization of the synthesis of synthetic rutile from titania slag. *Applied surface science,* 258(7), 3068–3073.

Chinweuba, D. C., Nwandikom, G. I., Okafor, V. C. and Nwajinka, C. O. (2016). Mathematical Modelling of Thin Layer Drying Behaviour of Parboiled Breadfruit (Treculia africana)

Seeds. *Greener Journal of Science Engineering and Technological Research*. 6 (1): 027-039.

Correia, A.F.K., Loro, A.C., Zanatta, S., Spoto, M. H. F., & Vieira, T. M. F. S. (2015). Effect of Temperature, Time, and Material Thickness on the Dehydration Process of Tomato, International Journal of Food Science, http://dx.doi.org/10.1155/2015/970724. (3), 26-41.

Coursey, D.G (1967). Yam storage—I: A review of yam storage practices and of information on storage losses. Journal of stored product research. 2(3); 229-244.

Cui, H.X., Li, T., Wang, L.P., Su, Y., & Xian, C.J. (2016). *Dioscorea bulbifera* polysaccharide and cyclophosphamide combination enhances anti-cervical cancer effects and attenuates immunosuppression and oxidative stress in mice. *Sci rep*.6: 19185.

Dandamrongrak R., Young G., & Mason R. (2002). Evaluation of various pre-treatments for the dehydration of banana and selection of suitable drying models. *Journal of Food Engineering*, 95, 139-146.

Daniel, M., Prasad, R., Anirban, D., Sawinder, K.,& Chayanika, S. (2017). Recent advances in convective drying of foods. *Journal of Food Technology and Preservation* (2017) Volume 1, Issue 1, 67-80.

Darvishi, H., Khoshtaghaza, M.H., & Minaei, S. (2014). Fluidized bed drying characteristics of soybeans, *Journal of Agric. Sci. Technol*. 16, 1017–1031.

Deb, A.C. (2002). Fundamental of Biochemistry. Eds 8, New Central Book Agency, Kolkata. DOI:http://dx.doi.org/10.1023/b:biry.0000040228.89036.46

Deepak, S., & Gattumane, M.M. (2015). Drying Kinetics and Mathematical Modeling of Casuarina Equisetifolia Wood Chips at Various Temperature. *Periodica Polytechnica Chemical Engineering*. *59(4), pp. 288-295, 2015 DOI:* 10.3311/PPch.7855

Diamente L.M. & Munro P.A., (1991). Mathematical modeling of hot air drying of sweet potato slices. *Int. J. Food Sci. Technol*., 26, 99-109.

Dincer, I., & Sahin, A.Z. (2004). A new model for thermodynamic analysis of a drying process, International Journal of Heat Mass Transfer., 47: 645-52, 2004.

Divine, N. B., Charles, F. A., Dzudie, T., Cesar, I., Clerge, T. and Zephirin, M. (2013). Indirect solar drying kinetics of sheanut (vitellaria paradoxa Gaetn) Kernels. Journal of Engineering and Applied science. 8(6) 183-191.

Dramani, Y. (2013). Effect of postharvest waxing treatments, yam variety and tuber size on shelf life of white yam (Dioscorea rotundata Poir). Thesis (MPHIL)-University of Ghana.1-93.

Dumont, R.; Vernier, P. (2000). "Domestication of yams (Dioscorea cayenensis-rotundata) within the Bariba ethnic group in Benin". *Outlook on Agriculture*. **29** (2): 137. *doi*:*10.5367/000000000101293149*

Dutta, B. (2015). Food and medicinal values of certain species of dioscorea with special reference to Assam. *Journal of pharmacog phytochemical*,3(4). 15-18.

Ehiem, J. C., & Eke, A. B. (2014). Determination of drying characteristics and kinetics of bitter kola (garcinia kola) using page's model. *Agric Eng Int: CIGR Journal*, 16(4): 278-284.

Ekechukwu, O. V., & Norton, B. (1998). Review of solar-energy drying systems III: low temperature air-heating solar collectors for crop drying applications. Energy Conversion and Management 1999. 40:657–67.

Emilio, R., Santiago, F.M., Isabel, R., Juan.L.,& Marina, P.A.(2015). Microstructure, Mechanical, and Thermogravimetric Characterization of CellulosicBy-Products Obtained from Biomass Seeds, International Journal of Food Properties, 18:6,1211-1222,

Erbay, Z., & Icier, F. (2010). A Review of Thin Layer Drying of Foods: Theory, Modelling and Experimental Results. *Critical Reviews in Food Science and Nutrition*. 50: 441-464.

Ertekin C., & Yaldiz O., (2004). Drying of eggplant and selection of a suitable thin layer drying model. *Journal of Food Eng*., 63, 349-359.

Etoamaihe, U. J. and Ibeawuchi, K. O. (2010) Prediction of the drying rates of cassava

slices during oven drying. Journal of Eng and Applies sciences 5(4) 308-311.

Evans, E., Yakubu, G., & Tawakalitu, B. (2013). "Evaluation of Ascorbic acid and Sodium Metabisulfite as inhibitors of browning in yam (D. rotundata) flour processing." Valahia University Press 14(2): 247-260.

Falade, K.O., & Solademi, O.J. (2010). Modelling of air drying of fresh and blanched sweet potato slices. *International Journal of Food Science & Technology,* 45(2):278 - 288

FAO. 2011. FAOSTAT database. [Online]. Available at: http://bit.ly/NmQzZf. [Accessed: 28. September 2018].

Falope, M.O., Ibrahim, H., & Takeda, Y. (1999). Screening of higher plants requested as pesticides using the brine shrimp lethality assay. *International Journal of Pharmacognosy*;37:230–254.

Farombi, O. E., Britton, G., & Emerole, O. G. (2000). Evaluation of the antioxidant activity and partial characterisation of extracts from browned yam flour diet. *Food Research International* 33:493-499.

Fatimah, B., Erni, M., Sari, F.D., & Happy., (2017). solar energy dryer kinetics using flat-plate finned collector and forced convention for potato drying. AIP conference proceedings 1855, 070002; Doi: 10.1063/1.4985529.

Fauziah, S., Nurhayati, A., & Zalila, A, (2013). Solar Drying System for Drying Empty Fruit Bunches. *Journal of Physical Science*, Vol. 24(1), 75–93.

Fellows, J. P. (2000). Food Processing Technology, Principles and Practice 2nd Edition. CRC Press, Woodhead Publishing Limited.

Fontana, A. J., Varith, J., Ikediala, J., Reyes, J., & Wacker, B. (1999). Thermal properties of selected foods using a dual needle heat-pulse sensor, ASAE Paper No. 996063, St. Joseph, MI: ASAE.

Galani, V.J., & Patel D. M. A. (2017). Comprehensive Phytopharmacological Review of Dioscorea bulbifera Linn. *International journal of environmental sciences and natural science.*vol 4 Issue. 5.

Gharehbeglou, P., Askari, B., Homayouni, R.A., Hoseini, S.S., Tavakoli, P.H., & Elhami, R.A.H. (2014). Investigating of drying kinetics and mathematical modelingof turnip. Agric Eng Int: *CIGR Journal*. Vol. 16, No.3, 194-204.

González, M. A.; Collazo De Rivera, A. (1972). Storage of Fresh Yam (Dioscorea alata L.) under Controlled Conditions.The Journal of Agriculture of the University of Puerto Rico**,** [S.l.],p.46-56,Availableat: http://revistas.upr.edu/index.php/jaupr/article/view/10886/9177>. Date accessed: 12 June 2018.

Goyalde, N. A., Melo, E., Rocha, R. P., Goneli, D. L., & Araujo, F. L. (2009). Mathematical Modelling of The Drying Kinetics Of Sugarcane Slices. *Revista Brasileira de Produtos Agroindustriais, Campina Grande*. 11(2): 117-121.

Guest, S., Essick, G., Patel, A., Prajapati, R., McGlone, F. (2007). Labeled magnitude scales for oral sensations of sweetness, dryness, pleasantness and unpleasantness, Food Qual Pref, vol. 18 (pg. 342-352).

Gupta R. K.,& Das, S. K. (2006). Some physical properties of green gram. *Journal of Food Engineering*. 66:1-8.

Haney, S.E., & Hangping, M, (2017). Theoretical and experimental analysis of drying kinetics of tomato slices by using infrared dryer. *International Journal of Advanced and Applied Sciences.* 4(1) 2017, Pages: 137-142

Harbone, J.B.(1998). Phytochemical Methods: A Guide to Modern Techniques of Plant Analysis. London New York Chapman and Hall. DOl: 10.1007/978-94-009-5921-7.

Hassan, L.G., Umar, K.J. & Umar, Z. (2007). Antinutritive factors in T*ribulus Terrestris* (Linn) leaves and predicted calcium and zinc bioavailability. *Journal of tropical bioscience,*7:33-36

Heshmatollah, N., Riccardo, L., & Mehdi, J. (2014). Experimental Design in Analytical Chemistry–Part I: Theory. *Journal of AOAC International*, 97(1), 1 – 10.

Hofsetz, K., Costa Lopes, C., Hubinger, M. D., Mayor, L., & Sereno, A. M. (2008). Effect of High Temperature on Shrinkage and Porosity of Crispy Dried Bananas, *J. of Food Engineering: Integrated Approach, 26:pp, 367-373.*

Huerta¤, E., Corona, J.E., & Oliva, A.I. (2010). Universal testing machine for mechanical properties of thin materials. *REVISTA MEXICANA DE FI´SICA*56 (4) 317–322

Ismail, M. A., & Ibn Idriss, E. M. (2013). Mathematical modelling of thin layer solar drying of whole okra (Abelmoschus esculentus (L.) Moench) pods. *International Food Research Journal*, 20(4): 1983-1989.

Jacques Y. A., Pamphile K. B. K., Gbocho S. E. E., Hubert K. K., & Lucien, P. K. (2016). Assessment of physicochemical properties and anti-nutritional factors of flour from yam (*Dioscorea bulbifera*) bulbils in southeast côte d'Ivoire. *International journal of advanced research. 4(12), 871-887.*

Jafari, V. S.M., Ghanbari, M.G., & Dehnad, D. (2016). Modeling the drying kinetics of green bell pepper ina heat pump assisted fluidized bed dryer. *Journal of food quality*, 39 98–108.

Jayarama, K. S., & D.K.D. (1995). Gupta. "Drying of fruits and vegetables". Handbook of Industrial drying, 2nd edition Vol.1. Edited by A. S. Mujumdar, chapter 21.

John, S. Roberts, David R. Kidd, Olga. Padilla. Zakour. (2008) Drying kinetics of grape seeds. Journal of food Engineering .89 (2008) 460- 465.

Josh, P., Chris, P., Rachel, L., & Gomes, M. (2014). Comparison of response surface methodology (RSM) and artificial neural networks (ANN) towards efficient extraction of artemisinin from Artemisia annua. *Industrial crops and products*, 58, 15–24.

Junling, S., Zhongli, P., Tara, H. M., Delilah, W., Edward, H. and Don, O. (2008) Elsevier – Food Science and Technology. 41, 1962 – 1972

Kadam, D. M., Samuel, D. V. K. & Pandey, A. K. (2005). "Influence of different treatments on dehydrated cauliflower quality." *International Journal of Food Science & Technology*40(8): 849-856.

Kajuna, S. T. A. R., Silayo, V. C. K., Mkenda, A. & Makungu, P. J. J. (2001). *African Journal of Science and Technology (AJST) Science and Engineering Series*. 2(2): 94-100.

Kaptso, K. G., Njintang, Y. N., Nguemtchoun, M. M. G., Scher, J., Hounhouigan, J. & Mbofung, C. M. F. (2013). Drying Kinetics of Two Varieties of Bambara Groundnuts (Vigna subterranean) seeds. *Journal of Food Technology*. 11(2): 30-37.

Kayode, R. M. O., Buhari, O. J., Otutu, L. O., Ajibola, T. B., Oyeyinka, S. A., Opaleke, D. O. & Akeem, S. A. (2017). Physicochemical Properties of Processed Aerial Yam (Dioscorea bulbifera) and Sensory Properties of Paste (Amala) Prepared with Cassava Flour. *The Journal of Agricultural Sciences*, Vol. 12(2), Pp 84-94.

Kirk, R.S, & Sawyer, R. (1991). Pearson's composition and chemical analysis of foods, 9th Edition Longman scientific and technical, Essex, England.

Kouassi, N.K., Nindjin, C; Tetchi, A.F & Amani, G.N. (2010). Evaluation of type of process and on nutritional and anti-nutritional composition of yams (Dioscorea cayanensis rotundata). *Journal of Food Tech*., 8: 191-199.

Lee, C., Yusof, S., Hamid, A., & Baharin, B. (2006). Optimizing conditions for hot water extraction of banana juice using response surface methodology (RSM). *Journal of food engineering*, 75, 473-479.

Leonel, P., & Lijauco., (2017). Drying Kinetics of Sweet Potato Chips in a Forced Convection Tray-Type Dryer, 7th Int'l Conf. on Innovations in Chemical, Biological, Environmental and Food Sciences (ICBEFS-17) Aug. 3-4, Pattaya (Thailand). 35-41.

Lewis, M. J. (1987). Physical properties of foods and food processing systems. VCH Publishers, Deerfield Beach, Florida. 465p.

Lihua, Z., Bo W., & Linglin, Z. (2014). Optimization of hot air drying of purple sweet potato using response surface methodology.*International Conference on Mechatronics, Electronic, Industrial and Control Engineering* (MEIC 2014). 719-723.

Luther, R. W., Dwayne, A. S. & Gerald, H. B. (2003). Food and Process Engineering Technology. ASAE Publication, USA.

Madamba, P.S., Driscoll, R.H., & Buckle, KA. (1996). The thin layer drying characteristics of garlic slices. J Food Eng. 29:75–97.

Mamman, E., Aviara, N. A., & Ogunjirin, O. A. (2012). Effects of heating temperature and time on some mechanical properties of balanites aegyptiaca nut. *Agricultural Engineering International: CIGR Journal*, *14*(2), 77–85.

Manoj, K.G., Sehgal, V.K., Dattatreya M. K., Singh, A.K., & Yadav, Y.K. (2012). Effect of Bed Thickness on Cauliflower Drying. *American Journal of Biochemistry*. 2(5): 56-61. doi: 10.5923/j.ajb.20120205.02.

Manpreet, S., Bhatti, K., Rajeev, K., Kalia, A., Reddy, & Ashwani K. (2011). RSM and ANN modeling for electrocoagulation of copper from simulated wastewater: multi objective optimization using genetic algorithm approach. *Desalination,* 274, 74–80.

Masud Alam, M.D., Nurul Islam, M.D., & Nazrul islam., M.D. (2014). Study on drying kinetics of summer onion. *Bangladesh j. Agril. Res*. 39(4): 661-673.

Mbaya, Y., Santuraki, H., and Jauro, S. A. (2013.). Acceptance of Aerial Yam (Dioscorea bulbifera) for food in Biu Emirate Council, Borno State, Nigeria. *Journal of Biology, Agriculture and Health Care*, 3(10), 18-23.

Meenakshi, G., Sadhana, S., Shivani, G.V., & Sushmita, D.S. (2014). Drying kinetics of thin layer pea pods using tray drying, *international journal of food and nutritional sciences*, vol.3, iss.3, 61-66.

Menon, A. S., & Mujumdar, A. S. (1987). Drying of Solids: Principles, Classification and Selection of Dryers. In: Mujumdar, A. S. (ed.) Handbook of Industrial Drying. New York: Marcel Dekker, Inc.

Mestres, C., Dorthe, S., Akissoe, N. and Hounhouigan, J. (2002). Prediction of sensorial mineral content of basil (*Ocimum basilicum* L.). *Journal of Food Eng*. 69, 375–379

Midilli A., Kucuk H.,& Yapar Z., (2002). A new model for single-layer drying. *Drying Technol*., 20(7), 1503-1513.

Mirzaee, E., Rafiee, S., Keyhani, A. and Emam-Djomeh, Z. (2009) Determination of moisture diffusivity and activation and activation energy in drying of apricots. Res. Agr. Eng. 55(3): 114 – 120.

Mohammad, Z., Seyed, H. S. and Barat, G. (2013) Kinetic drying and mathematical modeling of Apple slices in dehydration process. Journal of food process and technology. 4, (7) : 1-4.

Mohsen, B. (2017). Numerical simulation of potato slices drying using a two-dimensional finite element model*, Chem. Ind. Chem. Eng. Q. 23 (3) 431−440.*

Mohsen, B. (2016). Energy efficiency and moisture diffusivity of apple slices during convective drying. *Food Science Technology, Campinas*, 36(1): 145-150.

Mohsenin, N. N. (1986). Physical Properties of Plant and Animal Materials, 2nd edition. Gordon and Breach Science Publishers, New York cited in Varnamkhasti, M. G., Mobli, H. Jafari, A., Rafiee, S., Heidarysoltanabadi, M. & Kheiralipour, K. (2007) Some Engineering Properties of Paddy (var. sazandegi) *International journal of agriculture & biology*.(2), 22-35. Available at http://www.fspublishers.org [Accessed 10 June 2018].

Mohsenin, N. N. Thermal Properties of Foods and Agricultural Materials. Gordon and Breach, New York. 1980.

Motevali, A., Minaei, S., Khoshtaghaza, M.H., Kazemi, M., & Nikbakht A.M., (2010). Drying of pomegranate arils: comparisonof predictions from mathematical models and neuralnetworks. *International Journal of Food Engineering*, 6(3), Article 15, 1-19.

Munoz, A.M., & King, S.C. (eds.) 2007. International consumer product testing across cultures and countries. ASTM International, MNL 55.

Naghavi, Z., Moheb, A., & Ziaei-Rad, S. (2010). Numerical simulation of rough rice drying in a deep-bed dryer using non-equilibrium model. Energy Conversion and Management, 51(2), 258-264.

Ndukwu M. C., & Nwabuisi, K. (2011). Thin Layer drying kinetics of varieties of cocoyam corm slice with heated air. *Proceedings of the 11th International Conference and 32nd Annual General Meeting of the Nigerian Institution of Agricultural Engineers (NIAE Ilorin). Vol. 32: 347 – 353.*

Ndukwu, M.C., Ogunlowo, A.S., & Olukunle, O.J. (2010). Cocoa Bean (Theobroma cacao L) drying kinetics, *Chilean Journal of Applied Agric*. 70 (4) 633–639.

Nwabanne, J.T. (2009). Drying characteristics and engineering properties of fermented ground cassava, *African Journal of Biotechnology,* 8 (5), pp. 873-876.

Nwajinka, C.O., Okpala, C.D., & Udoye, B. (2014). Thin layer drying characteristics of cocoyam corn slices. *International journal of Bioscience*, 3(5): 241-244.

Nwosu, J. N. (2014). Evaluation Of The Proximate And Sensory Properties Of Biscuits Produced From Aerial Yam Flour (Dioscoreabulbifera), *American Journal of Research Communication,* Vol 2(3): 119-126.

Ogbuagu, M.N., (2008). Nutritive and Anti-Nutritive Composition of the Wild(Inedible)Species of Dioscorea bulbifera(Potato Yam) and Dioscorea dumentorum(Bitter Yam). *The Pacific Journal of Science and Technology*.Volume 9(1), 203-208.

Ogidi, I.A., Wariboko, C., & Alamene, A. (2017). Evaluation of some nutritional properties of water – yam (*Dioscorea* alata) cultivars in Bayelsa state, Nigeria. *European journal of food science and technology* Vol.5, no.3, pp.1-14,

Ojediran, J. (2013). Effect of Moisture Content and Processing Parameters on the Strength Properties of Brachystegia Eurycoma Seed, (July 2015).

Ojinnaka, M., Odimegwu, E., & Ilechukwu, R. (2016). Functional properties of flour and starch from two cultivars of aerial yam (Dioscorea bulbifera) in South East Nigeria. *Journal of Agriculture and Veterinary Science*, 9, 22-25.

Olorunda, O., &, Adesuyi, S.A. (19737. A comparison between the barn and clamp methods of storing yams. Rep. Nigerian Stored Prod. Res. Institute, 1970.

Okafor, N. (1966). Microbial Rotting of Stored Yams (Dioscorea spp.) in Nigeria. *Experimental Agriculture,2*(3), 179-182. DOI:10.1017/S0014479700026697.

Okigbo, R.N., Anuagasi, C.L., Amadi, J.E., & Ukpabi, U.J. (2009). Potential inhibitory effects of some African tuberous plant extracts on Escherichia coli, Staphylococcus aureus and Candida albicans. *International journal of green boil,* 6:91-98.

Okigbo, R.N., (2004). A review of biological control methods for postharvest yams (Dioscorea spp.) in storage in South Eastern Nigeria. *KMITL Sci Technol Journal*,4(1):207-215.

Oko, A.O., & Famurewa, A.C. (2015). Estimation of Nutritional and Starch Characteristics of Dioscorea alata (WaterYam) Varieties Commonly Cultivated in South-Eastern Nigeria. *British Journal of Applied Science & Technology 6(2): 145-152*, DOI: 10.9734/BJAST/2015/14095.

Oko, A. O., & Famurewa, A. C.(2014). Estimation of Nutritional and Starch Characteristics of *Dioscorea alata* (Water Yam) Varieties Commonly Cultivated in South-Eastern Nigeria. *British Journal of Applied Science & Technology*,6(2): 145-152.

Olabinjo O.O., Olajide J.O., & Olalusi A .P.(2017). Mathematical Modeling of Sun and Solar Drying Kinetics of Fermented Cocoa Beans. *International Journal of Environment, Agriculture and Biotechnology (IJEAB) Vol-2, Issue-5. 2419-2426.*

Olawale, A. S.,& S. O. Omole. (2012). Thin layer drying models for sweet potato in tray dryer. *Agric Eng Int: CIGR Journal*, 14 (2): Manuscript No. 2060.

Omid, M., Baharlooei, A., & Ahmadi, H., (2009). Modeling drying kinetics of pistachio nuts with multi-layer feed-forward neural network. *Drying technologies*, 27, 1069–1077.

Omodamiro, O.D. (2015). Anti-inflammatory and diuretic activities of ethanol extract of *Dioscorea bulbifera* leaf. *AJDDT*, 2(1): 029-038.

Onu, C. E., Igbokwe, P. K. and Nwabanne, J. T. (2017). Effective Moisture Diffusivity, Activation Energy and Specific Energy Consumption in the Thin-Layer Drying of Potato. International Journal of Novel Research in Engineering and Science. 3 (2) 10 – 22.

Opara, L. U. (1999). Yam storage. In: CGIAR Handbook of Agricultural Engineering 171 Volume IV Agro Processing. Bakker-Arkema (ed). *The American Society of Agricultural Engineers*, St. Joseph, M. I, U. S. A. pp. 182-214.

Osunde, Z.D. (2008). Minimizing Postharvest Losses in Yam(*Dioscorea spp.*): Treatments and Techniques: Chapter 12 from Using Food Science and Technology to Improve Nutrition and Promote National Development, Robertson, G.L. & Lupien, J.R. (Eds), © International Union of Food Science & Technology (2008).

Ozdemir, M., & Devres, Y. O. (1999). The thin layer drying characteristics of hazelnuts during roasting. Journal of Food Engineering. 42: 225-233.

Özge, S., Hande, D., & Seda, S. (2018). Convective and Microwave Drying of Onion Slices Regarding Texture Attributes, *Czech J. Food Sci.*, 36 (2): 187–193

Ozisik, M. N. (1993). Heat conduction. John Wiley & Sons, Mar 22, 1993 -Technology & Engineering–692.

Passam, H. C. (1977). Sprouting and apical dominance of yam tubers. *Tropical Science* 19: 29-39.

Paul, K. (2016). *Good Solid Modeling*, Bad FEA by H-Code vs. P-Code: The Facts (Why Mechanical (Pro/ENGINEER Structural Simulation Option) is a better Solution for

Design Engineers).Retrieved from https://deust.wordpress.com/2014/11/30/h-method-p-method/ February 25, 2019.

Princewill-Ogbonna, I.L. & Ibeji, C.C., (2015). Comparative Study on Nutritional and Anti nutritional Composition of three Cultivars (red, green and yellow) of AerialYam (Dioscorea bulbifera). *IOSR Journal of Environmental Science, Toxicology and Food Technology (IOSR-JESTFT)*, Volume 9, Issue 5 Ver. I PP 79-86.

Rafiee, S. H., Keyhani, A., Sharifi, M., Jafari, A., Mobli, H., & Tabatabaeefar, A. (2009). Thin Layer Drying Properties of Soybean (Viliamz Cultivar). *Journal of Agricultural Science Technology*, 11: 289-300.

Ramana, S. V., Taylor, A., &Wolf, W. (1992). Measurement of firmness in carrot tissue during cooking using dynamic, static and sensory tests. *Journal of the Science of Food and Agriculture*, 60 (3): 369-375.

Ramiro, T., Everaldo, J.M., Ricardo, D.A., Omar, A.P., & Hugo, T. (2012). Drying kinetics of two yams (Dioscorea alata) varieties.*Dyna rev.fac.nac.minas* vol.79 no.171.180-192.

Rhoda, H. G., & Negimote, B. (2015). Drying Characteristics and Kinetics of Bitter leave (Vernonia amygdalina) and Scent leave (Ocimum gratissimum).

Ronoh, E.K., Kanali, C.K., Mailutha, J.T., & Shitanda, D. (2010). Thin layer drying kinetics of amaranth (*Amaranthus cruentus*)grains in a natural convection solar tent dryer. *African journal of food agriculture nutrition and development*. Volume 3(3), 2218-2233.

Ryall. A.L. & W.J. Lipton.(1972). Vegetables as living products. Respiration and heat production. In *Transportation and Storage of Fruits andVegetables*, vol. 1. AVI Publishing, Westport, CT.

Sacilik, K. (2007). The Thin-Layer Modelling of Tomato Drying Process. *Agriculturae Conspectus Scientificus*. 72(4): 343-349.

Saeed, I.E., Sopian, K., & Zainol, A. Z. (2008). Thin-layer drying of Roselle Mathematical modeling and drying experiments. Agricultural engineering International: CIGR Journal S 3(1), 1-22.

Sahin A. Z., Dincer I., Yilbas, B. S. & Hussain M. M. (2002). Determination of drying times for regular multi-dimensional objects. *International Journal of Heat and Mass Transfer*, 45, pp. 1757–1766.

Sajith, K. G. & Muraleedharan, C. (2004) Economic Analysis of a Hybrid Photovoltaic/Thermal Solar Dryer for drying Amla. International Journal of Engineering Research and Technology. 3,(8) :907 – 911.

Sanfu, R.E. (2016). Effect of Blanching on the Proximate and Sensory Qualities of the Aerial Yam Composite Cookies. *Caribbean Journal of Science and Technology*. Vol.4, 963-968

Sanful, R.E., Addo A, Oduro, I., & Ellis, W.O. (2015). Air Drying Characteristics of Aerial Yam (*Dioscorea bulbifera*). *Scholars Journal of Engineering and Technology (SJET)*, 3(8):693-700.

Sanful, R.E., Addo, A., Oduro, I., & Ellis, W.O .(2013). Effect of pre-treatment and drying on the functional properties of *D. bulbifera* flour. *Sky Journal of Food Science*, Vol. 2(4), pp. 27 – 34.

Sharma, A., Chen, C. R., & Lan, V. (2009). Solar Energy drying system:A review, renewable and sustainable energy reviews,13, pp. 1185-1210.

Sharma, R. (2004). Agro-technique of medicinal plants. Daya Publishing House, New Delhi, 81-82. DOI: http://dx.doi.org/10.1002/pad.4230030118.

Severini C., Baiano A., Pilli T. De, Carbone B. F., & Derossi A. (2005). Combined treatments of blanching and dehydration: study on potato cubes. *Journal of Food Engineering*, 68(3), pp. 289–296.

Singh, R. P., & Heldman, D. R. (2009). Introduction to Food Engineering. Elsevier, Academic Press.

Sobukola, O.P., Samuel O. A., Sanni L.O., & Bamiro F.O. (2010). Optimization of pre-fry drying of yam slices using response surface methodology. *Journal of Food Process Engineering*.3, 626-648. DOI: 10.1111/j.1745-4530.2008.00293.x

Soyal, Y. (2004). Microwave Drying Characteristics of Parsley. *Biosystems Engineering*,89(2):167-173.

Srikiatden, J., & Robert, J.S. (2007). Moisture Transfer in Solid Food Materials: A Review of Mechanisms, Models, and Measurement. *International Journal of Food Properties*, 10(4), 77-90. DOI: 10.1080/10942910601161672.

Stroshine, R. & Hamann D. (1995). Physical Properties of Agricultural Materials and Food Products. Course Manual, Purdue University, Indiana.

Subhash, C., Sarla, S., Abhay, P., & Anoop, B. (2014). Nutritional Profile and Phytochemical Screening of Garhwal Himalaya Medicinal Plant Dioscorea bulbifera. *International Research Journal of Pharmacy*, 3(5), 289-294

Taran, M., & Aghaie, E., (2015). Designing and optimization of separation process of iron impurities from kaolin by oxalic acid in bench-scale stirred-tank reactor. *Applied clay science*, 107, 109-116.

Tewodros, M.(2008). Morphological characterization and preliminary evaluation of aerial yam accessions collected from southwest Ethiopia. M.Sc. thesis, Presented to School of Graduate Studies, Hawassa University, Awassa.

Thiex, N., & VanErem, T. (1999). Comparisons of Karl Fischer methodwith oven methods for determination of water in forages andanimalfeeds. *Journal of AOAC*.82:799-808.

Tiwari A (2016) A Review on Solar Drying of Agricultural Produce. J Food Process Technol 7: 623. doi: 10.4172/2157-7110.1000623

Tiwari, A.K and Rao, J.M. Diabetes mellitus and multiple therapeutic approaches of phytochemicals: present status and future prospects. Current Science 2002: 83 (1): 30-37.

Torki-Harchegani, M., Ghanbarian, D., & Sadeghi, M. (2015). Heat Mass Transfer 51, 121-1129

Umar, G., Sawinder, K., Sushma, G., & Prasad, R. (2015). Effect of Hot Water Blanching Time and Drying Temperature on the Thin Layer Drying Kinetics of and Anthocyanin Degradation in Black Carrot (Daucus carota L.) Shreds. *Food technology and biotechnology*. 53(3), 37-43.

Uyigue, L., & Achadu, M.A. (2018). Measurement and Modeling of the Thin Layer Drying Properties of Selected Varieties of Yam Assisted by Hot-Water Blanching. *International Journal of Engineering and Modern Technology*, Vol. 4 No. 1, 35-53.

Vasanthi, H.R., Mukherjee, S., Ray, D., Jayachandran, K.S.P., & Lekli., (2010). Protective role of air potato (*dioscoreabulbifera*) of yam family in myocardial ischemic reperfusion injury, *food funct.*1:278-283.

Vyazovkin S (2012). Thermogravimetric Analysis, Characterization of Materials, 2nd edition. John Wiley and Sons, Inc, USA, pp 1–12.

Wankhade, P. K., Sapkal, R. S. and Sapkal, V. S. (2012) Drying Characteristics of Okra Slices using Different Drying Methods by Comparative Evaluation. Proceedings of the World Congress on Engineering and Computer Science San Francisco, US October 24-26, 2012.

Wanasundera, J. P. D.,& Ravindran, G. (1994). Nutritional assessment of yam (*Dioscorea alata*) tubers. Plant Foods for Human Nutrition 46(1), 33–39.

Wang C.Y., & Singh R.P., (1978). Use of variable equilibrium moisture content in modeling rice drying. *Trans. ASAE*, 11,668-672.

Wang, G., Lin, B., Liu, J., Wang, G., & Wang, F. (2009). Chemical constituents from tubers of D. *bulbifera.Zhongguo Zhong Yao za zhi*, 34 (13): 1679-1682.

Wang, J., Jiang, R. S., & Yu, Y. (2004). Relationship between dynamic resonance frequency and egg physical properties. *Food Research International*. 37:45.

Wang Z., Sun J., Liao X., Chen F., Zhao G., Wu J., & Hu X., (2007). Mathematical modeling on hot air drying of thin layerapple pomace. *Food Research Int*ernational, 40, 39-46.

Wireko-manu, F.D., Ibok, O.,Elis, W.O.,Asiedu, R.,& Maziya-Dixon, B. (2013). Potential health benefits of water yam (D.alata). *Pubfacts Scientific Publication Data*. Retrieved from http://www.pubfacts.com/detail/24056383.

World Food Summit 1996, Rome Declaration on World Food Security.

Wu, L., Orikasa, T., Ogawa, Y., Tagawa, A. (2007). Vacuum drying characteristics of eggplants. J. Food Eng. 83, 422–429.

Wyasu G., Gimba C. E., Agbaji E. B., & Ndukwe G. I. (2016). Thermo-gravimetry(TGA) and DSC of thermal analysis techniques in production of active carbon from lignocellulosic materials. *Advances in Applied Science Research*, 7(2): 109-115

Zinash D.(2008). Minimizing postharvest losses in yam (Dioscorea spp.) treatments and techniques Minna, Nigeria: *International Union of Food Science & Technology*.

APPENDIX

APPENDIX A: VARIABLES FOR CONVECTIVE AIR DRYER/SOLAR DRYER

Table A1: Moisture Content variationof unblanched water yam dried at 40 ^{o}C

time (sec)	water yam(g)	MC(db)	MR	DR1
0	100	238.5	1	0
300	97.27	229.2582938	0.961250708	0.546
600	94.2	218.865606	0.917675497	0.614
1200	90.02	204.7153013	0.858345079	0.418
1800	85.78	190.3618822	0.798163028	0.424
3600	76.5	158.9468517	0.666443823	0.309333333
5400	68.4	131.5264049	0.551473396	0.27
7200	62.33	110.9779959	0.465316545	0.202333333
9000	57.06	93.13777928	0.390514798	0.175666667
10800	53.8	82.10189573	0.344242749	0.108666667
12600	51.46	74.18043331	0.31102907	0.078
14400	49.89	68.86560596	0.288744679	0.052333333
16200	47.03	59.18381855	0.248150183	0.095333333
18000	45.54	54.13981043	0.227001302	0.049666667
19800	44.15	49.43432634	0.207271809	0.046333333
21600	44.05	49.0958023	0.205852421	0.003333333
23400	43.88	48.52031144	0.203439461	0.005666667
25200	43.29	46.52301963	0.195065072	0.019666667

Table A2: Moisture Contentvariation of unblanched aerial yam dried at 40 ^{o}C

time (sec)	Aerial yam(g)	MC(db)	MR	DR2
0	100	191.46	1	0
300	96.34	180.7925561	0.944283694	0.732
600	92.4	169.3090236	0.884304939	0.788
1200	88.4	157.650615	0.823412802	0.4
1800	83.98	144.7680734	0.75612699	0.442
3600	74.37	116.7587467	0.60983363	0.320333333

5400	67.6	97.02689012	0.506773687	0.225666667
7200	60.45	76.1874847	0.397928991	0.238333333
9000	55.77	62.5471466	0.326685191	0.156
10800	52.29	52.4043311	0.273709031	0.116
12600	50.33	46.69171087	0.243871884	0.065333333
14400	48.51	41.38713495	0.216165961	0.060666667
16200	46.17	34.5669659	0.180544061	0.078
18000	45.75	33.34283299	0.174150386	0.014
19800	44.85	30.71969105	0.160449656	0.03
21600	44.64	30.1076246	0.157252818	0.007
23400	44.26	29.00007578	0.151468065	0.012666667
25200	44.09	28.50459341	0.148880149	0.005666667

Table A3: Moisture Content variation **of u**nblanched water yam dried at 50 ^{o}C

time (sec)	water yam(g)	MC(db)	MR	DR
0	100	238.5	1	0
300	98.43	233.1851726	0.977715609	0.314
600	96.62	227.0578876	0.952024686	0.362
1200	91.52	209.7931618	0.879635899	0.51
1800	82.48	179.190589	0.751323224	0.904
3600	70.05	137.1120515	0.574893298	0.414333333
5400	57.7	95.30433311	0.399598881	0.411666667
7200	49.78	68.49322952	0.287183352	0.264
9000	45.18	52.9211239	0.221891505	0.153333333
10800	42.58	44.11949898	0.184987417	0.086666667
12600	41.06	38.97393365	0.16341272	0.050666667
14400	40.09	35.69025051	0.149644656	0.032333333
16200	39.8	34.70853081	0.145528431	0.009666667
18000	39.42	33.42213947	0.140134757	0.012666667

Table A4: Moisture Content variation of unblanched aerial yam dried at 50 ^{o}C

time (sec)	Aerial yam(g)	MC(db)	MR	DR2
0	100	191.46	1	0
300	96.34	180.7925561	0.944283694	0.732
600	92.4	169.3090236	0.884304939	0.788
1200	88.4	157.650615	0.823412802	0.4
1800	83.98	144.7680734	0.75612699	0.442
3600	74.37	116.7587467	0.60983363	0.320333333
5400	67.6	97.02689012	0.506773687	0.225666667
7200	60.45	76.1874847	0.397928991	0.238333333
9000	55.77	62.5471466	0.326685191	0.156
10800	52.29	52.4043311	0.273709031	0.116
12600	50.33	46.69171087	0.243871884	0.065333333
14400	48.51	41.38713495	0.216165961	0.060666667
16200	46.17	34.5669659	0.180544061	0.078
18000	45.75	33.34283299	0.174150386	0.014
19800	44.85	30.71969105	0.160449656	0.03
21600	44.64	30.1076246	0.157252818	0.007
23400	44.26	29.00007578	0.151468065	0.012666667
25200	44.09	28.50459341	0.148880149	0.005666667

Table A5: Moisture Content variation **of u**nblanched water yam dried at 60 ^{o}C

time (sec)	water yam(g)	MC(db)	MR	DR
0	100	238.5	1	0
300	95.29	222.5555179	0.933146826	0.942
600	89.65	203.4627624	0.853093343	1.128
1200	78.61	166.0897089	0.696392909	1.104
1800	69.12	133.9637779	0.561692989	0.949
3600	53.95	82.60968179	0.346371831	0.505666667
5400	40.72	37.82295193	0.158586801	0.441
7200	35.47	20.05044008	0.084068931	0.175

9000	32.27	9.217670955	0.038648516	0.106666667
10800	31.05	5.087677725	0.021331982	0.040666667
12600	30.5	3.225795531	0.013525348	0.018333333
14400	30.4	2.887271496	0.01210596	0.003333333

Table A6: Moisture Content variation **of u**nblanched aerial yam dried at 60 ^{o}C

time (sec)	Aerial yam(g)	MC(db)	MR	DR
0	100	191.46	1	0
300	94.28	174.7884757	0.912924244	1.144
600	89.09	159.6616905	0.833916695	1.038
1200	77.31	125.3276771	0.654589351	1.178
1800	67.48	96.67713786	0.504946923	0.983
3600	54.71	59.45766832	0.310548774	0.425666667
5400	46.24	34.77098805	0.181609673	0.282333333
7200	44.64	30.1076246	0.157252818	0.053333333
9000	43	25.32767706	0.132287042	0.054666667
10800	41.41	20.69345963	0.108082417	0.053
12600	40.89	19.17786651	0.10016644	0.017333333
14400	40.44	17.86629554	0.093316074	0.015

Table A7: Moisture Content variation **of u**nblanched water yam dried at 70 ^{o}C

time (sec)	water yam(g)	MC(db)	MR	DR
0	100	238.5	1	0
300	92.71	213.8215978	0.896526616	1.458
600	83.89	183.9637779	0.771336595	1.764
1200	72.46	145.2704807	0.609100548	1.143
1800	66.25	124.2481381	0.520956554	0.621
3600	44.5	50.61916046	0.212239667	0.725
5400	35.63	20.59207854	0.086339952	0.295666667
7200	31.63	7.051117129	0.029564432	0.133333333
9000	30.7	3.902843602	0.016364124	0.031
10800	30.14	2.007109005	0.008415551	0.018666667
12600	30.01	1.567027759	0.006570347	0.004333333

Table A8: Moisture Content variation **of u**nblanched aerial yam dried at 70 ^{o}C

time (sec)	Aerial yam(g)	MC(db)	MR	DR
0	100	191.46	1	0
300	96.17	180.2970737	0.941695778	0.766
600	88.04	156.6013582	0.817932509	1.626
1200	73.75	114.9516934	0.600395348	1.429
1800	62.2	81.28803847	0.424569302	1.155
3600	52.16	52.02543282	0.271730037	0.334666667
5400	45.48	32.55589041	0.170040167	0.222666667
7200	42.64	24.27842029	0.12680675	0.094666667
9000	41.72	21.5969863	0.112801558	0.030666667
10800	40.97	19.41103468	0.101384282	0.025
12600	40.78	18.85726027	0.098491906	0.006333333

Table A9: Moisture Content variation of unblanched water yam dried at inlet velocity, 2.0 m/s

time (sec)	water yam(g)	MC(db)	MR	DR
0	100	238.5	1	0
300	93.74	217.3083954	0.911146312	1.252
600	88.1	198.2156398	0.831092829	1.128
1200	79.23	168.1885579	0.705193115	0.887
1800	72.31	144.7626947	0.606971466	0.692
3600	59.73	102.176371	0.428412457	0.419333333
5400	50.11	69.61035884	0.291867333	0.320666667
7200	45.87	55.25693974	0.231685282	0.141333333
9000	42.01	42.18991198	0.176896906	0.128666667
10800	40.19	36.02877454	0.151064044	0.060666667
12600	38.94	31.7972241	0.133321694	0.041666667
14400	37.99	28.58124577	0.119837508	0.031666667
16200	37.58	27.19329722	0.114018018	0.013666667

18000	37.56	27.12559242	0.11373414	0.000666667

Table A10: Moisture Contentvariation of unblanched aerial yam dried at inlet velocity, 2.0 m/s

time (sec)	Aerial yam(g)	MC(db)	MR	DR
0	100	191.46	1	0
300	92.7	170.1834043	0.888871849	1.46
600	87.62	155.3772253	0.811538835	1.016
1200	80.3	134.0423375	0.700106223	0.732
1800	72.84	112.2994054	0.586542387	0.746
3600	63.82	86.00969397	0.449230617	0.300666667
5400	56.83	65.63662489	0.342821607	0.233
7200	52.84	54.00736229	0.2820817	0.133
9000	49.62	44.62234334	0.233063529	0.107333333
10800	47.84	39.4343515	0.205966528	0.059333333
12600	46.07	34.27550568	0.179021757	0.059
14400	44.97	31.06944331	0.16227642	0.036666667
16200	44.16	28.70861556	0.149945762	0.027
18000	44.15	28.67946954	0.149793532	0.000333333

Table A11: Moisture Contentvariation of unblanched water yam dried at inlet velocity, 2.5 m/s

time (sec)	water yam(g)	MC(db)	MR	DR
0	100	238.5	1	0
300	91.43	209.4884902	0.878358449	1.714
600	85.7	190.091063	0.797027518	1.146
1200	75.84	156.7125931	0.657075862	0.986
1800	68.74	132.6773866	0.556299315	0.71
3600	51.75	75.16215301	0.315145296	0.566333333
5400	42.62	44.2549086	0.185555172	0.304333333
7200	38.65	30.8155044	0.129205469	0.132333333
9000	37.23	26.0084631	0.10905016	0.047333333

10800	37.18	25.83920108	0.108340466	0.001666667
12600	37.14	25.70379147	0.107772711	0.001333333
14400	37.11	25.60223426	0.107346894	0.001
16200	37.08	25.50067705	0.106921078	0.001

Table A12: Moisture Content variation of unblanched aerial yam dried at inlet velocity 2.5 m/s

time (sec)	Aerial yam(g)	MC(db)	MR	DR
0	100	191.46	1	0
300	92.43	169.3964617	0.88476163	1.514
600	86.44	151.9379948	0.793575654	1.198
1200	74.45	116.9919149	0.611051472	1.199
1800	68.2	98.77565141	0.515907508	0.625
3600	53.94	57.21342466	0.298827038	0.475333333
5400	47.34	37.97705042	0.198355011	0.22
7200	43.79	27.63021277	0.144313239	0.118333333
9000	41.87	22.03417662	0.115085013	0.064
10800	40.8	18.91555232	0.098796366	0.035666667
12600	40.57	18.24519382	0.095295069	0.007666667
14400	40.42	17.8080035	0.093011613	0.005
16200	40.39	17.72056543	0.092554922	0.001

Table A13: Moisture Contentvariation of unblanched water yam dried at inlet velocity 3.0 m/s

time (sec)	water yam(g)	MC(db)	MR	DR
0	100	238.5	1	0
300	93.62	216.9021666	0.909443046	1.276
600	85.78	190.3618822	0.798163028	1.568
1200	78.51	165.7511848	0.694973521	0.727
1800	70.01	136.9766418	0.574325542	0.85
3600	53.05	79.56296547	0.333597339	0.565333333
5400	46.12	56.10324983	0.235233752	0.231
7200	41.8	41.47901151	0.173916191	0.144
9000	39.8	34.70853081	0.145528431	0.066666667

10800	38.62	30.71394719	0.128779653	0.039333333
12600	37.61	27.29485443	0.114443834	0.033666667
14400	37.2	25.90690589	0.108624343	0.013666667
16200	37.18	25.83920108	0.108340466	0.000666667

Table A14: Moisture Content variation of unblanched aerial yam dried at inlet velocity, 3.0 m/s

time (sec)	Aerial yam(g)	MC(db)	MR	DR
0	100	191.46	1	0
300	93.91	173.7100729	0.907291721	1.218
600	87.43	154.8234509	0.808646458	1.296
1200	75.02	118.6532381	0.619728602	1.241
1800	66.46	93.70424366	0.489419428	0.856
3600	51.53	50.18923346	0.262139525	0.497666667
5400	45.16	31.62321772	0.165168796	0.212333333
7200	41.46	20.83918974	0.108843569	0.123333333
9000	39.68	15.6511979	0.081746568	0.059333333
10800	38.93	13.46524628	0.070329292	0.025
12600	38.48	12.15367531	0.063478927	0.015
14400	38.2	11.33758671	0.059216477	0.009333333
16200	38.2	11.33758671	0.059216477	0

Table A15: Moisture Content variation of unblanched water yam dried at inlet velocity 3.5 m/s

time (sec)	water yam(g)	MC(db)	MR	DR
0	100	238.5	1	0
300	95.03	221.6753555	0.929456417	0.994
600	91.03	208.134394	0.872680897	0.8
1200	84.02	184.4038592	0.773181799	0.701
1800	74.9	153.5304672	0.643733615	0.912
3600	60.06	103.2935003	0.433096437	0.494666667
5400	53.34	80.54468517	0.337713565	0.224
7200	44.24	49.73899797	0.208549258	0.303333333
9000	40.18	35.99492214	0.150922105	0.135333333

10800	37.46	26.78706838	0.112314752	0.090666667
12600	36.44	23.33412322	0.097836995	0.034
14400	35.95	21.67535545	0.090881994	0.016333333
16200	35.62	20.55822613	0.086198013	0.011

Table A16: Moisture Content variation of unblanched aerial yam dried at inlet, 3.5 m/s

time (sec)	Aerial yam(g)	MC(db)	MR	DR
0	100	191.46	1	0
300	94.75	176.1583387	0.92007907	1.05
600	89.4	160.5652171	0.838635836	1.07
1200	81.46	137.423276	0.717764943	0.794
1800	75.29	119.4401807	0.623838821	0.617
3600	57.29	66.97734188	0.349824203	0.6
5400	53.53	56.01843777	0.292585594	0.125333333
7200	46.64	35.93682891	0.187698887	0.229666667
9000	45.07	31.36090353	0.163798723	0.052333333
10800	43.4	26.49351792	0.138376256	0.055666667
12600	42.7	24.45329642	0.127720132	0.023333333
14400	42.43	23.66635383	0.123609912	0.009
16200	42.13	22.79197319	0.119043002	0.01

Table A17: Moisture Content variation of unblanched water yam dried at inlet velocity, 4.0 m/s

time (sec)	water yam(g)	MC(db)	MR	DR
0	100	238.5	1	0
300	93.73	217.274543	0.911004373	1.254
600	83.86	183.8622207	0.770910779	1.974
1200	75.57	155.7985782	0.653243514	0.829
1800	68.4	131.5264049	0.551473396	0.717
3600	60.08	103.3612051	0.433380315	0.277333333
5400	48.58	64.4309411	0.270150696	0.383333333
7200	44.87	51.87169939	0.217491402	0.123666667
9000	43.37	46.79383886	0.196200582	0.05

10800	34.18	15.68348003	0.065758826	0.306333333
12600	42.66	44.39031821	0.186122928	0.282666667
14400	42.19	42.79925525	0.179451804	0.015666667

Table A18: Moisture Content variation of unblanched aerial yam dried at inlet velocity, 4.0 m/s

time (sec)	Aerial yam(g)	MC(db)	MR	DR
0	100	191.46	1	0
300	92.12	168.492935	0.880042489	1.576
600	85.59	149.4605829	0.780636075	1.306
1200	75.47	119.9648091	0.626578967	1.012
1800	67.61	97.05603614	0.506925917	0.786
3600	58.61	70.82461673	0.369918608	0.3
5400	46.66	35.99512096	0.188003348	0.398333333
7200	42.68	24.39500437	0.127415671	0.132666667
9000	41.09	19.76078694	0.103211046	0.053
10800	40.64	18.44921597	0.096360681	0.015
12600	39.99	16.55472457	0.086465709	0.021666667
14400	39.43	14.92254736	0.077940809	0.018666667

Table A19: Moisture Content variation of unblanched water yam at thickness of 2.0 mm

time (sec)	water yam(g)	MC(db)	MR	DR
0	100	238.5	1	0
300	95.49	223.232566	0.935985602	0.902
600	90.39	205.9678402	0.863596814	1.02
1200	85.8	190.429587	0.798446906	0.459
1800	78.88	167.0037238	0.700225257	0.692
3600	61.85	109.3530806	0.458503482	0.567666667
5400	51.25	73.46953284	0.308048356	0.353333333
7200	45.09	52.61645227	0.220614056	0.205333333
9000	41.21	39.4817197	0.165541802	0.129333333

10800	39.26	32.88050102	0.137863736	0.065
12600	38.51	30.34157075	0.127218326	0.025
14400	38.42	30.03689912	0.125940877	0.003
16200	38.17	29.19058903	0.122392407	0.008333333

Table A20: Moisture Content variation of unblanched aerial yam at thickness of 2.0 mm

time (sec)	Aerial yam(g)	MC(db)	MR	DR
0	100	191.46	1	0
300	94.67	175.9251705	0.918861227	1.066
600	89.26	160.1571728	0.836504611	1.082
1200	82.53	140.5419003	0.73405359	0.673
1800	75.09	118.8572603	0.620794214	0.744
3600	59.55	73.56434276	0.384228261	0.518
5400	51.91	51.29678228	0.267924278	0.254666667
7200	47.52	38.50167881	0.201095157	0.146333333
9000	44.78	30.5156689	0.159384043	0.091333333
10800	43.73	27.45533664	0.143399857	0.035
12600	42.09	22.6753891	0.118434081	0.054666667
14400	41.95	22.2673448	0.116302856	0.004666667
16200	41.43	20.75175168	0.108386878	0.017333333

Table A21: Moisture Content variation of unblanched water yam at thickness of 4.0 mm

time (sec)	water yam(g)	MC(db)	MR	DR
0	100	238.5	1	0
300	96.69	227.2948544	0.953018258	0.662
600	92.73	213.8893026	0.896810493	0.792
1200	84.82	187.1120515	0.784536903	0.791
1800	79.26	168.2901151	0.705618931	0.556
3600	68.81	132.9143534	0.557292886	0.348333333
5400	60.98	106.4079215	0.446154807	0.261

7200	54.34	83.92992552	0.351907445	0.221333333
9000	50.11	69.61035884	0.291867333	0.141
10800	47.13	59.52234259	0.249569571	0.099333333
12600	44.82	51.70243737	0.216781708	0.077
14400	42.78	44.79654705	0.187826193	0.068
16200	41.46	40.32802979	0.169090272	0.044
18000	40.77	37.99221395	0.159296495	0.023
19800	40.4	36.73967502	0.154044759	0.012333333
21600	40.2	36.06262695	0.151205983	0.006666667
23400	40	35.38557888	0.148367207	0.006666667

Table A22: Moisture Content variation of unblanched aerial yam at thickness of 4.0 mm

time (sec)	Aerial yam(g)	MC(db)	MR	DR
0	100	191.46	1	0
300	97.81	185.0770213	0.966661555	0.438
600	94.34	174.9633518	0.913837626	0.694
1200	86.67	152.6083532	0.797076952	0.767
1800	81.72	138.1810726	0.721722932	0.495
3600	73.58	114.456211	0.597807432	0.271333333
5400	68.23	98.86308948	0.516364199	0.178333333
7200	63.5	85.07702128	0.444359246	0.157666667
9000	59.63	73.79751093	0.385446103	0.129
10800	56.83	65.63662489	0.342821607	0.093333333
12600	55.23	60.97326144	0.318464752	0.053333333
14400	52.31	52.46262314	0.274013492	0.097333333
16200	50.59	47.44950743	0.247829873	0.057333333
18000	49.09	43.0776042	0.224995321	0.05
19800	47.97	39.81324978	0.207945523	0.037333333
21600	46.96	36.8695016	0.192570258	0.033666667
23400	46.05	34.21721364	0.178717297	0.030333333

Table A23: Moisture content variation of unblanched water yam at thickness of 6.0 mm

time (sec)	water yam(g)	MC(db)	MR	DR
0	100	238.5	1	0
300	95.22	222.3185511	0.932153254	0.956

600	91.72	210.4702099	0.882474675	0.7
1200	86.14	191.5805687	0.803272825	0.558
1800	81.83	176.9901828	0.742097203	0.431
3600	70.71	139.3463101	0.584261258	0.370666667
5400	65.64	122.1831415	0.512298287	0.169
7200	59.61	101.7701422	0.426709192	0.201
9000	53.59	81.39099526	0.341262035	0.200666667
10800	49.76	68.42552471	0.286899475	0.127666667
12600	47.12	59.48849018	0.249427632	0.088
14400	45.38	53.59817197	0.224730281	0.058
16200	43.85	48.41875423	0.203013645	0.051
18000	41.76	41.3436019	0.173348436	0.069666667
19800	37.21	25.94075829	0.108766282	0.151666667
21600	34.01	15.10798917	0.063345867	0.106666667
23400	33.91	14.76946513	0.061926479	0.003333333
25200	33.7	14.05856466	0.058945764	0.007
27000	33.66	13.92315504	0.058378009	0.001333333
28800	33.55	13.55077861	0.056816682	0.003666667
30600	33.49	13.34766418	0.055965049	0.002
32400	33.4	13.04299255	0.0546876	0.003
34200	33.39	13.00914015	0.054545661	0.000333333
36000	33.37	12.94143534	0.054261783	0.000666667

Table A24: Moisture content variation of unblanched aerial yam at thickness of 6.0 mm

time (sec)	Aerial yam(g)	MC(db)	MR	DR
0	100	191.46	1	0
300	96.59	181.5212066	0.948089453	0.682
600	93.87	173.5934888	0.906682799	0.544
1200	90.74	164.470784	0.859034702	0.313
1800	87.17	154.0656543	0.804688469	0.357
3600	81.67	138.0353425	0.72096178	0.183333333
5400	76.9	124.1326902	0.648347906	0.159
7200	69.67	103.0601166	0.538285368	0.241
9000	68.55	99.79576217	0.52123557	0.037333333
10800	66.55	93.96655785	0.490789501	0.066666667
12600	64.15	86.97151268	0.454254219	0.08
14400	62.42	81.92925095	0.427918369	0.057666667
16200	59.05	72.10704168	0.376616743	0.112333333
18000	56.99	66.10296124	0.345257293	0.068666667

19800	54.44	58.67072574	0.306438555	0.085
21600	50.93	48.44047217	0.253005704	0.117
23400	50.23	46.40025066	0.24234958	0.023333333
25200	49.01	42.84443602	0.223777478	0.040666667
27000	48.64	41.76603323	0.218144956	0.012333333
28800	47.92	39.66751967	0.207184371	0.024
30600	47.32	37.91875838	0.19805055	0.02
32400	46.7	36.11170504	0.188612269	0.020666667
34200	46.38	35.17903235	0.183740898	0.010666667
36000	46.22	34.71269601	0.181305213	0.005333333

Table A25: Moisture content variation of blanched water yam dried at 40 ^{o}C

time (sec)	water yam(g)	MC(db)	MR	DR
0				
0	108.21	266.2928233	1	0
300	99.77	237.7213947	0.892706727	1.688
600	95.33	222.6909276	0.836263346	0.888
1200	89.56	203.1580907	0.762912377	0.577
1800	84.37	185.5886933	0.696934641	0.519
3600	69.69	135.8933649	0.510315536	0.489333333
5400	60.69	105.4262018	0.395903278	0.3
7200	58.45	97.84326337	0.367427339	0.074666667
9000	53.26	80.27386594	0.301449603	0.173
10800	48.79	65.14184157	0.244624849	0.149
12600	45.52	54.07210562	0.203055062	0.109
14400	43.85	48.41875423	0.181825231	0.055666667
16200	40.58	37.34901828	0.140255444	0.109
18000	39.43	33.45599188	0.1256361	0.038333333
19800	39.17	32.57582938	0.122330857	0.008666667
21600	38.79	31.28943805	0.117500118	0.012666667
23400	38.66	30.8493568	0.115847496	0.004333333
25200	38.51	30.34157075	0.113940625	0.005
27000	38.47	30.20616114	0.113432126	0.001333333
28800	38.45	30.13845633	0.113177877	0.000666667
30600	37.73	27.70108328	0.104024896	0.024
32400	37.72	27.66723087	0.103897771	0.000333333
34200	37.11	25.60223426	0.096143163	0.020333333

Table A26: Moisture content variation of blanched aerial yam dried at 40 ^{o}C

time (sec)	Aerial yam(g)	MC(db)	MR	DR
0			0	
0	131.98	284.668977	1.486832639	0
300	118.46	245.2635558	1.281017214	2.704
600	114.26	233.0222268	1.21708047	0.84
1200	110.64	222.4713669	1.161973085	0.362
1800	100.89	194.0539959	1.013548501	0.975
3600	84.93	147.5369455	0.770588872	0.532
5400	71.95	109.7054095	0.572993886	0.432666667
7200	63.63	85.45591956	0.446338241	0.277333333
9000	56.03	63.30494317	0.33064318	0.253333333
10800	51.29	49.48972894	0.258485997	0.158
12600	47.28	37.80217429	0.197441629	0.133666667
14400	45.18	31.68150976	0.165473257	0.07
16200	42.35	23.43318566	0.12239207	0.094333333
18000	40.53	18.12860973	0.094686147	0.060666667
19800	39.77	15.9135121	0.083116641	0.025333333
21600	39.92	16.35070242	0.085400096	-0.005
23400	38.34	11.74563101	0.061347702	0.052666667
25200	38.71	12.82403381	0.066980225	-0.012333333
27000	38.49	12.18282133	0.063631157	0.007333333
28800	38.23	11.42502477	0.059673168	0.008666667
30600	37.92	10.52149811	0.054954028	0.010333333
32400	37.46	9.180781113	0.047951432	0.015333333
34200	37.4	9.005904984	0.04703805	0.002

Table A27: Moisture content variation of blanched water yam dried at inlet velocity 2.5 m/s

time (sec)	water yam(g)	MC(db)	MR	DR
0				
0	111.76	278.3104265	1.045129279	0
300	100.36	239.7186865	0.900207086	2.28
600	86.46	192.6638456	0.72350371	2.78
1200	75.03	153.9705484	0.578200143	1.143
1800	67.05	126.9563304	0.476754607	0.798
3600	53.8	82.10189573	0.308314339	0.441666667
5400	45.95	55.52775897	0.208521425	0.261666667
7200	41.93	41.91909276	0.157417283	0.134
9000	40.07	35.6225457	0.133772083	0.062
10800	38.94	31.7972241	0.119406989	0.037666667
12600	38.03	28.71665538	0.107838638	0.030333333
14400	37.49	26.88862559	0.100973903	0.018
16200	36.99	25.19600542	0.094617666	0.016666667
18000	36.75	24.38354773	0.091566672	0.008
19800	36.47	23.43568043	0.08800718	0.009333333

Table A28: Moisture content variation of blanched aerial yam dried at inlet velocity 2.5 m/s

time (sec)	Aerial yam(g)	MC(db)	MR	DR
0				
0	131.4	282.9785077	1.478003279	0
300	118.18	244.4474672	1.276754764	2.644
600	100.03	191.5474381	1.000456691	3.63
1200	86.44	151.9379948	0.793575654	1.359
1800	74.18	116.2049723	0.606941253	1.226
3600	56.24	63.91700962	0.333840017	0.598
5400	50.51	47.21633926	0.24661203	0.191
7200	47.73	39.11374526	0.204291994	0.092666667
9000	46.3	34.94586418	0.182523055	0.047666667
10800	45.26	31.91467794	0.1666911	0.034666667
12600	44.41	29.4372661	0.15375152	0.028333333
14400	43.77	27.57192072	0.144008778	0.021333333

16200	43.17	25.82315943	0.134874958	0.02
18000	42.69	24.42415039	0.127567901	0.016
19800	42.2	22.99599534	0.120108615	0.016333333

Table A29: Moisture content variation of blanched water yam at thickness of 2.0 mm

time (sec)	water yam(g)	MC(db)	MR	DR
0			0	
0	108.57	267.5115098	1.00457649	0
300	99.56	237.0104942	0.890037108	1.802
600	92.98	214.7356127	0.806389035	1.316
1200	84.35	185.5209885	0.696680392	0.863
1800	74.55	152.345633	0.572098156	0.98
3600	60.56	104.9861205	0.394250657	0.466333333
5400	51.22	73.36797563	0.275516158	0.311333333
7200	45.1	52.65030467	0.197715823	0.204
9000	42.08	42.42687881	0.159324154	0.100666667
10800	39.81	34.74238321	0.13046684	0.075666667
12600	39.01	32.03419093	0.120296862	0.026666667
14400	38.46	30.17230873	0.113305001	0.018333333
16200	38.26	29.49526066	0.110762507	0.006666667
18000	38.26	29.49526066	0.110762507	0

Table A30: Moisture content variation of blanched aerial yam at thickness of 2.0 mm

time (sec)	Aerial yam(g)	MC(db)	MR	DR
0				
0	126.34	268.2306208	1.400974725	0
300	116.82	240.4836083	1.256051438	1.904
600	108.26	215.5346138	1.125742264	1.712
1200	95.91	179.5392772	0.93773779	1.235
1800	81.08	136.3157272	0.71198019	1.483
3600	65.63	91.28512387	0.476784309	0.515
5400	54.7	59.4285223	0.310396544	0.364333333
7200	50.41	46.92487904	0.245089727	0.143
9000	48.57	41.56201108	0.217079343	0.061333333
10800	46.54	35.6453687	0.186176584	0.067666667

12600	45.46	32.49759837	0.169735707	0.036
14400	44.33	29.20409793	0.152533678	0.037666667
16200	43.88	27.89252696	0.145683312	0.015
18000	43.67	27.28046051	0.142486475	0.007

Table A 31: Solar Radiation data during the experiment

Period	Ave. Min Temp.(^oC)	Ave. Max.Temp. (^oC)	Ave. Relative humidity (%)	Ave. Solar Radiation(W/m^2)
	33.78	35.90	61.0	160.21
	34.27	36.15	63.0	165.21
May	31.65	32.08	61.5	162.39
	30.03	33.53	63.5	173.42
	31.34	34.59	64.0	161.09
	32.61	36.11	65.0	175.31
	31.64	33.04	67.5	151.32
June	34.01	35.24	65.0	154.23
	32.49	36.23	69.5	149.00
	31.84	35.22	65.0	143.67
	30.22	33.41	63.0	144.23
	31.34	34.61	68.0	147.32
July	32.28	35.50	67.5	137.23
	33.41	35.69	70.0	139.09
	30.31	33.29	65.0	135.62
	30.40	33.88	59.5	130.30
	33.28	35.29	61.0	132.40
August	32.41	36.49	60.0	133.99
	31.23	35.39	61.5	130.01
	34.12	36.01	59.5	129.45

Table A32: Moisture content Variation of unblanched samples at thickness of 2.0 mm

Time(m)	W.Y(g)	M.C	A.Y(g)	M.C	Chamber Temp	Exit Temp	Max.Temp /RH	Min.Temp/RH
0	100	238.5	100	191.46	36	36.3	30.5/84	29/85
5	97.04	228.4797	98.33	186.5926144	36.2	37.2	32.4/82	30.3/82
10	87.54	196.3199	96.85	182.2790032	36.4	37.6	32.5/81	30.5/82
20	85.35	188.9062	94.1	174.2638473	36.3	37	33.2/80	31.2/82
30	83.52	182.7112	92	168.1431827	37.2	37.5	33.1/62	32.9/62
60	77.57	162.5691	84.5	146.2836666	37.8	39.3	34.2/64	32.9/61

90	71.84	143.1716	77.72	126.5226639	39.2	41.2	35.2/59	34.9/58
120	66.39	124.7221	72.44	111.1335646	39.9	42.3	35.6/58	35/57
150	61.65	108.676	67.3	96.15250947	40.2	44.2	37.2/54	35.9/55
180	57.14	93.4086	62.76	82.92021568	40.3	43.9	37.5/53	36.2/54
210	53.33	80.51083	59.05	72.10704168	40.8	42.8	38/51	37.2/51
240	59.03	99.8067	55.52	61.81849607	41.4	45	39.1/50	37.5/50
270	45.59	54.30907	53.27	55.26064121	41.4	44.2	39.2/50	37.6/49
300	43.08	45.81212	51.73	50.77215389	41.3	43.2	38.9/51	38.1/49
330	41.45	40.29418	50.84	48.17815797	42.3	43.7	39.9/50	38.9/48
360	38.05	28.78436	48.52	41.41628097	42.4	44.3	40.1/47	39.9/47
390	37.05	25.39912	47.92	39.66751967	42.3	45.1	39.9/47	39.1/47
420	35.87	21.40454	47.06	37.16096182	41.2	43.2	38.2/48	37.9/48
450	34.61	17.13913	46.34	35.06244827	39.2	41.2	35.2/68	34.4/69
480	34.43	16.52979	46.26	34.82928009	38.4	40.3	36.1/62	34.2/68

Table A33: Moisture content Variation of unblanched samples at thickness of 4.0 mm

Time(m)	W.Y(g)	M.C	A.Y(g)	M.C	Chamber Temp	Exit Temp	Max.Temp /RH	Min.Temp/RH
0	100	238.5	100	191.46	38.9	40.2	33.6/82	33.1/84
5	99.21	235.8257	98.85	188.1082075	39	42	34.6/81	34.2/81
10	97.84	231.1879	97.28	183.5322821	39.2	41.3	35.6/79	35/78
20	95.56	223.4695	94.71	176.0417546	38.4	40	36.2/78	35.2/81
30	93.61	216.8683	92.32	169.0758554	37.2	40.1	35.4/78	35/78
60	88.88	200.8561	86.94	153.3952958	37.9	40.4	34.7/74	33.8/73
90	84.85	187.2136	82.32	139.9298339	39.1	42.1	35.6/75	34.7/74
120	80.14	171.2691	77.41	125.6191373	40.2	43.8	36.7/64	35.2/62
150	74.85	153.3612	72.32	110.7838123	40.8	43.2	37.1/61	36.3/60
180	71.1	140.6666	68.55	99.79576217	41	41.9	37.9/58	36.4/59
210	64.28	117.5792	63.12	83.96947246	39.2	40.3	36.2/61	35.9/62
240	61.81	109.2177	60.8	77.20759545	39.4	42	35.8/62	34.1/70
270	59.61	101.7701	59.13	72.34020985	41.4	42.8	38.1/54	36.2/59
300	56.26	90.42959	56.76	65.43260274	41.6	41.9	38.5/55	36.7/54
330	53.54	81.22173	54.87	59.92400466	39.9	40.2	37.2/56	36.7/57
360	50.95	72.45396	53.29	55.31893326	38.2	39.2	36.2/68	35.4/67
390	48.46	64.02471	51.85	51.12190615	38	38.9	36/68	35/68
420	46.41	57.08497	50.66	47.65352958	37.8	39.5	35.7/59	34.2/60
450	44.14	49.40047	49.46	44.156007	37.2	39.2	35.8/70	34.9/69
480	42.48	43.78097	48.66	41.82432527	36.4	38.2	34.2/70	34/71
510	40.89	38.39844	47.84	39.4343515	36	37.3	34.6/68	33.8/70
540	39.57	33.92993	47.21	37.59815214	35.3	39	32.5/67	31.9/67

570	38.85	31.49255	46.88	36.63633343	35.1	38.4	33.9/71	32.9/70
600	37.43	26.68551	45.87	33.69258525	35	38.2	34.1/70	33.8/71
630	36.71	24.24814	45.5	32.61418245	36.5	37.5	34.8/60	34.6/58
660	36.08	22.11544	45.13	31.53577966	36.9	38.2	34.6/59	34.3/57
690	35.75	20.99831	44.84	30.69054503	37.2	39.1	34.4/68	34.1/64
720	35.01	18.49323	44.03	28.32971728	37.8	40.1	34.3/68	33.9/65
750	34.32	16.15741	43.38	26.43522588	37.8	39.6	34.5/58	34/56
780	33.01	11.72275	42.01	22.44222093	37.1	39.3	34.1/59	33/58

Table A34: Moisture content Variation of unblanched samples at inlet air velocity of 0.5 m/s

Time(m)	W.Y(g)	M.C	A.Y(g)	M.C	Chamber Temp	Exit Temp	Max.Temp /RH	Min.Temp/RH
0	100	238.5	100	191.46	36.7	38.3	33.1/62	32.9/62
5	97.41	229.7322	98.9	188.2539376	35.8	38.1	34.8/71	33.1/71
10	95.3	222.5894	96.93	182.5121714	35.9	38.8	34.2/69	32.2/72
20	91.47	209.6239	93.2	171.6407053	37.2	40.1	35.9/62	33.2/63
30	87.7	196.8615	88.87	159.020478	39.3	41.5	36.1/65	34.2/65
60	78.57	165.9543	80.77	135.4122005	35.4	39.2	33.4/68	33.3/67
90	70.14	137.4167	71.89	109.5305334	38.4	40.2	34.3/68	33.4/68
120	63.73	115.7173	65.34	90.43988925	37.5	40.8	35.8/64	34.2/61
150	59.82	102.481	61.51	79.27696298	37.8	40.6	35.9/61	34.8/60
180	57.57	94.86425	58.89	71.64070533	39.2	42.1	36/60	34.7/59
210	54.54	84.60697	55.8	62.63458467	36.3	40.1	34.5/59	34.4/59
240	51.2	73.30027	52.38	52.66664529	30.1	32.3	28.2/73	28.1/72
270	48.97	65.75118	50.35	46.75000291	30.2	33.4	28.4/72	28.1/72
300	47.83	61.89201	49.27	43.60223259	32.3	35.2	29/82	28.8/82
330	46.84	58.54062	48.21	40.5127543	32.7	35.8	30.4/81	28.9/80
360	46.56	57.59276	48.19	40.45446226	33	36.2	30.6/80	30.1/80
390	46.45	57.22038	48.12	40.2504401	37.8	39.3	34.7/74	32.2/74
420	45.81	55.05383	47.49	38.41424075	35.4	37.2	31.3/73	30.1/75
450	45.44	53.80129	47.18	37.51071408	37.1	40.1	35.5/70	32.3/74
480	45.08	52.5826	46.84	36.51974934	38	41.2	34.8/80	33.2/81
510	46.22	56.44177	46.22	34.71269601	37.2	40.3	35.4/82	34.1/81

APPENDIX B: VARIABLES FOR SOLAR DRYER

APPENDIX C: DRYING KINETIC MODELS

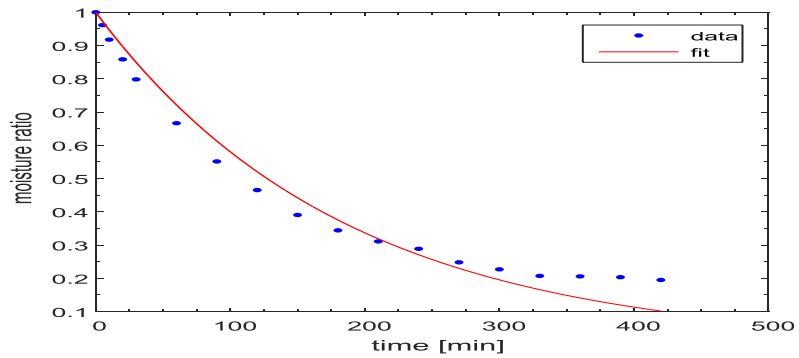

Fig. C1: Variation of experimental and Newton model based predicted moisture ratio with time

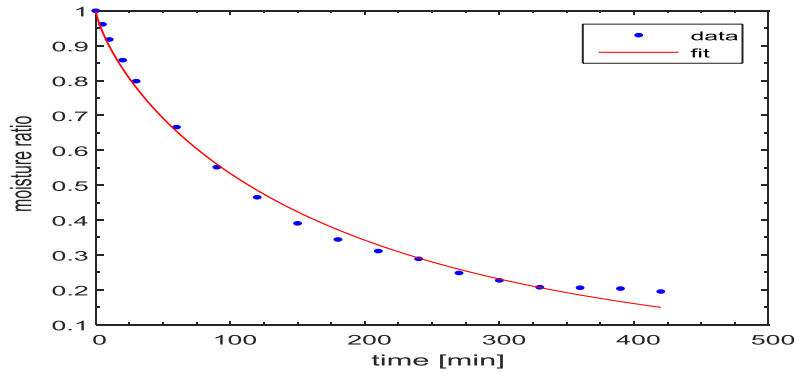

Fig C2: Variation of experimental and Page model based predicted moisture ratio with time

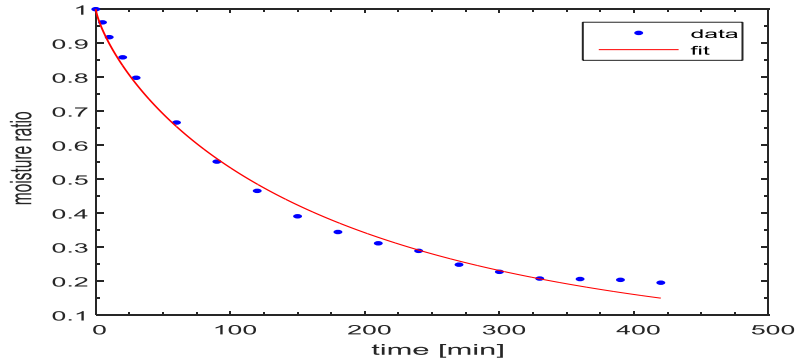

Fig.C3: Variation of experimental and Page modified model based predicted moisture ratio with time

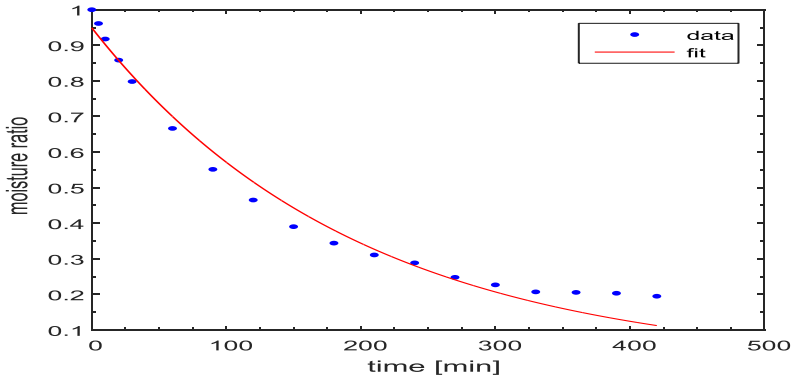

Fig. C4: Variation of experimental and Henderson et Pabis model based predicted moisture ratio with time

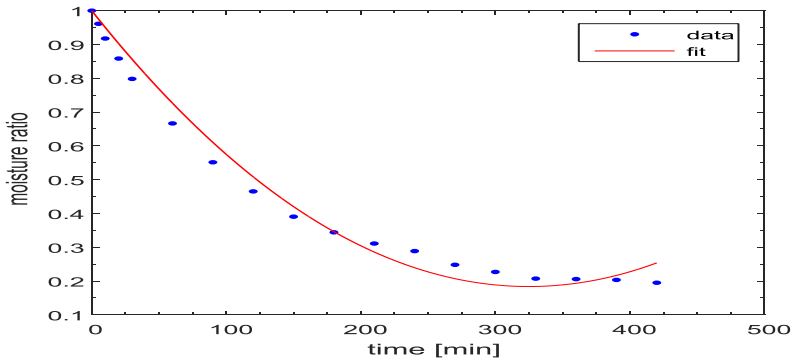

Fig. C5. Variation of experimental and Wang et Singh model based predicted moisture ratio with time

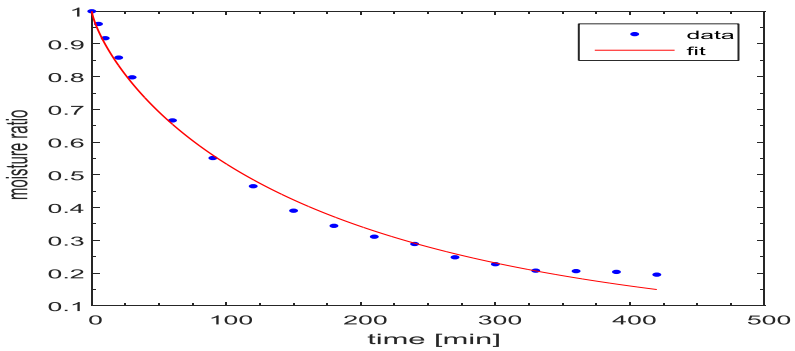

Fig. C6: Variation of experimental and Weibull model based predicted moisture ratio with time

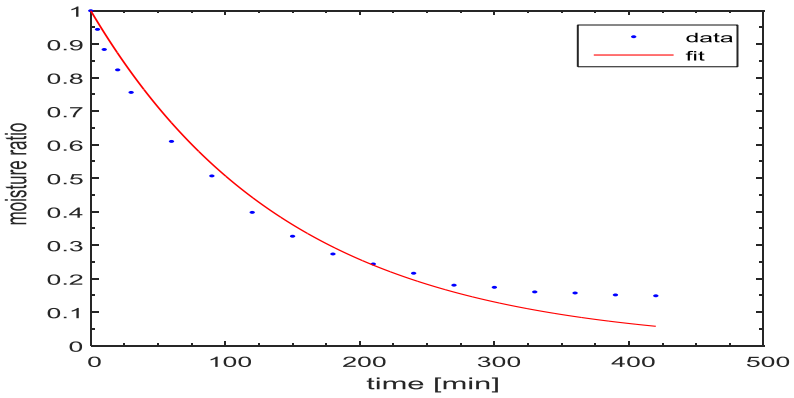

Fig. C7. Variation with time of experimental moisture ratio and Newton model-based predicted moisture ratio

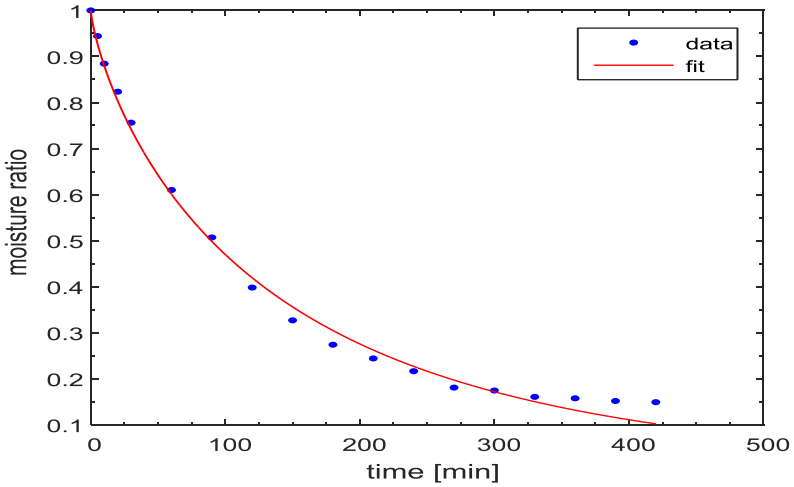

Fig. C8. Variation with time of experimental moisture ratio and Page model-based predicted moisture ratio

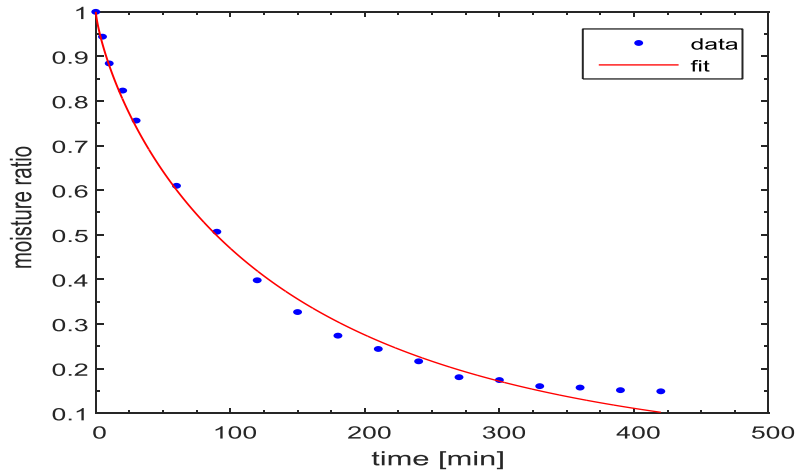

Fig. C9: Variation with time of experimental moisture ratio and Page Modified model-based predicted moisture ratio

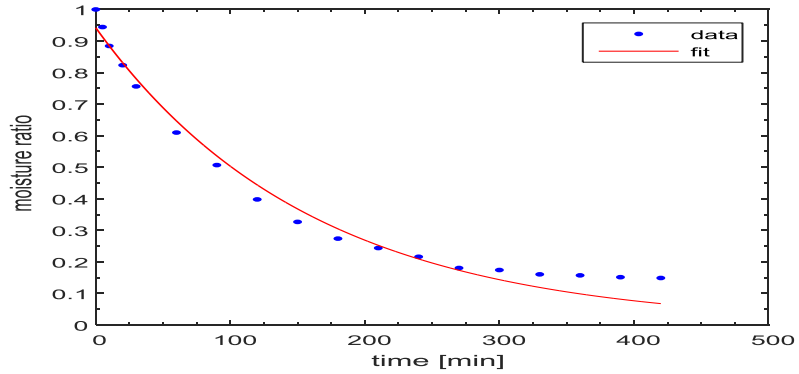

Fig C10: Variation with time of experimental moisture ratio and Henderson et Pabis model-based predicted moisture ratio

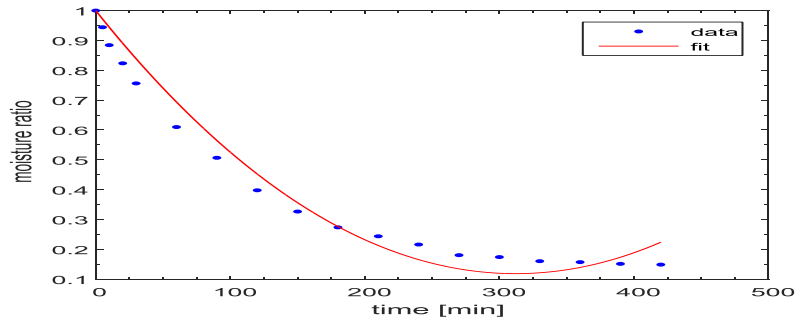

Fig. C11: Variation with time of experimental moisture ratio and Wang et Singh model-based predicted moisture ratio

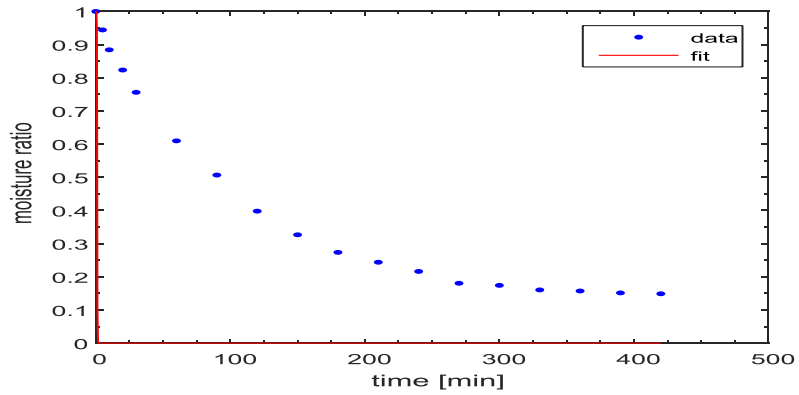

Fig. C12: Variation with time of experimental moisture ratio and Weibull model-based predicted moisture ratio.

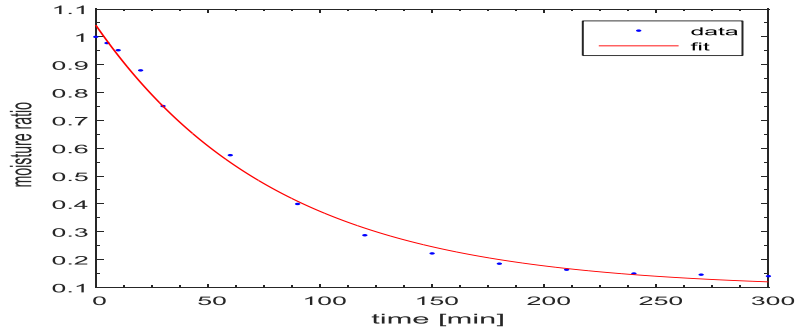

Fig. C13. Variation of experimental and Logarithmic model based predicted moisture ratio with time of Unblanched Water Yam dried at heater temp of 50^{o} C

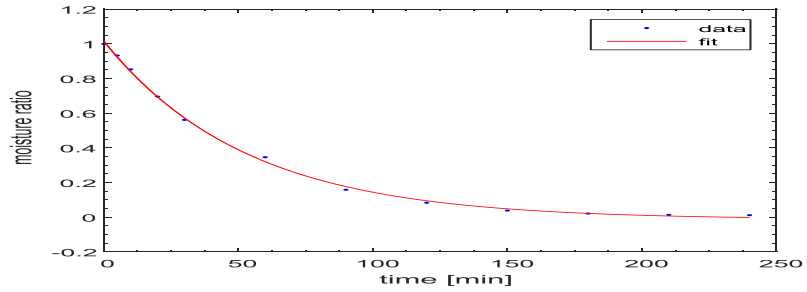

Fig. C14: Variation of experimental and Logarithmic model based predicted moisture ratio with time of Unblanched Water Yam dried at heater temp of 60^{o} C

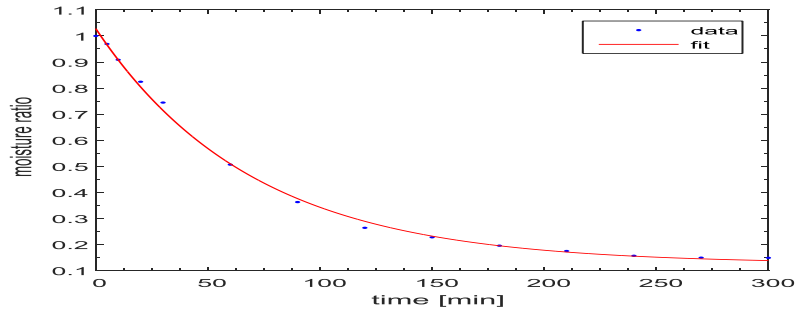

Fig. C15. Variation of experimental and Logarithmic model based predicted moisture ratio with time of Unblanched Aerial Yam dried at heater temp of 50^{o} C

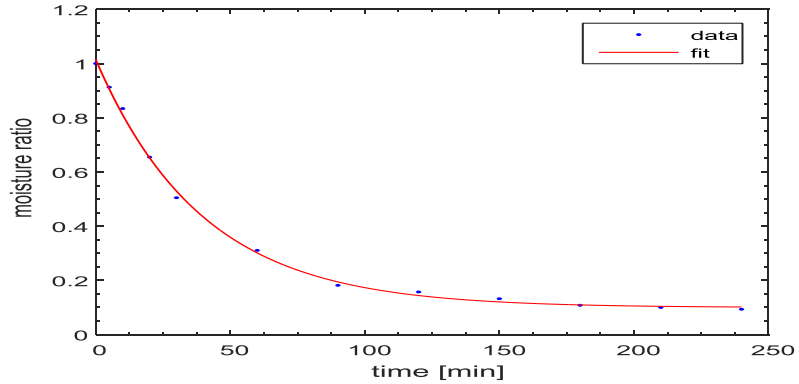

Fig. C16: Variation of experimental and Logarithmic model based predicted moisture ratio with time of Unblanched Aerial Yam dried at heater temp of 60^{o} C

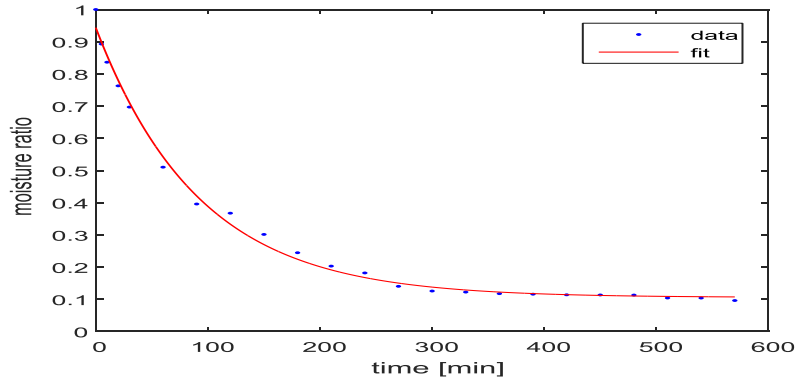

Fig. C17: Variation of experimental and Logarithmic model based predicted moisture ratio with time of blanched Water Yam dried at heater temp of 40^{o} C

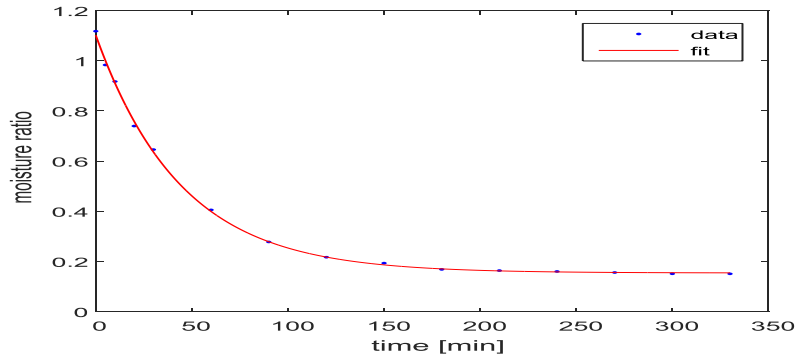

Fig. C18: Variation of experimental and Logarithmic model based predicted moisture ratio with time of blanched Water Yam dried at heater temp of 50^{o} C

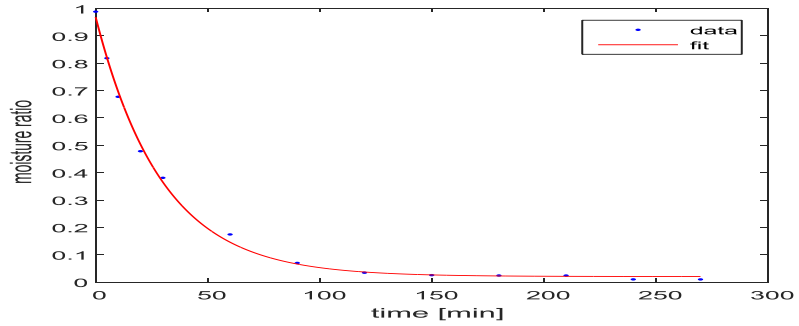

Fig. C19: Variation of experimental and Logarithmic model based predicted moisture ratio with time of blanched Water Yam dried at heater temp of 60^{o} C

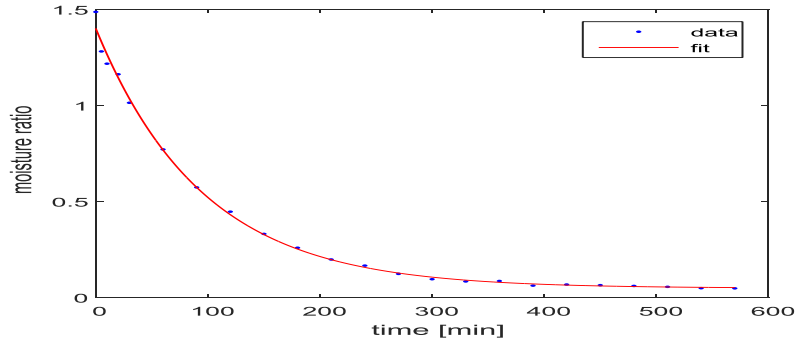

Fig. C20: Variation of experimental and Logarithmic model based predicted moisture ratio with time of blanched Arial Yam dried at heater temp of 40^{o} C

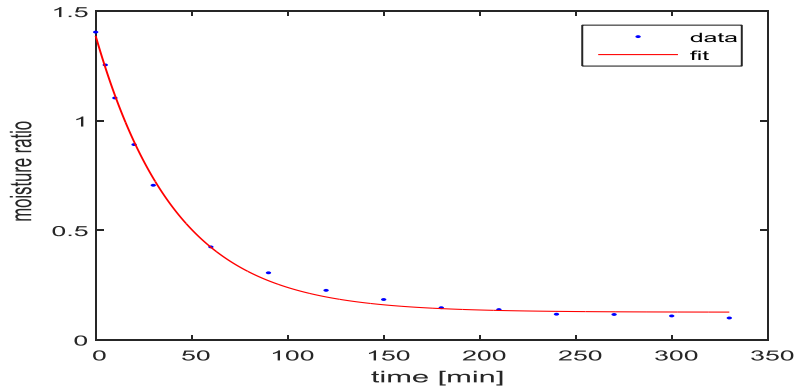

Fig. C21: Variation of experimental and Logarithmic model based predicted moisture ratio with time of blanched Arial Yam dried at heater temp of 50^{o} C

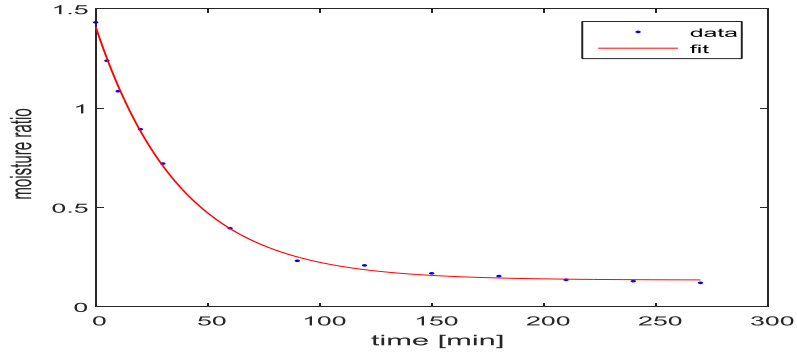

Fig. C22: Variation of experimental and Logarithmic model based predicted moisture ratio with time of blanched Arial Yam dried at heater temp of 60^{o} C

APPENDIX D: Table of design of experiment

Table D1 - Lack of Fit table for the convective drying of blanched WY

Source	Sum ofSquares	df	MeanSquare	F-Value	p-valueProb > F
Linear	2376.61	11	216.06	38.93	0.0004
2FI	2050.77	8	256.35	46.18	0.0003
Quadratic	67.8	5	13.56	2.44	0.1747
Cubic	16.24	1	16.24	2.93	0.1479

Table D2 - Lack of Fit table for the convective drying of blanched AY

Source	Sum ofSquares	df	MeanSquare	F-Value	p-valueProb > F
Linear	2671.68	11	242.88	108.68	< 0.0001
2FI	662.88	8	82.86	37.08	0.0005
Quadratic	8.67	5	1.73	0.78	0.6062
Cubic	3.46	1	3.46	1.55	0.2684

Table D3 - Model regression summerytable for the convective drying of blanched WY

Source	Sequ. p-value	Lack of Fit p-value	Adjusted R-Squared	Predicted R-Squared
Linear	0.0687	0.0004	0.2286	-0.012
2FI	0.5802	0.0003	0.1792	-1.0113
Quadratic	< 0.0001	0.1747	0.9509	0.8475
Cubic	0.2555	0.1479	0.9624	-0.2331

Table D4 - Model regression summerytable for the convective drying of blanched AY

Source	Sequ. p-value	Lack of Fit p-value	Adjusted R-Squared	Predicted R-Squared
Linear	0.4997	< 0.0001	-0.0286	-0.6141
2FI	0.0003	0.0005	0.6819	0.288
Quadratic	< 0.0001	0.6062	0.9878	0.9742
Cubic	0.7171	0.2684	0.985	0.6834

Table D5 - Model Summary Statistics for the convective drying of blanched WY

Source	Std.Dev.	R-Squared	AdjustedR-Squared	PredictedR-Squared
Linear	12.26	0.3504	0.2286	-0.012
2FI	12.64	0.4384	0.1792	-1.0113
Quadratic	3.09	0.9742	0.9509	0.8475
Cubic	2.71	0.9881	0.9624	-0.2331

Table D6 - Model Summary Statistics for the convective drying of blanched AY

Source	Std.Dev.	R-Squared	AdjustedR-Squared	PredictedR-Squared
Linear	12.95	0.1338	-0.0286	-0.6141
2FI	7.2	0.7824	0.6819	0.288
Quadratic	1.41	0.9936	0.9878	0.9742
Cubic	1.56	0.9953	0.985	0.6834

Table D7 - Lack of Fit table for the solar drying of unblanched WY

Source	Sum ofSquares	df	MeanSquare	F-Value	p-valueProb > F
Linear	7473.59	11	679.42	149.57	< 0.0001
2FI	5724.72	8	715.59	157.53	< 0.0001
Quadratic	4	5	0.8	0.18	0.9602
Cubic	9.82E-06	1	9.82E-06	2.16E-06	0.9989

Table D8 - Lack of Fit table for the solar drying of unblanched AY

Source	Sum ofSquares	df	MeanSquare	F-Value	p-valueProb > F
Linear	2769.3	11	251.75	230.91	< 0.0001
2FI	1815.09	8	226.89	208.1	< 0.0001
Quadratic	7.13	5	1.43	1.31	0.3878
Cubic	5.06	1	5.06	4.64	0.0838

Table D9 - Lack of Fit table for the solar drying of blanched WY

Source	Sum ofSquares	df	MeanSquare	F-Value	p-valueProb > F
Linear	2570.31	11	233.66	18.65	0.0023
2FI	1657.64	8	207.21	16.54	0.0034
Quadratic	173.19	5	34.64	2.76	0.1444
Cubic	3.89	1	3.89	0.31	0.6012

Table D10 - Lack of Fit table for the solar drying of blanched AY

Source	Sum ofSquares	df	MeanSquare	F-Value	p-valueProb > F
Linear	2660.47	11	241.86	24.48	0.0012
2FI	1740.26	8	217.53	22.01	0.0017
Quadratic	133.76	5	26.75	2.71	0.1492
Cubic	57.11	1	57.11	5.78	0.0613

Table D11 - Model regression summerytable for the solar drying of unblanched WY

Source	Sequ. p-value	Lack of Fit p-value	Adjusted R-Squared	Predicted R-Squared
Linear	0.0003	< 0.0001	0.6258	0.482
2FI	0.3106	< 0.0001	0.6469	0.4822
Quadratic	< 0.0001	0.9602	0.9979	0.9973
Cubic	0.8907	0.9989	0.997	0.9986

Table D12 - Model regression summerytable for the solar drying of unblanched AY

Source	Sequ. p-value	Lack of Fitp-value	AdjustedR-Squared	PredictedR-Squared
Linear	< 0.0001	< 0.0001	0.7549	0.6487
2FI	0.1285	< 0.0001	0.8021	0.6995
Quadratic	< 0.0001	0.3878	0.9982	0.9954
Cubic	0.871	0.0838	0.9975	0.9177

Table D13 - Model regression summerytable for the solar drying of blanched WY

Source	Sequ. p-value	Lack of Fit p-value	Adjusted R-Squared	Predicted R-Squared
Linear	< 0.0001	0.0023	0.7165	0.5678
2FI	0.1254	0.0034	0.772	0.681
Quadratic	0.0001	0.1444	0.9594	0.8722
Cubic	0.0708	0.6012	0.9809	0.9151

Table D14 - Model regression summerytable for the solar drying of blanched AY

Source	Sequ. p-value	Lack of Fitp-value	AdjustedR-Squared	PredictedR-Squared
Linear	< 0.0001	0.0012	0.6845	0.5322
2FI	0.1335	0.0017	0.7435	0.6754
Quadratic	< 0.0001	0.1492	0.9659	0.8932
Cubic	0.4435	0.0613	0.9669	-0.2231

Table D15 - Model Summary Statistics for the solar drying of unblanched WY

Source	Std.Dev.	R-Squared	AdjustedR-Squared	PredictedR-Squared
Linear	21.65	0.6849	0.6258	0.482
2FI	21.03	0.7584	0.6469	0.4822
Quadratic	1.63	0.9989	0.9979	0.9973
Cubic	1.95	0.999	0.997	0.9986

Table D16 - Model Summary Statistics for the solar drying of unblanched AY

Source	Std.Dev.	R-Squared	AdjustedR-Squared	PredictedR-Squared
Linear	13.17	0.7936	0.7549	0.6487
2FI	11.83	0.8646	0.8021	0.6995
Quadratic	1.12	0.9991	0.9982	0.9954
Cubic	1.32	0.9992	0.9975	0.9177

Table D17 - Model Summary Statistics for the solar drying of blanched WY

Source	Std.Dev.	R-Squared	AdjustedR-Squared	PredictedR-Squared
Linear	12.83	0.7613	0.7165	0.5678
2FI	11.5	0.844	0.772	0.681
Quadratic	4.86	0.9786	0.9594	0.8722
Cubic	3.33	0.994	0.9809	0.9151

Table D18 - Model Summary Statistics for the solar drying of blanched AY

Source	Std.Dev.	R-Squared	AdjustedR-Squared	PredictedR-Squared
Linear	13.01	0.7343	0.6845	0.5322
2FI	11.73	0.8245	0.7435	0.6754
Quadratic	4.28	0.982	0.9659	0.8932
Cubic	4.21	0.9896	0.9669	-0.2231

APPENDIX E

Fig. E1: Blanched aerial yam

Fig. E2: unblanched aerial yam

Fig. E3: Blanched water yam

Fig. E4: unblanched water yam

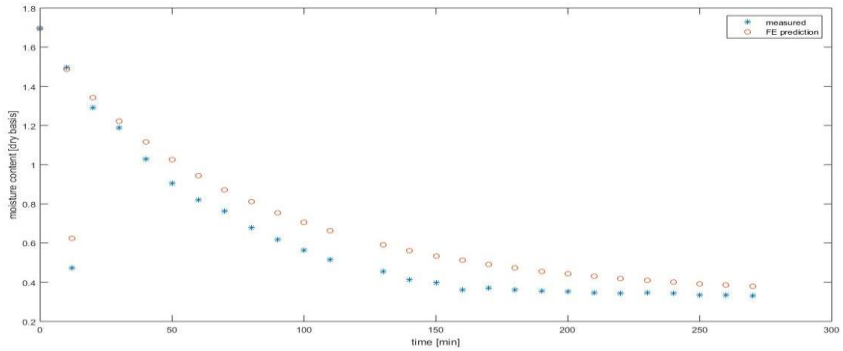

Fig. F1: Finite element prediction of water yam drying process at 90 ^{o}C.

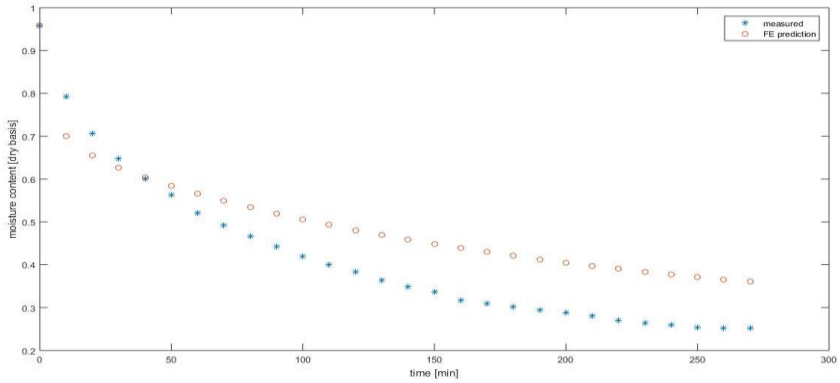

Fig. F2: Finite element prediction of aerial yam drying process at 90 ^{o}C.

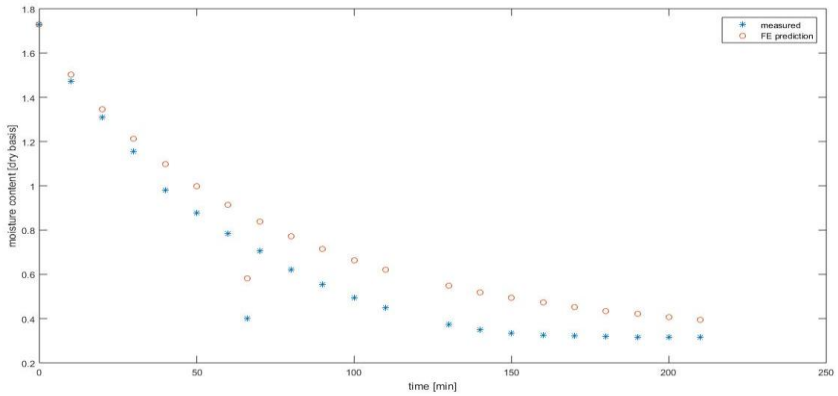

Fig. F3: Finite element prediction of water yam drying process at 110 ^{o}C.

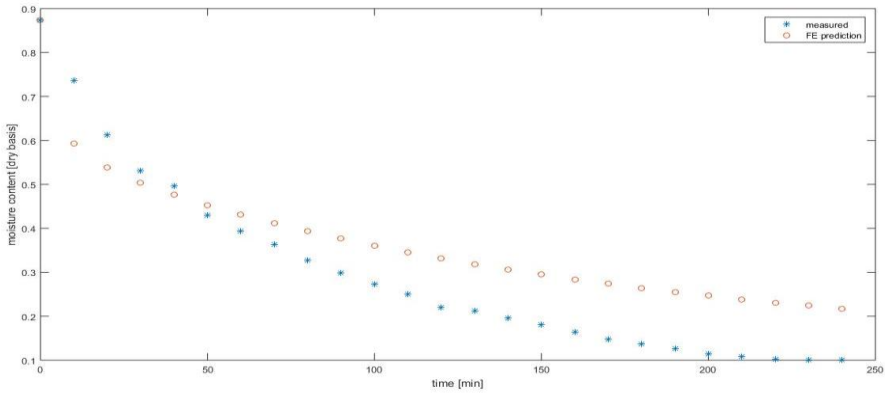

Fig. F4: Finite element prediction of water yam drying process at 110 ^{o}C.

FINITE ELEMENT PDE SCRIPT

```
% This script is written and read by pdetool and should NOT be edited.
% There are two recommended alternatives:
% 1) Export the required variables from pdetool and create a MATLAB script
% to perform operations on these.
% 2) Define the problem completely using a MATLAB script. See
% http://www.mathworks.com/help/pde/examples/index.html for examples
% of this approach.
function pdemodel1
[pde_fig,ax]=pdeinit;
pdetool('appl_cb',10);
set(ax,'DataAspectRatio',[1 1 1]);
set(ax,'PlotBoxAspectRatio',[1.5 1 1]);
set(ax,'XLim',[-1.5 1.5]);
set(ax,'YLim',[-1 1]);
set(ax,'XTickMode','auto');
set(ax,'YTickMode','auto');
% Geometry description:
pderect([1 -1 -0.20000000000000001 0.20000000000000001],'R1');
set(findobj(get(pde_fig,'Children'),'Tag','PDEEval'),'String','R1')
% Boundary conditions:
pdetool('changemode',0)
pdesetbd(4,...
'neu',...
1,...
'1.6246*10^(-6)*100',...
'1.6246*10^(-6)*100*0.2526')
pdesetbd(3,...
'neu',...
```

```
1,...
'1.6246*10^(-6)*100',...
'1.6246*10^(-6)*100*0.2526')
pdesetbd(2,...
'neu',...
1,...
'1.6246*10^(-6)*100',...
'1.6246*10^(-6)*100*0.2526')
pdesetbd(1,...
'neu',...
1,...
'1.6246*10^(-6)*100',...
'1.6246*10^(-6)*100*0.2526')
% Mesh generation:
setappdata(pde_fig,'Hgrad',1.3);
setappdata(pde_fig,'refinemethod','regular');
setappdata(pde_fig,'jiggle',char('on','mean',''));
setappdata(pde_fig,'MesherVersion','preR2013a');
pdetool('initmesh')
% PDE coefficients:
pdeseteq(2,...
'1.2241*10^(-10)*100*100',...
'0.0',...
'0',...
'1.0',...
'0:10*60:270*60',...
'0.9590',...
'0.0',...
'[0 100]')
setappdata(pde_fig,'currparam',...
['1.2241*10^(-10)*100*100';...
'0 '])
% Solve parameters:
setappdata(pde_fig,'solveparam',...
char('0','1000','10','pdeadworst',...
'0.5','longest','0','1E-4','','fixed','Inf'))
% Plotflags and user data strings:
setappdata(pde_fig,'plotflags',[1 1 1 1 1 1 1 1 0 0 0 28 1 0 0 0 0 1]);
setappdata(pde_fig,'colstring','');
setappdata(pde_fig,'arrowstring','');
setappdata(pde_fig,'deformstring','');
setappdata(pde_fig,'heightstring','');
% Solve PDE:
pdetool('solve')
```

```
% Thermophysical Charaterization
% Temp 110C
M_d=22.12/1000;
MC_eq=2.3375;
H=4/1000/2;
Time=60*[0 10 20 30 40 50 60 70 80 90 100 110 120 130 140 150 160 170 180 190 200 210];
Mass1=10^(-3)*
[61.409 57.002 53.672 49.702 44.412 41.978 39.844 38.15 36.232 34.798 33.31 32.18 30.85
30.3 29.731 29.322 29.017 28.908 28.882 28.85 28.7
Mass2=10^(-3)*
[59.328 52.383 48.494 45.708 43.236 41.156 39.074 37.25 35.54 34.023 32.835 31.909 31.174
30.464 30.001 29.763 29.64 29.567 29.498 29.442
Mass=(Mass1+Mass2)/2;
MC=(Mass-M_d)/M_d;
MR=(MC-MC_eq)/(MC(1)-MC_eq);
y=(4*H^2/pi/pi)*log(8./MR/pi/pi);
D_eff=inv(Time*Time')*y*Time'
plot(Time,D_eff*Time,Time,y)
xlabel('t [sec]'); ylabel('y=(4*H^2/pi^2)*log(8/MR/pi^2)');
legend ('Linear fit','Measured')
% Convective Mass Transfer Coefficient
l=30/1000;w=20/1000;h=4/1000;% length width and height of each sample
ns=12;% number of samples
rhow=1000; % density of water
V1=10^(-6)*[0 41 40.5 41 40 40 40 40 40 39.5 39.5 39 38.5 38 38 37.5 37.5 37 37 36.5 36.5
36.5]; % initial volume in the flask
V_i=ns*l*w*h;% initial volume of the samples
A_i=ns*2*(l*w+w*h+l*h);% initial area of the samples
V=V_i-(Mass(1)-Mass)/rhow;% volume at time t of the samples
V2=V1+V/ns; % volume of one sample at t
A=zeros(1,length(V));
for i=1:length(V)
if V(i)>0
A(i)=(1-((Mass(1)-Mass(i))./V_i/rhow))^(2/3)*A_i; % area at time t of the samples
h_m(i)=V(i)*log(MR(i))/A(i)/Time(i)/60; % convective mass transfer coefficient
else
A(i)=0;
h_m(i)=0;
end
end
10^6*V1'
V'
10^6*V2'
A'
h_m'
% Data at Temp 90C
```

```
M_d=22.12/1000;
MC_eq=2.2293;
H=4/1000/2;
Time=60*[0 10 20 30 40 50 60 70 80 90 100 110 12 130 140 150 160 170 180 190 200 210 220
230 240 250 260 270];
Mass1=10^(-3)*
[60.598 55.867 52.212 49.115 46.704 44.446 42.753 41.215 39.85 38.572 37.346 36.227 35.264
34.571 33.754 33.246 31.912 32.552 32.259 32.0
Mass2=10^(-3)*
[58.713 54.528 49.122 47.69 43.029 39.789 37.772 36.84 34.407 32.987 31.892 30.819 29.94
29.758 28.749 28.568 28.364 28.148 27.993 27.935
Mass=(Mass1+Mass2)/2;
MC=(Mass-M_d)/M_d;
MR=(MC-MC_eq)/(MC(1)-MC_eq);
y=(4*H^2/pi/pi)*log(8./MR/pi/pi);
D_eff=inv(Time*Time')*y*Time'
plot(Time,D_eff*Time,Time,y)
xlabel('t [sec]'); ylabel('y=(4*H^2/pi^2)*log(8/MR/pi^2)');
legend ('Linear fit','Measured')
% Convective Mass Transfer Coefficient
l=30/1000;w=20/1000;h=4/1000;% length width and height of each sample
ns=12;% number of samples
rhow=1000; % density of water
V1=10^(-6)*[0 61 60.5 60 60 59.5 59.5 59 59 58.5 58.5 58 58 57.5 57 57 56.5 56 56 55.5 55.5
55 55 54.5 54.5 54.5 54 54]; % initial volume in the
flask
V_i=ns*l*w*h;% initial volume of the samples
A_i=ns*2*(l*w+w*h+l*h);% initial area of the samples
V=V_i-(Mass(1)-Mass)/rhow;% volume at time t of the samples
V2=V1+V/ns; % volume of one sample at t
A=zeros(1,length(V));
for i=1:length(V)
if V(i)>0
A(i)=(1-((Mass(1)-Mass(i))./V_i/rhow))^(2/3)*A_i; % area at time t of the samples
h_m(i)=V(i)*log(MR(i))/A(i)/Time(i)/60; % convective mass transfer coefficient
else
A(i)=0;
h_m(i)=0;
end
end
10^6*V1'
V'
10^6*V2'
A'
h_m'
% Program for Plotting The Measured and the FEM predicted Kinetics
```

```
% Temp 110C
M_d=22.12/1000;
MC_eq=2.3375;
H=4/1000/2;
Time1=[0 10 20 30 40 50 60 70 80 90 100 110 120 130 140 150 160 170 180 190 200 210];
Mass1=10^(-3)*
[61.409 57.002 53.672 49.702 44.412 41.978 39.844 38.15 36.232 34.798 33.31 32.18 30.85
30.3 29.731 29.322 29.017 28.908 28.882 28.85 28.7
Time2=[0 10 20 30 40 50 60 70 80 90 100 110 12 130 140 150 160 170 180 190 200 210];
Mass2=10^(-3)*
[59.328 52.383 48.494 45.708 43.236 41.156 39.074 37.25 35.54 34.023 32.835 31.909 31.174
30.464 30.001 29.763 29.64 29.567 29.498 29.442
Time=(Time1+Time2)/2;
Mass=(Mass1+Mass2)/2;
MC=(Mass-M_d)/M_d;
% predicted values
[m,n]=size(u);
MCred=zeros(1,n);
for i=1:n
MCpred(i)=mean(u(:,i));
end
plot(Time,MC,'*',Time,MCpred,'o')
xlabel('time [min]');ylabel('moisture content [dry basis]')
legend('measured','FE prediction')
% error indices
T=MC;Y=MCpred;
Rsquared=1-sum((T-Y).^2)/sum((T-mean(T)).^2);
RMSE=sqrt(mean((Y-T).^2));
r=sum((Y-mean(Y)).*(T-mean(T)))/sqrt(sum((Y-mean(Y)).^2)*sum((T-mean(T)).^2));
Stat=[Rsquared RMSE r]'
% Data at Temp 90C
M_d=22.12/1000;
MC_eq=2.2293;
H=4/1000/2;
Time1=[0 10 20 30 40 50 60 70 80 90 100 110 12 130 140 150 160 170 180 190 200 210 220
230 240 250 260 270];
Mass1=10^(-3)*
[60.598 55.867 52.212 49.115 46.704 44.446 42.753 41.215 39.85 38.572 37.346 36.227 35.264
34.571 33.754 33.246 31.912 32.552 32.259 32.0
Time2=[0 10 20 30 40 50 60 70 80 90 100 110 12 130 140 150 160 170 180 190 200 210 220
230 240 250 260 270];
Mass2=10^(-3)*
[58.713 54.528 49.122 47.69 43.029 39.789 37.772 36.84 34.407 32.987 31.892 30.819 29.94
29.758 28.749 28.568 28.364 28.148 27.993 27.935
Time=(Time1+Time2)/2;
Mass=(Mass1+Mass2)/2;
```

```
MC=(Mass-M_d)/M_d;
% predicted values
[m,n]=size(u);
MCred=zeros(1,n);
for i=1:n
MCpred(i)=mean(u(:,i));
end
plot(Time,MC,'*',Time,MCpred,'o')
xlabel('time [min]');ylabel('moisture content [dry basis]')
legend('measured','FE prediction')
% error indices
T=MC;Y=MCpred;
Rsquared=1-sum((T-Y).^2)/sum((T-mean(T)).^2);
RMSE=sqrt(mean((Y-T).^2));
r=sum((Y-mean(Y)).*(T-mean(T)))/sqrt(sum((Y-mean(Y)).^2)*sum((T-mean(T)).^2));
Stat=[Rsquared RMSE r]'



% Thermophysical Charaterization
% Temp 110C
M_d=28.23/1000;
MC_eq=1.6065;
H=4/1000/2;
Time=60*[0 10 20 30 40 50 60 70 80 90 100 110 120 130 140 150 160 170 180 190 200 210
220 230 240];
Mass1=10^(-3)*
[52.33 49.786 46.307 44.323 43 41.894 40.977 40.016 39.135 38.345 37.648 36.959 35.755
35.906 34.944 34.193 33.433 32.612 32.062 31.55 31
Mass2=10^(-3)*
[53.486 48.221 44.75 42.154 41.498 38.848 37.68 36.92 35.838 34.959 34.199 33.656 33.157
32.584 32.552 32.466 32.334 32.183 32.094 32.008
Mass=(Mass1+Mass2)/2;
MC=(Mass-M_d)/M_d;
MR=(MC-MC_eq)/(MC(1)-MC_eq);
y=(4*H^2/pi/pi)*log(8./MR/pi/pi);
D_eff=inv(Time*Time')*y*Time'
plot(Time,-D_eff*Time,Time,-y)
xlabel('t [sec]'); ylabel('y=(4*H^2/pi^2)*log(8/MR/pi^2)');
legend ('Linear fit','Measured')
% Convective Mass Transfer Coefficient
l=30/1000;w=20/1000;h=4/1000;% length width and height of each sample
ns=12;% number of samples
rhow=1000; % density of water
V1=10^(-6)*[0 72.5 72 72 71.5 71.5 71 71 71 70.5 70 70 70 70 70 70 69 69 68.5 68.5 68 68 67.5
67.5 67]; % initial volume in the flask
V_i=ns*l*w*h;% initial volume of the samples
```

```
A_i=ns*2*(l*w+w*h+l*h);% initial area of the samples
V=V_i-(Mass(1)-Mass)/rhow;% volume at time t of the samples
V2=V1+V/ns; % volume of one sample at t
A=zeros(1,length(V));
for i=1:length(V)
if V(i)>0
A(i)=(1-((Mass(1)-Mass(i))./V_i/rhow))^(2/3)*A_i; % area at time t of the samples
h_m(i)=V(i)*log(MR(i))/A(i)/Time(i)/60; % convective mass transfer coefficient
else
A(i)=0;
h_m(i)=0;
end
end
10^6*V1'
V'
10^6*V2'
A'
h_m'
% MODEL FOR h_m
for i=1:length(Time)-1
t(i)=Time(i+1);
hm(i)=h_m(i+1);
end
f = fit( t', hm', 'poly2')% quadratic fit
Y=f(t); % fitted values at the indicated points of "time"
T=hm';
Rsquared=1-sum((T-Y).^2)/sum((T-mean(T)).^2);
RMSE=sqrt(mean((Y-T).^2));
r=sum((Y-mean(Y)).*(T-mean(T)))/sqrt(sum((Y-mean(Y)).^2)*sum((T-mean(T)).^2));
Stat=[Rsquared RMSE r]'
% Program for Plotting The Measured and the FEM predicted Kinetics
% Temp 110C
M_d=28.23/1000;
MC_eq=1.6065;
H=4/1000/2;
Time=[0 10 20 30 40 50 60 70 80 90 100 110 120 130 140 150 160 170 180 190 200 210 220
230 240];
Mass1=10^(-3)*
[52.33 49.786 46.307 44.323 43 41.894 40.977 40.016 39.135 38.345 37.648 36.959 35.755
35.906 34.944 34.193 33.433 32.612 32.062 31.55 31
Mass2=10^(-3)*
[53.486 48.221 44.75 42.154 41.498 38.848 37.68 36.92 35.838 34.959 34.199 33.656 33.157
32.584 32.552 32.466 32.334 32.183 32.094 32.008
Mass=(Mass1+Mass2)/2;
MC=(Mass-M_d)/M_d;
% predicted values
```

```
[m,n]=size(u);
MCred=zeros(1,n);
for i=1:n
MCpred(i)=mean(u(:,i));
end
plot(Time,MC,'*',Time,MCpred,'o')
xlabel('time [min]');ylabel('moisture content [dry basis]')
legend('measured','FE prediction')
% error indices
T=MC;Y=MCpred;
Rsquared=1-sum((T-Y).^2)/sum((T-mean(T)).^2);
RMSE=sqrt(mean((Y-T).^2));
r=sum((Y-mean(Y)).*(T-mean(T)))/sqrt(sum((Y-mean(Y)).^2)*sum((T-mean(T)).^2));
Stat=[Rsquared RMSE r]'
% Temp 90C
M_d=28.23/1000;
MC_eq=1.6934;
H=4/1000/2;
Time=60*[0 10 20 30 40 50 60 70 80 90 100 110 120 130 140 150 160 170 180 190 200 210
220 230 240 250 260 270];
Mass1=10^(-3)*
[54.487 49.6 46.845 45.004 43.599 42.36 40.978 39.875 39.082 38.275 37.531 36.937 36.389
35.706 35.216 34.88 34.51 34.276 34.031 33.863 3
Mass2=10^(-3)*
[56.116 51.596 49.541 48.024 46.794 45.907 44.916 44.382 43.751 43.116 42.615 42.13 41.703
41.29 40.909 40.569 39.864 39.654 39.499 39.21
Mass=(Mass1+Mass2)/2;
MC=(Mass-M_d)/M_d;
MR=(MC-MC_eq)/(MC(1)-MC_eq);
y=(4*H^2/pi/pi)*log(8./MR/pi/pi);
D_eff=inv(Time*Time')*y*Time'
plot(Time,-D_eff*Time,Time,-y)
xlabel('t [sec]'); ylabel('y=(4*H^2/pi^2)*log(8/MR/pi^2)');
legend ('Linear fit','Measured')
% Convective Mass Transfer Coefficient
l=30/1000;w=20/1000;h=4/1000;% length width and height of each sample
ns=12;% number of samples
rhow=1000; % density of water
V1=10^(-6)*[0 58 57 57 57 56.5 56 56 55 55 55 55 54 54 53.5 53.5 53 53 53 52.5 52 52 51.5 51
51 51 50.5 50]; % initial volume in the flask
V_i=ns*l*w*h;% initial volume of the samples
A_i=ns*2*(l*w+w*h+l*h);% initial area of the samples
V=V_i-(Mass(1)-Mass)/rhow;% volume at time t of the samples
V2=V1+V/ns; % volume of one sample at t
A=zeros(1,length(V));
for i=1:length(V)
```

```
if V(i)>0
A(i)=(1-((Mass(1)-Mass(i))./V_i/rhow))^(2/3)*A_i; % area at time t of the samples
h_m(i)=V(i)*log(MR(i))/A(i)/Time(i)/60; % convective mass transfer coefficient
else
A(i)=0;
h_m(i)=0;
end
end
10^6*V1'
V'
10^6*V2'
A'
h_m'
% MODEL FOR h_m
for i=1:length(Time)-1
t(i)=Time(i+1);
hm(i)=h_m(i+1);
end
f = fit( t', hm', 'poly2')% quadratic fit
Y=f(t); % fitted values at the indicated points of "time"
T=hm';
Rsquared=1-sum((T-Y).^2)/sum((T-mean(T)).^2);
RMSE=sqrt(mean((Y-T).^2));
r=sum((Y-mean(Y)).*(T-mean(T)))/sqrt(sum((Y-mean(Y)).^2)*sum((T-mean(T)).^2));
Stat=[Rsquared RMSE r]'
% Program for Plotting The Measured and the FEM predicted Kinetics
% Temp 90C
M_d=28.23/1000;
MC_eq=1.6934;
H=4/1000/2;
Time=[0 10 20 30 40 50 60 70 80 90 100 110 120 130 140 150 160 170 180 190 200 210 220
230 240 250 260 270];
Mass1=10^(-3)*
[54.487 49.6 46.845 45.004 43.599 42.36 40.978 39.875 39.082 38.275 37.531 36.937 36.389
35.706 35.216 34.88 34.51 34.276 34.031 33.863 3
Mass2=10^(-3)*
[56.116 51.596 49.541 48.024 46.794 45.907 44.916 44.382 43.751 43.116 42.615 42.13 41.703
41.29 40.909 40.569 39.864 39.654 39.499 39.21
Mass=(Mass1+Mass2)/2;
MC=(Mass-M_d)/M_d;
% predicted values
[m,n]=size(u);
MCred=zeros(1,n);
for i=1:n
MCpred(i)=mean(u(:,i));
end
```

```
plot(Time,MC,'*',Time,MCpred,'o')
xlabel('time [min]');ylabel('moisture content [dry basis]')
legend('measured','FE prediction')
% error indices
T=MC;Y=MCpred;
Rsquared=1-sum((T-Y).^2)/sum((T-mean(T)).^2);
RMSE=sqrt(mean((Y-T).^2));
r=sum((Y-mean(Y)).*(T-mean
```

SIMPLE MATLAB SCRIPT-1 FOR ARTIFICIAL NEURAL NETWORK (ANN)

```
% Solve an Input-Output Fitting problem with a Neural Network

% Script generated by Neural Fitting app

% Created 10-March-2019 11:25:52

%

% This script assumes these variables are defined:

%

%   input - input data.

%   target - target data.


x = input;

t = target;


% Choose a Training Function

% For a list of all training functions type: help nntrain

% 'trainlm' is usually fastest.

% 'trainbr' takes longer but may be better for challenging problems.

% 'trainscg' uses less memory. Suitable in low memory situations.

trainFcn = 'trainlm';  % Levenberg-Marquardt backpropagation.
```

```
% Create a Fitting Network
hiddenLayerSize = 10;
net = fitnet(hiddenLayerSize,trainFcn);

% Setup Division of Data for Training, Validation, Testing
net.divideParam.trainRatio = 70/100;
net.divideParam.valRatio = 15/100;
net.divideParam.testRatio = 15/100;

% Train the Network
[net,tr] = train(net,x,t);

% Test the Network
y = net(x);
e = gsubtract(t,y);
performance = perform(net,t,y)

% View the Network
view(net)

% Plots
% Uncomment these lines to enable various plots.
%figure, plotperform(tr)
%figure, plottrainstate(tr)
```

```
%figure, ploterrhist(e)

%figure, plotregression(t,y)

%figure, plotfit(net,x,t)
```

Advanced MATLAB Script

```
% Solve an Input-Output Fitting problem with a Neural Network
% Script generated by Neural Fitting app
% Created 10-March-2019 11:27:12
%
% This script assumes these variables are defined:
%
%   input - input data.
%   target - target data.

x = input;
t = target;

% Choose a Training Function
% For a list of all training functions type: help nntrain
% 'trainlm' is usually fastest.
% 'trainbr' takes longer but may be better for challenging problems.
% 'trainscg' uses less memory. Suitable in low memory situations.
trainFcn = 'trainlm';  % Levenberg-Marquardt backpropagation.

% Create a Fitting Network
hiddenLayerSize = 10;
net = fitnet(hiddenLayerSize,trainFcn);

% Choose Input and Output Pre/Post-Processing Functions
```

```
% For a list of all processing functions type: help nnprocess
net.input.processFcns = {'removeconstantrows','mapminmax'};
net.output.processFcns = {'removeconstantrows','mapminmax'};

% Setup Division of Data for Training, Validation, Testing
% For a list of all data division functions type: help nndivide
net.divideFcn = 'dividerand';  % Divide data randomly
net.divideMode = 'sample';  % Divide up every sample
net.divideParam.trainRatio = 70/100;
net.divideParam.valRatio = 15/100;
net.divideParam.testRatio = 15/100;

% Choose a Performance Function
% For a list of all performance functions type: help nnperformance
net.performFcn = 'mse';  % Mean Squared Error

% Choose Plot Functions
% For a list of all plot functions type: help nnplot
net.plotFcns = {'plotperform','plottrainstate','ploterrhist', ...
    'plotregression', 'plotfit'};

% Train the Network
[net,tr] = train(net,x,t);

% Test the Network
```

```
y = net(x);
e = gsubtract(t,y);
performance = perform(net,t,y)

% Recalculate Training, Validation and Test Performance
trainTargets = t .* tr.trainMask{1};
valTargets = t .* tr.valMask{1};
testTargets = t .* tr.testMask{1};
trainPerformance = perform(net,trainTargets,y)
valPerformance = perform(net,valTargets,y)
testPerformance = perform(net,testTargets,y)

% View the Network
view(net)

% Plots
% Uncomment these lines to enable various plots.
%figure, plotperform(tr)
%figure, plottrainstate(tr)
%figure, ploterrhist(e)
%figure, plotregression(t,y)
%figure, plotfit(net,x,t)

% Deployment
% Change the (false) values to (true) to enable the following code blocks.
```

```
% See the help for each generation function for more information.
if (false)
    % Generate MATLAB function for neural network for application
    % deployment in MATLAB scripts or with MATLAB Compiler and Builder
    % tools, or simply to examine the calculations your trained neural
    % network performs.
    genFunction(net,'myNeuralNetworkFunction');
    y = myNeuralNetworkFunction(x);
end
if (false)
    % Generate a matrix-only MATLAB function for neural network code
    % generation with MATLAB Coder tools.
    genFunction(net,'myNeuralNetworkFunction','MatrixOnly','yes');
    y = myNeuralNetworkFunction(x);
end
if (false)
    % Generate a Simulink diagram for simulation or deployment with.
    % Simulink Coder tools.
    gensim(net);
end
```

Simple MATLAB Script- for convective dryer

```
% Solve an Input-Output Fitting problem with a Neural Network
% Script generated by Neural Fitting app
% Created 10-March-2019 12:05:04
```

```
%
% This script assumes these variables are defined:
%
%   input - input data.
%   target - target data.

x = input;
t = target;

% Choose a Training Function
% For a list of all training functions type: help nntrain
% 'trainlm' is usually fastest.
% 'trainbr' takes longer but may be better for challenging problems.
% 'trainscg' uses less memory. Suitable in low memory situations.
trainFcn = 'trainlm';  % Levenberg-Marquardt backpropagation.

% Create a Fitting Network
hiddenLayerSize = 10;
net = fitnet(hiddenLayerSize,trainFcn);

% Setup Division of Data for Training, Validation, Testing
net.divideParam.trainRatio = 55/100;
net.divideParam.valRatio = 20/100;
net.divideParam.testRatio = 25/100;
```

```
% Train the Network
[net,tr] = train(net,x,t);

% Test the Network
y = net(x);
e = gsubtract(t,y);
performance = perform(net,t,y)

% View the Network
view(net)

% Plots
% Uncomment these lines to enable various plots.
%figure, plotperform(tr)
%figure, plottrainstate(tr)
%figure, ploterrhist(e)
%figure, plotregression(t,y)
%figure, plotfit(net,x,t)
```

Advanced MATLAB Script for solar dryer

```
% Solve an Input-Output Fitting problem with a Neural Network
% Script generated by Neural Fitting app
% Created 10-March-2019 11:08:18
%
% This script assumes these variables are defined:
```

```
%
%   input - input data.
%   target - target data.

x = input;
t = target;

% Choose a Training Function
% For a list of all training functions type: help nntrain
% 'trainlm' is usually fastest.
% 'trainbr' takes longer but may be better for challenging problems.
% 'trainscg' uses less memory. Suitable in low memory situations.
trainFcn = 'trainlm';  % Levenberg-Marquardt backpropagation.

% Create a Fitting Network
hiddenLayerSize = 10;
net = fitnet(hiddenLayerSize,trainFcn);

% Choose Input and Output Pre/Post-Processing Functions
% For a list of all processing functions type: help nnprocess
net.input.processFcns = {'removeconstantrows','mapminmax'};
net.output.processFcns = {'removeconstantrows','mapminmax'};

% Setup Division of Data for Training, Validation, Testing
% For a list of all data division functions type: help nndivide
```

```
net.divideFcn = 'dividerand';  % Divide data randomly
net.divideMode = 'sample';  % Divide up every sample
net.divideParam.trainRatio = 55/100;
net.divideParam.valRatio = 20/100;
net.divideParam.testRatio = 25/100;

% Choose a Performance Function
% For a list of all performance functions type: help nnperformance
net.performFcn = 'mse';  % Mean Squared Error

% Choose Plot Functions
% For a list of all plot functions type: help nnplot
net.plotFcns = {'plotperform','plottrainstate','ploterrhist', ...
    'plotregression', 'plotfit'};

% Train the Network
[net,tr] = train(net,x,t);

% Test the Network
y = net(x);
e = gsubtract(t,y);
performance = perform(net,t,y)

% Recalculate Training, Validation and Test Performance
trainTargets = t .* tr.trainMask{1};
```

```
valTargets = t .* tr.valMask{1};
testTargets = t .* tr.testMask{1};
trainPerformance = perform(net,trainTargets,y)
valPerformance = perform(net,valTargets,y)
testPerformance = perform(net,testTargets,y)

% View the Network
view(net)

% Plots
% Uncomment these lines to enable various plots.
%figure, plotperform(tr)
%figure, plottrainstate(tr)
%figure, ploterrhist(e)
%figure, plotregression(t,y)
%figure, plotfit(net,x,t)

% Deployment
% Change the (false) values to (true) to enable the following code blocks.
% See the help for each generation function for more information.
if (false)
    % Generate MATLAB function for neural network for application
    % deployment in MATLAB scripts or with MATLAB Compiler and Builder
    % tools, or simply to examine the calculations your trained neural
    % network performs.
```

```
    genFunction(net,'myNeuralNetworkFunction');
    y = myNeuralNetworkFunction(x);
end
if (false)
    % Generate a matrix-only MATLAB function for neural network code
    % generation with MATLAB Coder tools.
    genFunction(net,'myNeuralNetworkFunction','MatrixOnly','yes');
    y = myNeuralNetworkFunction(x);
end
if (false)
    % Generate a Simulink diagram for simulation or deployment with.
    % Simulink Coder tools.
    gensim(net);
end
```

QUESTIONNAIRE

9-Point Hedonic Rating on Water Yam and Aerial Yam Floor

Kindly assist in determining and rating of the floor samples labeled (A-H). Please tick (√) appropriately your observation using the hedonic scale below.

Age bracket: Below 20 years ( ) Between 20 and 40 years ( ) Above 40 years ( )

Gender: Male ( ) Female ( )

Occupation: _____

Hedonic Scale Ranking:

LE: Like extremely

LVM: Like very much

LM: Like moderately

LS: like slightly

NLS: Neither like nor dislike

DS: Dislike slightly

DM: Dislike moderately

DVM: Dislike very much

DE: Dislike extremely

Floor Samples		**LE**	**LVM**	**LM**	**LS**	**NLD**	**DS**	**DM**	**DVM**	**DE**
Floor A	(1). Appearance									
	(2). Colour									
	(3). Aroma									
	(4). Texture									
Floor B	(1). Appearance									
	(2). Colour									
	(3). Aroma									
	(4). Texture									
Floor C	(1). Appearance									
	(2). Colour									
	(3). Aroma									
	(4). Texture									
Floor D	(1). Appearance									
	(2). Colour									
	(3). Aroma									
	(4). Texture									
Floor E	(1). Appearance									
	(2). Colour									
	(3). Aroma									
	(4). Texture									
Floor F	(1). Appearance									
	(2). Colour									
	(3). Aroma									
	(4). Texture									
Floor G	(1). Appearance									
	(2). Colour									
	(3). Aroma									
	(4). Texture									
Floor H	(1). Appearance									
	(2). Colour									
	(3). Aroma									
	(4). Texture									